Functional Properties of the Intact and Compromised Midbrain Dopamine System

Anna-Kristin Kaufmann

St Cross College

University of Oxford

A thesis submitted for the degree of

Doctor of Philosophy

Hilary Term 2017

Acknowledgements

I would like to thank my supervisor Paul Dodson for his remarkable support, guidance and friendship. I am immensely grateful for his all-encompassing training, be it in hands-on experiments, building MacGyver-style lab equipment or critical scientific thinking. Also, I would like to thank him for his admirable attempts in trying to close my knowledge gaps when it came to pop cultural references. I further thank my excellent co-supervisor Peter Magill for his valuable input and scientific reasoning and Paul Bolam for his support.

I thank Rafal Bogacz, Kouichi Nakamura and Andrew Sharott for their input on data analysis. I thank the MRC and the German Academic Scholarship Foundation for their financial support and Prof. Peter Somogyi at the MRC ANU and Prof. Peter Brown at the MRC BNDU for providing access to a fantastic range of resources.

I thank past and present unit members and support staff for all their help and friendship: Jane Janson, Lisa Conyers, Katherine Shakespeare, Liz Norman, Hua Zhang, Ben Micklem, Savita Anderson, Vivienne Collins, Rahul Shah, Eszter Kormann, Abbey Becker, Farid Garas, Colin McNamara, Naomi Berry, Max Rothwell, Maaike van Swieten, Luke Bryden, Abhilasha Joshi, Linda Katona, Marco Bocchio, Mina Salib, Gunes Unal and Kouichi Nakamura. Special thanks go to Natalie Doig, Emilie Syed, Jennifer Kaufling, Amy Wolff, Claire Bradley, Alexander Morley and Matt Carr who made sure I took part in social activities. Also thanks to the Dupret-lab football team for matches in rain and sunshine.

I thank Sebastian Vasquez, Ayesha Sengupta and Santiago Herce Castanon for their friendship and shared time in Oxford. Thanks to Bastian Gastl for years of loyal friendship and humorous messages and thanks to Konstanze Winter for being the most wonderful companion.

I would *l*ike to thank m*y* parents for being there always, *m*y siblings Lisa-Katrin and Christopher for being my accomplices in life and Dan for our pas*t* and fu*tur*e life adventure *t*ogether.

Abstract

Functional Properties of the Intact and Compromised Midbrain Dopamine System
Anna-Kristin Kaufmann, St Cross College
Thesis submitted for degree of Doctor of Philosophy, Hilary Term 2017

The midbrain dopamine system is involved in many aspects of purposeful behaviour and, when compromised, can have devastating effects on movement and cognition as seen in diseases like Parkinson's. In the healthy brain, dopamine neurons are thought to play particularly important roles in learning by signalling errors in reward prediction.

The objective of this thesis was to investigate the diversity in the functional properties of the midbrain dopamine system, and how this is altered through genetic variation of relevance to Parkinson's and development of cell phenotype. This objective was addressed with a combination of behavioural experiments, *in vivo* single-cell recording and labelling (both in anaesthetised as well as awake rodents), immunofluorescence labelling, retrograde tracing and stereology.

In a first set of experiments, it was demonstrated that chronic as well as acute genetic challenges can alter the firing patterns of midbrain dopamine neurons. Using a novel bacterial artificial chromosome-transgenic rat model, it was shown that the R1441C mutation in human leucine-rich repeat kinase 2, which is linked to Parkinson's, leads to motor deficits and an age-dependent reduction in the *in vivo* firing variability and burst firing of substantia nigra pars compacta (SNc) dopamine neurons. These findings help reveal processes of early, pre-degenerative dysfunction in dopamine neurons in Parkinson's. Similar effects on firing variability and burst firing of SNc dopamine neurons were found in a mouse model with conditional knock-out of the transcription factors Forkhead box A1 and A2 (FoxA1/2) in midbrain dopamine neurons. These findings indicate that FoxA1/2 are not only crucial for the early development of dopamine neurons, but also their function in the mature brain.

In a second set of experiments in wildtype mice, it was demonstrated that midbrain dopamine neurons (located in SNc and ventral tegmental area) show diverse expression of the molecular markers Calbindin, Calretinin, Aldh1a1, Sox6, Girk2, SatB1 and Otx2. It was found that selective expression of these markers is of use for discriminating between midbrain dopamine neurons that project to dorsal striatum or nucleus accumbens. To elucidate whether the diverse molecular marker expression would map onto dopamine neurons whose firing correlates with distinct behavioural events, midbrain dopamine neurons were recorded and labelled in head-fixed awake mice either exposed to neutral sensory stimuli or performing a classical conditioning paradigm. The population activity of midbrain dopamine neurons was not modulated by neutral sensory stimuli. Interestingly, fewer than 50% of identified dopamine neurons showed phasic firing increases following reward-predicting cue and/or reward delivery, despite the common assumption that most (if not all) midbrain dopamine neurons signal reward prediction errors. Instead, firing was modulated by other explanatory factors, such as licking, or showed no modulation during the task. Response types of midbrain dopamine neurons were not correlated with their anatomical location nor the selective or combinatorial expression of the markers Aldh1a1, Calbindin and Sox6.

In conclusion, the first set of experiments identified how different genetic burdens can alter the *in vivo* firing of midbrain dopamine neurons, and provide new insights into how circuits can change in pathological or compensatory ways at early disease stages in Parkinson's. The second set of experiments revealed striking heterogeneity of midbrain dopamine neurons in the intact system, and established further a functional diversity in the response types of identified midbrain dopamine neurons that is only partially consistent with canonical reward prediction error signalling.

Contents

List of Figures

List of Tables

List of Abbreviations

6-OHDA . . . 6-hydroxydopamine

AAV . . . . . Adeno-associated virus

ACH . . . . . Autocorrelation histogram

Aldh1a1 . . . . Aldehyde dehydrogenase 1 family member A1

AP . . . . . Anteroposterior

BAC . . . . . Bacterial artificial chromosome

C57Bl/6J . . . C57 black 6J

cKO . . . . . Conditional knock-out

CLi . . . . . Caudal linear nucleus

CreERT2 . . . Cre-enzyme fused to a mutated ligand-binding domain of the human estrogen receptor

CTB . . . . . Cholera toxin subunit b

CV2 . . . . . Coefficient of variation 2

D1 . . . . . Dopamine receptor 1a

D2 . . . . . Dopamine receptor 2

DA . . . . . Dopamine

DAT . . . . . Dopamine transporter

DDC . . . . . DOPA-decarboxylase

DLS . . . . . Dorsolateral striatum

DMS . . . . . Dorsomedial striatum

DOPA . . . . . Dihydroxyphenylalanine

DOPAC . . . . 3,4-Dihydroxyphenylacetic acid

DOPAL 3,4-Dihydroxyphenylacetaldehyde

DV . . . . . Dorsoventral

DRN . . . . . Dorsal raphe nucleus

DS . . . . . Dorsal striatum

ECoG . . . . . Electrocorticogram

eGFP . . . . . Enhanced green fluorescent protein

EMG . . . . . Electromyogram

En1/2 . . . . . Engrailed homeobox 1 and 2

EP . . . . . Entopeduncular nucleus

FACS . . . . . Fluorescence-activated cell sorting

FCV . . . . . Fast-scan cyclic voltammetry

Fgf8 . . . . . Fibroblast growth factor 8

FoxA1 . . . . . Forkhead box A1

FoxA2 . . . . . Forkhead box A2

FoxP2 . . . . . Forkhead box protein P2

GA . . . . . Gauge

GABA . . . . . γ-aminobutyric acid

GAD65 . . . . Glutamate decarboxylase 65

GAD67 . . . . Glutamate decarboxylase 67

GBA . . . . . Glucocerebrosidase

Girk2 . . . . . G protein-activated inward rectifier potassium channel 2

GLO . . . . . Gaussian locking to a free oscillator

GPe . . . . . External part of the globus pallidus

GPi . . . . . Internal part of the globus pallidus

HCN channel Hyperpolarization-activated cyclic nucleotide–gated channel

IF . . . . . Interfascicular nucleus

iPSC . . . . . Induced pluripotent stem cells

ISI . . . . . Inter-spike interval

ITI . . . . . Inter-trial interval

K-ATP channel ATP-sensitive potassium channel

KCNJ6 . . . . Potassium voltage-gated channel subfamily J member 6

KI . . . . . Knock-in

KO . . . . . Knock-out

LCM . . . . . Laser-captured microdissection

LDT . . . . . Laterodorsal tegmental nucleus

LED . . . . . Light-emitting diode

Lm . . . . . Lumen

Lmx1a . . . . . LIM homeobox transcription factor 1 alpha

Lmx1b . . . . . LIM homeobox transcription factor 1 beta

LRRK2 . . . . Leucine-rich repeat kinase 2

MFB . . . . . Medial forebrain bundle

mPFC . . . . . Medial prefrontal cortex

ML . . . . . Mediolateral

MPTP 1-methyl-4-phenyl-1,2,3,6-tetrahydropyridine

MSN . . . . . Medium-sized densely spiny neuron

NAc . . . . . Nucleus accumbens

NeuroD6 . . . Neurogenic differentiation factor-6

Nkx2.1 . . . . NK2 Homeobox 1

NMDA . . . . N-methyl-d-aspartate

Nurr1 . . . . . Nuclear receptor related 1 protein

OPDC . . . . . Oxford Parkinson's Disease Centre

Otx2 . . . . . Orthodenticle homeobox 2

PARK2 . . . . Parkinson protein 2, E3 ubiquitin protein ligase (Parkin)

PBP . . . . . Parabrachial pigmented nucleus

PBS . . . . . Phosphate-buffered saline

PETH . . . . . Peri-event time histogram

PFA . . . . . 4% w/v paraformaldehyde in 0.1 M phosphate buffer, pH 7.4

PFC . . . . . Prefrontal cortex

PIF . . . . . Parainterfascicular nucleus

PINK1 . . . . PTEN-induced putative kinase 1

Pitx3 . . . . . Pituitary homeobox 3

PN . . . . . Paranigral nucleus

PPN . . . . . Pedunculopontine nucleus

PS . . . . . Poisson surprise

RGS . . . . . Robust gaussian surprise

RLi . . . . . Rostral linear nucleus

RPE . . . . . Reward prediction error

RRF . . . . . Retrorubral field

RS . . . . . Rank surprise

SatB1 . . . . . Special AT-rich sequence binding protein 1

Shh . . . . . Sonic hedgehog

SK channel . . Calcium-activated small-conductance potassium channel

Slc6a3 . . . . . Solute carrier family 6 member 3

SNc . . . . . Substantia nigra pars compacta

SNCA . . . . . α-synuclein

SNl . . . . . Substantia nigra pars lateralis

SNr . . . . . Substantia nigra pars reticulata

Sox6 . . . . . Sex determining region Y box 6

SPN . . . . . Striatal projection neuron

STN . . . . . Subthalamic nucleus

SWA . . . . . Slow-wave activity

TD . . . . . Temporal difference

TH . . . . . Tyrosine hydroxylase

TS . . . . . Tail of the striatum

UPSIT . . . . University of Pennsylvania smell identification test

VTA . . . . . Ventral tegmental area

VTAR . . . . . Rostral ventral tegmental area

Wnt1 . . . . . Wingless-type MMTV integration site family, member 1

ZDHHC2 . . . Zinc finger DHHC-type containing 2

1

General introduction

Contents

1.1 A brief overview of the basal ganglia

Dopamine neurons located in the midbrain are part of the basal ganglia network. The basal ganglia comprise a distributed set of subcortical nuclei that are involved in various limbic and motor functions (Alexander, DeLong, et al. 1986; DeLong 1990). In the rodent brain, the basal ganglia subdivide into the dorsal and ventral striatum (including the nucleus accumbens), the ventral pallidum, the external part of the globus pallidus (GPe), the entopeduncular nucleus (EP; equivalent to the internal part of the globus pallidus in primates (GPi)), the subthalamic nucleus (STN), the ventral tegmental area (VTA), and the substantia nigra pars compacta (SNc) and pars reticulata (SNr). An introduction will be given for each of these nuclei, with a focus on the midbrain dopamine nuclei SNc and VTA.

1.1.1 The dorsal and ventral striatum

The striatum is considered the major input nucleus to the basal ganglia circuitry receiving excitatory inputs from cortex and thalamus (Bolam, Hanley, et al. 2000; Gerfen 1992; Smith and Bolam 1990a). In primates, the dorsal striatum is spatially divided by a white matter tract - the internal capsule - into caudate nucleus and putamen. In rodents, there is no equivalent division of the dorsal striatum. The idea of a division between dorsal and ventral striatum is based on their preferential inputs from allocortical regions (ventral striatum) versus neocortical regions (dorsal striatum) (Heimer and Wilson 1975) rather than a clear demarcation in cyto- or chemoarchitecture (Prensa, Richard, et al. 2003). In the frame of this concept, the ventral parts of caudate nucleus and putamen, the olfactory tubercule and the nucleus accumbens (NAc) form the ventral striatum (Prensa, Richard, et al. 2003). However, varying ways of dividing ventral from dorsal striatum have been proposed (Voorn, Vanderschuren, et al. 2004). The NAc itself separates into a core and shell region (often subdivided into medial shell and lateral shell). These subregions were defined based on the clustering of cells, the intensity of immunohistochemical staining for various markers (e.g. enkephalin, dopamine, opiate receptors or acetylcholinesterase), and afferent projection patterns

(Herkenham et al. 1984; Voorn, Gerfen, et al. 1989; Záborszky, Alheid, et al. 1985). The striatum is composed of various neuron types. The most prominent type of neuron in the striatum is the striatal projection neuron (SPN), also known as medium-sized densely spiny neuron (MSN), which accounts for more than 95 % of neurons in the striatum (Graveland et al. 1985; Kemp et al. 1971; Seite et al. 1977) and sends striatal outputs to other basal ganglia nuclei (Grofová 1975; Preston et al. 1980; Somogyi and Smith 1979). Striatal projection neurons use γ-aminobutyric acid (GABA) as their principal neurotransmitter and typically display low firing rates in recordings from animals at rest (DeLong 1973; Schultz and Romo 1988; Stern et al. 1997; Wilson and Groves 1981). The remaining striatal neurons consist of aspiny interneurons that utilise GABA or acetylcholine as a neurotransmitter (Bolam, Clarke, et al. 1983; Kita and Kitai 1988; Tepper, Tecuapetla, et al. 2010). Striatal projection neurons in dorsal striatum can be divided into two major populations based on their molecular and anatomical properties: They differ in projection target, with one group preferentially targeting the SNr and the EP (forming the striatonigral or so-called 'direct pathway'; see section 1.1.7) and the other group of SPNs targeting solely the GPe (forming the striatopallidal or so-called 'indirect pathway'; see section 1.1.7) (Chang et al. 1981; Grofová 1975; Kawaguchi et al. 1990; Preston et al. 1980; Somogyi and Smith 1979). The striatonigral SPNs express the neuropeptides Dynorphin and Substance P and the Acetylcholine muscarinic receptor 4, whereas striatopallidal SPNs are enriched in the neuropeptide Enkephalin, the Adenosine 2a receptor and G protein coupled receptor 6 (Bernard et al. 1992; Gerfen and Young 1988; Kanazawa et al. 1977; Lobo et al. 2007; Mroz et al. 1977; Penny et al. 1986; Schiffmann et al. 1991; Vincent et al. 1982). Further, the striatonigral SPNs show highly selective expression of the dopamine receptor 1a (D1), whereas striatopallidal SPNs show highly selective expression of the dopamine receptor 2 (D2) (Gerfen, Engber, et al. 1990; Le Moine, Normand, Guitteny, et al. 1990; Le Moine, Normand, and Bloch 1991). The differential expression of dopamine receptors in SPNs is crucial for the way in which dopamine is thought to shape striatal output (see section 1.1.7). However, it was found that such projection-specific expression of D1

and D2 receptors does not hold true for the ventral striatum, where both D1- and D2-SPNs contribute to direct and indirect pathways (Kupchik et al. 2015). The striatum is composed of two different compartments, termed patch (or striosome) and matrix, which form an interlaced labyrinth-like structure. Patch and matrix were identified by their different neurochemical composition, as well as distinct afferent and efferent patterns (Gerfen 1984; Gerfen, Baimbridge, et al. 1985; Gerfen 1992; Gerfen, Herkenham, et al. 1987; Graybiel et al. 1978; Olson, Seiger, et al. 1972). Many SPNs located in striatal patch compartments innervate dopamine neurons in the midbrain (Gerfen, Baimbridge, et al. 1985; Gerfen, Herkenham, et al. 1987; Watabe-Uchida et al. 2012).

1.1.2 The globus pallidus pars externa

The GPe is located medial to the caudal striatum and laterorostral to the internal capsule and is considered an integrative hub in basal ganglia circuitry (Mallet, Micklem, et al. 2012). It receives its major afferents from the striatum (GABAergic) and the STN (glutamatergic) and sends efferents to the STN, the thalamus, the SNr, the EP, the cortex and striatum (Beckstead 1983; Canteras et al. 1990; Carter and Fibiger 1978; Furuta et al. 2004; Grofová 1975; Ingham et al. 1988; Kincaid et al. 1991; Kita and Kitai 1987; Van Der Kooy et al. 1981; Smith and Bolam 1989; Staines et al. 1981), and projects within GPe forming a network of local collaterals (Kita and Kitai 1994; Sadek et al. 2007). The majority of GPe neurons are molecularly heterogeneous GABAergic projection neurons (Dodson, Larvin, et al. 2015; Hoover et al. 1999; Hoover et al. 2002; Kita 2007; Kita and Kita 2001; Kita and Kitai 1994; Smith, Parent, et al. 1987). In addition to the prototypic GPe neurons, a subpopulation of GPe neurons - termed arkypallidal neurons - projects back to the striatum (Beckstead 1983; Bevan et al. 1998; Hoover et al. 2002; Kita 2007; Mallet, Micklem, et al. 2012; Staines et al. 1981). The prototypic GPe neuron fires tonically at a high rate (∼20-40 spikes per second) both under urethane anaesthesia (Magill et al. 2000; Mallet, Pogosyan, et al. 2008) and in awake animals (Anderson and Turner 1991; DeLong 1971; Dodson, Larvin, et al.

2015; Sachdev et al. 1989), while the arkypallidal neuron fires more sporadically at rest (Dodson, Larvin, et al. 2015; Mallet, Pogosyan, et al. 2008; Mallet, Micklem, et al. 2012). In addition to striatal and subthalamic input, the GPe was also shown to receive input from midbrain dopamine neurons, most of them being collaterals of striatum-projecting dopamine neurons (Gauthier et al. 1999; Jan et al. 2000; Lindvall and Björklund 1979; Matsuda et al. 2009; Prensa and Parent 2001), and to express moderate levels of dopamine receptors (Yung et al. 1995).

1.1.3 The subthalamic nucleus

The STN is a small basal ganglia nucleus bordered dorsally by the zona incerta and ventrally by the cerebral peduncle (Paxinos and Watson 2007; Paxinos and Franklin 2013). Like the striatum, the STN is considered an input structure to the basal ganglia (Nambu, Tokuno, and Takada 2002) and receives afferents mainly from the GPe (GABAergic), the thalamus (glutamatergic) (Lanciego et al. 2004; Sugimoto et al. 1983) and the cortex (glutamatergic) (Monakow et al. 1978; Nambu, Takada, et al. 1996; Takada et al. 2001). The so-called 'hyperdirect pathway' is a parallel path of information flow from cortex through the basal ganglia alongside the direct striatonigral and indirect striatopallidal pathway (see section 1.1.7) (Nambu, Tokuno, Hamada, et al. 2000; Nambu, Tokuno, and Takada 2002). Additionally, there is evidence for midbrain dopamine input to the STN (Campbell et al. 1985; Hassani et al. 1997; Hedreen 1999; Lavoie, Smith, et al. 1989; Meibach et al. 1979). The STN contains glutamatergic projection neurons sending efferents mostly to the GPe, EP and SNr (Smith and Parent 1988). STN neurons fire spontaneously *in vivo* at rates of ∼10-20 spikes per second and with a firing pattern that is strongly influenced by cortical activity (Magill et al. 2000; Magill et al. 2001).

1.1.4 The output nuclei of the basal ganglia: entopeduncular nucleus and substantia nigra pars reticulata

While striatum and STN are considered input nuclei, EP and SNr form the output nuclei of the basal ganglia. The SNr is located ventral to the SNc and comprises

predominantly GABAergic projection neurons (Gulley et al. 1999; Oertel et al. 1984; Paxinos and Franklin 2013; Sanderson et al. 1986). A small number of dopamine neurons are scattered throughout the SNr (González-Hernández and Rodríguez 2000). In addition to the glutamatergic input from STN, a major inhibitory input to GABAergic SNr neurons arises from striatal SPNs (Bolam, Hanley, et al. 2000; Chevalier et al. 1985; Deniau, Feger, et al. 1976; Parent et al. 1995), which is the connection that constitutes part of the direct pathway in the classic basal ganglia model (Albin et al. 1989; DeLong 1990) (see section 1.1.7). Additionally, the GPe provides inhibitory inputs to the SNr (Smith and Bolam 1990a; Smith and Bolam 1989; Smith and Bolam 1990b) which complements the direct striatum-SNr/EP pathway with the indirect striatum-GPe-STN-SNr/EP pathway (see section 1.1.7). SPNs can thus exert dual modulation of SNr and EP neurons: Inhibitory modulation through direct SNr/EP innervation and excitatory modulation through the GPe and STN relay (Smith, Bevan, et al. 1998). Furthermore, dendritic release of dopamine establishes modulation of SNr neurons by midbrain dopamine neurons (Björklund and Lindvall 1975; Ford et al. 2010; Geffen et al. 1976; Nieoullon et al. 1977). GABAergic SNr neurons target the superior colliculus, pedunculopontine nucleus (PPN) and the thalamus (Di Chiara, Porceddu, et al. 1979; Deniau, Mailly, et al. 2007; Herkenham 1979). Notably, SNr neurons are also equipped with a network of local axon collaterals (Mailly et al. 2003), enabling mutual inhibition as well as inhibition of nearby dopamine neurons (Celada et al. 1999; Deniau, Kitai, et al. 1982; Juraska et al. 1977; Paladini et al. 1999; Tepper, Martin, et al. 1995). EP is located rostral to STN and mediocaudal to GPe (Paxinos and Franklin 2013). It is mostly composed of GABAergic projection neurons (Oorschot 1996) and largely parallels the SNr in input and output structure (Adinolfi 1969; Bolam and Smith 1992; Moriizumi et al. 1987; Smith, Bevan, et al. 1998). GPi neurons recorded in non-human primates were linked to movement control (Anderson and Turner 1991; Brotchie et al. 1991; Georgopoulos et al. 1983; Mink et al. 1991), while SNr neuron activity was correlated with oculomotor functions and non-motor concepts such as attention (Hikosaka et al. 1983c; Hikosaka et al. 1983a; Hikosaka et al.

1983b; Wichmann et al. 2004). A specific subset of lateral habenula-targeting glutamatergic EP-neurons in mice was recently linked to value-coding of rewarding or aversive events (Stephenson-Jones et al. 2016).

1.1.5 Substantia nigra pars compacta

The first detailed descriptions of the substantia nigra identified its two subdivisions based on Nissl-staining (Mingazzini 1888; Ramón y Cajal 1909): While the SNr (see section 1.1.4) is relatively sparse in cells, the SNc is formed of dense cell clusters (hence the Latin name "compacta") with perpendicular oriented dendrites penetrating the SNr. Dopamine-containing neurons in the midbrain were divided into the A8, A9 and A10 cell groups in the rat brain by Dalhström and Fuxe (1964). The "A" nomenclature was chosen for dopamine and noradrenaline, "B" for serotonin and "C" for adrenaline. Numbers were allocated based on caudal to rostral location of cell groups (see Figure 1.1A-B). This nomenclature was introduced because cell groups immunoreactive for monoamines extended beyond defined anatomical borders (Bentivoglio et al. 2005). However, the A8 group of dopamine neurons co-locates largely with the retrorubral field (RRF), the A9 group with the SNc and the A10 group with the VTA.

Numbers of SNc dopamine neurons in the mouse lie in the range of 4,000 – 7,000 per hemisphere (Nelson et al. 1996; Záborszky and Vadasz 2001). In the rat brain, each hemisphere contains around 10,000 – 13,000 SNc dopamine neurons (German and Manaye 1993; Hardman et al. 2002; Nair-Roberts et al. 2008) and in the human brain, numbers are considerably higher with estimates of 400,000 SNc dopamine neurons per hemisphere (Hardman et al. 2002; McGeer et al. 1977). But the SNc is not exclusively composed of dopamine neurons, it also contains GABAergic neurons which were estimated to account for around 30% of SNc neurons in the rat brain (González-Hernández and Rodríguez 2000; Hardman et al. 2002; Nair-Roberts et al. 2008). However, these numbers are highly dependent on the delineation of nuclei and might represent overestimates due to the inclusion of GABAergic SNr neurons. It is further important to note that neurotransmitter-identity of

neurons (also in the above listed cell counting literature) is largely determined indirectly based on the expression of proteins historically known to be involved in the synthesis or vesicular packaging of the respective neurotransmitter. With respect to GABAergic neurons, this is often the expression of glutamate decarboxylase (GAD65 or GAD67). However, it has been shown that midbrain dopamine neurons themselves can co-release GABA (Tritsch, Ding, et al. 2012) either following GABA uptake from extracellular space (Tritsch, Oh, et al. 2014) or *de novo* synthesis of GABA independent of GAD65 or GAD67 involving the aldehyde dehydrogenase Aldh1a1 (for more details on Aldh1a1 see sections 1.2.2 and 5.1) (Kim, Ganesan, et al. 2015). This and other findings of neurotransmitter co-release (reviewed in e.g. Morales et al. 2017; Tritsch, Granger, et al. 2016) exemplify that neurotransmitter-based cell type definition does not have to be as definite as often communicated.

Inputs. Striatal SPNs provide the major GABAergic input to SNc dopamine neurons (Bolam and Smith 1990; Grofová and Rinvik 1970; Somogyi, Bolam, et al. 1981; Watabe-Uchida et al. 2012). More specifically, SNc dopamine neurons are innervated by SPNs mostly located in the striatal patch compartment (Gerfen, Baimbridge, et al. 1985; Gerfen, Herkenham, et al. 1987; Watabe-Uchida et al. 2012). Further GABAergic innervation to SNc dopamine neurons is provided by SNr and GPe (Hajós et al. 1994; Mailly et al. 2003; Nitsch et al. 1988; Smith and Bolam 1990b; Watabe-Uchida et al. 2012) with their electrical stimulation leading to inhibition of dopamine neurons (Paladini et al. 1999). Glutamatergic innervation of SNc dopamine neurons arises from the STN (Chergui, Akaoka, et al. 1994; Hammond et al. 1978; Kita and Kitai 1987; Shimo et al. 2009), diverse cortical areas (Carter 1982; Chiba et al. 2001; Usunoff et al. 1982; Watabe-Uchida et al. 2012), and the PPN (Charara et al. 1996; Futami et al. 1995; Tokuno et al. 1988). In addition to the glutamatergic innervation, SNc dopamine neurons receive cholinergic inputs, mainly from the PPN (Beninato et al. 1987; Beninato et al. 1988; Clarke et al. 1987; Futami et al. 1995; Gould et al. 1989). Additionally, SNc dopamine neurons are targeted by serotonergic neurons in the dorsal raphe nucleus (DRN) (Gervais et al. 2000; Nedergaard et al. 1988; Vertes 1991; Watabe-Uchida et al. 2012) and by

glutamatergic projections from the superior colliculus (Comoli et al. 2003; Watabe-Uchida et al. 2012). Besides these main inputs, the central nucleus of the amygdala, hypothalamic areas and the zona incerta also provide some projections to SNc dopamine neurons (Watabe-Uchida et al. 2012).

Outputs. The input-output pattern of SNc dopamine neurons is characterized by a high level of reciprocality: Many regions providing afferents, receive SNc dopamine efferents in return. The most extensive output (both in terms of neuron numbers projecting as well as in synaptic contacts) targets the dorsal striatum (Fallon, Koziell, et al. 1978; Van Der Kooy et al. 1981; Lindvall, Björklund, et al. 1974; Mattiace et al. 1989). The number of synapses formed by one SNc dopamine neuron in the rat dorsal striatum is estimated to be around 100,000 – 250,000 (Bolam and Pissadaki 2012). To put this number into perspective: Estimated from varicosity counts, a single SPN forms a few hundred synapses (Bolam and Moss 2010; Kawaguchi et al. 1990). In addition to the dorsal striatum, SNc dopamine neurons also project to STN, GPe, EP, amygdala and cortical regions (Campbell et al. 1985; Fallon, Koziell, et al. 1978; Francois et al. 2000; Fuxe et al. 1974; Gauthier et al. 1999; Hassani et al. 1997; Jan et al. 2000; Lindvall and Björklund 1979; Lindvall, Björklund, et al. 1974; Loughlin et al. 1983; Matsuda et al. 2009; Thierry et al. 1973). While SNc dopamine neurons do not give rise to local dopamine axon collaterals (Juraska et al. 1977; Wassef et al. 1981), they show somatodendritic dopamine release (Björklund and Lindvall 1975; Cheramy et al. 1981; Cragg et al. 1997; Geffen et al. 1976; Häusser et al. 1995; Nieoullon et al. 1977), giving them the ability to act locally on SNc and SNr neurons. While this Chapter describes the input- and output-pattern of SNc and VTA dopamine neurons separately, it is important to highlight that the delineation between these two nuclei is somewhat arbitrary with respect to projection patterns since they form more of an intermingled continuum, i.e. while the majority of neurons projecting to the NAc lie within the VTA, this region also contains neurons that project to the dorsal striatum (DS) and vice versa (see Figure 1.1C) (Bentivoglio et al. 2005; Fallon and Loughlin 1995; Gerfen 2004; Vogt Weisenhorn et al. 2016).

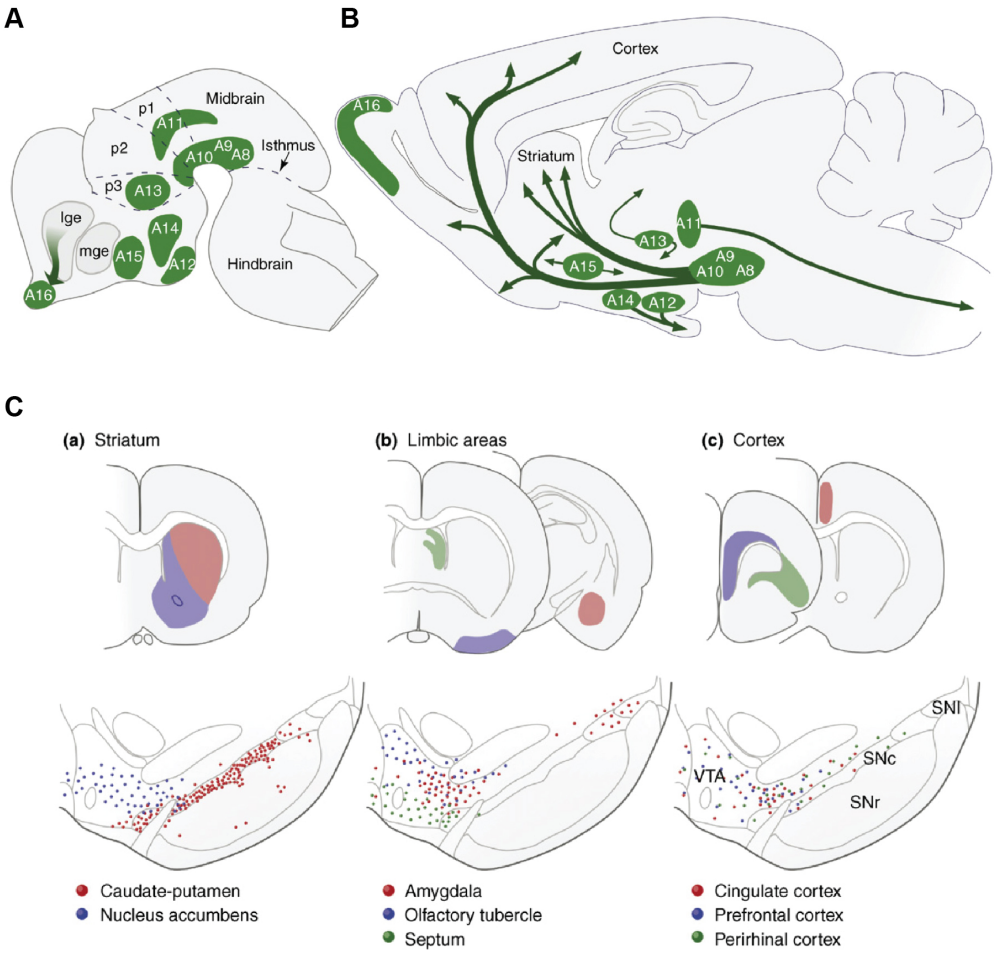

Figure 1.1: Dopamine neurons in the rodent brain (reproduced from Björklund and Dunnett 2007). (A-B) Distribution of dopamine neuron groups in the developing (A) and adult (B) rodent brain in parasagittal view (rostral to the left). Dopamine neurons are divided into 9 distinct cell groups (A8 – A16; A8 – A10 form the midbrain dopamine nuclei) from caudal to rostral. (C) Locations of dopamine neurons projecting to (a) striatal, (b) limbic and (c) cortical regions form an intermingled continuum. Bottom schematics show coronal midbrain sections with the location of dopamine neurons (circles) colour-coded by projection target. Top schematics show a coronal view of the innervated area. lge, lateral ganglionic eminence; mge, medial ganglionic eminence; p1 – p3, prosomeres 1-3; SNc, substantia nigra pars compacta; SNl, substantia nigra pars lateralis; SNr, substantia nigra pars reticulata; VTA, ventral tegmental area.

1.1.6 Ventral tegmental area

The VTA was originally described as a circumscribed nucleus in the opossum and named nucleus tegmenti ventralis (Tsai 1925). The dopamine cell group A10 co-locates largely with the VTA. Cytoarchitecturally, A10 dopamine neurons have been divided into different clusters, e.g. the paranigral nucleus (PN), interfascicular

nucleus (IF), parainterfascicular nucleus (PIF), parabrachial pigmented nucleus (PBP), caudal linear nucleus (CLi), rostral linear nucleus (RLi) and rostral ventral tegmental area (VTAR) (Fu et al. 2012; Halliday et al. 1986; Oades et al. 1987; Swanson 1982) but are commonly summarised with the collective term VTA. In mice and rats, SNc and VTA contain similar numbers of dopamine neurons with 10,000 – 15,000 VTA dopamine neurons per hemisphere in mice (Nelson et al. 1996) and 10,000 – 20,000 VTA dopamine neurons per hemisphere in rats (German and Manaye 1993; Nair-Roberts et al. 2008). The ratio is shifted towards SNc dopamine neurons in humans with roughly 60,000 – 150,000 VTA dopamine neurons – only around 25% of the total number of midbrain dopamine neurons (Bentivoglio et al. 2005; Brichta and Greengard 2014). Like the SNc, the VTA is not exclusively composed of dopamine neurons but also contains glutamatergic (Kawano et al. 2006; Yamaguchi et al. 2007) and GABAergic (Van Bockstaele and Pickel 1995; Carr et al. 2000a) neurons accounting for 20 – 30 % of neurons in the VTA (Olson and Nestler 2007). Additionally, some neurons in the VTA are capable of neurotransmitter co-release (reviewed in Barker et al. 2016).

Inputs. Inhibitory inputs onto VTA dopamine neurons arise from SPNs located in the NAc – also forming patches of projecting neurons similar to the SNc-projecting SPNs in the dorsal striatum (Watabe-Uchida et al. 2012) – and local GABAergic neurons within VTA (Beier et al. 2015; Johnson and North 1992; Kalivas et al. 1993; Ogawa et al. 2014; Watabe-Uchida et al. 2012). Besides input from GABAergic VTA neurons, VTA dopamine neurons are also innervated by local glutamatergic neurons (Dobi et al. 2010). Other inputs onto VTA dopamine neurons originate in PPN, laterodorsal tegmental nucleus (LDT), amygdala, lateral hypothalamus, DRN and cortex (Beier et al. 2015; Van Bockstaele, Cestari, et al. 1994; Charara et al. 1996; Fadel et al. 2002; Mena-Segovia et al. 2008; Ogawa et al. 2014; Omelchenko et al. 2005; Omelchenko et al. 2006; Phillipson 1979; Sesack et al. 1992; Vertes 1991; Watabe-Uchida et al. 2012). Generally, when grossly divided into SNc and VTA dopamine neurons, input regions targeting dopamine neurons are remarkably similar for SNc and VTA, mostly just differing in number and density (e.g. VTA

dopamine neurons receive more input from DRN and lateral hypothalamus; Ogawa et al. 2014; Watabe-Uchida et al. 2012). However, there is often a mediolateral topography in the inputs to midbrain dopamine neurons (Ikemoto 2007; Yetnikoff et al. 2014).

Outputs. As for SNc dopamine neurons, VTA dopamine neurons largely project to brain regions that innervate the VTA in return. The main target of VTA dopamine neurons is the ventral striatum, including NAc core, NAc shell and olfactory tubercule (Fallon and Moore 1978a; Ikemoto 2007; Swanson 1982). It was estimated that VTA dopamine neurons projecting to the ventral striatum form considerably fewer synaptic contacts than SNc dopamine neurons projecting to the dorsal striatum with 12,000 – 30,000 synapses per VTA-projecting dopamine neuron in the rat brain (Bolam and Moss 2010; Bolam and Pissadaki 2012). Other regions innervated by VTA dopamine neurons include lateral septum, cortical areas (e.g. medial prefrontal cortex (mPFC)), amygdala, hippocampus, and cerebellum (Beckstead, Domesick, et al. 1979; Fallon and Loughlin 1995; Fallon, Koziell, et al. 1978; Fallon and Moore 1978a; Ikai et al. 1994; Oades et al. 1987; Swanson 1982).

1.1.7 A working model of the functional organization of basal ganglia

Given the extensive data collected on structure and function of the basal ganglia nuclei over two decades, Albin and colleagues (1989) suggested a synthesized model of the basal ganglia accounting both for the healthy as well as the diseased system. The model incorporates the idea of parallel processing of cortical information by the basal ganglia through a direct striatonigral and an indirect striatopallidal pathway and built the basis for refined models of the basal ganglia ever since (Alexander and Crutcher 1990; Chesselet 1996; DeLong 1990; Smith, Bevan, et al. 1998). According to this model, cortical information is funneled through the striatum to the basal ganglia output nuclei GPi/EP and SNr directly or indirectly relayed via GPe and STN (Figure 1.2). These two pathways have functionally opposing effects on the target regions in the thalamus and the brain stem (Alexander

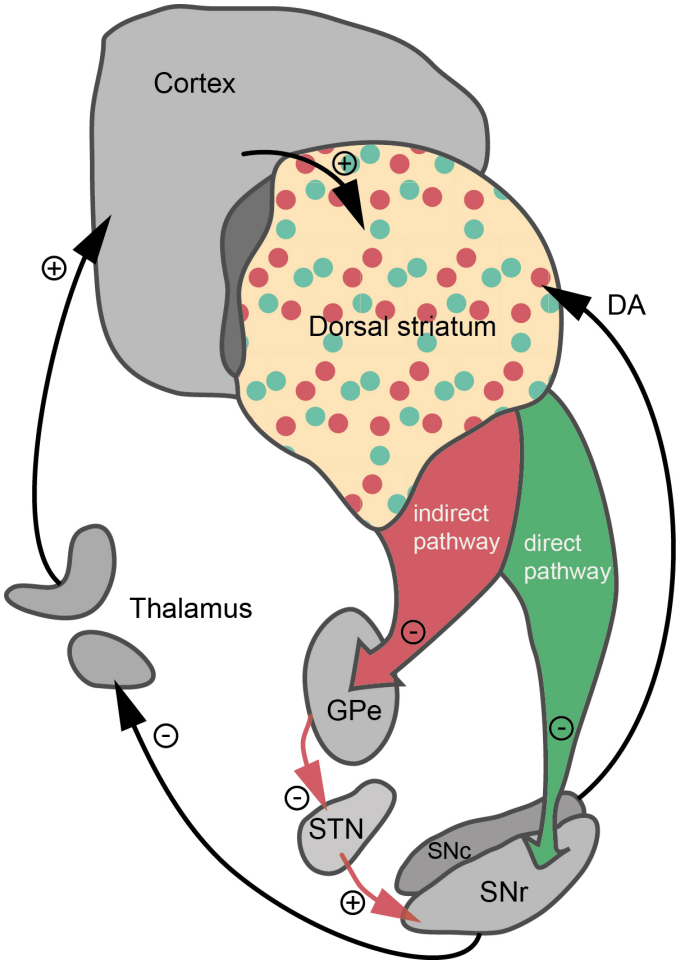

Figure 1.2: Concept of direct and indirect pathways in the basal ganglia network. The direct pathway (green) conveys cortical information through D1-SPNs (green circles) in the striatum directly to basal ganglia output nuclei (EP and SNr; only SNr depicted). The indirect pathway (red) conveys cortical information through D2-SPNs (red circles) in the striatum via GPe and STN to basal ganglia output nuclei. The network is modulated by dopamine (DA) from SNc dopamine neurons. EP and SNr output to the thalamus which innervates the cortex. ⊕ excitatory; ⊖ inhibitory. Adapted from Gerfen (1992). SNr, substantia nigra pars reticulata; GPe, globus pallidus pars externa; STN, subthalamic nucleus.

and Crutcher 1990): Increased activity along the direct pathway is proposed to disinhibit, while increased activity along the indirect pathway is proposed to inhibit neurons in the target regions. At the level of the striatum, signaling of direct and indirect pathway SPNs is differentially modulated by dopamine which "inhibits" D2-expressing indirect pathway SPNs but "excites" D1-expressing direct pathway SPNs by gating and trafficking ion channels, which alter SPNs' response to glutamatergic inputs (Alexander and Crutcher 1990; Surmeier et al. 2007). While the direct and

indirect pathway model of the basal ganglia has proven heuristically useful, it is an oversimplification at the same time, leaving many anatomical and other findings aside. An example is the direct cortical input to the STN which bypasses the striatum and was hence termed hyperdirect pathway (Nambu, Tokuno, Hamada, et al. 2000; Nambu, Tokuno, and Takada 2002). Furthermore, it was found that while the gross separation of indirect and direct pathway SPNs holds true, some SPNs express both D1 and D2 receptors (Aizman et al. 2000), some SPNs project along both pathways, direct and indirect (Lévesque et al. 2005), and stimulation of direct and indirect pathway SPNs both excites and inhibits firing of subpopulations of SNr neurons (Freeze et al. 2013). Additionally, GPe is not just recipient of striatal projections but also projects back to the striatum (Kita 2007; Kita and Kita 2001; Mallet, Micklem, et al. 2012), the thalamus itself projects directly to the striatum (Doig et al. 2010; Macchi and Bentivoglio 1986; Macchi, Bentivoglio, et al. 1984; McFarland et al. 2000; Powell et al. 1956) and midbrain dopamine neurons receive SPN input and innervate other basal ganglia nuclei in addition to the striatum (see section 1.1.5). Additionally, a direct projection from midbrain dopamine neurons to the thalamus was described in primates (García-Cabezas, Martínez-Sánchez, et al. 2009; García-Cabezas, Rico, et al. 2007; Sánchez-González et al. 2005). Further, while some of the organisational principles laid out hold true for the ventral striatum, they were shown to be less prominent than in the dorsal striatum (Kupchik et al. 2015; Smith, Lobo, et al. 2013). Functional implications for many of these potential complications remain to be investigated.

1.2 Segregation of midbrain dopamine neurons

Midbrain dopamine neurons were originally classified as one ‘cell type’ based on their shared neurotransmitter identity (Carlsson et al. 1962; Dahlström et al. 1964; Ehringer et al. 1960). However, a range of other characteristics might be used to separate midbrain dopamine neurons into subtypes. Such characteristics can include their anatomical location in VTA or SNc, developmental origin, precise molecular makeup (besides their shared expression of enzymes required for dopamine synthesis,

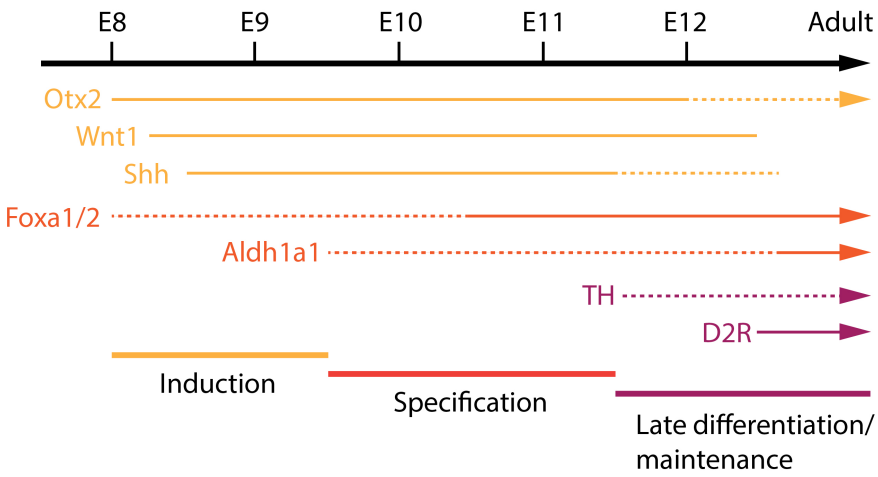

Figure 1.3: Simplified time scale of molecular marker expression in midbrain dopamine neurons during development in the mouse brain. Black bar on top depicts time interval (e.g. E8, embryonic day 8). Coloured thin lines depict expression onset and offset for individual molecular markers (only a selection shown). Solid bars indicate a requirement of the respective marker during time period; dashed lines indicate that a respective marker is not required for dopamine neuron development during time period. Arrowheads indicate maintained expression in the adult system. Not all markers are expressed in all mature midbrain dopamine neurons. Thick bars at bottom show three approximate developmental phases of midbrain dopamine neurons. Shh, sonic hedgehog; Wnt1, wingless-type MMTV integration site family, member 1; Otx2, orthodenticle homeobox 2; Foxa1/2, Forkhead box A1/2; Aldh1a1, aldehyde dehydrogenase 1 family member A1; TH, tyrosine hydroxylase; D2R, dopamine receptor 2. Adapted from Wurst and Prakash (2010).

tyrosine hydroxylase and DOPA-decarboxylase), input and output patterns, or different behavioural correlates of their activity. This section will focus on the anatomical and molecular characteristics.

1.2.1 Midbrain dopamine neurons in development

In brain development, 'organising centres' serve to signal instructions to their surroundings and pattern neural tissue into brain regions in a temporally and spatially specific manner (Rhinn et al. 2001). In the mouse, the ventral midbrain is induced around embryonic day 8 (E8), marking the beginning of midbrain dopamine neuron development (Di Porzio et al. 1990). Essential for this induction is combined signalling of the glycoprotein sonic hedgehog (Shh), wingless-type MMTV integration site family, member 1 (Wnt1) and the fibroblast growth factor 8 (Fgf8) (Hynes, Porter, et al. 1995; Hynes, Poulsen, et al. 1995; Prakash et al. 2006; Roussa et al.

2004; Zervas et al. 2004). Midbrain dopamine neurons are derived from radial glia-like progenitors located in a domain in the ventral midline, the floor plate (Bonilla et al. 2008; Hynes and Rosenthal 1999; Ono et al. 2007). While the floor plate defines the dorso-ventral origin of midbrain dopamine neurons, the precise site along the anterio-posterior axis is still debated (Blaess et al. 2015; Wurst et al. 2010) and some studies suggest that SNc dopamine neurons originate in the caudal diencephalon, while only VTA dopamine progenitors migrate from the mesencephalon (Jacobs et al. 2007; Maxwell et al. 2005; Smits, Burbach, et al. 2006; Smits, Oerthel, et al. 2013). However, the collective term 'midbrain dopamine neurons' will be used in this report to refer to the A8, A9 and A10 cell clusters of dopamine neurons, irrespective of their developmental origin. Following the establishment of the floor plate, other molecular regulators (often transcription factors) ensure the specification / early differentiation of migratory midbrain dopamine neurons (Ang 2009). These regulators include the LIM homeobox transcription factor 1 alpha and beta (Lmx1a/b) (Andersson et al. 2006; Burbach et al. 2000; Guo et al. 2007), the transcription factor Orthodenticle homeobox 2 (Otx2) (Acampora et al. 1997; Omodei et al. 2008; Puelles et al. 2004), the Engrailed homeobox 1 and 2 (En1/2) (Simon, Saueressig, et al. 2001; Simon, Bhatt, et al. 2003) and/or the Forkhead/winged helix transcription factors Foxa1 and Foxa2 (Mavromatakis et al. 2011; Metzakopian et al. 2012). Notably, while some developmental factors cease to be expressed in mature midbrain dopamine neurons, the above listed transcription factors are examples of regulators that retain expression throughout late differentiation and maintenance of all or just some midbrain dopamine neurons (see Figure 1.3) (reviewed in Blaess et al. 2015; Bodea et al. 2015; Smidt and Burbach 2007; Wurst et al. 2010). While Poulin et al. (2014) describe molecularly defined subpopulations of midbrain dopamine neurons in adult mice, a recent study showed the presence of molecularly distinct subpopulations already at postnatal day 0 (La Manno et al. 2016). This highlights the establishment of molecular diversity in midbrain dopamine neurons early on in postnatal development.

1.2.2 Molecular diversity of mature midbrain dopamine neurons

If midbrain dopamine neurons do comprise different molecular subtypes, what might be the purpose of this diversity and why is it useful to unravel? One possibility is that molecular diversity might allow for distinct computation within neural circuits; an example are striatal SPNs whose differential expression of dopamine receptors results in their opposing modulation by dopamine (Alexander and Crutcher 1990; Surmeier et al. 2007). In a similar way, unique transcriptional codes in midbrain dopamine neurons might account for differential neural circuit integration and functional roles. Unraveling them could be used to gain genetic access to defined subtypes and target them specifically with the help of intersectional transgenic strategies (Cardozo Pinto et al. 2017; Luo et al. 2008; Madisen et al. 2015). Furthermore, revealing molecular subtypes of midbrain dopamine neurons is of particular interest, because only some of them are vulnerable in Parkinson's (Fearnley et al. 1991; Hirsch et al. 1988; Hirsch et al. 1989). Many studies have tried to correlate this differential vulnerability with selective protein expression. One example is the calcium-binding protein Calbindin, a molecule involved in the regulation of intracellular levels of calcium, which was shown to be expressed in midbrain dopamine neurons spared from degeneration in Parkinson's (German, Manaye, et al. 1992; Iacopino, Christakos, et al. 1992; Yamada et al. 1990). While such early reports could only focus on a few marker characteristics per study, more recent technology allows for larger-scale profiling. Identifying extensive barcodes of subtype identity, as revealed for other nervous tissue like the retina (Siegert et al. 2012), could help distinguish the selectively vulnerable dopamine neuron population based on combinatorial molecular characteristics. Laser-captured microdissection (LCM) combined with microarray analysis was used to perform comparative expression analysis of SNc and VTA dopamine neurons in rats and mice (Chung, Seo, et al. 2005; Greene, Dingledine, et al. 2005; Grimm et al. 2004). LCM allows for averaged expression analysis across captured neurons (tens to hundreds of cells; Poulin, Tasic, et al. 2016). These studies identified some transcriptional differences between SNc and VTA tissue

samples. For instance, while SNc neurons were enriched in transcripts linked to metabolism or cellular transport, VTA neurons were enriched in transcripts linked to axon guidance (Brichta and Greengard 2014; Chung, Seo, et al. 2005; Greene, Dingledine, et al. 2005). However, these studies are based on the premise that VTA and SNc dopamine neurons are homogeneous in their molecular makeup. Gene-expression profiling following fluorescent tagging of midbrain dopamine neurons and fluorescence-activated cell sorting (FACS) helped reveal molecular subtypes of midbrain dopamine neurons with single-cell resolution. Poulin et al. (2014) analysed the expression of 96 different genes in midbrain dopamine neurons in an anatomically unbiased way and identified six different clusters with principal component analysis. Each of these clusters was characterised by a distinct combinatorial expression of molecular markers, including Calbindin, Sex determining region Y box 6 (Sox6), and Aldehyde dehydrogenase 1 family member A1 (Aldh1a1) (Poulin, Zou, et al. 2014). This work was further extended by La Manno et al. (2016) who tracked subtype emergence across development. In embryonic mouse tissue, they identified two molecularly distinct groups but showed that full diversity emerged postnatally (postnatal day 7) (La Manno et al. 2016). While Poulin et al. (2014) correlated one of the defined subtypes to selective vulnerability in a neurotoxic Parkinson's model, a separate study using translatome and regulatory network analysis identified the transcriptional regulators Special AT-rich sequence binding protein 1 (SatB1) and Zinc finger DHHC-type containing 2 (ZDHHC2) as potential neurodegenerative factors in Parkinson's (Brichta, Shin, et al. 2015). However, while these studies concentrate on molecularly separated subtypes of midbrain dopamine neurons, they show few if any links to specific projection targets or electrophysiological characteristics of these subtypes. Projection target specificity was only shown for one molecularly defined subtype targeting the extended amygdala (Poulin, Zou, et al. 2014). A separate study profiled gene expression in NAc-projecting midbrain dopamine neurons using a technique called retroTRAP but did not compare it to gene expression of midbrain dopamine neurons targeting other regions in the brain (Ekstrand et al. 2014).

1.2.3 Inputs and outputs of midbrain dopamine neurons

As outlined in section 1.1.5 and 1.1.6, SNc and VTA dopamine neurons receive synaptic inputs from and send outputs to a diverse range of regions in the brain. A major input arises from dorsal and ventral striatum (Beier et al. 2015; Bolam and Smith 1990; Grofová and Rinvik 1970; Lerner et al. 2015; Somogyi, Bolam, et al. 1981; Watabe-Uchida et al. 2012). Striatal neurons projecting to dopamine neurons in the midbrain are not homogeneously distributed but form patches of neurons both in dorsal and ventral striatum (Gerfen, Baimbridge, et al. 1985; Gerfen, Herkenham, et al. 1987; Watabe-Uchida et al. 2012). Additionally, striatal inputs to midbrain dopamine neurons are arranged in a topographical manner in medio-lateral, anterio-posterior and inverted dorso-ventral orientation (Fallon, Koziell, et al. 1978; Fallon and Moore 1978a; Fallon, Riley, et al. 1978; Fallon and Moore 1978b; Haber 2014; Ikemoto 2007; Joel et al. 2000; Moore 1978). This topography is also preserved in the reciprocal projections from midbrain dopamine neurons to the striatum: Midbrain dopamine neurons receiving inputs from the lateral NAc send more outputs to the lateral NAc, midbrain dopamine neurons projecting to the dorso-medial striatum (DMS) receive more inputs from the DMS, and midbrain dopamine neurons projecting to the dorso-lateral striatum (DLS) also receive more inputs from the DLS (Beier et al. 2015; Lerner et al. 2015; Watabe-Uchida et al. 2012). Input-output dependencies were investigated using anterograde and retrograde tract-tracing combined with immunocytochemistry and electron microscopy in a triple-labeling design (Carr et al. 2000b) and more recently using whole-brain mapping of input-output relationships of genetically defined neural populations with rabies-virus based (Cre-dependent) monosynaptic tracing (Beier et al. 2015; Lerner et al. 2015; Menegas, Bergan, et al. 2015). Such whole-brain approaches allow for parallel comparison of multiple input and output regions. Beier et al. (2015) focused on VTA dopamine neurons and mapped inputs from 22 brain regions to midbrain dopamine neurons projecting to amygdala, mPFC, medial and lateral NAc. While gross input patterns were relatively similar, midbrain dopamine neurons projecting to the lateral part of the NAc received more total inputs from lateral NAc and NAc

core and fewer inputs from the dorsal raphe nucleus (Beier et al. 2015). Other input regions they included were cortical areas, ventral pallidum, amygdala, bed nucleus of the stria terminalis, GPe, hypothalamus, lateral habenula and zona incerta, largely confirming previously identified input regions to midbrain dopamine neurons (see section 1.1.5 and 1.1.6). Lerner et al. (2015) focused on DMS- and DLS-projecting midbrain dopamine neurons and 26 input regions showing that they only differed in the amount of inputs coming from the DMS and DLS (Lerner et al. 2015). Menegas et al. (2015) extended a similar experimental approach to midbrain dopamine neurons projecting to eight target regions, including the dorsal and ventral striatum, lateral habenula, GPe, orbitofrontal cortex, mPFC and amygdala. Additionally, they investigated inputs to midbrain dopamine neurons projecting to the posterior part of the striatum which was the only subset of midbrain dopamine neurons with distinctly different input pattern: They received more inputs from GPe, STN and zona incerta and less inputs from the shell region of the NAc and the hypothalamus (Menegas, Bergan, et al. 2015). However, these monosynaptic tracing studies only address the question of input regions of midbrain dopamine neurons but do not differentiate inputs based on other criteria such as their neurotransmitter identity. Thus, while midbrain dopamine neurons might all be innervated by similar brain regions, suborganisation of such innervation might differ.

1.3 Functional heterogeneity of midbrain dopamine neurons

Electical activity of midbrain dopamine neurons is subject of extensive investigation and has been studied *in vitro* and *in vivo* both in anaesthetised and awake animals. This section will give a brief overview of midbrain dopamine neuron firing *ex vivo* and *in vivo* and introduce the behavioural concepts this activity was correlated with.

1.3.1 Firing properties of midbrain dopamine neurons

In vivo, extracellularly recorded midbrain dopamine neurons are characterised by broad action potentials of multiphasic shape and a firing rate of typically below

10 spikes per second (Aebischer et al. 1984; Brown et al. 2009; Janezic et al. 2013; Schultz 1986; Ungless 2004). They show diverse firing patterns including regular (pacemaker) and burst firing as extremes (see Figure 1.4) (Grace and Bunney 1984b; Grace and Bunney 1984a). Burst firing is thought of as a mechanism for supra-linear dopamine release in target regions; burst-like electrical stimulation patterns of medial forebrain bundle or the midbrain increase dopamine levels more effectively than single stimulations (Ammari et al. 2009; Chergui, Suaud-Chagny, et al. 1994; Cragg 2003; Gonon 1997; Gonon 1988; Nissbrandt et al. 1994; Overton et al. 1997; Suaud-Chagny, Chergui, et al. 1992; Suaud-Chagny, Brun, et al. 1992). Grace and Bunney's definition of a burst was based on cut-off criteria for the length of inter-spike intervals (ISI) and defined as a group of three or more action potentials whose first ISI is shorter than 80 ms and last ISI longer than 160 ms, often accompanied by a decrease in spike height (Grace and Bunney 1984a). Since these criteria are somewhat arbitrary and only applicable to dopamine neurons with a narrow firing frequency band, more quantitative and objective detection methods have been developed, including Poisson surprise (PS), Gaussian locking to a free oscillator (GLO), Rank surprise (RS) and Robust gaussian surprise (RGS) methods (Bingmer et al. 2011; Gourévitch et al. 2007; Ko et al. 2012; Legéndy et al. 1985). Burst firing is present both in awake and anaesthetised state, but can be affected by the anaesthetic or brain state (Brown et al. 2009; Kelland et al. 1990; Walczak et al. 2017). For instance, reduced burst-occurrence in midbrain dopamine neurons was shown in rats under urethane anaesthesia (Kelland et al. 1990). Firing regularity and burst firing of midbrain dopamine neurons was shown to depend on cortically measured brain state activity, with an activated brain state resulting in more regular firing patterns (Brown et al. 2009; Walczak et al. 2017). *In vivo* bursting was shown to be regulated through N-methyl-d-aspartate (NMDA) glutamate receptors with glutamatergic inputs arriving from the STN, PPN and LDT (Chergui, Akaoka, et al. 1994; Floresco et al. 2003; Lodge et al. 2006b; Lokwan et al. 1999; Overton et al. 1992; Suaud-Chagny, Chergui, et al. 1992; Zweifel et al. 2009). Further, calcium and potassium (e.g. calcium-activated small-conductance potassium (SK)) channels

are intrinsic modulators of firing pattern and burst firing (Grace and Bunney 1984a; Ji et al. 2006; Waroux et al. 2005; Wolfart, Neuhoff, et al. 2001).

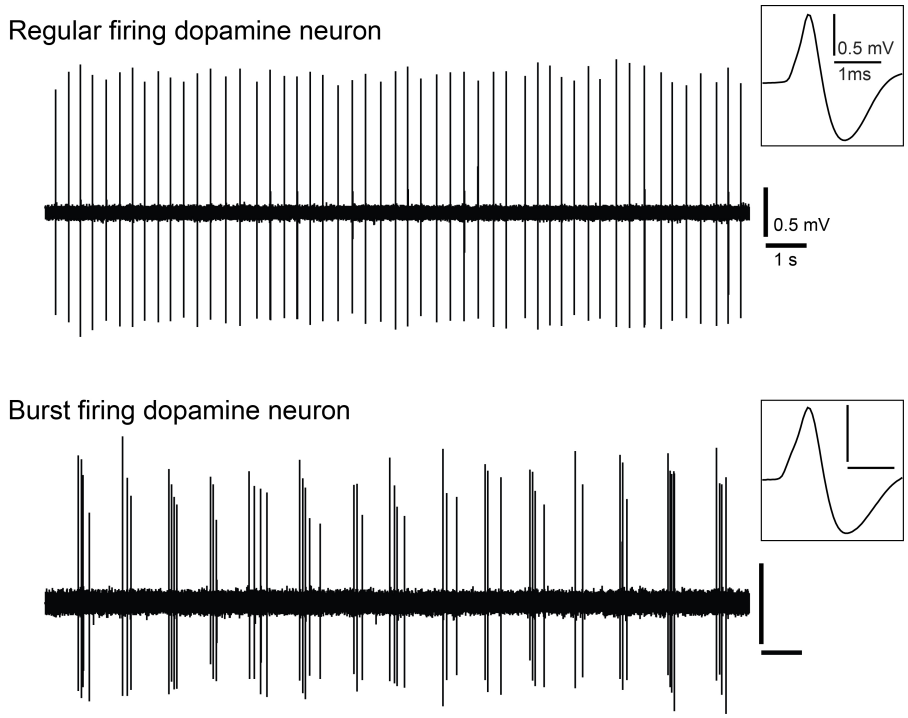

Figure 1.4: Firing modes of midbrain dopamine neurons. Extracellular *in vivo* recording of 'regular firing' (top) and 'burst firing' (bottom) midbrain dopamine neurons recorded in anaesthetised rats. Insets: Average waveforms of the extracellularly-recorded action potentials shown on the left.

Ion channels contributing to the characteristic firing patterns of midbrain dopamine neurons were revealed through *in vitro* slice recordings. In slice preparations, midbrain dopamine neurons fire spontaneously with a regular low-frequency pattern, often described as pacemaker-firing (Grace and Onn 1989; Kita, Kita, and Kitai 1986). Such activity has been recorded with both sharp microelectrodes as well as patch-clamp techniques and was shown to be independent of synaptic inputs (Grace and Onn 1989; Silva et al. 1990). Individual action potentials *in vitro* are characterised by broad action potential shape, elicited at relatively depolarised thresholds and with a prominent after-hyperpolarisation (Grace and Onn 1989; Kita, Kita, and Kitai 1986; Silva et al. 1990). Action potentials in midbrain dopamine neurons are initiated at the axon initial segment but also backpropagate

along dendrites (Häusser et al. 1995). A range of ion channels contribute to pacemaker-activity in midbrain dopamine neurons (reviewed in Liss and Roeper 2010), but calcium channel-driven autonomous oscillations in membrane potential are particularly important (Chan et al. 2007; Puopolo et al. 2007). However, in some midbrain dopamine neurons, located mainly in the VTA, pacemaker activity is dependent on sodium and hyperpolarisation-activated cyclic nucleotide-gated cation (HCN) channels (Chan et al. 2007; Puopolo et al. 2007). Notably, midbrain dopamine neurons can further regulate their firing through D2-receptor mediated autoinhibition (Groves et al. 1975).

1.3.2 Midbrain dopamine neurons and perceptual salience

Salience can be defined as the quality of being particularly noticeable or important. Some of the earliest work measuring firing of midbrain dopamine neurons showed modulation of their electrical activity by perceptually salient but neutral sensory stimuli, such as light flashes or sounds (Chiodo, Caggiula, et al. 1979; Chiodo, Antelman, et al. 1980; Fiorillo et al. 2013; Horvitz et al. 1997; Schultz and Romo 1990; Steinfels et al. 1983a; Steinfels et al. 1983b; Strecker et al. 1985). These stimuli were categorised as perceptually or physically salient because they are noticeable but considered neutral since they should not carry value information (i.e. they have not been associated with a rewarding or punishing event) (Schultz 2007a). Modulation of the firing of midbrain dopamine neurons can be bidirectional, reflected in firing increase or decrease (compared to a window of baseline firing). Midbrain dopamine neurons responded heterogeneously to neutral sensory stimuli, ranging from phasic increases to phasic decreases (Chiodo, Caggiula, et al. 1979; Chiodo, Antelman, et al. 1980; Fiorillo et al. 2013; Horvitz et al. 1997; Kobayashi et al. 2014; Schultz and Romo 1990; Steinfels et al. 1983a; Steinfels et al. 1983b; Strecker et al. 1985). However, some of these responses might be attributable to other factors such as movement or averseness of the stimulus. Despite heterogeneous responses, conceptual frameworks largely focused on phasic increases in firing in response to neutral sensory stimuli and interpreted them as attention-attracting novelty responses to surprising events

(Bromberg-Martin et al. 2010; Schultz 2007a; Schultz 2015) or the result of stimulus generalisation occurring in rewarded contexts (Kakade et al. 2002; Kobayashi et al. 2014; Matsumoto, Tian, et al. 2016; Sadacca et al. 2016; Schultz 2010; Schultz 2016). Kakade and Dayan (2002) tried to incorporate these findings into models of dopamine-guided reinforcement learning and suggested that stimulus generalisation represents initial uncertainty of the animal as to whether the respective stimulus will lead to an outcome, especially in a context where other similar stimuli do result in outcomes. They further interpret that novelty responses occur because stimuli are given a high initial value: An "optimistic" signalling mechanism which could support initial exploration of novel environments (Gershman et al. 2015; Kakade et al. 2002). However, other studies suggested an anatomical segregation of a dopamine system carrying novelty-responses and a dopamine system involved in reward signalling, arguing for functional separation and against convergence within the same set of dopamine neurons (Menegas, Babayan, et al. 2017).

1.3.3 Midbrain dopamine neurons and reward prediction

Learning is fundamental for survival and associative learning paradigms have been employed to study its neural correlates. Associative learning comprises classical and operant conditioning. Classical conditioning was discovered by Ivan Pavlov and shows how a behavioural response (e.g. salivation) elicited by an innately valued stimulus like food (unconditioned stimulus) can be evoked by an initially neutral stimulus (conditioned stimulus; e.g. a sound) if it is repeatedly and reliably paired with the unconditioned stimulus (Pavlov et al. 1928). For classical conditioning to occur, it is not required that conditioned and unconditioned stimulus overlap in time, they can be separated by short constant delays whereby the conditioned stimulus predicts the unconditioned stimulus. While classical conditioning is a passive form of learning, operant conditioning, also known as instrumental learning, requires action and is based on reinforcement through outcomes that only occur after a defined action is executed (e.g. a lever press) (Thorndike 1911). In the early 1990s, Schultz and colleagues linked the phasic firing increases of single midbrain dopamine

neurons recorded in non-human primates to unexpected food and liquid rewards, laying the cornerstone for extensive research into their role in reward-associated learning (Ljungberg et al. 1992; Schultz and Romo 1990; Schultz, Apicella, et al. 1993). In brief, firing of midbrain dopamine neurons is considered to change with learning. Before conditioning takes place, midbrain dopamine neurons respond with phasic increases to reward (at this point unexpected and thus, an unconditioned stimulus). After extensive conditioning, however, this phasic response was found to no longer occur at the time of reward but at the time of the reward-predicting conditioned stimulus instead (see Figure 6.1B) (Mirenowicz et al. 1994; Schultz and Hollerman 1998; Schultz and Hollerman 1998). Furthermore, if a predicted reward was omitted, midbrain dopamine neurons responded with a firing decrease at the time of expected reward delivery (see Figure 6.1C). Combined, these results were interpreted as prediction error signal implemented in the firing of midbrain dopamine neurons: Firing at the outcome period increases if an outcome is better than expected (e.g. unexpected or bigger reward), firing decreases if an outcome is worse than expected (e.g. omitted reward) and firing remains unchanged if expectation matches the outcome (Schultz and Hollerman 1998; Schultz, Dayan, et al. 1997; Tobler, Dickinson, et al. 2003; Tobler, Fiorillo, et al. 2005). This error signalling suggested that midbrain dopamine neurons may contribute to learning (Schultz, Dayan, et al. 1997) as prediction error terms are central in reinforcement learning theories (Rescorla et al. 1972; Sutton 1988; Sutton and Barto 1990). The idea behind these theories is that learning occurs whenever there is a discrepancy between expectation and outcome which serves to update prediction. Sutton and Barto's (1988; 1990) temporal difference (TD) learning model is based on the calculation of real-time prediction errors at any time point t:

$$\delta(\mathrm{t}) = \mathrm{r(t)} + \gamma\ \mathrm{V(t+1)} - \mathrm{V(t)}$$

δ(t) is the TD prediction error at time t, r(t) corresponds to the actual reward at time t and V(t) is the predicted reward at time t. The temporal discount

factor γ accounts for the preference of rewards lying in the near as opposed to more distant future (biologically, this makes sense because of limited life spans and uncertainty about future rewards). However, midbrain dopamine neurons are commonly recorded following extensive training in conditioning or instrumental learning tasks, leaving it unclear whether the response shift in midbrain dopamine neurons follows the same time course as task learning. Most non-human primate studies comparing midbrain dopamine neuron responses at multiple time points do so after extensive initial task training (Schultz, Apicella, et al. 1993; Takikawa et al. 2004). Non-human primate studies comparing reward responses at earlier stages of learning show retained reward responses even after performance criteria are met (Schultz and Hollerman 1998). Similarly, reward responses of midbrain dopamine neurons and dopamine terminals recorded in mice do not, or only incompletely, exhibit a response shift from the time of reward to the time of reward-predicting cue after learning, going against what would be expected if prediction errors were signalled (Cohen et al. 2012; Eshel, Tian, et al. 2016; Menegas, Babayan, et al. 2017; Parker et al. 2016; Tian et al. 2016).

In the framework of value-signalling, it might be expected that midbrain dopamine neurons respond to aversive outcomes and aversive outcome-predicting cues with phasic firing decreases, since they represent worse than expected events. The finding of both phasic firing increases as well as phasic firing decreases to aversive events in putative midbrain dopamine neurons (Matsumoto and Hikosaka 2009) led to the idea of "motivational value" coding midbrain dopamine neurons (phasic increases to positive valued and phasic decreases to negative valued events) and a separate group of "motivational salience" coding midbrain dopamine neurons (phasic increases to positive and negative valued events) (Bromberg-Martin et al. 2010). However, other studies on mice showed less clear results with aversive events resulting in biphasic responses both to cue and aversive outcome (Eshel, Tian, et al. 2016) or hardly any detectable cue-response and a brief phasic firing increase to the aversive outcome (Cohen et al. 2012). This is further complicated

by the finding that reward context modifies responses to aversive outcomes (Lerner et al. 2015; Matsumoto, Tian, et al. 2016).

1.3.4 Midbrain dopamine neurons and movement

Despite the general notion that the firing of midbrain dopamine neurons does not correlate with movement *per se* (DeLong et al. 1983; Schultz 2007a), there is evidence that the activity of putative dopamine neurons represents movement in a heterogeneous manner (Fan et al. 2012; Schultz 1986; Schultz, Ruffieux, et al. 1983). Given the degeneration of SNc dopamine neurons in Parkinson's and the resulting motor symptoms, it is of particular interest that firing of midbrain dopamine neurons was shown to signal onset of spontaneous movements in a subtype-specific manner and that this signalling was abolished in a Parkinson's mouse model (Dodson, Dreyer, et al. 2016). This finding was further supported by a study showing that movement-related signals can be found in dopamine terminals in striatal target regions (Howe et al. 2016). Other studies concluded that postural disturbances and even direction-selective movement kinematics like acceleration or velocity are represented in the firing of midbrain dopamine neurons (Barter, Castro, et al. 2014; Barter, Li, et al. 2015).

1.4 The midbrain dopamine system in Parkinson's

Parkinson's is one of the most common neurodegenerative diseases and is typically diagnosed by its motor symptoms which can include resting tremor, postural instability and muscular rigidity (Hughes et al. 1992). However the motor symptoms of Parkinson's are often preceded by non-motor symptoms including sleep disorders, loss of olfaction and gastrointestinal disturbances (Magerkurth et al. 2005; Ross et al. 2008; Samii et al. 2004). Arvid Carlsson speculated in 1959 that dopamine in the brain might be somehow linked to Parkinson's (Carlsson 1959) and Ohle Hornykiewicz and Herbert Ehringer then showed that caudate and putamen in postmortem brains of Parkinson's patients displayed marked dopamine depletion

(Ehringer et al. 1960). Further studies revealed that midbrain dopamine neurons are progressively lost in Parkinson's with a regional selectivity for SNc dopamine neurons (Fearnley et al. 1991; German, Manaye, et al. 1992; Hirsch et al. 1988; Hirsch et al. 1989). However, some VTA dopamine neurons and also non-dopamine neurons from other brain regions (e.g. serotonergic, cholinergic and adrenergic) were shown to degenerate (Alberico et al. 2015; Fearnley et al. 1991; Hirsch et al. 1989; McRitchie et al. 1997; Sulzer et al. 2013). Additionally, non-degenerated dopamine neurons in brains of Parkinson's patients typically contain intraneuronal protein aggregates termed Lewy bodies (Spillantini et al. 1997). While there is no cure or disease-slowing therapy for Parkinson's, dopamine replacement through administration of the dopamine precursor L-DOPA is still the standard treatment used to alleviate motor symptoms (Birkmayer et al. 1961). Unlike dopamine, L-DOPA crosses the blood brain barrier and is then metabolised to dopamine. However, prolonged treatment with L-DOPA results in adverse effects such as dyskinesia (Cotzias et al. 1967).

Since the etiology of Parkinson's is still largely unknown, extensive effort has been put towards studying the disease and potential therapies over the last decades. Due to the similarities in mammalian nervous systems, animal models are often used to gain insights into disease mechanisms and progression.

1.4.1 Neurotoxin-induced rodent models of Parkinsonism

The earliest models of Parkinsonism were based on the administration of neurotoxins. For example the administration of the agents 6-hydroxydopamine (6-OHDA) or 1-methyl-4-phenyl-1,2,3,6-tetrahydropyridine (MPTP) was found to result in the loss of monoaminergic neurons (Deumens et al. 2002; Smeyne et al. 2005; Ungerstedt 1968). 6-OHDA injections into the medial forebrain bundle (MFB), the striatum or the midbrain results in the rapid loss of dopamine neurons (Jeon et al. 1995). 6-OHDA is relatively selective for catecholamine neurons because it enters neurons through dopamine or noradrenaline transporters (Luthman et al. 1989). It leads to fairly rapid loss of dopamine neurons detectable 12 hours after nigral 6-OHDA

injection which then progresses with time (Jeon et al. 1995). Mechanistically, it is thought that 6-OHDA causes oxidative stress in affected neurons, ultimately followed by their death (Schober 2004). Since bilaterally injected 6-OHDA models require intense care (Cenci et al. 2002), unilateral injections are more commonly used. As symptomatic readout, contralateral body rotations induced through systemic administration of amphetamine or apomorphine are measured (Perese et al. 1989). While 6-OHDA is unable to cross the blood brain barrier, MPTP does and can thus be administered systemically. The neurotoxic effect of MPTP was discovered accidentally and shown to cause irreversible Parkinsonian symptoms in humans (Langston, Ballard, et al. 1983; Langston, Forno, et al. 1999). MPTP is spontaneously converted to MPP+ in the brain which has high affinity to the dopamine transporter (as well as noradrenaline and serotonin transporters) (Javitch and Snyder 1984; Javitch, D'Amato, et al. 1985). Inside dopamine neurons, MPP+ impairs respiratory function of mitochondria and leads to their loss (Mizuno et al. 1987). However, not all model species respond in a similar way to MPTP treatment. While MPTP is commonly used in both non-human primate and mouse studies, mice are less sensitive to the chemical. Furthermore, rats are relatively insensitive to the drug at low doses and conversely show high mortality rates at higher doses (Giovanni et al. 1994; Przedborski et al. 2001).

Taken together, while neurotoxin-induced animal models replicate the loss of dopamine neurons seen in Parkinson's, they do not reflect the slow progressive nature of Parkinson's and are not well suited for studying early disease processes. With the discovery of Parkinson's associated genes (Satake et al. 2009; Simón-Sánchez et al. 2009), it became possible to employ transgenic approaches to investigate early dysfunctions and disease progression in genetically modified animal models.

1.4.2 Transgenic rodent models of Parkinsonism

A range of different genetic risk loci for Parkinson's have been identified in humans (e.g. Nalls et al. 2014; Satake et al. 2009). The very first gene found to be implicated in Parkinson's was α-synuclein (*SNCA*) and both dominant point mutations as

well as locus multiplications have been linked with the disease (Chartier-Harlin et al. 2004; Krüger et al. 1998; Polymeropoulos et al. 1997; Singleton et al. 2003; Zarranz et al. 2004). Subsequently, other genes such as leucine-rich repeat kinase 2 (*LRRK2*), Parkin (*PARK2*), Phosphatase and tensin homolog-induced novel kinase 1 (*PINK1*) or Glucocerebrosidase (*GBA*) were identified as risk loci for Parkinson's (Di Fonzo et al. 2005; Gilks et al. 2005; Saunders-Pullman et al. 2006; Shimizu et al. 1998; Sidransky et al. 2012; Valente, Abou-Sleiman, et al. 2004). Modelling Parkinson's on the basis of these or other genetic risk factors was thought to help replicate different age-dependent disease stages and to get closer to an "ideal" disease model allowing testing of novel therapeutics. Such an ideal disease model would replicate most symptoms of Parkinson's, including its progressive nature, age-dependence, L-DOPA responsive motor symptoms, loss of dopamine neurons and human disease-relevant neuropathology. A model based on overexpression of human α-synuclein under the control of the Thy1 promoter was described with progressive sensorimotor, olfactory and digestive deficits accompanied by molecular changes (Chesselet, Fleming, et al. 2008; Fleming, Salcedo, et al. 2004). While this model did not display overt neurodegeneration, a more recent BAC-transgenic model overexpressing α-synuclein was described with age-dependent dopamine neuron loss, decreased SNc dopamine neuron firing and motor impairments following early-onset dopamine transmission deficits (Dodson, Dreyer, et al. 2016; Janezic et al. 2013). Notably, it was also shown that precise movement-related firing of SNc dopamine neurons in this model was compromised (Dodson, Dreyer, et al. 2016), shedding light on potential characteristics of the disease that occur at early stages. In a similar manner, *LRRK2* transgenic models were suggested to be most relevant to the investigation of early circuit alterations in Parkinson's (Dawson et al. 2010); rodent models of *LRRK2*-linked Parkinson's are summarised in section 3.1. LRRK2 is a multidomain protein that localises to membranous structures (Biskup et al. 2006) and it was shown that the overexpression of *LRRK2* can enhance α-synuclein-linked neuropathologies in mice (Lin et al. 2009). In this context, it is of interest to highlight that mutations in *SNCA* are completely penetrant, while mutations in

LRRK2 show incomplete penetrance. This suggests that additional factors might contribute to *LRRK2*-linked Parkinson's (Dawson et al. 2010).

Only few Parkinson's studies have addressed the question whether *in vivo* firing properties of SNc dopamine neurons change prior to their loss. However, given the extensive striatal innervation arising from SNc dopamine neurons (Matsuda et al. 2009), changes in their firing rate or pattern are likely to impact on the basal ganglia network at early stages of the disease. In-depth phenotyping of transgenic animal models of Parkinson's might contribute to a more complete picture of circuit changes that take place prior to the loss of dopamine neurons, potentially revealing new starting points for the development of neuroprotective therapies.

1.5 Aims of research

The midbrain dopamine system has been linked to diverse behavioural concepts in the healthy brain including associative learning or movement. Additionally, its necessity becomes apparent in brain disorders like Parkinson's where midbrain dopamine neurons are subject to degeneration. While extensively studied, the functional diversity of midbrain dopamine neurons has only recently been acknowledged and become focus of investigation. Since a critical readout of a neuron's function is its electrical activity, this thesis aimed at investigating firing activity of identified midbrain dopamine neurons under disruptive conditions pertinent to Parkinson's and the maintenance of dopamine neurons and expanding onto the healthy brain to gain deeper understanding of their functional diversity. Specific aims were to:

- Define the *in vivo* firing properties of identified SNc dopamine neurons in a *LRRK2* rat model of Parkinson's following its behavioural characterisation (Chapter 3).
- Define *in vivo* firing properties of identified SNc dopamine neurons in a mouse with conditional knock-out of the transcription factors Foxa1 and Foxa2 in midbrain dopamine neurons (Chapter 4).
- Characterise projection target-specific expression of molecular markers in midbrain dopamine neurons targeting the nucleus accumbens or the dorsal striatum (Chapter 5).
- Assess functional diversity of identified midbrain dopamine neurons recorded in awake head-fixed mice during the presentation of sensory stimuli or the performance of a classical conditioning paradigm (Chapter 6).

2

Materials and methods

Contents

2.1 Animals

All experiments were carried out in accordance with the Animals (Scientific Procedures) Act of 1986 (United Kingdom). Animals were maintained under a 12/12-h light/dark cycle, and all experimental procedures were performed during the light phase of the cycle.

2.1.1 *LRRK2* transgenic rats

LRRK2 transgenic male rats used for behavioural and electrophysiological experiments in Chapter 3 were generated on a Sprague Dawley (Charles River Laboratories) background by our collaborators in the Oxford Parkinson's Disease Centre (OPDC) (Sloan et al. 2016). Bacterial artificial chromosome (BAC)-transgenic rats expressed either the full human 'wildtype' leucine-rich repeat kinase 2 (LRRK2) gene (referred to as hWT) or the R1441C point mutated variant (referred to as R1441C) at 4-5 times the level of endogenous rat Lrrk2. Additionally, non-transgenic littermates (referred to as nTG) were used for behavioural and electrophysiological experiments. Young-adult (6 month old) nTG and R1441C male rats and aged (16-22 month old) hWT male rats were only used for electrophysiological recordings. Aged (16-22 month old) nTG and R1441C male rats were used for behavioural and electrophysiological experiments (numbers shown in Table 2.1, Table 2.2 and Table 2.3). All experiments and subsequent analyses were performed blind to genotype. For electrophysiological recordings in young adult rats, I performed recordings in n = 5 rats (nTG n = 2; R1441C n = 3) and combined them with recordings from n = 6 rats (nTG n = 4; R1441C n = 2) performed by Dr. Paul Dodson to complete the dataset.

Table 2.1: Aged non-transgenic rats (rows) used for experiments (columns) in Chapter 3. A cross marks all experiments individual rats were included in.

rat ID	Odour discrimination	Hidden food	Balance beam	Open field	Electro-physiology
268.3.04	x	x		x	x
268.4.02		x	x	x	
268.4.03		x	x	x	
268.4.14			x	x	
268.4.15			x	x	
268.4.16		x	x	x	
268.3.32	x	x		x	
268.3.34	x	x		x	x
268.3.35	x	x		x	x
268.4.26			x	x	
268.4.27			x	x	
268.4.32		x	x	x	x
268.4.33		x	x	x	
268.3.82	x	x	x	x	
268.3.91	x	x	x	x	
268.3.92	x		x	x	
M00027406					x
M00027407					x
Total number	**7**	**11**	**12**	**16**	**6**

Table 2.2: Aged R1441C *LRRK2* mutant rats (rows) used for experiments (columns) in Chapter 3. A cross marks all experiments that each rat was included in.

rat ID	Odour discrimination	Hidden food	Balance beam	Open field	Electro-physiology
268.4.01		x	x	x	
268.4.04		x	x	x	
268.3.18				x	x
268.3.20		x		x	
268.4.11		x	x	x	
268.4.12		x	x	x	
268.4.17		x	x	x	
268.4.18	x	x	x	x	
268.4.19		x	x	x	
268.4.20	x	x	x	x	x
268.3.36	x	x		x	x
268.3.37	x	x		x	x
268.3.75	x	x	x	x	x
268.3.76	x	x	x	x	x
268.3.78	x	x	x	x	x
268.3.80	x		x	x	x
Total number	**8**	**14**	**12**	**16**	**8**

Table 2.3: Numbers of young adult nTG and R1441C *LRRK2* and aged hWT rats used for experiments in Chapter 3. Young adult rats and aged hWT rats were not used for behavioural experiments.

Genotype	Odour discrimination	Hidden food	Balance beam	Open field	Electro-physiology
nTG 6 months	0	0	0	0	6
R1441C 6 months	0	0	0	0	5
hWT 16-22 months	0	0	0	0	5

2.1.2 Foxa1/2 conditional knock-out mice

Mice used for electrophysiological experiments in Chapter 4 were obtained as part of a collaboration with Siew-Lan Ang (NIMR, London) (Ferri et al. 2007; Pristerà et al. 2015). Mice with floxed Foxa1 and Foxa2 alleles ($Foxa1^{flox/flox}$;$Foxa2^{flox/flox}$) were crossed with Slc6a3-CreERT2/+ mice (conditional dopamine transporter-Cre heterozygous mice) to generate Slc6a3-CreERT2/+; $Foxa1/2^{flox/flox}$ mice (Foxa1/2 cKO) which were then maintained on an outbred MF1 background. Littermates with floxed Foxa1 and Foxa2 alleles ($Foxa1^{flox/flox}$;$Foxa2^{flox/flox}$) served as controls. Cre-dependent recombination (deletion) of Foxa1/2 alleles was achieved by intraperitoneal injection of tamoxifen (10 mg/mL in 10% ethanol / 90% corn oil) in 8 week old Foxa1/2 cKO and control mice. Tamoxifen is a synthetic estrogen receptor ligand that binds to the cytoplasmic CreERT2 recombinase (Cre-enzyme fused to a mutated ligand-binding domain of the human estrogen receptor). Upon binding tamoxifen, the CreERT2 enzyme enters the cell nucleus and excises loxP-flanked Foxa1 and Foxa2 genes resulting in their conditional knock-out (cKO) (Feil et al. 1997; Weber et al. 2001). Foxa1/2 cKO as well as the control mice were injected with 1 mg of tamoxifen twice a day, for 5 consecutive days. Electrophysiological recordings were performed on male control (n = 6) and Foxa1/2 cKO mice (n = 6) up to 2 weeks after Cre-mediated deletion of Foxa1/2. Experiments and subsequent analyses were performed blind to genotype.

2.1.3 C57Bl/6J mice

3 – 5 month old male C57Bl/6J mice used for Chapter 5 and 6 were obtained from Charles River Laboratories (for numbers see Table 2.4). Animals were housed with littermates.

Table 2.4: Numbers of C57Bl/6J mice included in experiments in Chapter 5-6.

	Experiment	Total number
Anatomy	Cell counting	17
Electrophysiology	Sensory stimuli	9
Electrophysiology	Cued reward	28

2.2 Behavioural testing of *LRRK2* rats

2.2.1 Hidden food

Olfactory impairments are symptoms detectable at preclinical stages of Parkinson's (Hawkes 2008; Hawkes et al. 2010). Using olfaction as a biomarker might help develop treatments applicable at early disease stages when SNc dopamine neuron loss is less severe and motor symptoms have not yet developed. To test whether the *LRRK2* mutant rats had olfactory impairment, they were tested on a hidden food and odour discrimination paradigm. With the hidden food test, the rat's performance in spatially locating an odour, as opposed to differentiating between two odours (see odour discrimination task, section 2.2.2), is tested (Gusmão et al. 2012). Each rat was familiarised with chocolate drops (Cadbury Dairy Milk Chocolate Buttons; ∼1 g per chocolate drop) for three consecutive days prior to testing. To increase the rat's motivation to search for the hidden chocolate drop, rats were put on food restriction with 21 g lab chow per animal 21-27 hours before testing. All animals were tested between 3 and 8 pm. The testing box (51 x 36 x 28 cm) was filled with sawdust consisting of a uniform mixture taken from individual cages of all testing animals. For each trial, a chocolate drop was randomly placed in one of four locations ∼1 cm underneath the sawdust (Figure 2.1B). After one adaptation trial without any buried chocolate, each animal was tested on six consecutive hidden food trials (Figure 2.1A). To ensure the rats' motivation to find the hidden chocolate, four visible trials, in which a pile of three chocolate drops was placed on top of the sawdust, were added after the hidden trials. Possible locations for the visible trials were the same as for the hidden trials (Figure 2.1B). In between trials, faeces

were removed from the box and the sawdust was extensively mixed to ensure a homogeneous background odour. The time to find the hidden chocolate drop was recorded and a maximum search time of 300 seconds was allowed. Individual trials were concluded as soon as the animal started eating the chocolate drop. Animals which took longer than 300 seconds on the first visible trial were excluded from analysis due to a potential lack in motivation.

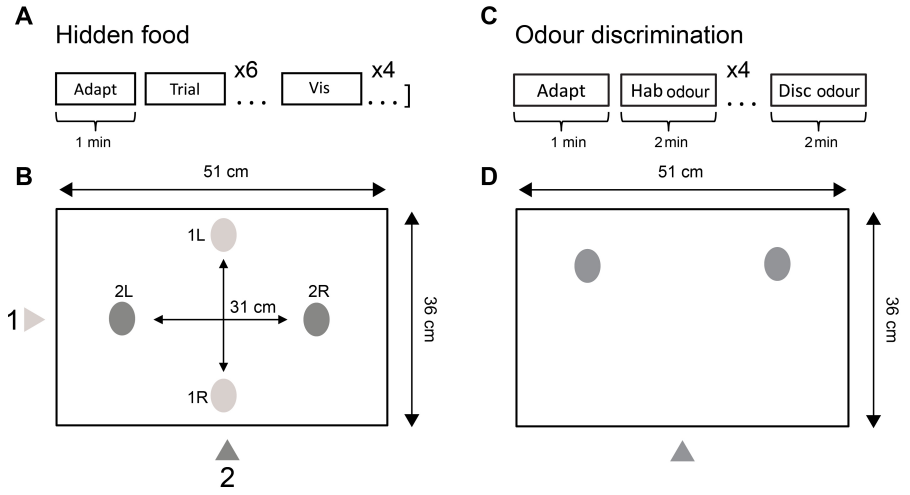

Figure 2.1: Experimental design for olfactory tasks. (A-B) Experimental design for the hidden food task. (A) Trial sequence: nTG and R1441C rats were familiarised with the experimental box for 1 minute (Adapt) followed by six trials with a chocolate drop randomly hidden at 1 of 4 locations (Trial) and four visible trials where a pile of chocolate drops was visibly placed in 1 of the 4 locations on top of the sawdust in the experimental box (Vis). A maximum of 300 seconds was given on each hidden and visible trial. (B) Schematic of the experimental box. Grey arrows indicate the starting positions of the animal. Grey ovals represent the four locations for chocolate drops. For starting position 1, chocolate was either placed in 1L or 1R and for starting position 2 chocolate was either placed in 2L or 2R. (C-D) Experimental design of the odour discrimination task. (C) Trial sequence: nTG and R1441C rats were familiarised with the experimental box for 1 minute (Adapt) and then exposed to the habituation odour for two minutes each on four successive trials (Hab odour). On the fifth and last trial, a novel odour was presented for two minutes in one of the two locations (Disc odour). The experiment was repeated with three odour pairs per animal. (D) Schematic of the experimental box. The grey arrow indicates the starting position of the animal and the two ovals represent the two locations for odour presentation. Animals were video recorded on all trials.

2.2.2 Odour discrimination

An odour discrimination task was used to assess the rats' ability to differentiate between two different odours. If a rat discriminates odours, novel odours elicit

investigative behaviour (e.g. sniffing) of the site perceived to give rise to the odour (Mandairon et al. 2009; Veyrac, Nguyen, et al. 2007; Veyrac, Sacquet, et al. 2009). During the habituation phase, rats were presented with two identical odours (Hab odour; Figure 2.1C) one of which was replaced with a new odour in the discrimination trial (Disc odour; Figure 2.1C). If the new odour could not be discriminated from the habituation odour, there should be no increased investigation in response to the new odour. Each rat was presented with three pairs of odorants with approximately 5 minutes between odour pairs (Table 2.5). Dilutions were chosen so that odour pairs were theoretically emitting the same vapour-phase partial pressure (Cleland et al. 2002; Mandairon et al. 2009). 20 µl of each odour was applied to porous filter stones (Fluval Biomax) in glass vials in the experimental box (51 x 36 x 28 cm; Figure 2.1D). The box contained a 2 cm layer of sawdust which consisted of a uniform mixture taken from individual cages of all testing animals. Odours were presented in two locations with equal distance from the rats' starting position (Figure 2.1D). Odours of a pair were randomized for habituation and discrimination phase. To avoid a place preference bias, odours for the discrimination trial were randomly placed in one or the other location.

Table 2.5: Odours and dilutions used for the odour discrimination task. When necessary, odours were diluted in mineral oil (chemicals were purchased from Sigma-Aldrich).

Pair	Odorant	Dilution
1	(+)Limonene	Pure
	(–)Carvone	Pure
2	Anisole	1 % v/v
	Amyl acetate	1 % v/v
3	Decanal	1.78 % v/v
	Pentanol	0.07 % v/v

Rats were first familiarised with the experimental box in a 1 minute adaptation trial with no odorants. This was followed by four 2 minute presentations of the habituation odour (separated by approximately 1 minute) and by one 2 minute

presentation of the discrimination odour (Figure 2.1C). Sniffing time at each vial was manually assessed from video recordings. Onset of sniffing was taken as the time when the animal's nose was in close proximity to, or above, the glass vial and offset of sniffing was taken as the time when the animal turned its nose away from the vial. Individual sniffing times were then taken as the time between onset and offset of sniffing. Total sniffing time per vial was taken as the sum of all individual sniffing times. To test whether investigation time of the discrimination odour was significantly higher than investigation time of the habituation odour during its fourth presentation, investigation time per trial was averaged over all three odour pairs. The recognition index was calculated as Disc/(Disc+Hab4) × 100 where Disc is the time spent exploring the novel odour and Hab4 is the time spent exploring the familiarised odour on the fourth trial (Veyrac, Sacquet, et al. 2009). A recognition index of 50 implies that time spent exploring the novel odour is identical to the time spent exploring the familiar odour.

2.2.3 Balance beam

Balance beam tests are used to assess coordination and balance in rodents (Deacon 2013). For the balance beam test, a plastic tube of 4.5 cm diameter and 130 cm length was clamped to a platform 60 cm above a cushioned surface. Following two guided habituation trials, male rats were placed on top of the end section of the tube, facing away from the platform. Rats were required to turn 180° and traverse the beam. The distance travelled along the beam before falling was video recorded for five subsequently repeated trials and analysed off-line. Completed trials were rated as 100% and falling off the beam before turning as 0%.

2.2.4 Open field

Open field recordings were made to test general locomotor and explorative behaviour. A black circular board with a diameter of 120 cm and without walls, placed 30 cm above ground, was used as an arena. Each rat was placed in the centre of the board and left to explore for 6.5 minutes in dim light conditions. Activity was

recorded with an overhead video camera and analysed off-line using the EthoVision tracking system (Version 3.1; Noldus). For analysis, the arena was subdivided into an inner circle and an outer ring (ring width 22.5 cm). Total distance moved and time spent in the outer ring was measured.

2.3 Anaesthetised electrophysiological recordings

2.3.1 Preparation of anaesthetised rats

Anaesthesia was induced with 4% isoflurane (Isoflo; Shering-Plough), and maintained with urethane (1.2 g/kg, i.p.; ethyl carbamate, Sigma-Aldrich), with a ketamine (30 mg/kg, i.p.; Ketaset, Willows Francis) and xylazine (3 mg/kg, i.p.; Rompun, Bayer) mix given as required. Anaesthesia was monitored during experiments using electrocorticogram recordings (ECoG, see below) and by testing reflexes to a cutaneous pinch or gentle corneal stimulation. Wound margins were infiltrated with the local anaesthetic bubivacaine (0.75% w/v, Marcain Polyamp, Astra Zeneka) and corneal dehydration was prevented with application of Hypromellose eye drops (Norton Pharmaceuticals) and eye ointment (Lacri-Lube, Allergan). Animals were placed in a stereotaxic frame (Kopf) and their body temperature maintained at 37 ± 0.5°C using a homeothermic heating device (Harvard Apparatus). For ECoG recordings, a stainless steel screw was juxtaposed on the dura mater above the right frontal cortex (anteroposterior 4.2 mm, mediolateral 2 mm distance from Bregma; Paxinos and Watson 2007) and was referenced against a screw positioned above the cerebellum. The raw ECoG was bandpass filtered (0.3 – 1500 Hz, -3 dB limits) and amplified (2000 times, DPA-2FS filter/amplifier, NPI Electronic Instruments) prior to acquisition. For single-cell recordings in the midbrain (see section 2.4), a craniotomy was performed above the right and/or left substantia nigra pars compacta (SNc) and the dura mater removed.

2.3.2 Preparation of anaesthetised mice

The mouse recording setup was identical to the protocol described for rats (see section 2.3.1) except that anaesthesia was maintained with urethane only (1.5

g/kg, i.p.; ethyl carbamate, Sigma-Aldrich) and coordinates for ECoG recordings were anteroposterior and mediolateral 2 mm distance from Bregma (Paxinos and Franklin 2013) and the dura mater was left intact.

2.4 Single-unit recordings and juxtacellular labelling

2.4.1 Single-unit recordings in rats and mice

Saline solution (0.9% w/v NaCl) was frequently applied around the craniotomy to prevent dehydration of the exposed cortex. Extracellular single-unit recordings were made with borosilicate glass electrodes (tip diameter ~1.3 µm, *in situ* resistance 10-25 MΩ; GC120F-10, 30-0044, Harvard Apparatus) filled with saline solution (0.5 M NaCl) containing Neurobiotin (1.5% w/v, Vector Laboratories). Electrodes were lowered down into the brain using a micromanipulator (IVM-1000; Scientifica). Electrode signals were filtered at 0.3 – 5 kHz and amplified 1000 times (ELX-01MX and DPA-2FS amplifiers from NPI Electronic Instruments). A Humbug (Quest Scientific) was used to eliminate mains noise at 50 Hz. To avoid possible sampling bias, generous on-line criteria were applied to guide recordings of SNc dopamine neurons (spike duration threshold to-trough for bandpass-filtered spikes above 0.8 ms and firing rates below 20 spikes/s) (Janezic et al. 2013).

2.4.2 Juxtacellular labelling and perfuse-fixation

Following the recording, single neurons were filled with Neurobiotin using a juxtacellular method (Brown et al. 2009; Janezic et al. 2013; Pinault 1996) to allow for their unambiguous identification and localization. In brief, the electrode was advanced slowly toward the neuron and then a microiontophoretic current was applied (1–10 nA positive current, 200 ms duration, 50% duty cycle). The optimal position of the electrode was identified when the firing pattern of the neuron was robustly modulated by the applied current. Ideal modulation duration was between 3 – 5 minutes; this was sufficient to label somata and proximal dendrites. The Neurobiotin was then left to transport along neuronal processes (up to 12 h). At

the end of the experiment, animals were given a lethal dose of anaesthetic and transcardially perfused with 200 mL (rats) or 20 mL (mouse) of 0.01 M phosphate-buffered saline (PBS) at pH 7.4 followed by 300 mL (rats) or 40 mL (mice) of 4% w/v paraformaldehyde in 0.1 M phosphate buffer, pH 7.4 (PFA). Brains were left in PFA for 12 hours at 4°C and then stored in PBS with 0.05% w/v sodium-azide until they were sectioned 12–72 h later.

2.4.3 Tissue processing to identify recorded and labelled neurons

For tissue processing, fixed brains were sectioned at 50 µm in the coronal plane on a vibrating blade microtome (VT1000S; Leica Microsystems), collected and washed in PBS. Free-floating sections were incubated for 4 h at room temperature in PBS with 0.3% (vol/vol) Triton X-100 (PBS-Triton, Sigma-Aldrich) and Cy3-conjugated streptavidin (diluted 1:1000, PA43001, GE Healthcare) or in some cases AlexaFluor 488-conjugated streptavidin (diluted 1:1000, S-32354, Invitrogen). Tissue sections were then mounted on slides for viewing with an epifluorescence microsope (Axiophot, Carl Zeiss) and sections containing Neurobiotin-labelled neuronal somata (i.e. those labelled with Cy3 or 488) were identified and isolated. To identify dopamine neurons, immunoreactivity for tyrosine hydroxylase (TH; an enzyme involved in the synthesis of dopamine) was visualised in all Neurobiotin-labelled neurons. Sections were incubated overnight at room temperature in PBS-Triton with mouse anti-TH (1:1000, T2928/T1299, Sigma-Aldrich) or chicken anti-TH (1:500, ab76442, Abcam), washed in PBS, and then incubated for 4 h at room temperature in PBS-Triton with AMCA-conjugated secondary antibody (donkey anti-mouse IgG, 1:500; 715-155-150 or donkey anti-chicken IgG, 1:500, 703-155-155; Jackson Immunoresearch Laboratories). After washing in PBS, sections were mounted in Vectashield (Vector Laboratories) and viewed on an epifluorescence microscope (AxioImager.M2, Carl Zeiss) using Axiovision software (Carl Zeiss). Precise anatomical locations of individually labelled cells were obtained by registering their position on the coronally cut section to a standard rat (Paxinos and Watson

2007) or mouse brain atlas (Paxinos and Franklin 2013) using TH-labelling and anatomical landmarks as guidance (Fu et al. 2012). Images were acquired using a 40x oil immersion objective (numerical aperture 1.3; for figures in Chapter 3 and Chapter 4) or a 63x oil immersion objective (numerical aperture 1.4; for figures in Chapter 6) on a confocal laser-scanning microscope (LSM710, Carl Zeiss) and ZEN software (2008; Carl Zeiss). Each fluorescence channel was imaged in a separate track. AMCA fluorescence was imaged with excitation from a diode 405 m laser, with emission restricted at 409-485 nm. CY3 signal was imaged with excitation from a helium/neon 543 nm laser, with emission restricted at 552-639 nm. AlexaFluor 488 fluorescence was imaged with excitation from an argon 488 nm laser, with emission restricted at 493-542 nm. AlexaFluor 647 fluorescence was imaged with excitation from a helium/neon 633 nm laser, with emission at 637-757 nm. Digital images were cropped to regions of interest and brightness and contrast adjusted when needed (Photoshop software, Adobe Systems).

In addition to Neurobiotin- and TH-labelling, identified dopamine neurons in Chapter 6 were also tested for the expression of the molecular markers Sox6, Aldh1a1 and Calbindin (see section 2.6.2; Table 2.6). To be able to test for expression of these three additional markers with only two spectrally distinct fluorescent 'channels' left on the confocal microscope, a sequential protocol was used (Figure 2.2). In a first step, all sections containing identified (i.e. Neurobiotin-containing and TH-positive) dopamine neurons were incubated overnight at room temperature in PBS-Triton with guinea pig anti-Sox6 (1:1000, gift from M. Wegner, Friedrich-Alexander University Erlangen-Nuremberg; Stolt et al. 2006), washed in PBS and then incubated overnight at room temperature in PBS-Triton with AlexaFluor 647-conjugated secondary antibody to visualise immunoreactivity of Sox6 (donkey anti-guinea pig IgG, 1:500; 706-605-148; Jackson Immunoresearch Laboratories). After washing in PBS, sections were mounted in Vectashield (Vector Laboratories) and images of individually labelled cells were acquired using a confocal laser-scanning microscope (LSM710; see above) to confirm whether they expressed Sox6 (see Figure 2.2). Following immunolabelling for Sox6 and image acquisition,

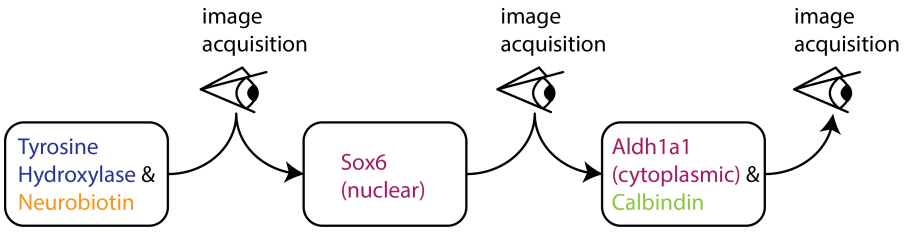

Figure 2.2: Schematic for sequential immunolabelling and image acquisition of individual identified midbrain dopamine neurons in Chapter 6. In a first stage, juxtacellularly labelled neurons were identified by Neurobiotin-labelling and confirmed to be dopamine neurons by tyrosine hydroxylase expression. In a second stage, identified dopamine neurons were tested for the expression of the nuclear marker Sox6. Following image acquisition, identified dopamine neurons were tested for the expression of the molecular markers Calbindin and Aldh1a1. Aldh1a1, visualised with the same Fluorophor as Sox6, was differentiated from Sox6 by its cytoplasmic expression.

all sections were incubated overnight at room temperature in PBS-Triton with rabbit anti-Aldh1a1 (1:500, HPA002123; Sigma-Aldrich) and goat anti-Calbindin (1:500, sc7691; Santa Cruz), washed in PBS and then incubated overnight at room temperature in PBS-Triton with AlexaFluor 647- and 488-conjugated secondary antibodies to visualise immunoreactivity for Aldh1a1 (donkey anti-rabbit IgG, 1:500; 711-605-152; Jackson Immunoresearch Laboratories) and Calbindin (donkey anti-goat IgG, 1:500; A11055; Life Technologies) respectively. An AlexaFluor 647-conjugated secondary antibody was first used to reveal Sox6 expression (nuclear labelling) and then re-used to reveal Aldh1a1 immunoreactivity (nuclear plus cytoplasmic labelling; Figure 2.2). After washing in PBS, sections were mounted in Vectashield (Vector Laboratories) and images of individually labelled cells were acquired a second time using a confocal laser-scanning microscope (LSM710; see above) to evaluate Aldh1a1 and Calbindin expression.

2.4.4 Analysis of anaesthetised recordings

All biopotentials were digitised online at 20 kHz using a Power 1401 mk 3 analog-digital converter (Cambridge Electronic Design) and acquired using Spike2 software (version 7.12; Cambridge Electronic Design). Because firing properties of midbrain dopamine neurons were shown to be brain state dependent (Brown et al. 2009; Walczak et al. 2017), only unit activity recorded during robust cortical slow-wave

activity (SWA) was included in the analysis. For the extraction of SWA periods, electrocorticogram data were Fourier-transformed (frequency resolution 0.2 Hz) and the power ratio in the SWA band (0.5-2 Hz) to the power in the gamma band (30-80 Hz) was calculated. Epochs of contiguous data with a power ratio of >13 for each data point were concatenated for further analysis (Janezic et al. 2013). Mean power of concatenated epochs was calculated for comparison between genotypes. Putative single-unit activity was isolated using template matching, principal component analysis and supervised clustering within Spike2. Firing variability was calculated using CV2 (Holt et al. 1996), which compares the variability of adjacent ISIs within a spike train, then a mean CV2 value was obtained for each neuron (lower CV2 values indicate more regular unit activity). Bursts in SNc dopamine neurons were determined using the Robust gaussian surprise method (RGS) (Ko et al. 2012), a statistical method to detect clusters of spikes with significantly lower ISIs than a central distribution obtained from the pooled and normalised spike trains. Percentage of total numbers of spikes emitted in bursts was calculated from RGS obtained clusters. RGS parameters were set to a minimum of three spikes per burst. While the RGS method was used to measure burst occurrence, the overall *in vivo* firing pattern of individual midbrain dopamine neurons was classified based on autocorrelation histograms (ACH). The ACH of each individual neuron was plotted (5 ms bins, 2 s window) and classified by visual inspection as one of three modes: regular (≥3 equally spaced peaks), irregular (<3 peaks increasing from zero approximating a steady state) or bursty (narrow peak with increase at short ISIs; see Figure 2.3) (Brown et al. 2009; Tepper, Martin, et al. 1995; Wilson, Young, et al. 1977). Classifications were then used to ascribe a firing mode to individual cells within each genotype.

2.4.5 Statistical approach for anaesthetised recordings

The Shapiro-Wilk test was used to judge whether data were normally distributed ($p \leq 0.05$ to reject). If data failed normality tests, a Mann–Whitney rank sum

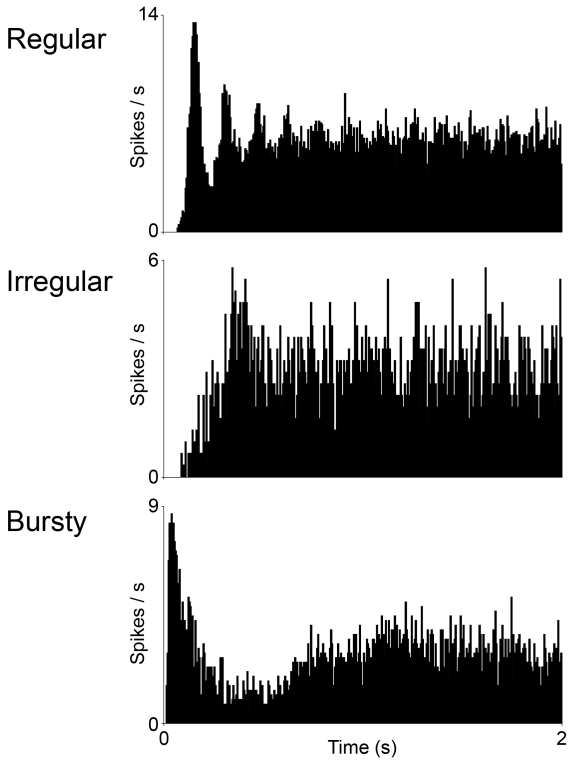

Figure 2.3: Autocorrelation histograms of midbrain dopamine neurons classified as regular firing (top), irregular firing (middle) and burst-firing (bottom).

test or Kruskal-Wallis one-way ANOVA on ranks with Dunn's method for multiple comparison was used (SigmaStat, Systat Software Inc). Significance for all statistical tests was set at $p \leq 0.05$. Boxplots display first quartile, median and third quartile. This approach was also taken for the analysis of behavioural data in Chapter 3.

2.5 Recordings in head-fixed awake mice

2.5.1 Headpost implantation

For electrophysiological recordings in awake behaving mice, animals were attached to a stereotaxic frame with a headpost (Dodson, Larvin, et al. 2015; Dodson, Dreyer, et al. 2016; Schiemann, Puggioni, et al. 2015). For headpost implantation, mice were anaesthetised using 3% (vol/vol) isoflurane for induction, and 1 – 2% isoflurane for maintenance of anaesthesia. Mice were placed in a stereotaxic frame (Kopf Instruments) and on a homeothermic heating mat (Harvard Apparatus) to ensure stable body temperature. Corneal dehydration was prevented using carbomer

liquid gel (Viscotears, Alcon) and the mouse was perioperatively injected with buprenorphine (0.03 mg/kg s.c., Vetergesic) to provide analgesia. A custom L-shaped headpost (with a weight of ∼0.7 – 0.8 g) made from stainless steel was attached to the skull using cyanoacrylate-based glue. The 3 mm diameter hole in the headpost-base was positioned above the substantia nigra of the right hemisphere (centre of the hole at AP –3 mm and ML +1.6 mm from Bregma; Paxinos and Franklin 2013). The craniotomy for single-unit recordings was made within the hole of the headpost either on the day of headpost implantation or 3 – 7 days prior to recording. For ECoG recordings, stainless steel screws (0.8 mm diameter; M1.0 X 3 slot cheese machine screw DIN 84 A2 St/St; Precision Technology Supplies) were implanted in the skull, one above the frontal cortex (AP +2 mm and ML -2 mm from Bregma; Paxinos and Franklin 2013) and one above the cerebellum of the left hemisphere. 0.023 cm diameter coiled stainless steel wire (AM Systems) was implanted between the layers of left and right nuchal neck muscle to record electromyogram activity (EMG; filtered at 0.3 – 0.5 kHz using a differential amplifier/filter module; DPA-2FS; npi Electronic Instruments). Exposed skull, screws and EMG wire were covered with dental acrylic (Jet Denture Repair; Lang Dental). The craniotomy was sealed with fast set removable silicone rubber (Body Double Skin Safe Lifecasting Silicone Rubber; Smooth-On). Following implantation, animals were allowed to recover until their weight was above 95% of the pre-surgery weight. This criterion was generally met after one day (irrespective of weight, every animal was given a minimum of one day recovery time). Recovery was followed by training sessions in cued reward experiments or recording in sensory stimuli experiments.

2.5.2 Treadmill, cue box and reward delivery system

For task training and electrophysiological recording in head-fixed awake mice, custom self-powered linear treadmills were used (Figure 2.4). Treadmills consisted of two rotatable 10 cm diameter cylinders enclosing a 14 x 11 cm suspended platform. Circular treadmill belts were made from black polyester webbing (similar to that used for seatbelts; width 9.5 cm, length 75 cm, thickness ∼1 mm; www.extremtextil.de).

Mice were placed on the treadmill platform and their headpost attached to either the treadmill stand (training treadmill) or a stereotaxic frame (recording treadmill; Figure 2.4) using custom headpost holders. Tone and light stimuli were delivered using a custom stimulus box attached to the treadmill at a distance of 10 cm anterior to the centre of the mouse's head. The stimulus box was equipped with LEDs (green: 520 nm, ∼2.1 lm, 815-4363, RS components; blue: 455 nm, ∼0.03 lm, 247-1690, RS components and 480 nm, ∼1.03 lm, 810-0451, RS components) and piezo speakers/transducers (∼70 dB sound pressure level; ∼1, 4, 5 kHz, 457-065 and 535-8253, RS components; or ∼10 kHz, 2400-106, Technobots). Light wavelengths and tone frequencies were chosen to lie within the visible and audible range of C57Bl/6 mice (Ehret 1983; Henry et al. 1980; Huberman et al. 2011; Willott 1986) and to avoid auditory startle responses (Ison et al. 2007). Rewards were delivered using a 16 GA metal spout attached to a custom stepper-motor-powered syringe pump. Blackcurrant juice (25% vol/vol in tap water, Ribena) or strawberry flavoured milk (undiluted, Yazoo) were used as rewarding liquids (individual animals only ever experienced either Ribena or Yazoo liquid) and reward size was 8-9 µL. The stimulus box and reward delivery system were manipulated and monitored through custom programmed microcontrollers (Arduino Mega2560). Individual licks during training sessions were detected using capacitive sensing at the reward delivery spout (AT42QT1919, N51DQ momentary capacitive touch sensor; Adafruit). During electrophysiological recording, capacitive sensing could not be used due to high electrical noise induced by the sensor and so licking was monitored by video (30 frames/s).

2.5.3 Sensory stimuli experiment

Animals used for the sensory stimuli experiment were not food restricted or trained prior to recording. Extracellular single-unit recordings were performed as described in section 2.4.1. The recording room had lighting conditions of ∼50 lx and an ambient noise of ∼60 dB. Four different sensory stimuli were pseudorandomly presented to the mouse while recording a single-unit (one stimulus at a time; Figure

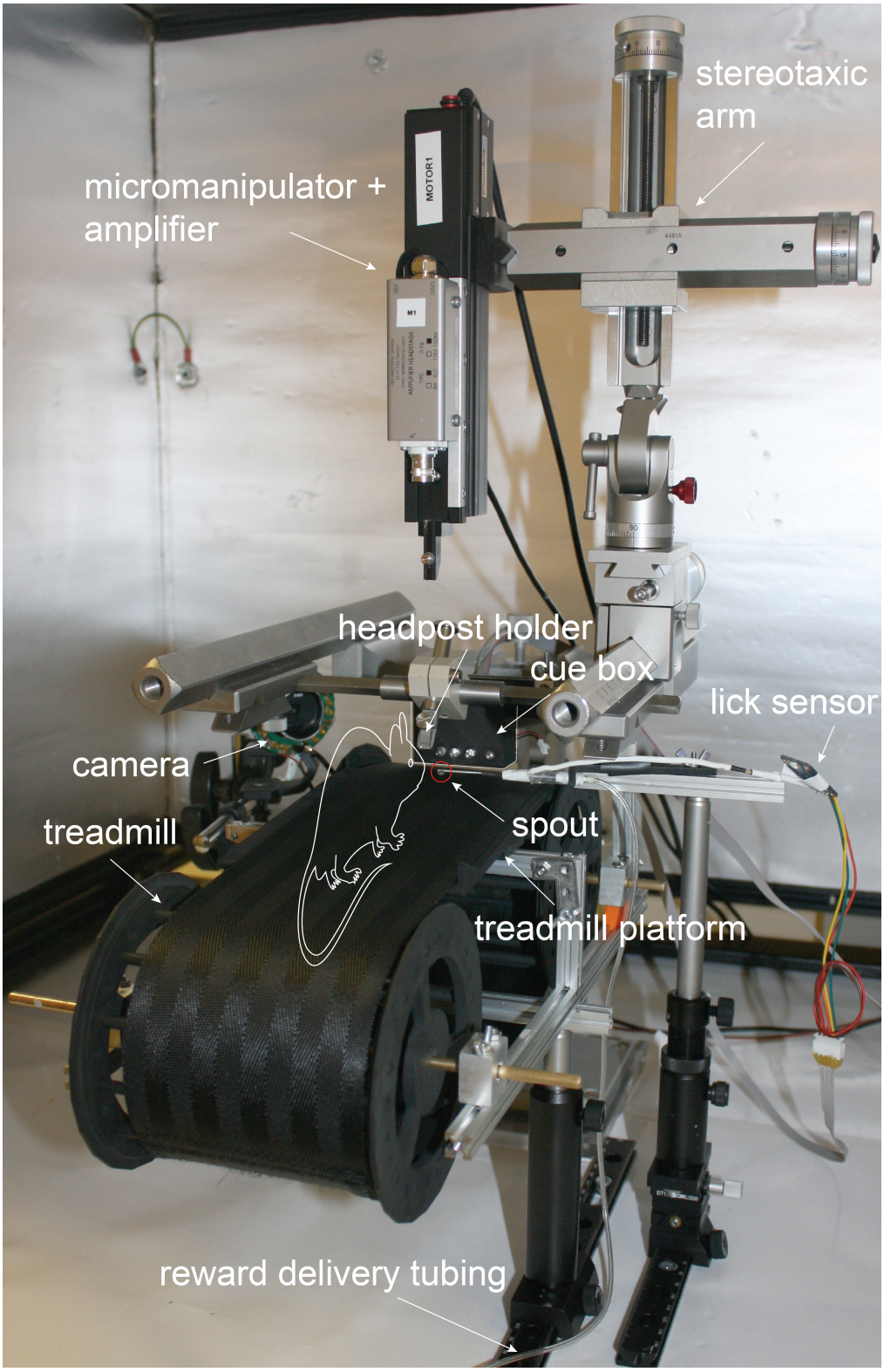

Figure 2.4: Recording setup for head-fixed awake mice. The setup is equipped with LED lights and speakers (cue box), a reward delivery spout and a lick sensor. Mice were placed on the treadmill and head-fixed using a custom headpost holder attached to the stereotaxic frame.

2.5A). The stimuli set consisted of two lights (green and blue; see section 2.5.2), a low frequency tone (1 kHz) and a high frequency tone (5 kHz or 10 kHz). Minimum inter-stimulus interval was 2 seconds (median inter-stimulus interval was 2.5 s; Figure 2.5C) and stimulus duration was 0.5 s for each stimulus. On average, 17 (median) stimuli were presented per recording (minimum 6, maximum 30; excluding movement-overlapping stimulus trials; see section 2.5.5). Median trial numbers for individual stimuli were 5 (blue LED), 6 (green LED), 5 (high tone) and 3 (low tone). Due to constraints of the experimental equipment, recordings were not performed in a sound-isolated environment, but brief and sudden distractor noises were minimised. Following recording, individual neurons were labelled using the juxtacellular method outlined in section 2.4.2 and processed as described in section 2.4.3. Movement periods were ascribed off-line using cervical EMG (filtered at 0.3 – 0.5 kHz) combined with video recordings.

2.5.4 Cued reward experiment

Animals used for cued reward experiments were food restricted and trained prior to recording. While animals were on a food restriction protocol, their weight was maintained above 85 % of baseline. Training sessions consisted of cue-paired reward deliveries identical to the task design on recording days (forward trace conditioning; Figure 2.5B) (Solomon et al. 1986): 1 second cue (4 kHz piezo sounder, ∼70 dB; 535-8253, RS components), 1 second inter-cue-reward interval, followed by reward delivery (Ribena or strawberry Yazoo, 8 – 9 µL). A single training session was terminated after 100 consumed rewards or 30 minutes of head-fixation (whichever occurred first). Animals received typically 1, rarely 2 training sessions per day. Number of training sessions before recording ranged from 2 – 15 (median 6). The cue predicted the reward with near 100 % probability (i.e. almost every cue was followed by a reward; reward delivery was occasionally omitted due to equipment failure) and inter-trial intervals were randomly drawn from an exponential distribution with a flat hazard function to ensure equal distribution of expectation (Zariwala et al. 2013) (Figure 2.5D-E). Licking during training was monitored using

a capacitive sensor. Extracellular single-unit recordings were performed identically to recordings in sensory stimuli experiments and are described in section 2.4.1. For electrophysiological recordings, animals were enclosed in a dark Faraday cage with 18 mm thick foam walls resulting in dim light conditions. The recording room had lighting conditions of ∼50 lx and an ambient noise of ∼60 dB. Following recording, single neurons were labelled using the juxtacellular method (see section 2.4.2) and tissue was processed as described in section 2.4.3. Movement and licking periods for single-unit recordings were determined off-line using cervical EMG and video recordings (30 frames/s). Lick-onset was defined as the first video frame with visually detectable lower lip movement, lick-offset was defined as the first of a series of at least three subsequent video frames with no visually detectable lip movement.

2.5.5 Analysis of head-fixed awake recordings

All biopotentials were digitised online at 20 kHz using a Power 1401 mk 3 analog-digital converter (Cambridge Electronic Design) and acquired in addition to time stamps of events (e.g. cue, reward delivery) using Spike2 software (version 7.12; Cambridge Electronic Design). Single-unit activity was isolated using template matching, principal component analysis and supervised clustering within Spike2. All data was then exported to MATLAB (Mathworks).

Sensory stimuli experiments: Firing activity of individually labelled neurons was normalised as z-scores (using baseline mean and standard deviation) and used to construct peri-event time histograms (PETH; bin size 40 ms). Baseline was taken as 1 second preceding stimulus onset. Because the activity of some midbrain dopamine neurons is modulated by movements (Dodson, Dreyer, et al. 2016), individual stimuli were excluded from the analysis if movements of the animal overlapped with a stimulus trial (a trial being defined as the time period from 1 s prior to stimulus onset to 1 s after stimulus offset). PETHs were smoothed with a 5-point Gaussian filter (half-width: 70 ms). A neuron was considered responsive to the stimuli if its PETH deviated at least 2 standard deviations (i.e. $|\text{z-score}| \geq 2$) from the baseline mean during the 500 ms of stimulus presentation. Population

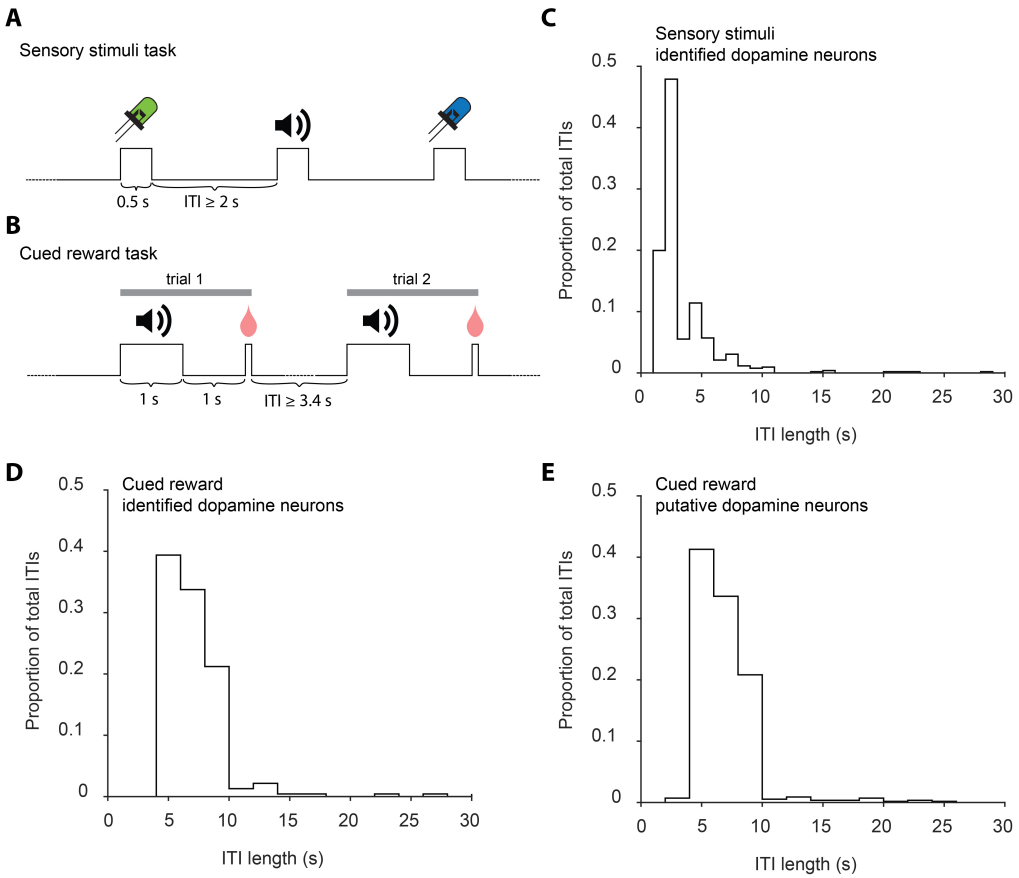

Figure 2.5: Task design and inter-trial interval (ITI)-distribution for head-fixed awake recordings. (A) Task design for sensory stimuli tasks: light and tone stimuli were presented in a pseudorandom fashion with random inter-stimulus intervals. (B) Task design for cued reward experiments. Forward conditioning consisted of a 1 second cue (a tone), a 1 second inter-cue-reward period followed by reward delivery (8 – 9 µL strawberry milk) and a random inter-trial interval. (C) ITI-distribution from recordings of dopamine neurons in the sensory stimuli task. (D-E) ITI-distribution from recordings of (D) identified and (E) putative dopamine neurons in the cued reward task.

activity was considered responsive if the population PETH (including error margins) deviated at least 2 standard deviations from the baseline mean during stimulus presentation (500 ms). To assess the relationship between response magnitude and stimulus-novelty in sensory stimuli experiments, Pearson's linear correlation was used. Stimulus-novelty per recorded cell was measured as the total number of prior experienced sensory stimuli and minimal and maximal rate (z-score) during stimulus presentation was taken as response magnitude. To obtain examples of shuffled data, corresponding stimulus periods were randomly positioned along the recording trace (randperm, MATLAB).

Cue-reward conditioning experiment: In cue-reward conditioning experiments, diverse responses of individual midbrain dopamine neurons to cues, rewards and movements (licking) were observed. To analyse which of these factors accounted best for changes in firing of individual midbrain dopamine neurons recorded in the conditioning experiment, a generalised linear regression model (glmfit, MATLAB) was used to obtain a least-squares fit of the selected predictors to the recording data. Predictors were defined as licking, cue and reward. Regression coefficients were estimated for each labelled neuron in 0.1 second windows spanning the entire recording duration of a neuron (i.e. for 100 seconds of recording of a cell, 1000 windows were analysed). All predictors were taken as binaries (e.g. the predictor "lick" was set to 1 if the animal was licking within a 0.1 second window and 0 otherwise). Cue windows were set to 0.6 seconds from cue onset and reward windows to 0.4 seconds from reward onset (based on visual inspection of the population PETH) (Eshel, Tian, et al. 2016). An individual cell was considered responsive to one of the three variables if the corresponding p-value was equal to or lower than 0.05. Signs of coefficients were used to determine whether firing rate increased (positive sign) or decreased (negative sign). For figures, reward- or licking-aligned average PETHs were constructed identically to sensory stimuli experiments (see above). Firing during 1 second preceding cue onset was considered as baseline. Firing variability was measured as mean CV2 during baseline (see section 2.4.4). The total number of prior received rewards was taken as the amount of cued-reward trials the animal had experienced prior to the start of the recording. This included all training trials (summed over training days) and trials received on the recording day. Pearson's linear correlation was used to describe the 2-dimensional relationship between response magnitudes and recording parameters.

Unlabelled, putative dopamine neurons were analysed in addition to identified dopamine neurons. Neurons with a spike duration (threshold-to-trough) for bandpass-filtered spikes more than 1 ms (see inset Figure 6.14A) and a firing rate below 10 spikes/s were considered as putative dopamine neurons (Barter, Li, et al. 2015; Hyland et al. 2002; Janezic et al. 2013; Pan et al. 2005; Wang and Tsien 2011).

To obtain examples of shuffled data, corresponding reward periods were randomly positioned along the recording trace (randperm, MATLAB).

2.5.6 Statistical approach for head-fixed awake recordings

The Shapiro-Wilk test was used to judge whether data sets were normally distributed ($p \leq 0.05$ to reject). For normally distributed data, a two-tailed t-test or one-way ANOVA was used. If data failed normality tests, Mann-Whitney rank sum or Kruskal-Wallis one-way ANOVA on ranks with Tukey Kramer post-hoc method for multiple comparisons were used (MATLAB, Mathworks). Significance for all statistical tests was set at $p \leq 0.05$. Boxplots display first quartile, median and third quartile. For the generalised linear regression used for cue-reward conditioning experiments, no correction for multiple comparisons was included. Given relatively small sample sizes of response groups for some statistical tests performed, non-significant results should be treated with caution.

2.6 Stereological cell counting in the midbrain

2.6.1 Retrograde tracer injections

For retrograde tracing experiments of midbrain dopamine neurons projecting to the nucleus accumbens (NAc) and the dorsal striatum (DS) in Chapter 5, adult 3-4 month old male C57Bl/6J mice (see Table 2.4) were anaesthetised using 3% (vol/vol) isoflurane for induction and 1-2% isoflurane for maintenance of anaesthesia. Mice were placed in a stereotaxic frame (Kopf Instruments) on a homeothermic heating mat (Harvard Apparatus) to ensure stable body temperature. Corneal dehydration was prevented using carbomer liquid gel (Viscotears; Alcon) and the mouse was perioperatively injected with buprenorphine (0.03 mg/kg s.c., Vetergesic) to provide analgesia. A small craniotomy was performed above the target region (NAc or DS) to allow access to the brain. For injections, calibrated glass micropipettes (708707; Blaubrand IntraMark) with an inner tip diameter of ∼18 µm were filled with a solution of the retrograde tracer Cholera toxin subunit b (CTB; 0.5% w/v diluted in saline; C9903; Sigma-Aldrich). The micropipette was then lowered into the target

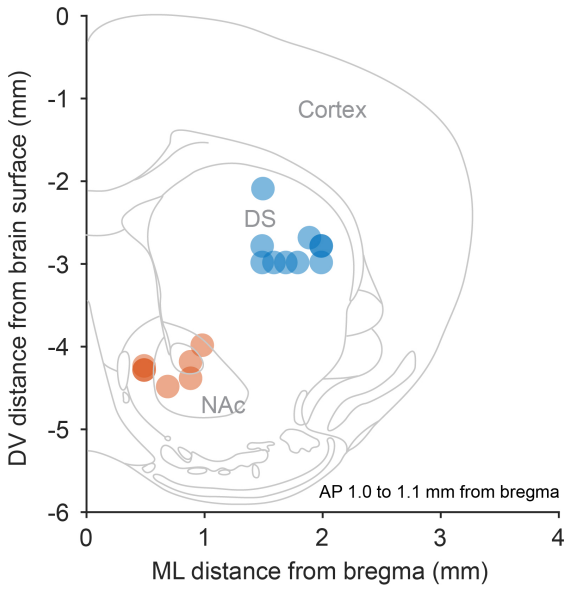

Figure 2.6: Approximate injection sites from retrograde tracing experiments targeted at the nucleus acumbens (orange circles; n = 7 animals) and the dorsal striatum (blue circles; n = 10 animals). NAc, nucleus accumbens; DS, dorsal striatum; AP, anteroposterior; ML, mediolateral; DV, dorsoventral distance from Bregma (Paxinos and Franklin 2013).

region in the brain under stereotaxic control and 150-300 nL CTB were manually ejected at a rate less than 0.05 µL min^{-1} using a 5 mL syringe attached to the micropipette with plastic tubing (inner diameter 0.08 cm; Tygon Lab Tubing, 06407-70, Cole-Parmer). All injections were unilateral (right hemisphere) targeted at the NAc (n = 7; AP: 1.0, ML: 0.7, DV: -4.3) or DS (n = 10; AP: 1.1, ML: 1.8, DV: -3; Figure 2.6) (Paxinos and Franklin 2013). Pipettes were left in place for 5-10 minutes after CTB injection (to minimise reflux) before they were retracted from the brain.

2.6.2 Tissue preparation and indirect immunofluorescence

9 – 13 days after tracer injection, mice were given a lethal dose of anaesthetic and transcardially perfused with 20 mL of 0.01 M phosphate-buffered saline (PBS) at pH 7.4 followed by 40 mL of 4% w/v paraformaldehyde in 0.1 M phosphate buffer, pH 7.4 (PFA). Brains were left in PFA at 4°C for 12 hours after perfusion and then stored in PBS with 0.05% w/v sodium-azide. Fixed brains were sectioned at 50 µm in the coronal plane on a vibrating blade microtome (VT1000S; Leica Microsystems). To ensure comparability between animals, midbrain sections were sampled with an

equal distance of 200 µm along the rostro-caudal axis (i.e. distance between two sections was 200 µm) and washed in PBS. Sections were preincubated for 1 h in 10% normal-donkey-serum in PBS with 0.3% (vol/vol) Triton X 100 (PBS-Triton; Sigma-Aldrich). Using a combinatorial protocol with partial overlap, free-floating sections of individual series were incubated overnight at room temperature in PBS-Triton with chicken anti-TH (1:250/500, ab76442; Abcam), mouse anti-CTB (1:500, ab35988; Abcam) and one or two of the primary antibodies listed in bold in Table 2.6. Sections were then washed in PBS and incubated for > 4 h at room temperature in PBS-Triton with AMCA-conjugated secondary antibody to visualise immunoreactivity for TH (donkey anti-chicken IgG, 1:500, 703-155-155; Jackson Immunoresearch Laboratories), CY3-conjugated secondary antibody to visualise immunoreactivity for CTB (donkey anti-mouse IgG, 1:500, 715-165-151; Jackson Immunoresearch Laboratories) and AlexaFluor 488- and/or 647-conjugated secondary antibodies to reveal immunoreactivity for the additional marker(s) (for secondary antibodies see Table 2.7). Tissue sections were then mounted on slides with fluorescence mounting medium (Vectashield; Vector Laboratories) for viewing and imaging. In addition to midbrain series, CTB immunoreactivity was visualised in sections containing NAc and DS to confirm the location of the injection site (protocol for CTB labelling identical to midbrain sections). Additionally, for Figure 5.4A, striatal sections of a non-injected male C57Bl/6J mouse were processed for Aldh1a1 immunoreactivity with an identical protocol using rabbit anti-Aldh1a1 (1:500, HPA002123; Sigma-Aldrich) and AlexaFluor 488-conjugated secondary antibody (1:500, A21206; Life technologies).

2.6.3 Tiled image acquisition and counting strategy for stereology

Projection target-specific molecular marker expression in midbrain dopamine neurons was assessed on 6 coronal sections of the midbrain (approximate rostro-caudal distance from Bregma: -3.8 / -3.6 / -3.4 / -3.2 / -3.0 / -2.8 mm). Stereological sampling of midbrain dopamine neurons was performed of the entire SNc and

Table 2.6: Primary antibody information. Antibodies used for combinatorial protocols in section 2.6.2 are highlighted in bold.

Antigen	Species	Supplier and code	Dilution
Tyrosine hydroxylase	Chicken	Abcam ab76442	1:500
Tyrosine hydroxylase	Mouse	Sigma T2928/T1299	1:1000
Calbindin	Rabbit	Swant CB38	1:1000
Calbindin	Goat	Santa Cruz sc7691	1:500
Calretinin	Rabbit	Synaptic Systems 214102	1:1000
Calretinin	Goat	Swant CG1	1:500
Sox6	Rabbit	Abcam ab30455	1:4000
Sox6	Guinea pig	Gift from M.Wegner	1:1000
Aldh1a1	Rabbit	Sigma HPA002123	1:500
SatB1	Goat	Santa cruz sc5989	1:1000
Girk2	Goat	Abcam ab65096	1:1000
Otx2	Goat	R&D systems AF1979	1:1000
Cholera toxin subunit b	mouse	Abcam ab35988	1:500

VTA ipsilateral to the CTB tracer injection site (right hemisphere) excluding the dopamine neuron group A8 (located in the retrorubral field). Regions of interest on each section (defined with immunofluorescence labelling for tyrosine hydroxylase) were first determined using a 5x objective lense (numerical aperture 0.16). A series of completely tessellated z-stacked images was then acquired of each region of interest with a 20x objective (numerical aperture 0.8) on an epifluorescence microscope (AxioImage.M2; Carl Zeiss) equipped with Stereoinvestigator software 9.0 (MBF Bioscience) using appropriate sets of filter cubes: AMCA (excitation 299 – 392 nm, beamsplitter 395 nm, emission 420 – 470 nm), AlexaFluor 488 (excitation 450 – 490 nm, beamsplitter 495 nm, emission 500 – 550 nm), CY3 (excitation 532 – 558 nm, beamsplitter 570 nm, emission 570 – 640 nm) and AlexaFluor 647 (excitation 625 – 655 nm, beamsplitter 660 nm, emission 665 – 715 nm). Z-stacked images were acquired with 1 µm steps ('optical sections') at 0 – 10 µm from the upper surface of the section. This defined a 10 µm optical disector that

Table 2.7: Secondary antibody information.

Antigen	Fluorophor	Supplier and code	Dilution
Chicken IgG	AMCA	Jackson Immunoresearch 703-155-155	1:500
Mouse IgG	CY3	Jackson Immunoresearch 715-165-151	1:500
Rabbit IgG	AlexaFluor 488	Life technologies A21206	1:500
Rabbit IgG	AlexaFluor 647	Jackson Immunoresearch 711-605-152	1:500
Goat IgG	AlexaFluor 488	Life technologies A11055	1:500
Goat IgG	AlexaFluor 647	Jackson Immunoresearch 705-605-147	1:500
Guinea pig IgG	AlexaFluor 647	Jackson Immunoresearch 706-605-148	1:500

was overlaid with 2-dimensional counting frames (320 x 420 µm; consisting of two perpendicular exclusion lines and two perpendicular inclusion lines) to perform cell counts. Individual neurons were counted if their nucleus was in focus within the 10 µm optical disector (West 1993). A neuron was classified as not expressing the tested molecular marker only when positive immunoreactivity could be observed in other cells on the same optical section as the tested neuron. Every marker-combination was counted in a minimum of three animals per injection site (i.e. six series per marker). Absolute counts were exported from Stereoinvestigator to Excel (Microscoft) and into MATLAB (Mathworks) for further analysis.

2.6.4 Analysis of stereological cell counts

For the analysis of cell counts, data were sorted by marker combination. All numbers reported are based on the total number of counts on six rostro-caudal sections. Counted combinations included: all neurons expressing TH; neurons expressing TH and the respective marker (listed in bold in Table 2.6); TH-neurons containing the tracer (CTB); TH-neurons expressing the respective marker, and containing the tracer. To obtain proportions of midbrain dopamine neurons co-expressing a particular marker (or co-expressing marker and tracer), counts were collapsed across

sections and divided by the collapsed number of TH-positive neurons in the same series. Sample plots of marker distributions on three rostro-caudal sections (Figure 5.1C) were obtained by importing 2-dimensional coordinates (relative to an arbitrary reference point set in Stereoinvestigator) of all TH neurons and TH-marker-positive neurons into MATLAB (Mathworks) and plotting them onto custom drawn reference sections (based on Fu et al. 2012). Total numbers of TH-neurons and TH-neurons co-expressing the tracer were plotted for each of the six rostro-caudal levels. A projection target discrimination index was calculated as the difference between the proportion of TH-marker-tracer positive neurons targeting the DS and the proportion of TH-marker-tracer positive neurons targeting the NAc (positive indices indicate a preference for DS- over NAc-projection and negative indices indicate a preference for NAc- over DS-projection). Displayed images were acquired using a confocal laser-scanning microscope (LSM710, 20x objective, numerical aperture 0.8; Carl Zeiss) and ZEN software (2008, Carl Zeiss). Example images of injection sites were acquired as tiled single images in Stereoinvestigator (MBF Bioscience) using a combination of transmitted and reflected light illumination on an epifluorescence microscope (AxioImager.M2, Carl Zeiss, 10x objective, numerical aperture 0.45).

3

R1441C *LRRK2* BAC transgenic rats show motor impairment and progressive changes in firing of SNc dopamine neurons

Contents

3.1 Introduction

Dopamine neuron circuits are involved in motor and cognitive functions as well as motivationally guided behaviour, and their dysfunction plays a role in multiple diseases such as addiction, schizophrenia or Parkinson's (Di Chiara and Imperato 1988; Fearnley et al. 1991; Hassler 1938; Koob et al. 1988; Seeman et al. 1993). Age is the biggest risk factor for Parkinson's which in turn is one of the most common neurodegenerative diseases: It affects over 1 % of the population over the age of 60 and 5 % of the population over the age of 85 (Guttmacher et al. 2003; Lau et al. 2006; Wood-Kaczmar et al. 2006). Parkinson's is clinically described by motor symptoms such as resting tremor, postural instability and muscular rigidity and non-motor symptoms such as disorders of sleep or loss of olfaction (Ross et al. 2008; Samii et al. 2004). Post mortem, Parkinson's patients are typically found to have a severe loss of dopamine neurons in the substantia nigra pars compacta (SNc) together with Lewy bodies, abnormal intraneuronal protein aggregates with α-synuclein as a major component (Spillantini et al. 1997). Olfactory impairments are considered an early feature of Parkinson's, detectable at preclinical stages in motor asymptomatic individuals (Hawkes 2008; Hawkes et al. 2010). Using olfaction as a biomarker might thus help develop new therapeutic approaches applicable at early stages of the development of Parkinson's when SNc dopamine neuron loss is less severe.

Investigating the dopamine system *in vivo* is critical for understanding the properties of SNc dopamine neurons in intact brain circuitry and how their properties might change during disease progression. To do this in humans is challenging because of the invasive nature of directly recording the electrical activity of dopamine neurons (and would not be ethical in healthy controls). However, the similarities in mammalian nervous systems allow the use of animal models to study disease-related mechanisms. Neurotoxin-induced models, using for example 6-hydroxydopamine (6-OHDA) or 1-methyl 4-phenyl 1,2,3,6-tetrahydropyridine (MPTP) (reviewed in Deumens et al. 2002; Smeyne et al. 2005), have helped to elucidate the effects of midbrain dopamine neuron loss on neuronal networks, but are not well suited for

studying the progressive nature of the disease. Following the discovery of human genes associated with familial and non-familial forms of Parkinson's (Satake et al. 2009; Simón-Sánchez et al. 2009), it was tried to capture such genetic burden in transgenic animals to model Parkinson's with a view to understanding why those genes are harmful, what early disease stages look like and how the disease progresses. One of the most common genetic susceptibility locus for Parkinson's are mutations in the gene encoding for leucine-rich repeat kinase 2 (LRRK2) (Di Fonzo et al. 2005; Gilks et al. 2005; Saunders-Pullman et al. 2006) with the most prevalent mutations occurring in the MAP kinase-like domain (e.g. G2019S) and in the GTPase domain (e.g. R1441C) (Gilks et al. 2005; Paisan-Ruiz et al. 2004; Zimprich et al. 2004). Globally, the G2019S mutation accounts for 4 % of familial and 1-2 % of so-called sporadic cases of Parkinson's (Gilks et al. 2005; Healy et al. 2008). However, in Ashkenazi Jews with Parkinson's, the G2019S mutation was detected in 14 – 18 % of cases (Orr-Urtreger et al. 2007; Ozelius et al. 2006; Saunders-Pullman et al. 2006) and in almost 40 % of a North African population with Parkinson's (Lesage et al. 2006). In other populations, the R1441C mutation is more frequent (Criscuolo et al. 2011).

LRRK2 is involved in a diversity of cellular functions, including vesicular trafficking, autophagy and mitochondrial dynamics (Plowey et al. 2008; Shin et al. 2008; Wang, Yan, et al. 2012). LRRK2 is expressed in many human tissue types, including lung, heart, thyroid, and most brain regions (Su et al. 2004; Zimprich et al. 2004).

Different transgenic mouse and rat models have been generated to study the function of wild-type LRRK2 or compare it with its pathogenic forms, including gene knock-in, gene knock-out, overexpression and vector-based (e.g. bacterial-artificial chromosome (BAC)) approaches (Beccano-Kelly et al. 2015; Chen, Weng, et al. 2012; Lee et al. 2014; Li, Liu, et al. 2009; Ramonet et al. 2011; Stafa et al. 2013; Tong et al. 2009; Tsika et al. 2014). Mouse models with gene knock-in (KI) were created with the G2019S, the R1441G and the R1441C mutated *LRRK2* (Liu, Lu, et al. 2014; Longo et al. 2014; Tong et al. 2009). While motor deficits in the bar test (a test that measures the animal's ability to respond to an imposed

static posture), drag test (a test that measures the animal's ability to balance during imposed backward dragging) and open field activity were detected in aged G2019S-KI animals (Longo et al. 2014), no motor impairments were found in aged R1441G-KI (12 months) or R1441C-KI (12 and 24 months) animals in the absence of additional drug treatment (Liu, Lu, et al. 2014; Tong et al. 2009). Aged (20 months) inducible or conditional mouse and rat models for R1441C- and G2019S-mutated *LRRK2* did not display motor changes (Lin et al. 2009; Tsika et al. 2014), apart from increased travelled distance in the G2019S rat model (Zhou, Huang, et al. 2011). Vector-based models were created with the G2019S, R1441G, I2020T and R1441C mutant version of *LRRK2*: Some G2019S mouse models showed no change in locomotor activity or balance beam performance (Li, Patel, et al. 2010; Ramonet et al. 2011), others showed increased locomotor activity (Melrose et al. 2010). G2019S BAC-transgenic rat models showed increased postural instability and rear counts (Lee et al. 2014) or decreased fall latency on the rotarod (Walker et al. 2014). I2020T *LRRK2* transgenic mice showed motor impairments on the balance beam and the rotarod at variable ages of the animals (e.g. at 4 months but not 18 months) (Maekawa et al. 2012). Aged R1441G BAC mouse models showed decreased rearing activity (Bichler et al. 2013; Li, Liu, et al. 2009) and in one study also decreased fall latency on the rotarod (Dranka, Gifford, Ghosh, et al. 2013). Loss of SNc dopamine neurons was not reported in any of these models. An aged R1441C *LRRK2* mouse model showed decreased locomotor activity accompanied by loss of SNc dopamine neurons (Ramonet et al. 2011).

Taken together, while this shows the extensive range of different transgenic *LRRK2* models of Parkinson's, few of them replicate the hallmark symptoms and progressive nature of the disease. Additionally, none of these models were tested for altered function of midbrain dopamine neurons. In this Chapter, a novel BAC-transgenic rat model expressing the R1441C mutant or the wild-type form of the human *LRRK2* genomic locus was used to investigate the impact of the mutation on behaviour and *in vivo* firing properties of midbrain dopamine neurons (see also Sloan et al. 2016).

3.2 Aims

The overall objective of the research detailed in this Chapter was to use a novel transgenic rat model of Parkinson's to define the impact of the R1441C *LRRK2* mutation on (1) behavioural phenotype and (2) the *in vivo* firing properties of SNc dopamine neurons. The specific aims of this research were to:

- Define the olfactory performance of aged R1441C *LRRK2* rats.
- Test the motor function of aged R1441C *LRRK2* rats.
- Measure *in vivo* firing properties of SNc dopamine neurons in aged R1441C *LRRK2* mutant rats.
- Measure *in vivo* firing properties of SNc dopamine neurons in young adult R1441C *LRRK2* mutant rats.

3.3 Methods

LRRK2 transgenic rats used for experiments in this Chapter were generated by our collaborators in the Oxford Parkinson's Disease Centre (OPDC) (Sloan et al. 2016). Young-adult (6 month old) or aged (16-22 month old) male rats were used for experiments. For recordings, only histochemically identified (i.e. tyrosine hydroxylase-expressing) neurons located within the SNc were included in the analysis (see section 2.4.3). Experiments and analysis were performed blind to genotype. Detailed experimental methods are described in:

2.1 Animals

2.1.1 *LRRK2* transgenic rats

2.2 Behavioural testing of *LRRK2* rats

2.2.1 Hidden food

2.2.2 Odour discrimination

2.2.3 Balance beam

2.2.4 Open field

2.3 Preparations for anaesthetised electrophysiological recordings

2.3.1 Preparation of anaesthetised rats

2.4 Single-unit recordings and juxtacellular labelling

2.4.1 Single-unit recordings in rats and mice

2.4.2 Juxtacellular labelling and perfuse-fixation

2.4.3 Tissue processing to identify recorded and labelled neurons

2.4.4 Analysis of anaesthetised recordings

2.4.5 Statistical approach for anaesthetised recordings

3.4 Results

3.4.1 Aged R1441C *LRRK2* rats display no impaired olfactory performance

Loss of olfaction is one of the earliest non-motor symptoms frequently reported in Parkinson's patients (Doty, Deems, et al. 1988; Ward et al. 1983) and might potentially be used as a biomarker to detect the disease at a stage of less progressed neurodegeneration (Hawkes 2008; Hawkes et al. 2010). To determine whether overexpression of the human R1441C *LRRK2* variant affects olfactory performance in aged rats, an odour discrimination and a hidden food test was performed on 16-22 month old R1441C *LRRK2* rats (R1441C) and non-transgenic controls (nTG). In the hidden food test (see section 2.2.1), food-restricted rats had to locate a buried chocolate drop using olfaction. R1441C rats did not show a significant increase in search time for the hidden chocolate compared to nTG rats, indicating similar olfactory capabilities of nTG and R1441C rats in locating hidden food (Figure 3.1A). In the odour discrimination task (see section 2.2.2), rats were familiarised with one odour over four trials and presented with a new, unfamiliar odour on the fifth trial. If rats are able to distinguish between the familiar and the new odour, they will spend longer sniffing the new odour (Mandairon et al. 2009; Veyrac, Nguyen, et al. 2007; Veyrac, Sacquet, et al. 2009). Non-transgenic (nTG), but not R1441C *LRRK2* mutant rats spent significantly more time sniffing the new odour (Figure 3.1B). However, to avoid a type 2 statistical error, a discrimination index was calculated as the percentage of total sniffing time spent sniffing the novel odour (a discrimination index of 50 implies equal amounts of time were spent exploring novel and familiar odour; section 2.2.2); nTG and R1441C rats had similar discrimination indices (Figure 3.1C). Taken together, these results indicate that nTG and R1441C *LRRK2* mutant rats have similar olfactory capabilities allowing them to spatially locate and discriminate different odours.

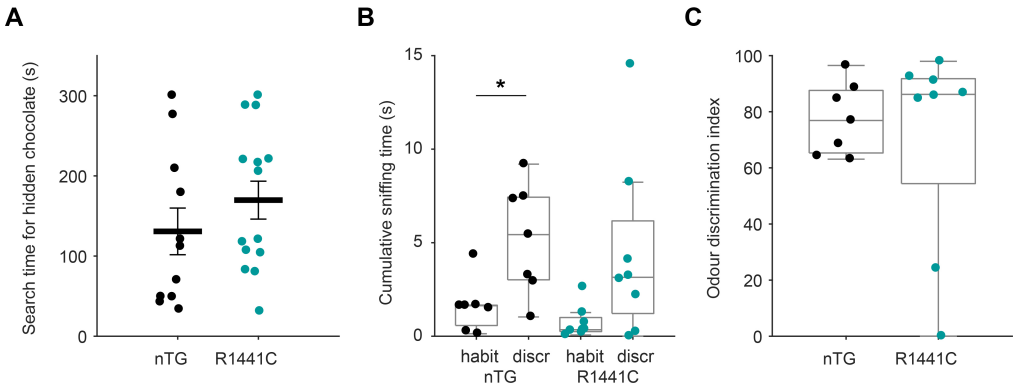

Figure 3.1: Olfactory performance is unaltered in aged R1441C *LRRK2* mutant rats. (A) 16-22 month old R1441C *LRRK2* rats do not show increased search time on a hidden food task compared to non-transgenic controls (nTG n = 11; R1441C n = 14; t-test, p = 0.30). (B-C) Olfactory discrimination is similar between 16-22 month old nTG controls and R1441C mutant rats (nTG n = 7, R1441C n = 8). (B) nTG controls show significantly increased sniffing time of a novel odour (discr) compared to a familiar odour (measured on habituation trial 4 (habit)) (Mann-Whitney rank sum, p = 0.03). (C) R1441C *LRRK2* mutant rats as well as nTG controls show similar odour discrimination indices (calculated as discr/(discr-habit)*100; see section 2.2.2; Mann-Whitney rank sum, p = 0.61). Black bars in (A) indicate mean ± SEM; boxplots in (B-C) display first quartile, median and third quartile.

3.4.2 Aged R1441C *LRRK2* rats display motor impairment

Motor impairments are hallmark symptoms of Parkinson's. To determine whether R1441C *LRRK2* rats display impaired motor performance, 16-22 month old R1441C *LRRK2* rats were compared with non-transgenic controls in a balance beam task (see section 2.2.3). R1441C *LRRK2* rats performed significantly worse on the balance beam test compared to nTG controls (Figure 3.2A). Non-transgenic controls managed to traverse on average ∼50 % of the total beam length (130 cm) but R1441C *LRRK2* transgenic rats traversed only ∼20 %. Comparison of the average weight showed no difference between genotypes (nTG 689 ± 32 g and R1441C 693 ± 20 g; mean ± SEM; t-test, p = 0.91), indicating that the impaired balance beam performance in R1441C *LRRK2* mutant rats was not due to differences in weight. Open field recordings were made to assess the locomotor and explorative activity of R1441C *LRRK2* rats. Both distance travelled, as well as time spent in the surrounding of the arena, were similar between nTG and R1441C *LRRK2*

rats (Figure 3.2B-D). These data indicate that aged R1441C *LRRK2* rats show motor impairments in a balance beam task.

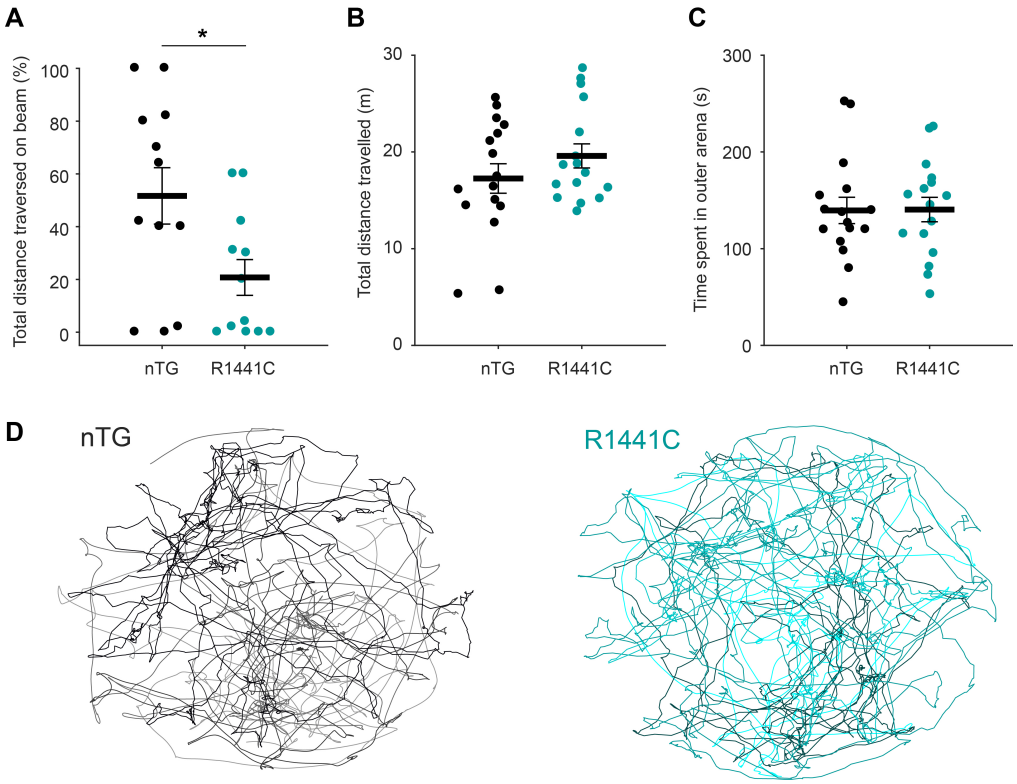

Figure 3.2: Aged R1441C *LRRK2* mutant rats exhibit motor impairment on the balance beam. (A) Mean distance travelled along a 130 cm balance beam with a diameter of 4.5 cm was significantly shorter for R1441C compared to nTG control rats (nTG n = 12, R1441C n = 12; t-test, p = 0.02). (B-D) In an open field arena, R1441C *LRRK2* rats and nTG controls showed similar total distance travelled (t-test, p = 0.25) (B) as well as exploration time of the outer ring of the arena (t-test, p = 0.96) (C) (nTG n = 16; R1441C n = 16). (D) shows overlaid example trajectories in the open field arena for four nTG control rats (left) and four R1441C rats (right). Data from each individual rat are displayed in a different colour shade. Black bars in (A-C) indicate mean ± SEM.

3.4.3 *In vivo* firing of SNc dopamine neurons is more regular in aged R1441C *LRRK2* rats

Rate or pattern changes in the firing of midbrain dopamine neurons can impact on extracellular dopamine concentrations in target structures (Dreyer et al. 2010). To investigate whether the R1441C mutation in *LRRK2* influences the firing of midbrain dopamine neurons, extracellular recordings of the action potentials fired by individual substantia nigra pars compacta (SNc) neurons were made in anaesthetised

16-22 month old nTG and R1441C rats (Figure 3.3). To test whether potential changes in firing rate or pattern were a result of the R1441C mutation in *LRRK2 per se*, or caused by elevated expression of human LRRK2, recordings from SNc dopamine neurons in 16-22 month old hWT rats (which express the human wild-type form of the protein at 4-5 times the level of endogenous rat *Lrrk2* (Sloan et al. 2016)) were also made. Following recordings, each individual neuron was juxtacellularly labelled to verify its location within the SNc and confirm its dopaminergic identity (by immunoreactivity for tyrosine hydroxylase, Figure 3.3).

No difference was observed in the average firing rate of SNc dopamine neurons recorded in nTG, hWT and R1441C rats (Figure 3.4A). However, a significant decrease in the variability of SNc neuron firing in R1441C *LRRK2* rats (as assessed by CV2, a measure of variability in the interspike interval) compared to nTG rats was identified (Figure 3.4B). Since increased power of cortical brain state activity is associated with increased firing variability of SNc dopamine neurons (Brown et al. 2009; Walczak et al. 2017), the average power of the extracted SWA epochs was compared between genotypes. There was no difference in mean power of cortical SWA between recordings from nTG, R1441C or hWT rats (Figure 3.4C).
To explore whether the decrease in firing variability of SNc dopamine neurons in R1441C *LRRK2* compared to nTG rats might be due to a change in burst firing, burst occurrence and percentage of spikes fired in bursts were compared. Both the frequency of bursts and the percentage of spikes fired as bursts were significantly lower in R1441C rats (Figure 3.4D-F). These results did not survive multiple comparisons when data from hWT rats was included (Kruskal-Wallis one-way ANOVA, $p = 0.072$ for frequency of bursts and $p = 0.054$ for percentage of spikes fired as bursts).

3.4.4 *In vivo* firing of SNc dopamine neurons is unaltered in young adult R1441C *LRRK2* rats

The greatest risk factor for Parkinson's is age. To test whether the reduced firing variability and burst firing in SNc dopamine neurons of R1441C rats were

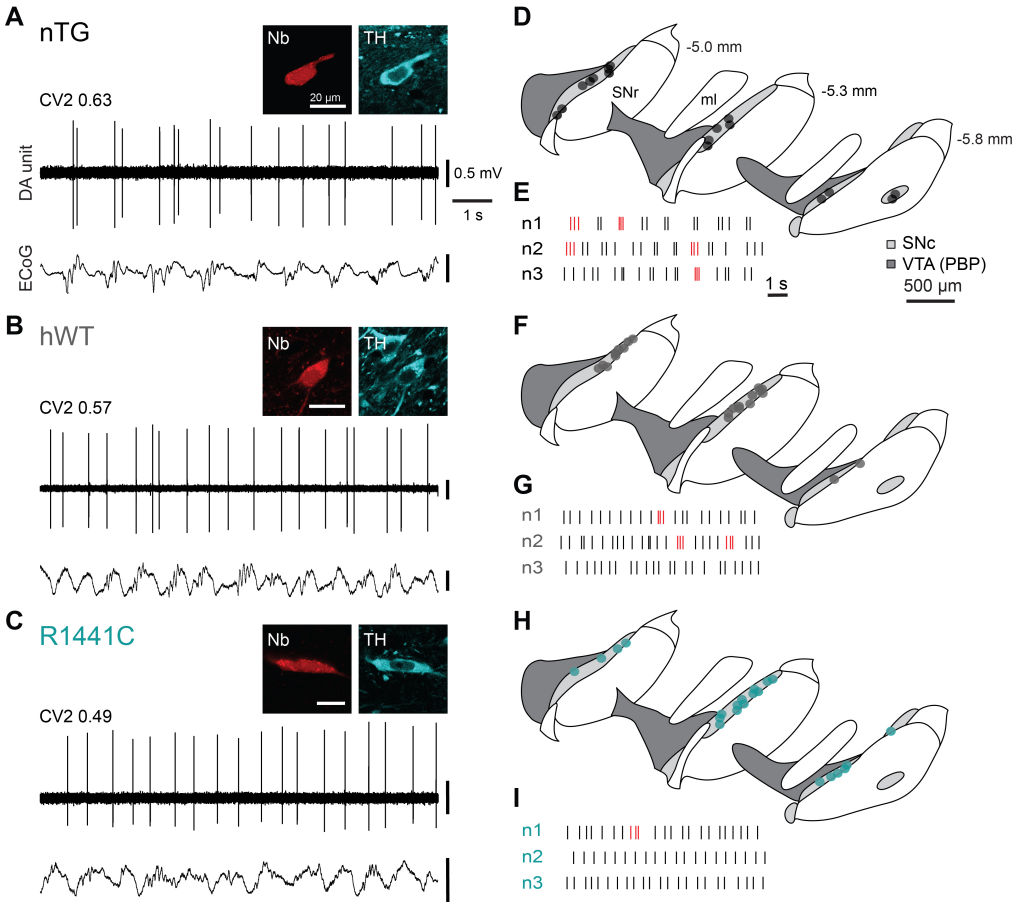

Figure 3.3: Spontaneous activity of identified SNc dopamine neurons in 16-22 month old nTG (A, D, E), hWT (B, F, G), and R1441C rats (C, H, I) during robust cortical slow-wave activity (measured in the electrocorticogram; ECoG). After recording, individual neurons were juxtacellularly labelled with Neurobiotin (Nb) and confirmed to be dopaminergic by expression of tyrosine hydroxylase (TH) immunoreactivity. (E,G,I) Example raster plots denoting 10 s of spike firing in 3 example neurons from each genotype. Spikes detected as occurring within bursts are highlighted in red. (D,F,H) Coronal schematics with approximate locations of recorded and labelled dopamine neurons for each genotype on three rostro–caudal levels (distance caudal to Bregma shown in (D); dorsal top, lateral right). PBP, parabrachial pigmented area of the VTA; SNr, substantia nigra pars reticulata; ml, medial lemniscus (adapted from Paxinos and Watson 2007).

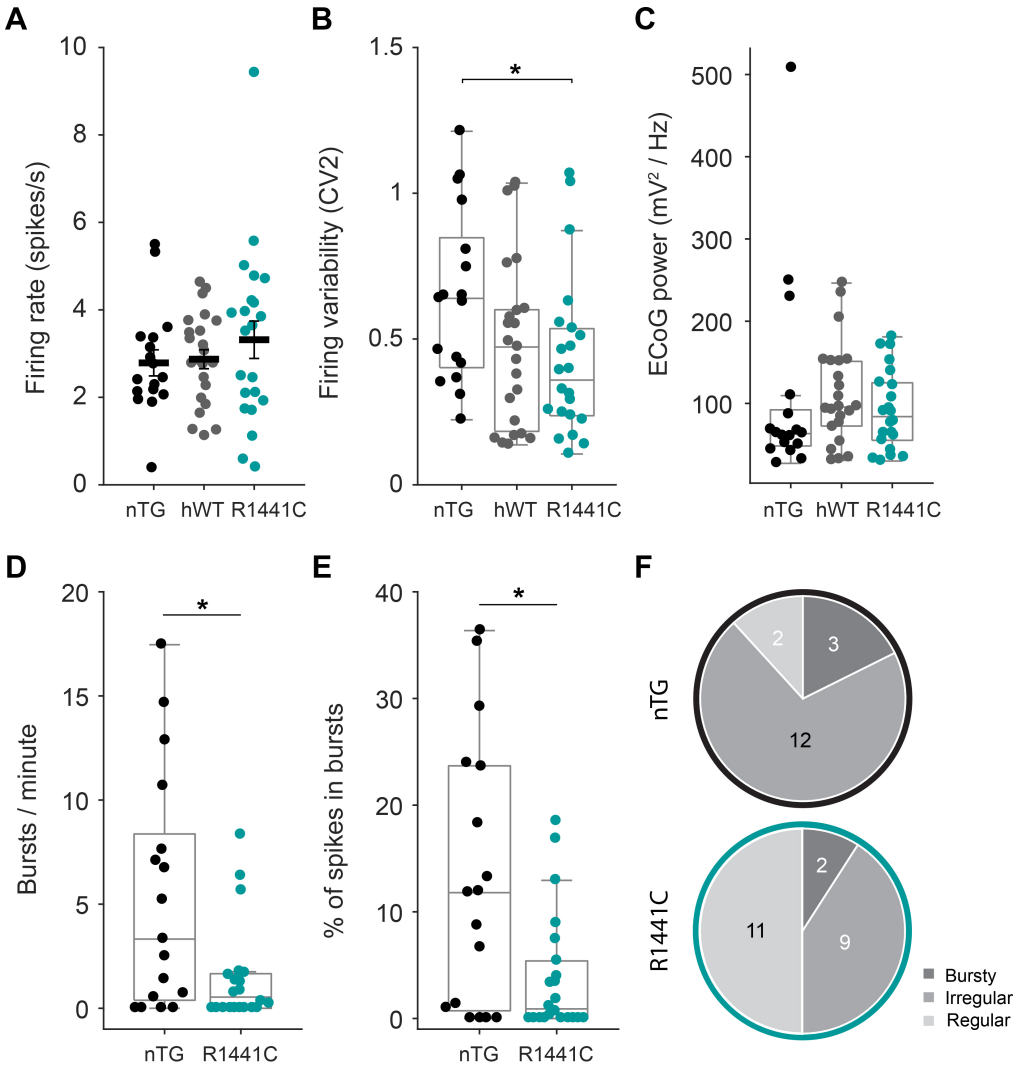

Figure 3.4: SNc dopamine neurons in aged R1441C *LRRK2* rats show reduced burst firing. (A) Mean firing rate (nTG n = 17, hWT n = 23, R1441C n = 22; t-test, p = 0.60) and (B) firing variability of SNc dopamine neurons (nTG n = 17, hWT n = 23, R1441C n = 22, p = 0.045, Kruskal-Wallis one-way ANOVA, Dunn's post hoc test). (C) Mean power of cortical SWA extracted from ECoG recordings (Kruskal-Wallis one-way ANOVA, p = 0.23). (D-E) Mean number of bursts per minute and mean percentage of spikes occurring within bursts (Mann-Whitney rank sum, p = 0.03). (F) Distribution of autocorrelation histogram-based firing pattern classification of dopamine neurons recorded in nTG (top; regular n = 2; irregular n = 12; bursty n = 3) and R1441C rats (bottom; regular n = 11; irregular n = 9; bursty n = 2). Data in (A) are displayed with mean ± SEM. (A-E) each circle represents data from a single neuron. Boxplots in (B-E) indicate first quartile, median and third quartile.

age-dependent, individual substantia nigra pars compacta (SNc) neurons were extracellulary recorded in anaesthetised young adult (6 month) nTG and R1441C rats (Figure 3.5). One would not expect to observe changes in the regularity or 'burstiness' of SNc neuron firing in younger rats if such changes were age-dependent.

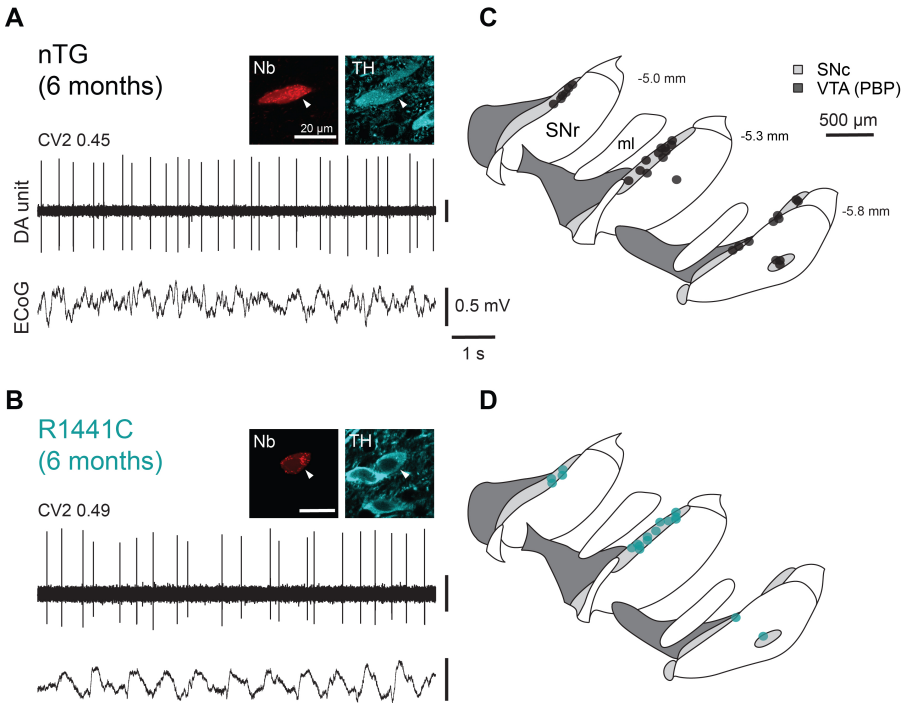

Figure 3.5: Spontaneous activity of identified SNc dopamine neurons in 6-month old nTG (A,C) and R1441C rats (B,D) during robust slow-wave activity (measured in the electrocorticogram; ECoG). Individual neurons were juxtacellularly labelled with Neurobiotin (Nb) and confirmed to be dopaminergic by tyrosine hydroxylase (TH) expression. (C-D) Coronal schematics with approximate locations of recorded and labelled dopamine neurons for each genotype on three rostro–caudal levels (distances caudal from Bregma shown in (C); dorsal top, lateral right). PBP, parabrachial pigmented area of the VTA; SNr, substantia nigra pars reticulata; ml, medial lemniscus (adapted from Paxinos and Watson 2007). Some of the identified SNc dopamine neurons were recorded by Dr. Paul Dodson.

There was no difference in the firing rate, regularity or 'burstiness' of SNc dopamine neurons in 6 month old nTG and R1441C rats (Figure 3.6A-B,D-E). While the average power of cortical SWA was significantly higher in SNc dopamine neurons recorded in nTG rats compared to R1441C rats (Figure 3.6C), this does not argue against the finding of unaltered firing regularity and burst firing in SNc dopamine neurons of young adult R1441C rats compared to nTG rats in this section:

Increased cortical brain state activity leads to increased firing variability (Brown et al. 2009; Walczak et al. 2017), potentially biasing the data recorded from SNc dopamine neurons in 6 month old nTG rats in this section towards higher but not lower CV2 values.

In a previous study, it was shown that SNc dopamine neurons from aged mice display more variable firing *in vitro* (Branch, Sharma, et al. 2014). To test for general age-related changes in firing regularity in the present study, firing regularity was compared between recordings from aged and young adult nTG rats as well as between recordings from aged and young adult R1441C mutant rats. No significant difference in CV2 values was found when comparing recordings obtained from aged and young adult nTG rats (Mann-Whitney rank sum, $p = 0.15$) or when comparing recordings obtained from aged and young adult R1441C rats (Mann-Whitney rank sum, $p = 0.95$).

Taken together, data in this Chapter suggest that the reduction in burst firing of SNc dopamine neurons in R1441C *LRRK2* is age-dependent.

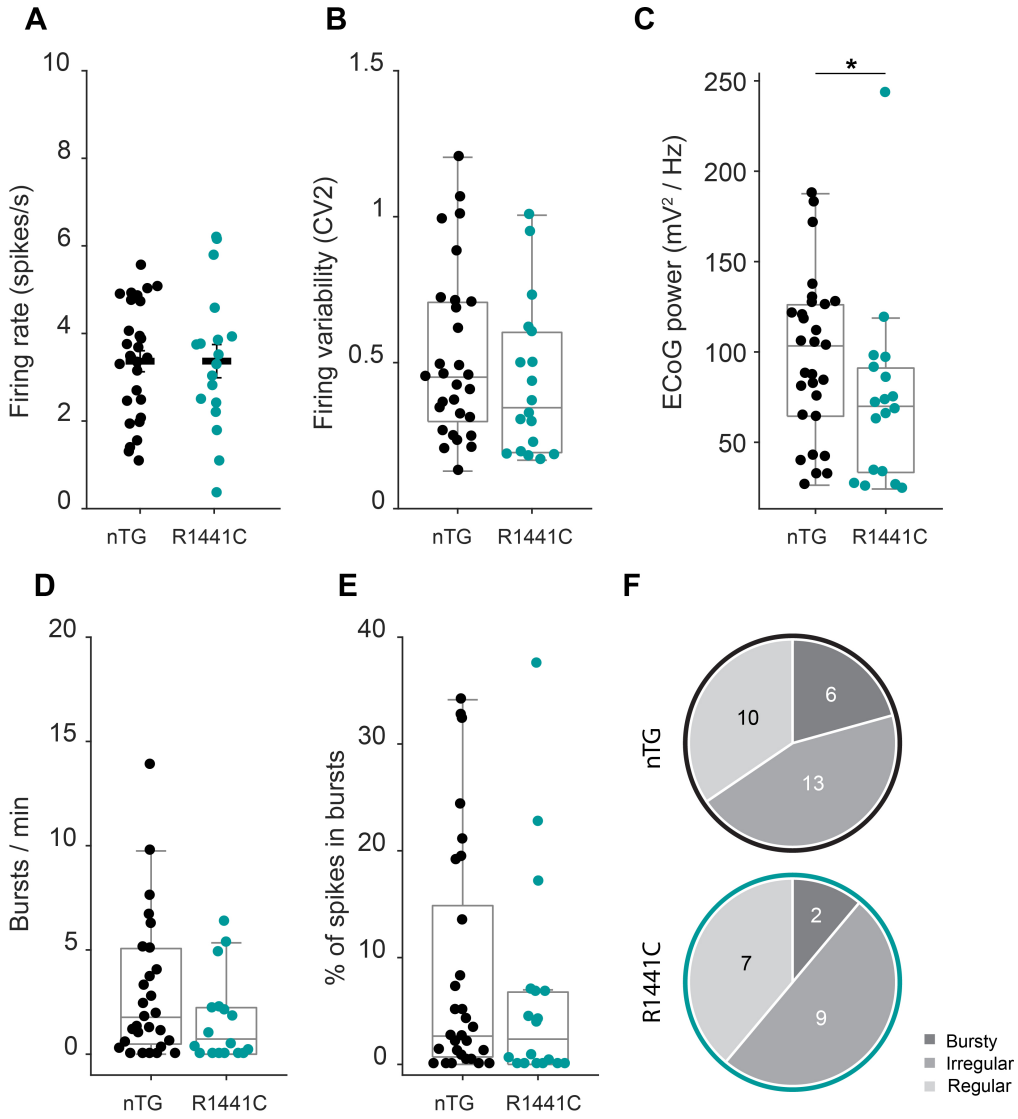

Figure 3.6: *In vivo* firing of SNc dopamine neurons in young adult R1441C *LRRK2* rats and nTG rats is similar. Mean firing rate (t-test, p = 0.996; nTG n = 29 and R1441C n = 18) (A) and firing variability (Mann-Whitney rank sum, p = 0.25; nTG n = 29 and R1441C n = 18) (B) were not significantly different between genotype. (C) Mean power of cortical SWA extracted from ECoG recordings was higher in SNc dopamine neurons recorded in nTG compared to R1441C rats (Mann-Whitney rank sum, p = 0.02; nTG n = 29 and R1441C n = 18), potentially biasing CV2 obtained from SNc dopamine neurons recorded in nTG rats towards higher values (Brown et al. 2009; Walczak et al. 2017). Mean number of bursts per minute (Mann-Whitney rank sum, p = 0.21; nTG n = 29 and R1441C n = 18) (D) and mean percentage of spikes occurring within bursts (Mann-Whitney rank sum, p = 0.34; nTG n = 29 and R1441C n = 18) (E) were not significantly different between genotype. (F) Distribution of autocorrelation histogram-based firing pattern classification in nTG (top; regular n = 10; irregular n = 13; bursty n = 6) and R1441C rats (bottom; regular n = 7; irregular n = 9; bursty n = 2). Data in (A) are displayed with mean ± SEM. (A-E) each circle represents data from a single neuron. Boxplots in (B-E) indicate first quartile, median and third quartile.

3.5 Discussion

In Parkinson's, dopamine neurons in the substantia nigra pars compacta (SNc) degenerate and this degeneration is thought to contribute to motor and non-motor symptoms. However, there might be other changes (e.g. in the firing properties of dopamine neurons or the release of dopamine from terminals) that precede the degenerative phase of the disease. In this Chapter, the behavioural phenotype of a new BAC-transgenic R1441C *LRRK2* transgenic rat model for Parkinson's was assessed in combination with the *in vivo* firing properties of dopamine neurons located within the SNc. Work in collaboration with colleagues from the OPDC demonstrated that this model has no overt loss of dopamine neurons in the SNc and lacks accumulation of neuropathological markers of Parkinson's such as α-synuclein, (pSer202/Thr205) tau or ubiquitin in SNc dopamine neurons (Sloan et al. 2016). However, aged R1441C *LRRK2* mutant rats showed impaired motor performance on the balance beam (within this thesis) and on the rotarod (see Sloan et al. 2016). Previously published studies on rodent models bearing the R1441C *LRRK2* mutation did not show such motor deficits (Ramonet et al. 2011; Tong et al. 2009; Tsika et al. 2014) and changes in locomotor activity were reported in only one case (Ramonet et al. 2011). In previous studies, mice were used as the model species with either heterologous promoter-driven (Ramonet et al. 2011), or Cre-recombinase dependent expression of R1441C *LRRK2* (Tsika et al. 2014), whereas the model used in this Chapter is a BAC-transgenic rat model. Different experimental approaches and species may explain phenotypic differences between models tested for motor behaviour.

Aged R1441C *LRRK2* transgenic rats showed similar olfactory performance compared to non-transgenic controls. This is in accordance with previously published work on R1441C and R1441G *LRRK2* models (Bichler et al. 2013; Tsika et al. 2014) but not a separate R1441G *LRRK2* mouse model which showed olfactory impairment on the hidden food task (Dranka, Gifford, McAllister, et al. 2014). Again, this may be the result of different transgenic approaches or experimental designs. Identifying odour detection thresholds of control animals would allow

determining the optimal level of difficulty applied in the actual olfactory task. This is often impractical due to the number of aged animals that would be required for such an experiment. Lack of olfactory impairment in the R1441C *LRRK2* model of this study could also be due to the specific type of mutation. In Parkinson's patients carrying the R1441C *LRRK2* mutation - and more generally in cases of LRRK2-related Parkinson's - mixed results are obtained when tested for olfactory impairments in the UPSIT (University of Pennsylvania Smell Identification Test) (Doty, Shaman, et al. 1984) with some individuals being affected but not others (Ferreira, Guedes, et al. 2007; Khan, Jain, et al. 2005; Markopoulou et al. 1997; Marras et al. 2011; Silveira-Moriyama, Guedes, et al. 2008; Silveira-Moriyama, Munhoz, et al. 2010). Furthermore, while the UPSIT, which is commonly used to assess olfactory function in humans, tests a whole range of odours and how well they can be identified (Doty, Shaman, et al. 1984), the olfactory tests commonly used in rodents might not provide the same level of granularity and sensitivity to detect olfactory impairments. Thus, it remains a possibility that more subtle olfactory changes remain undetected in rodent models of Parkinson's.

Besides *LRRK2*, other susceptibility genes have been implicated in Parkinson's, e.g. point mutations in or locus multiplication of the α-synuclein gene (Chartier-Harlin et al. 2004; Krüger et al. 1998; Polymeropoulos et al. 1997; Singleton et al. 2003; Zarranz et al. 2004) or mutations in the PTEN-induced putative kinase 1 (*PINK1*) gene (Valente, Bentivoglio, et al. 2001; Valente, Brancati, et al. 2002; Valente, Abou-Sleiman, et al. 2004). Transgenic models of α-synuclein or *PINK1*-related Parkinson's show olfactory deficits in similar tests as described in this Chapter (Chesselet, Richter, et al. 2012; Farrell et al. 2014; Fleming, Tetreault, et al. 2008; Glasl et al. 2012; Hansen et al. 2013). However, like LRRK2-linked Parkinson's, olfactory function in patients with α-synuclein- or *PINK1*-related Parkinson's is variable and not reliably impaired (Bostantjopoulou et al. 2001; Krüger et al. 1998). In addition to altered olfaction, cognitive deficits are known non-motor symptoms of Parkinson's (Foltynie et al. 2003). R1441C *LRRK2* rats showed impaired cognitive performance on a spatial short-term memory task (Sloan et al. 2016) and cognitive

changes were also reported for *LRRK2* knock-out (KO) and overexpression models (Beccano-Kelly et al. 2015; Hinkle et al. 2012).

Importantly, the progressive motor and cognitive deficit in R1441C *LRRK2* rats was accompanied by an age-dependent decrease in firing variability and burst firing in SNc dopamine neurons. Changes in the firing of midbrain dopamine neurons were only observed in the 16-22 month old but not in the 6 month old cohorts. No changes in firing properties were observed in transgenic rats expressing human wild-type LRRK2 (hWT). However, there were also no significant differences between hWT and R1441C *LRRK2* rats, leaving open the question whether the level of LRRK2 expression may have some impact on dopamine neuron firing. A reduction in striatal dopamine following degeneration of midbrain dopamine neurons is thought to underlie major symptoms (e.g. motor symptoms) of Parkinson's (Ehringer et al. 1960) but R1441C *LRRK2* transgenic rats did not show detectable loss of SNc dopamine neurons (Sloan et al. 2016). However, not only neurodegeneration but also changes in dopamine release or firing properties of midbrain dopamine neurons are likely to influence striatal dopamine levels. Aged but not young adult R1441C *LRRK2* transgenic rats displayed progressively impaired dopamine release in dorsal striatum as well as altered *in vivo* burst firing (Sloan et al. 2016). Burst firing, rather than increases in tonic activity (i.e. single spike firing), is thought to be a crucial means by which midbrain dopamine neurons can transiently increase striatal dopamine release. It was suggested that burst firing increases dopamine release non-linearly and thus more potently than increased overall tonic activity (Ammari et al. 2009; Chergui, Suaud-Chagny, et al. 1994; Cragg 2003; Gonon 1997; Gonon 1988; Nissbrandt et al. 1994; Overton et al. 1997; Suaud-Chagny, Brun, et al. 1992; Suaud-Chagny, Chergui, et al. 1992). Firing mode-related differences in dopamine release differentially affect postsynaptic dopamine receptor occupancy (Dreyer et al. 2010; Venton et al. 2003), ultimately shaping striatal outputs. Changes in the firing pattern of SNc dopamine neurons in aged R1441C *LRRK2* rats may thus result in diminished dopamine release, changed striatal outputs and contribute to the observed motor deficit. Indeed, motor deficits in R1441C *LRRK2* rats were reversed

by L-DOPA treatment indicating that they were induced by altered dopamine function (Sloan et al. 2016). It is yet to be tested, however, whether the observed cognitive deficits also result from an impaired dopamine system. Interestingly, a recent study showed that lateral – presumably SNc – dopamine neurons were involved in a working memory task (Matsumoto and Takada 2013). Additionally, a study showing impaired object recognition and location in a model overexpressing *LRRK2* linked this deficit to altered presynaptic dopamine receptor 2 signalling at glutamatergic terminals in the striatum (Beccano-Kelly et al. 2015), indicating that the dopamine system might underlie changes in cognitive performance. To test whether cognitive deficits in R1441C *LRRK2* animals were also dopamine-dependent, the spatial short-term working memory task could be performed under L-DOPA treatment. However, since LRRK2 is highly expressed both in cortex and hippocampal regions (Taymans et al. 2006), cognitive deficits could also be explained by the impact of mutated *LRRK2* on cortical or hippocampal brain regions associated with cognitive and memory functions.

None of the other R1441C *LRRK2* transgenic models were tested for changes in electrophysiological properties of the midbrain dopamine system and thus cannot be compared to the decreased burst firing of SNc dopamine neurons in *LRRK2* rats that was observed here. However, altered SNc dopamine neuron firing activity has been reported for other transgenic Parkinson's models. SNc dopamine neurons in α-synuclein overexpressing mice displayed reduced firing rates both *in vivo* in anaesthetised animals (Janezic et al. 2013) as well as in awake animals during quiet rest, with more spikes elicited in bursts (Dodson, Dreyer, et al. 2016). In mice expressing the A53T point mutated variant of α-synuclein, the firing rate of SNc dopamine neurons was increased (Subramaniam et al. 2014). A *PINK1*-deleted mouse model displayed increased firing variability and increased burst firing in putative dopamine neurons (Bishop et al. 2010). Comparing the characteristics of these different models might help shed light on mechanistic aspects of early stages of the disease and its progression, and help answer the question whether changes in firing activity of dopamine neurons are compensatory (e.g. counteract pathological

changes in striatal dopamine), are just by-products of an imbalanced network, or themselves promote the disease phenotype. Abnormal bursting has been suggested as a pathophysiological mechanism elsewhere in the basal ganglia of Parkinson's patients (reviewed in Lobb 2014) but much of the focus in Parkinson's research has been on the degeneration of dopamine neurons. However, changes in their firing might precede protein aggregation and/or cell death and studying them could help disentangle causes of different Parkinson's related symptoms. It remains unclear why changes in firing of midbrain dopamine neurons in Parkinson's models are of such heterogeneous nature ranging from increased firing rate, decreased firing rate to changes in firing pattern. Different types and causes (e.g. different genetic forms) of Parkinson's might underlie these differences. A more causal rather than correlative approach to help answer this question would be the use of optogenetic manipulations of SNc dopamine neurons. If altered firing patterns or rate were pathogenic, then mimicking or restoring normal firing patterns or rate through optical manipulations might help restore otherwise impaired motor function in Parkinson's models.

In the absence of identified external stimuli (e.g. in anaesthetised rodents), dopamine neurons are characterised by low-frequency tonic background firing with embedded spontaneous bursts (Grace and Bunney 1980; Grace and Bunney 1984a; Grace and Bunney 1984b; Sanghera, Trulson, et al. 1984). Burst (but not tonic) firing is abolished in *in vitro* slice recordings, indicating that intact synaptic inputs are required for burst generation. In contrast, tonic firing relies predominantly on intrinsic mechanisms (Khaliq et al. 2008; Khaliq et al. 2010; Morikawa et al. 2011): The small-conductance, calcium-activated potassium (SK) channel for example regulates the precision of tonic firing frequency in midbrain dopamine neurons (Wolfart and Roeper 2002; Wolfart, Neuhoff, et al. 2001), slowly gating hyperpolarization-activated cyclic nucleotide-gated cation (HCN) channels, which mediate Ih currents, contribute to pacemaker frequency control (Chan et al. 2007; Puopolo et al. 2007). Additionally, L-type calcium channels define the TTX-resistant membrane oscillations in most dopamine neurons which stop firing when L-type

calcium channels are blocked (Chan et al. 2007; Puopolo et al. 2007) (see section 1.3.1). Synaptic inputs from the subthalamic nucleus (STN), the pedunculopontine nucleus (PPN) and the laterodorsal tegmental nucleus (LDT) mediate burst firing in midbrain dopamine neurons via postsynaptic N-methyl-d-aspartate (NMDA) receptors (Chergui, Akaoka, et al. 1994; Floresco et al. 2003; Lodge et al. 2006a; Lokwan et al. 1999; Suaud-Chagny, Brun, et al. 1992; Zweifel et al. 2009). In the A53T α-synuclein model, impaired A-type potassium channel function was shown to be an intrinsic mechanism contributing to the increased firing rate in SNc dopamine neurons (Subramaniam et al. 2014), while increased firing variability in the *PINK1*-model was linked to reduced SK channel function (Bishop et al. 2010). A potential means to study mechanisms underlying altered burst firing in SNc dopamine neurons of R1441C *LRRK2* rats would be *ex vivo* slice recordings to reveal whether changes are of afferent or intrinsic nature. A candidate intrinsic mechanism for the reduced burst frequency might be altered NMDA receptor expression or phosphorylation. Since application of NMDA (the agonist for NMDA receptors) was shown to induce burst firing in midbrain dopamine neurons *in vitro* (Blythe et al. 2007; Johnson, Seutin, et al. 1992), possible failure to do so in SNc dopamine neurons of R1441C *LRRK2* rats might indicate that NMDA receptors underlie impaired burst firing. Additionally, mRNA expression levels of NMDA receptor subunits in midbrain dopamine neurons (e.g. NR1) could be measured using UV-laser microdissection to evaluate expression differences between non-transgenic controls and R1441C LRRK2 rats (Gründemann et al. 2008).

Taken together, this Chapter shows that the R1441C *LRRK2* mutation leads to an age-dependent motor deficit and decreases in the *in vivo* burst firing of SNc dopamine neurons. The neurophysiological changes induced by mutant *LRRK2* occur prior to detectable loss of midbrain dopamine neurons.

4

Foxa1 and Foxa2 maintain firing properties of midbrain dopamine neurons in adult life

Contents

4.1 Introduction

Midbrain dopamine neurons are generated in the floor plate region of the mesencephalon during embryonic development (Hynes, Poulsen, et al. 1995). Following proliferation and neurogenesis, midbrain dopamine neurons acquire their molecular phenotype during the differentiation step and migrate to form the different dopaminergic nuclei of the midbrain (Blaess et al. 2015; Wurst et al. 2010). Each step in the development of midbrain dopamine neurons is characterised by the expression of distinct subsets of genes, including transcription factors (reviewed in Blaess et al. 2015). The winged-helix/forkhead transcription factors Foxa1 and Foxa2 (Foxa1/2) are important for the specification and differentiation of midbrain dopamine neurons (Ang 2009; Ferri et al. 2007). They act as so-called 'pioneer proteins' and help other transcription factors bind to highly condensed chromatin in enhancer and promoter regions (Cirillo et al. 2002). In addition to the roles that Foxa1/2 play during development, midbrain dopamine neurons retain expression of Foxa1/2 into adulthood (Besnard et al. 2004; Kittappa et al. 2007). A number of developmental transcription factors were shown to remain expressed in mature midbrain dopamine neurons, e.g. Nurr1, Lmx1a and Lmx1b, Otx2 or Pitx3 (Burbach et al. 2000; Chung, Seo, et al. 2005; Di Salvio, Di Giovannantonio, Omodei, et al. 2010; Smidt, Schaick, et al. 1997; Zetterström et al. 1996). Various studies have addressed the issue of the function of these adult-expressed developmental transcription factors and how they might contribute to the neuron's maintenance (phenotype) and survival. For example, Nurr1 was shown to be important for nuclear-encoded mitochondrial gene expression (Kadkhodaei et al. 2013) and Otx2 negatively controls mRNA levels of the dopamine transporter (Di Salvio, Di Giovannantonio, Acampora, et al. 2010). In addition to their role in early development (Ang 2009), Foxa1/2 were also shown to be important at late embryonic stages to retain the phenotype of midbrain dopamine neurons (Stott et al. 2013). This raises the possibility that Foxa1/2 are not only required to define features of the dopamine system during early and late development but also in the function of the mature dopamine system. It was shown that Foxa1/2 are necessary to preserve expression of transcripts

characteristic for midbrain dopamine neurons such as tyrosine hydroxylase (TH) or DOPA-decarboxylase (DDC) and that protein levels for TH are significantly reduced in the absence of Foxa1/2 (Pristerà et al. 2015). Additionally, conditional Foxa1/2 knock-out led to a reduction in overall dopamine content (Pristerà et al. 2015). However, a largely understudied question is whether and how the expression of developmental transcription factors like Foxa1/2 contributes to the maintenance of the electrophysiological properties of midbrain dopamine neurons *in vivo* in the adult system. This is of particular interest to help reveal how progressive diseases like Parkinson's might affect midbrain dopamine systems prior to overt degeneration of neurons. While some studies report a 40 % loss of SNc dopamine neurons in Foxa1/2 conditional knock-out animals (Domanskyi et al. 2014), there was thus far no study investigating pre-degenerative impact of Foxa1/2 deletion on the firing activity of SNc dopamine neurons. While our collaborators have shown that Foxa1/2 are required to preserve intact striatal dopamine release (Pristerà et al. 2015), the same conditional (tamoxifen-induced) recombinase-based gene knock-out model was used in this Chapter to investigate the role of Foxa1/2 for the maintenance of *in vivo* firing properties of midbrain dopamine neurons in adult mice (see also Pristerà et al. 2015).

4.2 Aims

The research detailed in this Chapter was designed to define the role of the transcription factors Foxa1 and Foxa2 in the maintenance of *in vivo* firing properties of midbrain dopamine neurons. The specific aim of this research was to:

- Quantify *in vivo* firing properties of identified SNc dopamine neurons in adult Foxa1/2 conditional knock-out mice and their genetic controls.

4.3 Methods

Foxa1/2 conditional knock-out and control mice used for experiments in this Chapter were generated by Siew-Lan Ang's group (NIMR, London). 8 week old male control and Foxa1/2 cKO mice received tamoxifen injections; electrophysiological recordings were made up to 2 weeks after the Cre-mediated deletion of Foxa1/2. The use of Slc6a3 (DAT)-Cre mice ensured that Foxa1/2 were deleted only from dopamine neurons. Only histochemically identified (i.e. tyrosine hydroxylase-expressing) neurons located within the SNc were included in the analysis. Experiments and analyses were performed blind to genotype. Detailed experimental methods are described in:

2.1 Animals

2.1.2 Foxa1/2 conditional knock-out mice

2.3 Preparations for anaesthetised electrophysiological recordings

2.3.2 Preparation of anaesthetised mice

2.4 Single-unit recordings and juxtacellular labelling

2.4.1 Single-unit recordings in rats and mice

2.4.2 Juxtacellular labelling and perfuse-fixation

2.4.3 Tissue processing to identify recorded and labelled neurons

2.4.4 Analysis of anaesthetised recordings

2.4.5 Statistical approach for anaesthetised recordings

4.4 Results

4.4.1 SNc dopamine neurons in Foxa1/2 conditional knock-out mice show decreased firing variability and a reduction in burst firing

To test the possibility that Foxa1/2 are important for maintaining appropriate firing of dopamine neurons, extracellular recordings of the action potentials fired by individual dopamine neurons located in the substantia nigra pars compacta (SNc) were made in anaesthetised control mice ($Foxa1^{flox/flox}$;$Foxa2^{flox/flox}$) and Foxa1/2 cKO mice (Slc6a3-iCreERT2/+; $Foxa1^{flox/flox}$;$Foxa2^{flox/flox}$) (Figure 4.1). Identified SNc dopamine neurons fired at less than 10 spikes per second (Figure 4.1A-B and Figure 4.2A) and were located throughout the SNc (Figure 4.1C,E). Electrocorticogram (ECoG) recordings were used to monitor the brain state (Figure 4.1A-B). Only recordings of SNc neuron activity made during cortical slow-wave activity (SWA; see section 2.4.4) were included in the analysis. Changes in firing rate or pattern of SNc dopamine neurons are likely to alter basal ganglia network activity. To assess whether Foxa1/2 were required for appropriate firing activity of SNc dopamine neurons, firing rate and pattern were compared between neurons recorded in Foxa1/2 cKO and control mice. The average firing rate of SNc neurons in Foxa1/2 cKO mice was not significantly different from that of neurons in control mice (Figure 4.2A). However, there was a significant decrease in firing variability of SNc dopamine neurons in Foxa1/2 cKO mice when compared to controls (Figure 4.2B). One possible cause of a decrease in firing variability is a reduction in burst firing (see Chapter on R1441C *LRRK2* transgenic rats, section 3.4.3). Therefore, the frequency of burst firing in SNc dopamine neurons was examined using an unbiased, statistical method of burst detection (Ko et al. 2012). Foxa1/2 cKO mice showed a significant reduction in the occurrence and 'magnitude' of bursts (Figure 4.2D-E). The reduction of burst firing in Foxa1/2 cKO mice was also reflected in the overall firing pattern (defined based on autocorrelation histograms). Firing patterns of SNc dopamine neurons in control mice could be almost evenly divided into those that were regular, irregular or bursty (Figure 4.2F). However, this heterogeneity in

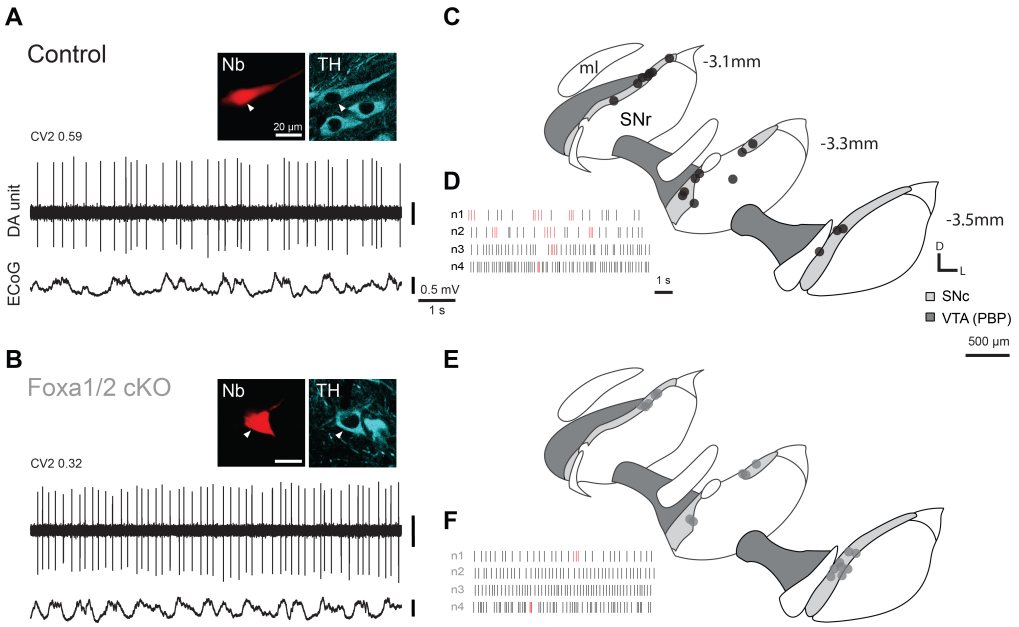

Figure 4.1: Spontaneous activity of identified SNc dopamine neurons in control (A,C-D) and Foxa1/2 cKO mice (B,E-F) during robust cortical slow-wave activity (electrocorticogram; ECoG). Following recording, individual neurons were juxtacellularly labelled with Neurobiotin (Nb) and confirmed to be dopaminergic by expression of tyrosine hydroxylase (TH) immunoreactivity. (C,E) Coronal schematics with locations of recorded and labelled dopamine neurons for control (C) and Foxa1/2 cKO mice (E) on three rostro–caudal levels (distance caudal to Bregma shown in (C)). (D,F) Example raster plots denoting 10 s of spike firing of 4 example neurons (n1-n4) from each genotype. Spikes detected as occurring within bursts by Robust gaussian surprise are highlighted in red. D, dorsal; L, lateral; PBP, parabrachial pigmented area of the VTA; SNr, substantia nigra pars reticulata; SNc, substantia nigra pars compacta; ml, medial lemniscus (adapted from Paxinos and Franklin 2013).

firing was heavily biased towards regular firing in Foxa1/2 cKO mice, with none of the neurons being characterised as bursty based on autocorrelation histograms (Figure 4.2F). To verify that the brain states were equivalent for recordings in both genotypes, the mean SWA power for each recorded neuron was extracted and compared. There was no significant difference in the power of cortical SWA between control and Foxa1/2 cKO mice (Figure 4.2C).

These findings suggest that the Foxa1/2 transcription factors are required for the maintenance of appropriate firing patterns of SNc dopamine neurons.

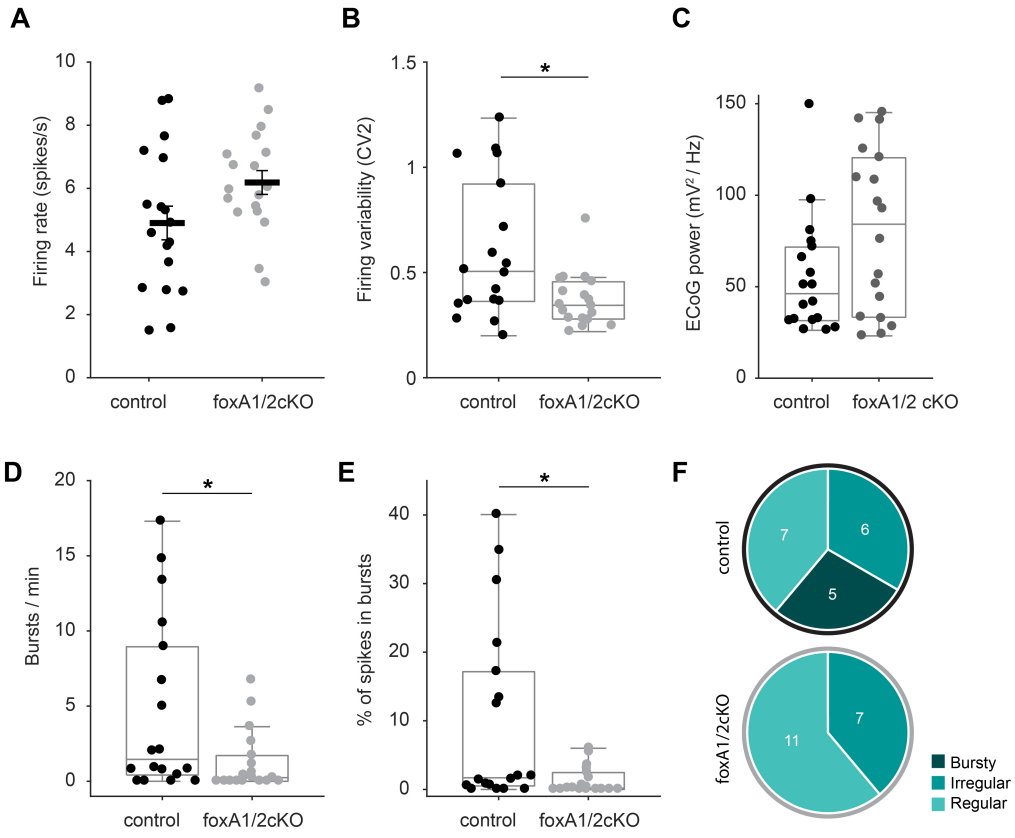

Figure 4.2: SNc dopamine neurons of adult Foxa1/2 cKO mice show a reduction in burst firing *in vivo*. Mean firing rate (t-test, p = 0.06; control n = 18, Foxa1/2 cKO n = 18) (A) and firing variability (B) of SNc dopamine neurons (control n = 18, Foxa1/2 cKO n = 18, Mann-Whitney rank sum, p = 0.02). (C) Mean power of cortical brain state activity in control and Foxa1/2 cKO mice (extracted from ECoG recordings; Mann-Whitney rank sum, p = 0.10; control n = 18, Foxa1/2 cKO n = 18). (D-E) Mean number of bursts per minute as detected by Robust gaussian surprise (Mann-Whitney rank sum, p = 0.04) and mean percentage of spikes occurring within bursts (Mann-Whitney rank sum, p = 0.04). (F) Distribution of autocorrelation histogram-based firing pattern classification in control (top; regular n = 7; irregular n = 6; bursty n = 5) and Foxa1/2 cKO mice (bottom; regular n = 11; irregular n = 7). (A-E) Each circle represents data from a single neuron. Black bars in (A) indicate mean ± SEM; boxplots in (B-E) display first quartile, median and third quartile.

4.5 Discussion

The transcription factors Foxa1 and Foxa2 play crucial roles in the early development as well as the maturation of midbrain dopamine neurons (Ang 2009; Ferri et al. 2007; Stott et al. 2013). Unlike other transcription factors key for development, like Sonic hedgehog (Shh) or Corin (Blaess et al. 2015), Foxa1/2 remain expressed in midbrain dopamine neurons into adulthood, suggesting a functional role in the mature brain. In work with our collaborators, we found that conditional knock-out of Foxa1/2 in midbrain dopamine neurons of adult animals led to a reduction in tyrosine hydroxylase protein levels and dopamine content in midbrain dopamine neurons and dopamine transmission deficits in the dorsal striatum (Pristerà et al. 2015). Notably, Foxa1/2 are not expressed in other dopamine transporter (DAT)-expressing dopamine nuclei in the adult brain, including e.g. the arcuate nucleus, hypothalamus or olfactory bulb, indicating that molecular, physiological and behavioural (see later) changes observed in conditional knock-out animals trace back to altered midbrain dopamine neuron function (Pristerà et al. 2015). To assess whether Foxa1/2 are important for the maintenance of accurate firing properties in midbrain dopamine neurons, extracellular *in vivo* recordings were made from individual midbrain dopamine neurons located in the SNc of control and conditional Foxa1/2 knock-out mice. This revealed a significant reduction in firing variability as well as a reduction in burst frequency in SNc dopamine neurons of conditional Foxa1/2 knock-out mice. Burst firing is thought to be a crucial means of midbrain dopamine neurons to transiently increase striatal dopamine release (Dreyer et al. 2010; Gonon 1988; Nissbrandt et al. 1994) (see discussion section 3.5). The decrease in burst firing of SNc dopamine neurons in conditional Foxa1/2 knock-out mice might therefore lead to a reduction in extracellular striatal dopamine concentration. Bursting in dopamine neurons is controlled largely by synaptic input (Overton et al. 1997; Redgrave et al. 2008; Tepper, Martin, et al. 1995) with NMDA receptors playing a prominent role (Zweifel et al. 2009). More recently, it was also shown that the expression of ATP-sensitive potassium (K-ATP) channels is important for burst firing in SNc dopamine neurons (Schiemann, Schlaudraff, et al. 2012). Interestingly,

expression of the K-ATP channel subunits Sur1 and Kir6.2 in pancreatic β-cells is dependent upon the presence of Foxa2 (Lantz et al. 2004; Sund et al. 2001). Analogous regulation of K-ATP channel subunit expression by Foxa transcription factors could explain the reduction in burst firing of SNc neurons of conditional Foxa1/2 knock-out mice. This hypothesis could be tested by first evaluating whether SNc dopamine neurons of Foxa1/2 knock-out mice show reduced expression of K-ATP channel subunits (e.g. through mRNA expression analysis following laser microdissection; Schiemann, Schlaudraff, et al. 2012) and whether their (e.g. virus-mediated) restoration would lead to a rescued burst firing phenotype. In support of this hypothesis, it was shown that K-ATP channels promote degeneration of SNc dopamine neurons (Liss, Haeckel, et al. 2005) and that their subunit Sur1 shows elevated mRNA levels in SNc dopamine neurons of Parkinson's patients (Schiemann, Schlaudraff, et al. 2012). While the conditional Foxa1/2 knock-out mice displayed reduced burst firing in SNc dopamine neurons (potentially due to decreased K-ATP channel activity), it was suggested that increased K-ATP channel activity in (surviving) SNc dopamine neurons of Parkinson's patients results in increased burst firing (Schiemann, Schlaudraff, et al. 2012). Such up-regulation in burst-promoting channels in patients with Parkinson's could hint at compensatory network measures to counteract lack of striatal dopamine as result of the loss of midbrain dopamine neurons.

Unlike the *LRRK2* rat model discussed in Chapter 3, conditional Foxa1/2 knock-out mice used in this study did not show motor deficits at the time point tested but were instead affected by severe feeding deficits (Pristerà et al. 2015). Foxa1/2 knock-out mice had significantly reduced water and food intake when compared to control animals and this was not linked to reduced locomotor activity, motor coordination, muscle strength or feeding zone entries (Pristerà et al. 2015). However, feeding deficits could be substantially delayed by the administration of L-DOPA, indicating that the dysfunctional dopamine system was involved in the insufficient food and water intake. Aphagic and adipsic behaviour has been linked to the dopamine system in other studies, showing that disruption of the TH gene or

chemical lesioning of the (dorsal striatum-projecting) midbrain dopamine system using 6-OHDA resulted in feeding and drinking deficits (Ligmond et al. 1972; Sotak et al. 2005; Szczypka et al. 1999; Ungerstedt 1971b; Zhou and Palmiter 1995). But unlike in the conditional knock-out model used in this study, these deficits were often accompanied by hypoactivity, leaving it unclear whether they were the result of an impaired motor system or lack in motivation – both of which are linked to the dopamine system (Matsumoto and Takada 2013). However, in other examples, 6-OHDA lesioned rats were shown to retain the ability to perform motor actions required for food intake (Berridge, Venier, et al. 1989). Strikingly, not only dopamine depletion in the striatum but also prolonged dopamine signalling has been shown to lead to feeding deficits: Amphetamine and methamphetamine, cocaine, other blockers of dopamine reuptake or dopamine receptor agonists can result in aphagic behaviour (Al-Naser et al. 1994; Balopole et al. 1979; Chen, Duh, et al. 2001; Kraeuchi et al. 1985; Kuo 2002; Morley et al. 1987; Wellman et al. 2002; Hoek et al. 1994). This led to the hypothesis that adequate feeding behaviour relies on "optimal" levels of dopamine which are neither too high nor too low. Such optimal levels might be provided by the specific dynamics of midbrain dopamine neurons (Heffner et al. 1977), including adequate firing and burst rates. To test the direct effects of reduced burst firing on feeding behaviour, targeted optogenetic stimulation of SNc dopamine neurons using appropriate stimulation patterns could be used to restore burst firing and potentially reverse feeding deficits acutely. Alternatively, stimulation of brain regions implicated in burst generation (e.g. PPN; Floresco et al. 2003; Lokwan et al. 1999) or pharmacological activation of burst-promoting channels (e.g. K-ATP; Schiemann, Schlaudraff, et al. 2012) could help restore burst firing in SNc dopamine neurons to investigate its effect on Foxa1/2 induced aphagia. Taken together, the results in this Chapter show that the developmental transcription factors Foxa1 and Foxa2 are also crucial for the functioning of the dopamine system in the mature brain. Their conditional knock-out decreases *in vivo* burst firing and firing variability of SNc dopamine neurons.

5

Molecular diversity of midbrain dopamine neurons

Contents

5.1 Introduction

Historically, dopamine neurons located in the midbrain were anatomically divided into A9 (co-located with the SNc), A10 (co-located with the VTA) and A8 dopamine neurons (co-located with the RRF) (Dahlström et al. 1964). However, despite their common neurotransmitter phenotype, dopamine neurons in these anatomically defined nuclei show multifaceted heterogeneity (Björklund and Dunnett 2007; Bromberg-Martin et al. 2010; Roeper 2013). For instance, dopamine neurons in the midbrain send efferent projections to different brain regions. Broadly, more lateral located dopamine neurons in SNc preferentially target the dorsal striatum (DS), while more medial located VTA dopamine neurons predominantly target the nucleus accumbens (NAc) and send projections to the prefrontal cortex (PFC) (Bentivoglio et al. 2005; Ferreira, Del-Fava, et al. 2008; Lindvall, Björklund, et al. 1974; Moore and Bloom 1979; Swanson 1982; Thierry et al. 1973; Ungerstedt 1971a). Additionally, dopamine neurons located in SNc but not VTA are preferentially lost in Parkinson's disease (Fearnley et al. 1991; German, Manaye, et al. 1992; Hirsch et al. 1988; Hirsch et al. 1989). One hypothesis is that underlying diverse molecular profiles of midbrain dopamine neurons could account for their differential vulnerability in Parkinson's. Defining molecular diversity of midbrain dopamine neurons contributes to a better understanding of functional diversity in health, and is crucial to allow subtype generation from induced pluripotent stem cells (iPSCs), to widen the genetic tools available to study midbrain dopamine circuits and to develop novel targeted therapeutics for Parkinson's. This Chapter focuses on a selection of seven molecular markers that were shown by others to be differentially expressed in subsets of midbrain dopamine neurons: The calcium-binding proteins Calbindin (Calb1) and Calretinin (Calb2), the G protein-activated inward rectifier potassium channel 2 (Girk2/Kcnj6), the aldehyde dehydrogenase 1 family member A1 (Aldh1a1) as well as the transcription factors Nuclear sex determining region Y box 6 (Sox6), Special AT-rich sequence binding protein 1 (SatB1) and Orthodenticle homeobox 2 (Otx2). These molecules are just a small subset of differentially expressed markers revealed through detailed single-cell gene expression profiling

and microarray studies (Chung, Seo, et al. 2005; Greene, Dingledine, et al. 2005; Greene 2006; Grimm et al. 2004; La Manno et al. 2016; Poulin, Zou, et al. 2014) and were selected in this study for three reasons: (1) Expression is limited to a subset of midbrain dopamine neurons, (2) Expression can be detected with commercially available antibodies, (3) Expression is linked to an intact midbrain dopamine system. Early studies showed that some midbrain dopamine neurons express Calbindin (Celio 1990; Cote et al. 1991; Gerfen, Baimbridge, et al. 1985; Jande et al. 1981) and that they are relatively spared in tissue from Parkinson's patients and animal models (German, Manaye, et al. 1992; Iacopino, Christakos, et al. 1992; Yamada et al. 1990). Calbindin serves as an intracellular calcium buffer and might protect cells from toxic levels of free calcium (Reisner et al. 1992; Schmidt 2012). Calretinin – a calcium-binding protein with some homology to Calbindin – was also shown to be expressed in a subset of midbrain dopamine neurons (González-Hernández, Cruz-Muros, et al. 2010; Isaacs et al. 1994; Liang, Sinton, Sonsalla, et al. 1996; Rogers 1987; Rogers 1992) with some but not complete overlap with Calbindin expression (Nemoto et al. 1999). In addition to calcium-binding proteins, it was also shown that ion channels like Girk2 are selectively expressed in midbrain dopamine neurons. Striatal-projecting dopamine neurons which express Girk2 were selectively affected in so-called weaver mice, a line which carries a spontaneously occurred point missense mutation in the *Kcnj6* gene (Patil et al. 1995; Roffler-Tarlov et al. 1984). Girk2 is a member of the inwardly rectifying potassium channel family that is activated by G protein subunits and is the downstream target of D2-like autoreceptors in dopamine neurons; their activation leads to hyperpolarisation of the plasma membrane (Beckstead, Grandy, et al. 2004; Hille 1992; Kofuji et al. 1995; Wickman et al. 1994). It has also been shown that Aldh1a1 correlates with the differential pattern of midbrain dopamine neuron loss in Parkinson's: Aldh1a1 was shown to be selectively expressed in ventrally located dopamine neurons of the midbrain and to have lower expression levels in post-mortem tissue from Parkinson's patients (Galter et al. 2003; Mandel et al. 2007; McCaffery et al. 1994). Aldh1a1 mediates oxidation of the highly reactive 3,4-Dihydroxyphenylacetaldehyde

(DOPAL) to the less reactive 3,4-Dihydroxyphenylacetic acid (DOPAC) and was shown to be involved in GABA synthesis in dopamine neurons (Kim, Ghazizadeh, et al. 2015; Marchitti et al. 2007). While knock-out of Aldh1a1 alone did not lead to an apparent behavioural phenotype or cell loss (Anderson, Schray, et al. 2011; Wey et al. 2012), Aldh1a1-positive midbrain dopamine neurons in an A53T alpha-synuclein transgenic mouse model were preferentially spared from degeneration (Liu, Yu, et al. 2014) but were differentially affected by the neurotoxin MPTP (Poulin, Zou, et al. 2014), a chemical used to mimic Parkinson's symptoms in animal models. Overexpression of Aldh1a1 had protective effects on dopamine neurons (Liu, Yu, et al. 2014) and post-mortem Parkinson's patient tissue revealed a reduced number in Aldh1a1-positive dopamine neurons (Liu, Yu, et al. 2014). Likewise, it was shown that the developmental transcription factor Otx2, which remains expressed in a subset of VTA dopamine neurons into adulthood (Chung, Seo, et al. 2005; Di Salvio, Di Giovannantonio, Omodei, et al. 2010), confers resistance to MPTP (Di Salvio, Di Giovannantonio, Acampora, et al. 2010). Furthermore, Otx2 is not the only selectively expressed transcription factor in midbrain dopamine neurons, both Sox6 and SatB1 are predominantly expressed in SNc rather than VTA dopamine neurons (Brichta, Shin, et al. 2015; Grimm et al. 2004; Panman, Andersson, et al. 2011; Panman, Papathanou, et al. 2014; Poulin, Zou, et al. 2014). As mentioned above, VTA dopamine neurons predominantly target the NAc and PFC (mesolimbic and mesocortical pathway) and SNc dopamine neurons send efferents largely to the DS (nigrostriatal pathway). While this is a separation of great utility, it remains a simplified conceptual scheme. Rather than constituting a clear cut in their projection targets, SNc and VTA dopamine neurons form an intermingled continuum of neurons projecting to DS, NAc, olfactory tubercle, prefrontal cortex, amygdala, lateral septum and sparsely to other areas (reviewed in Bentivoglio et al. 2005; Fallon and Loughlin 1995) (see Figure 1.1C) organised in a partially topographical pattern (Fallon, Koziell, et al. 1978; Fallon and Moore 1978a; Fallon, Riley, et al. 1978; Fallon and Moore 1978b; Moore 1978). Supporting the idea of separated pathways carrying distinct information, axon collateralization was only

shown for a minority of projection targets including projections to cortical areas (Loughlin et al. 1984), cerebellum (Ikai et al. 1994) or NAc medial shell (Beier et al. 2015) and seemed to be overall minimal (Fallon 1981; Hosp et al. 2015; Matsuda et al. 2009; Yetnikoff et al. 2014). Since these pathways originate from interspersed midbrain dopamine neurons, identifying underlying molecular expression patterns might help place molecules in the context of projection target patterns (Khan, Stott, et al. 2017). In this Chapter, retrograde tracing, immunofluorescence labelling of molecular markers and stereological cell counts were combined to correlate projection targets with molecular marker expression. More specifically, the proportions of NAc- or DS-projecting midbrain dopamine neurons expressing Calbindin, Calretinin, Girk2, Aldh1a1, Sox6, SatB1 or Otx2 were defined.

5.2 Aims

The research detailed in this Chapter was designed to study projection target-specific molecular marker expression in midbrain dopamine neurons of adult C57Bl/6J mice. A set of seven molecular markers known to be expressed in subpopulations of midbrain dopamine neurons was selected and mapped onto NAc- and DS-projecting midbrain dopamine neurons. The specific aims of this research were to:

- Examine the distribution of seven molecular markers expressed amongst midbrain dopamine neurons, including Calbindin, Calretinin, Girk2, Aldh1a1, Sox6, SatB1 and Otx2.
- Assess the proportion of DS-projecting midbrain dopamine neurons, revealed through retrograde tracing with Cholera toxin subunit b, which expressed one of the seven markers.
- Assess the proportion of NAc-projecting midbrain dopamine neurons, revealed through retrograde tracing with Cholera toxin subunit b, which expressed one of the seven markers.

5.3 Methods

3-4 month old male C57Bl/6J mice used for experiments in this Chapter were obtained from Charles River Laboratories. A total of 17 animals were used for the combined retrograde tracing, immunofluorescence labelling and stereology experiments (n = 10 DS-injected and n = 7 NAc-injected). Note that, for cell counts in this Chapter, no boundaries were drawn between VTA and SNc to not conform to preconceptions about location of neurons innervating DS and NAc. Detailed experimental methods are described in:

2.1 Animals

2.1.3 C57Bl/6J mice

2.6 Stereological cell counting in the midbrain

2.6.1 Retrograde tracer injections

2.6.2 Tissue preparation and indirect immunofluorescence

2.6.3 Tiled image acquisition and counting strategy for stereology

2.6.4 Analysis of stereological cell counts

5.4 Results

5.4.1 Overall expression of molecular markers

To assess projection target-specific expression of molecular markers in midbrain dopamine neurons, retrograde tracing was combined with immunofluorescence labelling and a stereological counting strategy. Animals were injected with the retrograde tracer Cholera toxin subunit b (CTB) either into the dorsal striatum (DS) or the nucleus accumbens (NAc) (see section 2.6.1). 9 – 13 days post-injection, brains were removed following perfuse-fixation through the vascular system and cut at 50 µm thickness per section. Midbrain sections were divided into 4 series so that each series contained six sections spaced 200 µm apart. Series were then processed to reveal tyrosine hydroxylase (TH), tracer (CTB) and selected markers. Neurons were identified as dopamine neurons by positive immunolabelling for TH. Additionally, sections containing DS and NAc were processed for CTB immunolabelling to confirm injection sites (Figure 5.2C-D and Figure 5.3C-D). A maximum of two markers (in addition to TH and tracer) could be used per series due to limited availability of fluorophores with non-overlapping emission/excitation spectra. Counts were performed on a series of six midbrain sections (spanning the rostrocaudal extent of the dopaminergic midbrain), scanned as tiled z-stacks using Stereoinvestigator (with a step size of 1 µm at 0 – 10 µm from the surface of the section). Drawings of contours for the scanning area were guided by TH-labelling and counts were performed on the entire midbrain containing TH-positive neurons (excluding A8; see section 2.6.3). The subset of markers tested were the calcium-binding proteins Calbindin and Calretinin, the potassium channel Girk2, the aldehyde dehydrogenase Aldh1a1 and the transcription factors Otx2, Sox6 and SatB1. All seven markers were previously shown to be expressed in subsets of dopamine neurons (Chung, Seo, et al. 2005; Greene 2006; Greene, Dingledine, et al. 2005; Grimm et al. 2004; La Manno et al. 2016; Poulin, Zou, et al. 2014).

Firstly, marker expression pattern on midbrain sections was assessed qualitatively (irrespective of CTB tracer labelling). The overall pattern of marker expression was

in accordance with the literature. Girk2 was expressed in SNc and to a lesser extent in VTA dopamine neurons (Schein et al. 1998) (Figure 5.1C). SatB1 and Sox6 had largely overlapping expression patterns with positive dopamine neurons located mostly in SNc (Brichta, Shin, et al. 2015; Panman, Papathanou, et al. 2014) (Figure 5.1C). Aldh1a1 was expressed in ventral populations of SNc and VTA dopamine neurons (Liu, Yu, et al. 2014) (Figure 5.1C). Calbindin was expressed in many medially located VTA dopamine neurons, scattered throughout the extent of VTA and expressed in sparse cell populations in lateral aspects of SNc and substantia nigra pars lateralis (SNl) (Liang, Sinton, Sonsalla, et al. 1996) (Figure 5.1C). Calretinin displayed a similar but not entirely overlapping expression pattern as Calbindin (Liang, Sinton, and German 1996) (Figure 5.1C). Otx2 was restricted to a ventral portion of medial dopamine neurons (Di Salvio, Di Giovannantonio, Omodei, et al. 2010) (Figure 5.1C). Collapsing data across injection sites, rostrocaudal sections, and SNc/VTA, an average of 53 ± 2 % (mean ± SEM) of all counted TH-positive neurons co-expressed Girk2, 51 ± 3 % (mean ± SEM) co-expressed SatB1, 36 ± 2 % (mean ± SEM) co-expressed Sox6, 40 ± 1 % (mean ± SEM) co-expressed Aldh1a1, 29 ± 2 % (mean ± SEM) co-expressed Calretinin, 45 ± 2 % (mean ± SEM) co-expressed Calbindin, and 12 ± 2 % (mean ± SEM) co-expressed Otx2 (Figure 5.1B).

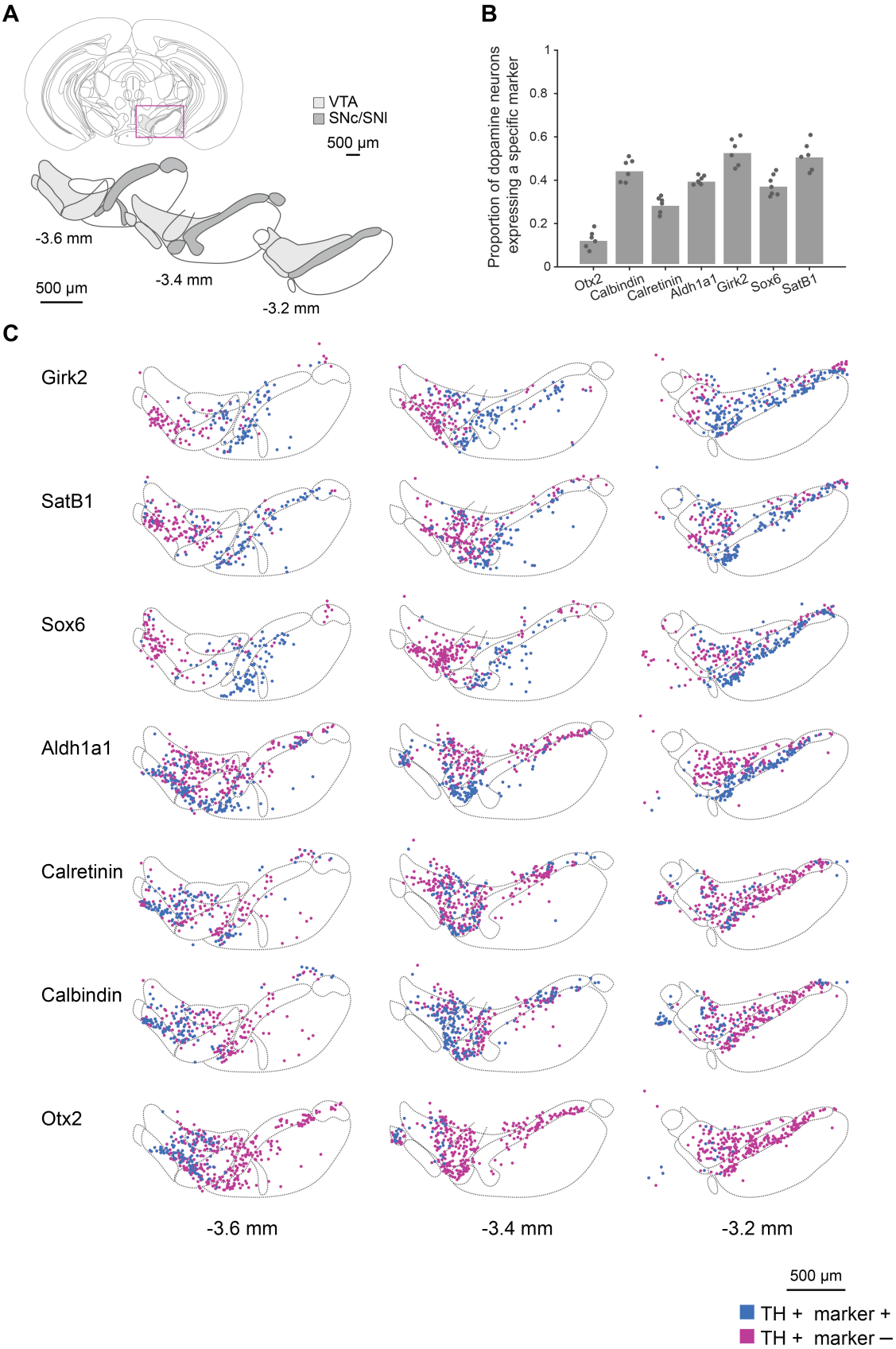
A
VTA
SNc/SNl
500 µm
-3.6 mm
500 µm
-3.4 mm
-3.2 mm
B
Proportion of dopamine neurons expressing a specific marker
1
0.8
0.6
0.4
0.2
0
Otx2
Calbindin
Calretinin
Aldh1a1
Girk2
Sox6
SatB1
C
Girk2
SatB1
Sox6
Aldh1a1
Calretinin
Calbindin
Otx2
-3.6 mm
-3.4 mm
-3.2 mm
500 µm
TH + marker +
TH + marker –

Figure 5.1: Co-expression pattern of selected molecular markers in midbrain dopamine neurons. (A) Schematics of three coronal midbrain sections (whole brain section adapted from Paxinos and Franklin 2013). (B) Proportions of midbrain dopamine neurons (identified by the expression of tyrosine hydroxylase, TH) co-expressing the markers Otx2, Calbindin, Calretinin, Aldh1a1, Girk2, Sox6 and SatB1. Proportions are calculated from summed counts across 6 midbrain sections spanning the rostrocaudal axis (see Figure 5.2 and Figure 5.3). (C) Examples of the distribution of TH-positive neurons (magenta) and TH-positive neurons co-expressing the respective marker (blue) on three coronal midbrain sections. Distances taken relative to Bregma (Paxinos and Franklin 2013). VTA, ventral tegmental area; SNc, substantia nigra pars compacta; SNl, substantia nigra pars lateralis; TH, tyrosine hydroxylase.

5.4.2 Molecular markers of dorsal striatum-projecting midbrain dopamine neurons

To assess the proportion of DS-projecting midbrain dopamine neurons expressing a specific marker, the number of triple-positive neurons (TH, marker, tracer) was counted on the six selected rostrocaudal levels of DS-injected brains (with no borders between SNc and VTA) (Figure 5.2C-D). The distribution of total counts of TH-positive neurons across the six coronal midbrain sections of all counted series (n = 15) is shown in Figure 5.2E. Fewest TH-positive neurons were found in the most rostral and caudal sections, similar to the counts obtained from NAc-injected tissue (see section 5.4.3; Figure 5.3E). Collapsed across rostrocaudal sections, 104 (interquartile range [60 124]) of TH-neurons per series were tracer-positive.

To assess marker expression of DS-projecting dopamine neurons, the proportion of triple-positive neurons (TH, tracer, marker) was calculated. Two of seven markers were expressed in more than 90 % of DS-projecting dopamine neurons; on average, 95 % of DS-projecting dopamine neurons were positive for Girk2 and 94 % were positive for SatB1 (Figure 5.2A-B). Additionally, Sox6 was expressed in 88 % and Aldh1a1 in 83 % of DS-projecting dopamine neurons (Figure 5.2A-B). The remaining three markers were expressed at substantially lower levels in DS-projecting dopamine neurons: on average 14 % were positive for Calretinin, 1 % expressed Calbindin and none of them were positive for Otx2 (Figure 5.2A-B). This indicates that some markers (Girk2, SatB1, Sox6 and Aldh1a1) are preferentially expressed in DS-projecting dopamine neurons whereas others (Calretinin, Calbindin and Otx2) are rarely expressed by DS-projecting dopamine neurons (Figure 5.2G).

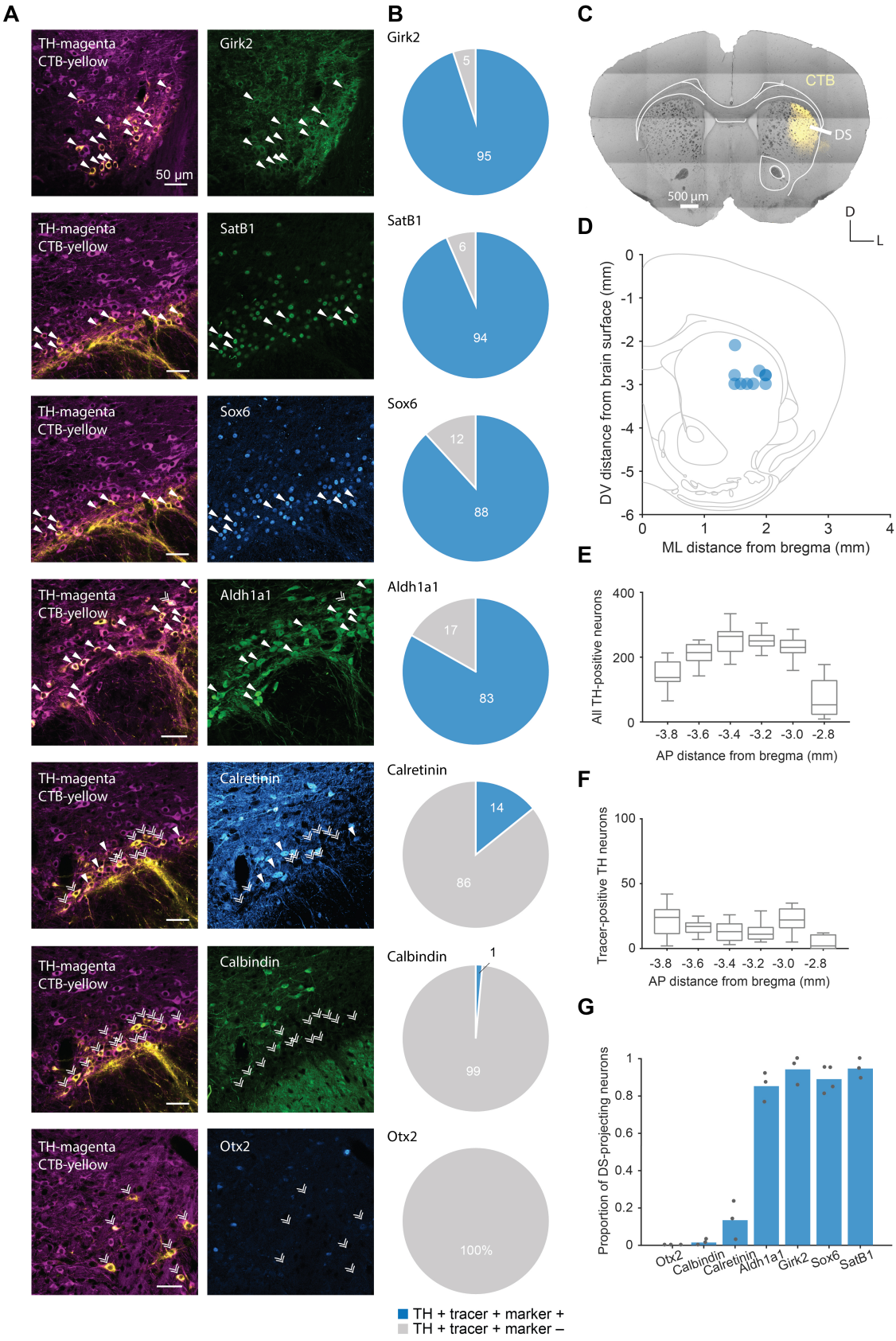
A
TH-magenta
CTB-yellow
50 µm
Girk2
SatB1
Sox6
Aldh1a1
Calretinin
Calbindin
Otx2
B
Girk2
5
95
SatB1
6
94
Sox6
12
88
Aldh1a1
17
83
Calretinin
14
86
Calbindin
1
99
Otx2
100%
TH + tracer + marker +
TH + tracer + marker –
C
CTB
DS
500 µm
D
L
D
DV distance from brain surface (mm)
ML distance from bregma (mm)
E
All TH-positive neurons
AP distance from bregma (mm)
F
Tracer-positive TH neurons
AP distance from bregma (mm)
G
Proportion of DS-projecting neurons
Otx2
Calbindin
Calretinin
Aldh1a1
Girk2
Sox6
SatB1

Figure 5.2: Marker expression in dorsal striatum-projecting dopamine neurons. (A-B,G) Proportion of dorsal striatum-projecting midbrain dopamine neurons co-expressing the molecular markers Girk2, SatB1, Sox6, Aldh1a1, Calretinin, Calbindin and Otx2 across the rostrocaudal axis. Because corresponding markers were counted on the same series, some TH-CTB images apply to multiple marker panels. (A) Single-headed arrows depict examples of TH-tracer neurons positive for a marker; double-headed arrows depict examples of TH-tracer neurons negative for a marker. (B) Proportion of TH-tracer-marker triple-positive neurons shown in blue and TH-tracer double-positive but marker-negative neurons shown in grey. (C) Representative example of retrograde tracer injection site in the dorsal striatum and (D) distribution of tracer injection sites in the dorsal striatum (n = 10 injected animals). Circles denote injection site. Coronal schematic adapted from Paxinos and Franklin (2013). (E) Counts of TH-positive neurons across the rostrocaudal axis (n = 15 sections per level). (F) Counts of TH-tracer double-positive neurons across rostrocaudal axis (n = 15 sections per level). TH, tyrosine hydroxylase; CTB/tracer, cholera toxin subunit b retrograde tracer; DS, dorsal striatum; D, dorsal; L, lateral; DV, dorsoventral; ML, mediolateral; AP, anteroposterior. (+): expression detected; (-): no expression detected. AP levels are approximate.

5.4.3 Molecular markers of nucleus accumbens-projecting midbrain dopamine neurons

To assess the proportion of NAc-projecting midbrain dopamine neurons expressing a specific marker, counts of triple-positive neurons (TH, marker, tracer) were assessed on the six selected rostrocaudal levels of NAc-injected brains (Figure 5.3C-D). The distribution of total counts of TH-positive neurons across the six coronal midbrain sections of all counted series (n = 13) is shown in Figure 5.3E; lowest numbers of TH-positive neurons were found in the most rostral and caudal sections. Collapsed across rostrocaudal sections, 71 (interquartile range [52 106]) neurons per series were TH-tracer double-positive. They had a similar distribution across rostrocaudal levels as TH-positive neurons (Figure 5.3F). Marker expression in NAc-projecting midbrain dopamine neurons was assessed by calculating the proportion of TH-tracer-marker triple-positive neurons. While a high proportion of DS-projecting dopamine neurons were Girk2, SatB1 and Sox6 positive (Figure 5.2G), only minor fractions of NAc-projecting dopamine neurons expressed one of these markers (Figure 5.3A-B, G); 32 % were positive for Girk2 (Figure 5.3A-B), 5 % were positive for SatB1 (Figure 5.3A-B) and 13 % were positive for Sox6. Notably, when assessing the expression of Aldh1a1 in NAc-projecting dopamine neurons, two of the counted series (obtained from two different brains) showed relatively low levels in overlap (1 % and 6 %; Figure 5.3G), while a third series showed markedly higher overlap between NAc-projecting dopamine neurons and Aldh1a1 expression (47 %; Figure 5.3G). Unreliable levels in immunolabelling were unlikely to be the reason for this variability given the consistency in overall numbers for Aldh1a1-expressing midbrain dopamine neurons (Figure 5.1B) and differences in the precise location of the injection site were considered as alternative explanation. Indeed, upon closer examination of the injection sites on the three brains used to count overlap between TH, tracer and Aldh1a1, the two injection sites with low overlap between TH, tracer and Aldh1a1 were found to be located more laterocaudal in the NAc (marked with asterisks in Figure 5.3D). Subsequently, counts were repeated on a series corresponding to a more medially and rostrally targeted injection site (marked with

an arrowhead in Figure 5.3D) and a considerably higher proportion in TH-marker-tracer triple-positive neurons was found (59 %; Figure 5.3G). Since Aldh1a1 is specific to midbrain dopamine neurons (McCaffery et al. 1994) and highly expressed in projections and fibres in striatum (similar to TH), coronal NAc sections were processed for Aldh1a1 fibre expression for qualitative analysis. Aldh1a1-positive fibres were not distributed evenly throughout the NAc, but strongest in the NAc medial shell (Figure 5.4A) while the NAc core was almost devoid of Aldh1a1-positive fibres (Figure 5.4A). This suggests a NAc subregion-specific innervation by Aldh1a1-positive midbrain dopamine neurons.

To assess how well a marker discriminated between DS- and NAc-projections, a discrimination index was calculated by subtracting the proportion of NAc-projecting dopamine neurons expressing a specific marker from the corresponding proportion of DS-projecting dopamine neurons. An index of +100 would indicate strongest discrimination with all identified DS-projecting dopamine neurons but no NAc-projecting dopamine neurons expressing the respective marker. An index of -100 would indicate strongest discrimination with all identified NAc-projecting dopamine neurons but no DS-projecting dopamine neurons expressing the respective marker. An index of 0 indicates no target preference. The best discrimination indices were obtained for SatB1 (+89), Sox6 (+75) and Calbindin (-87; Figure 5.4B), with selective expression in DS-projecting (SatB1 and Sox6) or NAc-projecting dopamine neurons (Calbindin). While Otx2 was exclusively found in NAc-projecting dopamine neurons, it was expressed in relatively few of them resulting in an index of only -33 (Figure 5.4B). Taken together, although marker expression did not show complete target-specific discrimination for any of the tested markers, some were expressed in a highly selective manner in neurons innervating either DS (SatB1, Sox6) or NAc (Calbindin). It is important to highlight that only two projection targets of midbrain dopamine neurons were tested against each other. This leaves it unclear whether Sox6 or Calbindin, while being useful for discriminating between neurons projecting to DS or NAc, would retain this level of discrimination when tested for other projection targets of midbrain dopamine neurons like the PFC.

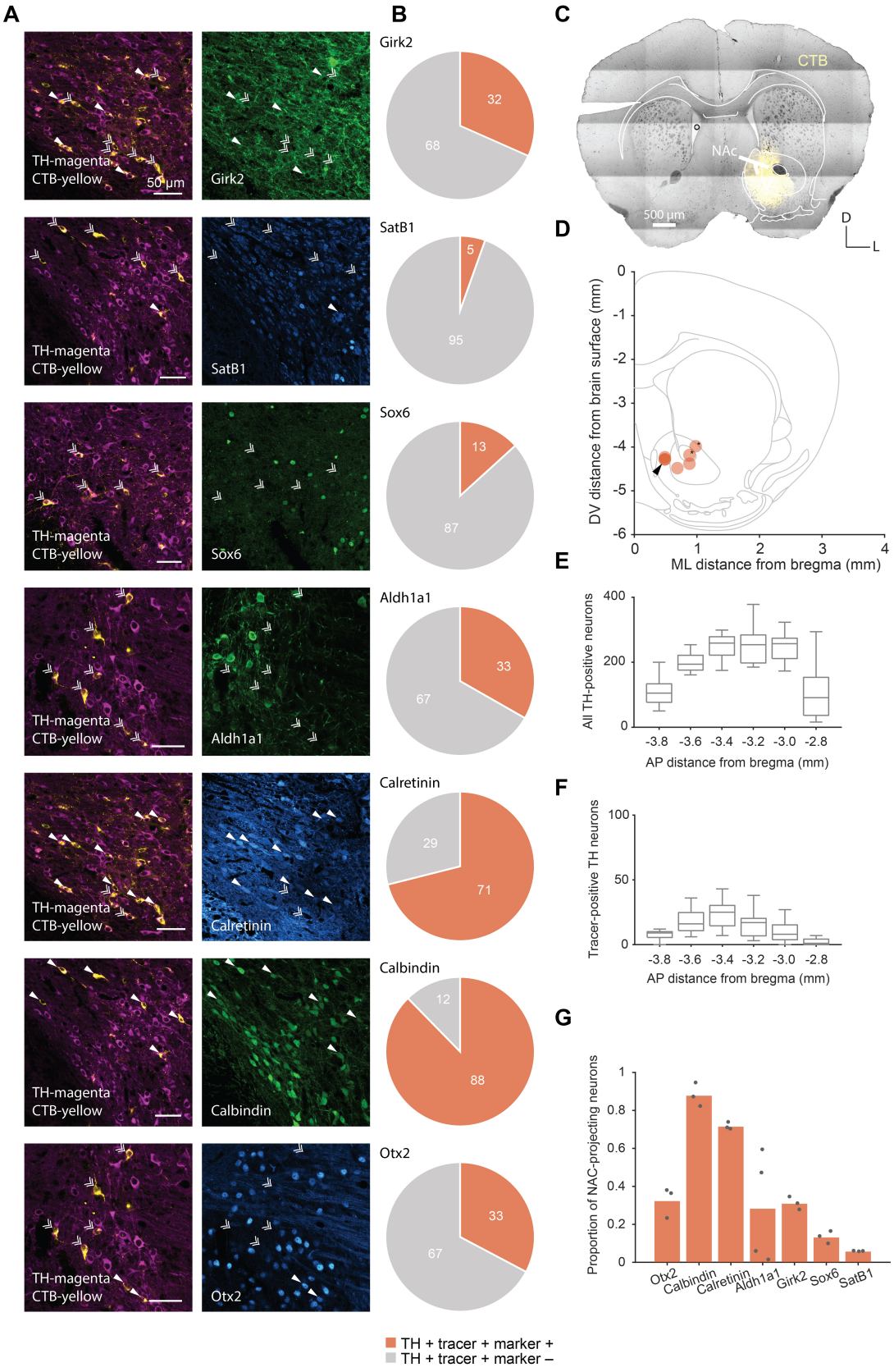
A
TH-magenta
CTB-yellow
50 µm
Girk2
SatB1
Sox6
Aldh1a1
Calretinin
Calbindin
Otx2
B
Girk2
32
68
SatB1
5
95
Sox6
13
87
Aldh1a1
33
67
Calretinin
29
71
Calbindin
12
88
Otx2
33
67
TH + tracer + marker +
TH + tracer + marker –
C
CTB
NAc
500 µm
D
L
D
DV distance from brain surface (mm)
0
-1
-2
-3
-4
-5
-6
0
1
2
3
4
ML distance from bregma (mm)
E
All TH-positive neurons
400
200
0
-3.8 -3.6 -3.4 -3.2 -3.0 -2.8
AP distance from bregma (mm)
F
Tracer-positive TH neurons
100
50
0
-3.8 -3.6 -3.4 -3.2 -3.0 -2.8
AP distance from bregma (mm)
G
Proportion of NAC-projecting neurons
1
0.8
0.6
0.4
0.2
0
Otx2
Calbindin
Calretinin
Aldh1a1
Girk2
Sox6
SatB1

Figure 5.3: Marker expression in nucleus accumbens-projecting dopamine neurons. (A-B,G) Proportion of NAc-projecting midbrain dopamine neurons co-expressing the molecular markers Girk2, SatB1, Sox6, Aldh1a1, Calbindin, Calretinin, Otx2 across the rostrocaudal axis. Because corresponding markers were counted on the same series, some TH-CTB images apply to multiple marker panels. (A) Single-headed arrows depict examples of TH-tracer neurons positive for a marker; double-headed arrows depict examples of TH-tracer neurons negative for a marker. (B) Proportion of marker triple-positive neurons are shown in orange and TH-tracer double-positive but marker-negative neurons in grey. (C-D) Distribution of retrograde tracer injection sites in the NAc (n = 7 injected animals). Asterisks in (D) highlight most lateral injections used to count Aldh1a1 co-expression, the arrowhead marks the most medial injections used to count Aldh1a1 co-expression. Coronal schematic adapted from Paxinos and Franklin (2013). (E) Counts of TH-positive neurons across rostrocaudal axis (n = 13 sections per level). (F) Counts of TH-tracer double-positive neurons across rostrocaudal axis (n = 13 sections per level). TH, tyrosine hydroxylase; CTB/tracer, cholera toxin subunit b retrograde tracer; NAc, nucleus accumbens; D, dorsal; L, lateral; DV, dorsoventral; ML, mediolateral; AP, anteroposterior. (+): expression detected; (-): no expression detected.

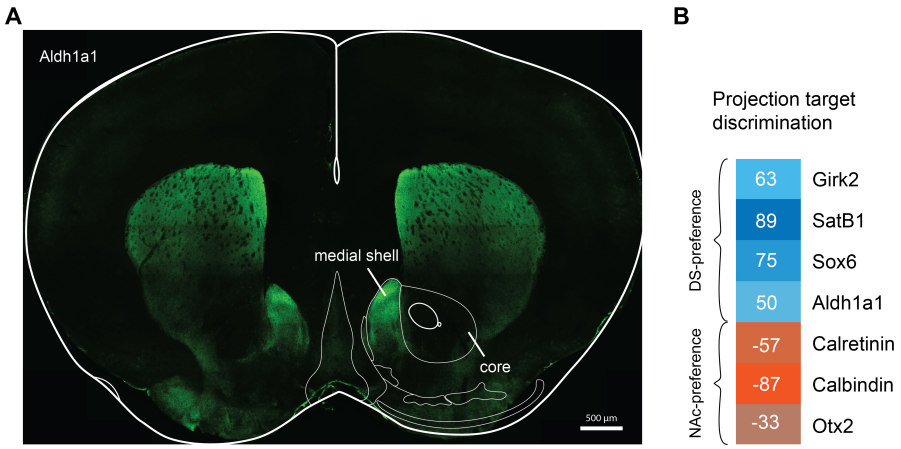

Figure 5.4: (A) Aldh1a1-positive fibres (green) preferentially innervate dorsal striatum and NAc medial shell but not NAc core (core). (B) Projection target discrimination for individual markers. Indices were calculated as the difference in the proportions of DS- and NAc-projecting midbrain dopamine neurons expressing the respective marker (i.e. DS-proportion minus NAc-proportion; proportions shown in pie charts in Figure 5.2 and Figure 5.3). Values > 0 and ≤ 100 indicate preference for DS (shades of blue), values < 0 and $\geq$ -100 indicate preference for NAc (shades of orange).

5.5 Discussion

While midbrain dopamine neurons share a common neurotransmitter, they show multidimensional diversity in their afferents, efferents, molecular and electrophysiological properties as well as encoding of behaviour (Beier et al. 2015; Berridge and Robinson 1998; Bromberg-Martin et al. 2010; Charara et al. 1996; Fallon and Moore 1978a; Fallon and Moore 1978b; Fallon, Riley, et al. 1978; Gerfen, Herkenham, et al. 1987; Lerner et al. 2015; La Manno et al. 2016; Menegas, Bergan, et al. 2015; Moore 1978; Phillipson 1979; Poulin, Zou, et al. 2014; Watabe-Uchida et al. 2012). A question arising from this diversity is whether its different dimensions can be collapsed onto each other, for instance whether molecular codes correspond to projection targets or differential encoding of behaviour (see Chapter 6). This is especially relevant in structures like the midbrain, where molecular identities, efferent targets and behavioural correlates span traditionally used boundaries of subnuclei. Mapping of distinct transcriptional codes onto projection- and functionally-defined cell types has proven useful for other basal ganglia nuclei like the GPe and striatum. GABAergic GPe neurons separate into STN-projecting prototypic neurons positive for the transcription factor Nkx2.1 and striatum-projecting arkypallidal neurons positive for the transcription factor FoxP2 (Abdi et al. 2015; Dodson, Larvin, et al. 2015; Mallet, Micklem, et al. 2012). GABAergic SPNs of the dorsal striatum separate into direct pathway MSNs expressing D1-receptors and indirect pathway SPNs expressing D2-receptors (Gerfen, Engber, et al. 1990; Le Moine, Normand, and Bloch 1991; Stoof et al. 1981). The aim of work in this Chapter was to assess projection target-specific molecular marker expression in midbrain dopamine neurons, through combining retrograde tracing with immunofluorescence labelling and stereological cell counting. A subset of seven molecular markers, known to be expressed in subpopulations of midbrain dopamine neurons, were selected for this evaluation: The two calcium-binding proteins Calbindin and Calretinin, the dehydrogenase Aldh1a1, the potassium channel Girk2 and the transcription factors Otx2, SatB1 and Sox6 (La Manno et al. 2016; Poulin, Zou, et al. 2014). Marker expression was assessed in midbrain dopamine neurons projecting to the two major

targets nucleus accumbens (NAc) and dorsal striatum (DS). Though none of the markers could be used for perfect discrimination of neurons innervating NAc or DS, some markers were nevertheless highly selective for neurons projecting to those two forebrain sites. For example, most (88 %) of midbrain dopamine neurons projecting to the NAc were positive for Calbindin, whereas only 1 % of midbrain dopamine neurons projecting to the DS expressed this calcium-binding protein (Figure 5.3 and Figure 5.4B). Calbindin became one focus of the dopamine and Parkinson's field because it was ascribed neuroprotective properties. Early on, it was shown that Calbindin expression in the cerebellum reduced with age, hinting at a possible role of the protein in neuron maintenance (Iacopino, Rhoten, et al. 1990). Follow-on studies have attributed neuroprotective properties to Calbindin because the Calbindin-positive population of midbrain dopamine neurons appears to be spared from degeneration in Parkinson's, both in VTA and SNc (German, Manaye, et al. 1992; Iacopino, Christakos, et al. 1992; Lavoie and Parent 1991; Liang, Sinton, Sonsalla, et al. 1996; Yamada et al. 1990). However, it remained unclear whether the relationship between loss of dopamine neurons in Parkinson's and Calbindin expression was causal or merely correlative. A correlative rather than causal relationship was supported by the finding that the pattern and extent of neural loss in MPTP-treated mice were unaltered in Calbindin-deficient mice (Airaksinen et al. 1997). Additionally, studies have shown selective vulnerability, rather than survival, of Calbindin-positive neurons in other neurodegenerative conditions like Alzheimer's (cortex) (Ichimiya et al. 1988) or Huntington's (striatum) (Kiyama et al. 1990). DS-projecting dopamine neurons have massive, unmyelinated axonal arbors exceeding the axonal arbor size of NAc- or PFC-projecting midbrain dopamine neurons (Aransay et al. 2015; Matsuda et al. 2009). This unusual morphological feature was suggested to lead to substantially higher bioenergetic demands and thus explain their differential vulnerability (Bolam and Pissadaki 2012; Pissadaki et al. 2013). Interestingly, Calbindin-expressing midbrain dopamine neurons in this study almost never projected to the DS, even if they were located in close proximity to DS-projecting midbrain dopamine neurons (Figure 5.2; Figure 5.3);

an observation also made in monkeys (Dopeso-Reyes et al. 2014). This finding supports the idea that projection target, rather than Calbindin-expression, might underlie differential vulnerability in midbrain dopamine neurons. In accordance with the literature, Calbindin was expressed in about 45 % and Calretinin in 29 % of midbrain dopamine neurons (Bentivoglio et al. 2005; Liang, Sinton, Sonsalla, et al. 1996; Nemoto et al. 1999), although other studies performed in rats report higher numbers (Rogers 1992). Projection-target preference of Calretinin-positive midbrain dopamine neurons was less pronounced than for Calbindin-expressing neurons with 71 % of NAc-projecting and 14 % of DS-projecting midbrain dopamine neurons expressing Calretinin. It was shown that TH-Calretinin double-positive fibres are largely restricted to the patch compartment in the dorsal striatum and to the matrix compartment of the NAc core (Seifert et al. 1998). The potential for differential innervation of patch and matrix compartments in DS and NAc could not be assessed in the current study. It was noted, however, that the proportion of NAc-projecting midbrain dopamine neurons co-expressing Aldh1a1 was much higher after injections targeting more rostromedial parts (e.g. medial shell; up to ∼60 %) compared to more caudolateral targeted injections (as low as 1 %) (Figure 5.3 and Figure 5.4). NAc subregions were first defined based on neurochemical properties and cell morphology (Herkenham et al. 1984; Záborszky, Alheid, et al. 1985), followed by descriptions of their partially distinct afferent (Brog et al. 1993) and efferent systems – including differences in inputs from midbrain dopamine neurons (Beier et al. 2015; Heimer, Zahm, et al. 1991; Zahm and Heimer 1990; Zahm and Heimer 1993; Zahm, Williams, et al. 1996) – and functional differences (Baldo et al. 2002; Hernandez et al. 2005; Lammel et al. 2008; Swanson et al. 1997). Future experiments with subterritory-confined NAc injections could be used to describe such differences in more detail.

Most midbrain dopamine neurons projecting to the DS were Girk2, SatB1 and Sox6 positive (95 %, 94 % and 88 % respectively; see Figure 5.2) but varied in their level of target discrimination with 32 % of NAc-projecting midbrain dopamine neurons expressing Girk2, 13 % expressing Sox6 and 5 % expressing SatB1 (Figure 5.3).

Thus, although more DS-projecting midbrain dopamine neurons were positive for Girk2 than Sox6 or SatB1, expression of Girk2 had low target discrimination between DS and NAc (Figure 5.4B). Initial studies in mice, rats and humans supported the idea that Girk2 expression in midbrain dopamine neurons is restricted to SNc and only laterodorsal parts of VTA (Eulitz et al. 2007; Mendez et al. 2005; Di Salvio, Di Giovannantonio, Acampora, et al. 2010; Schein et al. 1998), other studies indicated that Girk2 is expressed in almost all midbrain dopamine neurons albeit at varying levels (Fu et al. 2012; Reyes et al. 2012). This is supported by gene-expression profiling of single midbrain dopamine neurons, showing Girk2 expression in all subpopulations, although again at significantly different levels (Poulin, Zou, et al. 2014). Levels of co-expression in other studies performed in C57Bl/6J mice were reported to range from 50 % (subregions of VTA) up to 100 % (ventral SNc) (Fu et al. 2012). Co-expression levels in this study were on average 53 % (SNc and VTA combined; Figure 5.1), potentially excluding midbrain dopamine neurons with low Girk2 expression levels which were not detected with the immunolabelling protocol used in this study.

The best target discrimination for DS-projecting midbrain dopamine neurons in this study was found for the transcriptional regulator SatB1 (Figure 5.4B), which was detected in 51 % of all midbrain dopamine neurons but in 94 % of DS-projecting and only 5 % of NAc-projecting midbrain dopamine neurons (Figure 5.2 and Figure 5.3). However, other studies report that overall 95 % of both VTA and SNc dopamine neurons co-expressed SatB1 (Huang et al. 2011). A possible reason for these divergent findings are differences in immunolabelling protocols: Although both studies used the same antibody, Huang et al. (2011) applied it at a concentration of 1:100 following heat-treatment in citrate buffer (theoretically to increase immunoreactivity) while the present study used a concentration of 1:1000 without any pre-treatment. This suggests differential expression levels of SatB1 in different subpopulations of midbrain dopamine neurons, in agreement with expression profiling studies (Chung, Seo, et al. 2005; Grimm et al. 2004; Poulin, Zou, et al. 2014). SatB1 has previously been linked to vulnerability of SNc dopamine

neurons showing decreased regulatory activity of SatB1 through translatome and network analysis in MPTP mice and Parkinson's patients and degeneration of SNc midbrain dopamine neurons after knock-down of SatB1 (Brichta, Shin, et al. 2015). After SatB1, the transcription factor Sox6 showed the next strongest projection target discrimination, with 88 % of DS-projecting and 13 % of NAc-projecting midbrain dopamine neurons expressing Sox6 (Figure 5.2 and Figure 5.3). At the progenitor cell stage, Sox6 was shown to be selectively expressed in a subpopulation of midbrain dopamine progenitors (Panman, Papathanou, et al. 2014), preceding its differential expression in mature midbrain dopamine neurons (Chung, Seo, et al. 2005; Grimm et al. 2004; Poulin, Zou, et al. 2014). Conditional ablation of Sox6 in mice was shown to result in decreased TH-density in the dorsal striatum, further highlighting the potential importance of Sox6 for maintaining the integrity of DS-projecting midbrain dopamine neurons (Panman, Papathanou, et al. 2014). Furthermore, post-mortem tissue from Parkinson's patients shows diminished expression of Sox6 in neuromelanin positive cells (Panman, Papathanou, et al. 2014). A case study identified a *SOX6* mutation to underlie developmental delay and parkinsonian symptoms of a 4-year-old child (Scott et al. 2014). Interestingly, Sox6 expression in neural progenitors was shown to be restricted by Otx2 expression (Panman, Papathanou, et al. 2014).

Otx2 expression in the mature midbrain dopamine system is restricted to a subset of medially-located midbrain dopamine neurons (Di Giovannantonio et al. 2013; Panman, Papathanou, et al. 2014; Poulin, Zou, et al. 2014; Di Salvio, Di Giovannantonio, Omodei, et al. 2010; Di Salvio, Di Giovannantonio, Acampora, et al. 2010). In this study, Otx2 was the least widely expressed molecular marker, expressed in 12 % of midbrain dopamine neurons (Figure 5.1B). While none of the DS-projecting midbrain dopamine neurons expressed Otx2 (Figure 5.2), Otx2 was not expressed by many NAc-projecting midbrain dopamine neurons either (33 % co-expression; Figure 5.3). This might indicate that Otx2-positive midbrain dopamine neurons innervate other output structures in addition to NAc. Indeed, it was shown that eliminating Otx2 in development not only leads to neuron loss

in the midbrain but also loss of TH-positive fibres in target structures like the olfactory tubercle, prefrontal cortex, lateral septum and the amygdala, while leaving the dorsal striatum unaffected (Borgkvist et al. 2006; Chung, Licznerski, et al. 2010). Recently, it was shown that a subpopulation of midbrain dopamine neurons positive for the transcription factor Neurogenic differentiation factor-6 (NeuroD6) and located in the ventral VTA selectively innervates the lateral septum (Khan, Stott, et al. 2017). Since Otx2 expression is largely restricted to the same area in the VTA, subsequent tracing studies could help identify whether Otx2 expression in midbrain dopamine neurons colocalises with this lateral septum-innervating subpopulation.

Given that midbrain dopamine neurons with different projection targets are intermingled throughout SNc and in particular VTA (see e.g. Figure 1.1), molecular marker expression might serve as better indication of projection target than simply using anatomical location. However, expression patterns for some markers are largely confined to a specific anatomical location (e.g. Sox6 is most abundant in SNc; see Figure 5.1), indicating that both marker expression as well as anatomical location of a midbrain dopamine neuron might be predictive of its projection target. Thinking further, a combinatorial approach using both the information on molecular marker expression as well as the precise anatomical location might improve predictions of projection target, especially for markers expressed in subpopulations of midbrain dopamine neurons located in SNc as well as VTA such as Aldh1a1 (see Figure 5.1). It is important to note that only two projection targets of midbrain dopamine neurons were tested in this study. This leaves it unclear whether markers like Sox6 or Calbindin, which were highly discriminative for DS- and NAc-projections, would retain this level of discrimination when tested against other projection targets. Furthermore, the study design used in this Chapter only allows for 'one-dimensional' conclusions when looking at positive marker expression: While it is true that most NAc-projecting midbrain dopamine neurons express Calbindin, it cannot be concluded that most Calbindin-positive midbrain dopamine neurons project to the NAc. The reason for this is that any one tracer injection is likely to capture only a

fraction of midbrain dopamine neurons that project to that specific region. Furthermore, while this study differentiated DS- and NAc-projecting midbrain dopamine neurons, it did not account for potential compartment-specific innervation of striatum (i.e. patch and matrix). Early studies concluded that ventral SNc dopamine neurons preferentially innervate the patch compartment, while dorsal SNc dopamine neurons project to the striatal matrix (Gerfen, Herkenham, et al. 1987; Jimenez-Castellanos et al. 1987; Langer et al. 1989) and it would be of importance to test whether these two populations of midbrain dopamine neurons might differ in their molecular fingerprint. Given recent developments of (Cre-dependent) monosynaptic rabies virus tracing techniques (Wickersham et al. 2007) and patch- and matrix-specific Cre-driver mouse lines (Gerfen, Paletzki, et al. 2013), they could be combined to investigate whether the two striatal compartments are innervated by molecularly distinct populations of midbrain dopamine neurons. First, helper virus expression needed for infection with modified rabies virus could be targeted to patch-located SPNs via the patch-specific Cre-driver mouse line Sepw1-NP67 (Gerfen, Paletzki, et al. 2013), followed by infection with modified rabies virus resulting in monosynaptic tracing of midbrain dopamine neurons projecting to patch-SPNs. Secondly, expression profiles of those midbrain dopamine neurons could be obtained through fluorescence-activated cell sorting (FACS; to select exclusively dopamine neurons projecting to the patch, the patch-specific Cre-driver mouse line could be crossed with a Slc6a3-reporter mouse followed by multi-colour FACS, selecting only neurons that have two fluorophores; one fluorophore identifying them as patch-projecting and a second one identifying them as dopamine neuron) followed by single cell expression-profiling. Alternatively, an immunolabelling approach similar to the one presented in this study could be used. Thirdly, by repeating the same protocol with the matrix-specific Cre-driver mouse line Plxnd1-OG1 (Gerfen, Paletzki, et al. 2013), expression profiles of patch-projecting midbrain dopamine neurons could be compared to the ones projecting to the matrix. Data from a first study that employed a similar approach did not further analyse differences in SNc inputs to the two compartments but might indicate that input is provided

by populations that are spatially dispersed (Smith, Klug, et al. 2016). However, reconstructions of individual SNc dopamine neurons indicated that innervation of patch or matrix compartments by individual neurons was biased but not specific, i.e. individual neurons preferentially innervated one compartment or the other but their axon terminals were not exclusively restricted to a single type of compartment (Matsuda et al. 2009).

Taken together, some markers displayed a degree of projection target-selective innervation of either NAc or DS. Given the multitude of regions innervated by midbrain dopamine neurons and the manifold functions attributed to them, it is of particular interest to investigate whether they send distinct information to defined projection targets. Projection-selective markers could then be used to manipulate functionally defined midbrain dopamine neurons (e.g. through optogenetics) in a much more targeted fashion than the "blanket" approaches commonly used, where light-sensitive channels are expressed under the control of promoters of genes that are ubiquitously expressed in midbrain dopamine neurons (e.g. Slc6a3). Whether the markers selected in this study correspond to distinct behavioural correlates of midbrain dopamine neurons will be addressed in Chapter 6.

6

Functional diversity of midbrain dopamine neurons

Contents

6.1 Introduction

Different approaches have been used to study the roles that dopamine play in the brain. These include: assessing which functions are lost in the absence of dopamine, what functions are enhanced if dopamine transmission or content is increased, or what functions are 'encoded' by the firing of dopamine neurons or the dopamine they release (measured with fast-scan cyclic voltammetry (FCV)) (Berridge 2007; Gan et al. 2010), i.e. which aspects of a behaviour it correlates with. The firing of midbrain dopamine neurons or dopamine terminal signals have been correlated with many different behavioural concepts such as movement, motivation, working memory or decision making (Dodson, Dreyer, et al. 2016; Howe et al. 2016; Matsumoto and Takada 2013; Morris et al. 2006). In Parkinson's patients, midbrain dopamine neurons degenerate, leading to the characteristic motor symptoms (Samii et al. 2004); this highlights the importance of an intact midbrain dopamine system for normal motor function. Recordings of individual (identified and putative) midbrain dopamine neurons in mice and monkeys have provided evidence for action and movement representation in their activity (Barter, Castro, et al. 2014; Dodson, Dreyer, et al. 2016; Fan et al. 2012; Jin et al. 2010; Schultz, Ruffieux, et al. 1983). Other studies have shown that dopamine signals are involved in motivation, e.g. signalling effort in cost-based decision-making tasks (Day et al. 2010; Hamid et al. 2015; Salamone, Correa, Farrar, et al. 2007; Salamone, Correa, Nunes, et al. 2012). Some of the earliest work investigating putative midbrain dopamine neurons showed changes in their activity following the presentation of neutral (not reward-paired or aversive) sensory stimuli (Chiodo, Caggiula, et al. 1979; Chiodo, Antelman, et al. 1980; Fiorillo et al. 2013; Horvitz et al. 1997; Steinfels et al. 1983b; Steinfels et al. 1983a; Strecker et al. 1985). Such studies were performed in rats (Chiodo, Caggiula, et al. 1979; Chiodo, Antelman, et al. 1980), cats (Horvitz et al. 1997; Steinfels et al. 1983b; Steinfels et al. 1983a; Strecker et al. 1985) and monkeys (Fiorillo et al. 2013). Notably, the response types seen in those studies are heterogeneous and include 'non-responsive', as well as neurons which show phasic increases, phasic decreases, or combinations of both in time with the presentation

of neutral auditory or visual stimuli. These responses have often been interpreted as "alerting" (Bromberg-Martin et al. 2010; Schultz 1998) or perceptually "salient" (Schultz 2007b), informing the animal about potentially value-bearing events. For instance, the availability of food (positive value) or the presence of a predator (negative value). Responses of midbrain dopamine neurons to value-bearing events are often studied in classical conditioning paradigms where stimuli are paired with outcomes (Miller et al. 1981). Through conditioning, formerly neutral stimuli with no intrinsic value become cues for positively or negatively valued outcomes, so-called conditioned stimuli, and gain the ability to elicit responses otherwise seen following unconditioned stimuli such as rewards (Coon 1982; Pavlov et al. 1928). Neural activity of midbrain dopamine neurons, typically measured as firing rate, was shown to phasically increase following outcomes with positive value (Figure 6.1A) (Cohen et al. 2012; Mirenowicz et al. 1996; Schultz 1986). After classical forward conditioning (typically assessed after hundreds or thousands of repeated pairings of cue and reward), the phasic increase in firing rate of midbrain dopamine neurons was shown to no longer appear following the outcome but to have shifted to the outcome-predicting cue (Figure 6.1B) (Mirenowicz et al. 1994; Schultz, Dayan, et al. 1997). This response-shift in forward conditioning was used to infer that midbrain dopamine neurons carry prediction error signals. In this schema, if the outcome is identical with the prediction then no firing rate change occurs. However, if it is better or worse than predicted, this is reflected by an increase or decrease in firing rate respectively (Schultz 1998; Schultz, Dayan, et al. 1997) (Figure 6.1C). Consequently, midbrain dopamine neuron firing would then not signal reward itself but the discrepancy between prediction and actual outcome. Reward and reward prediction error (RPE) signalling of single dopamine neurons has been studied in monkeys (Schultz 2007a; Schultz 1998), rats (Kosobud et al. 1994; Pan et al. 2005) and mice (Cohen et al. 2012; Eshel, Tian, et al. 2016; Matsumoto, Tian, et al. 2016). The ascribed value to conditioned stimuli is thought to be stimulus-specific. However, stimulus generalisation can occur if a second similar stimulus is presented to the animal in addition to the original, outcome-predicting one (e.g. if they have

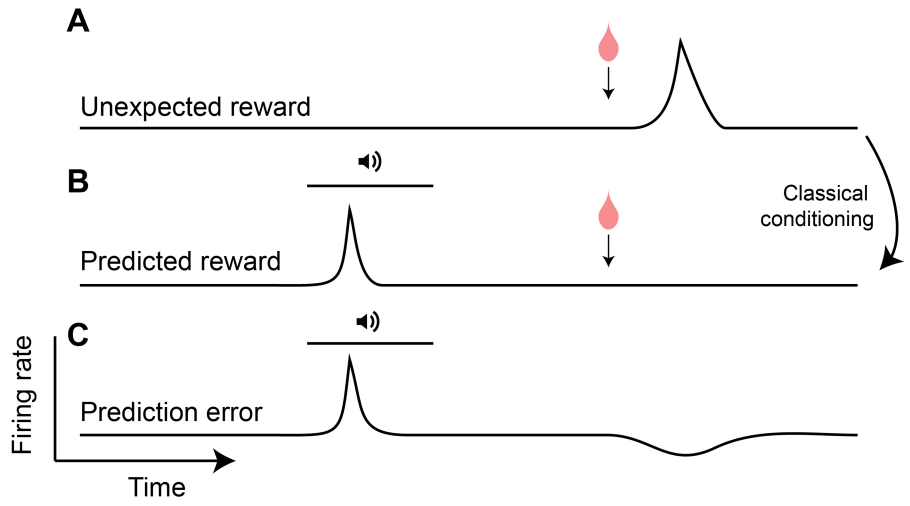

Figure 6.1: Concept of reward prediction error signalling of midbrain dopamine neurons after classical conditioning. (A) Midbrain dopamine neurons phasically increase firing to unexpected rewards (red drop). (B) This response shifts to the reward-predicting cue through conditioning. (C) Midbrain dopamine neurons do not signal reward itself but the difference between prediction (cue will be followed by reward) and the actual outcome (e.g. reward was omitted): the reward prediction error (RPE) signal (adapted from Schoenbaum et al. 2013).

the same sensory modality) (Kakade et al. 2002; Kobayashi et al. 2014; Matsumoto, Tian, et al. 2016; Sadacca et al. 2016; Schultz 2010; Schultz 2016).

The goal of the research in this Chapter was to investigate responses of identified midbrain dopamine neurons to neutral sensory stimuli, conditioned cues and predicted rewards in mice, and to correlate responses with the precise location of identified dopamine neurons and their molecular phenotype. Since it was shown that animals generalise from conditioned cues to neutral stimuli if presented with both (Kakade et al. 2002; Kobayashi et al. 2014; Matsumoto, Tian, et al. 2016; Sadacca et al. 2016; Schultz 2010; Schultz 2016), the experiment was designed to include two separate groups of mice. (1) A group of naïve animals were used in the sensory stimuli experiment and exposed to neutral auditory and visual stimuli while recording single-unit activity of midbrain dopamine neurons. These animals had never experienced classical conditioning training. (2) A separate group of mice were trained in a classical conditioning task, with one stimulus-outcome pair with an auditory cue predicting liquid reward.

6.2 Aims

The research detailed in this Chapter was designed to elucidate the behavioural correlates of the firing properties of individual midbrain dopamine neurons in head-fixed awake male C57Bl/6J mice. The specific aims of this research were to:

- Measure firing properties of identified midbrain dopamine neurons during the presentation of neutral auditory and visual stimuli to naïve adult C57Bl/6J mice.
- Measure firing properties of putative and identified midbrain dopamine neurons in a classical cue-reward conditioning task in food-restricted adult C57Bl/6J mice.
- Assess expression of molecular markers of subsets of dopamine neurons in recorded and identified (i.e. neurobiotin-labelled) midbrain dopamine neurons to correlate diverse responses with molecular phenotype.

6.3 Methods

For experiments in this Chapter, 3-5 month old male C57Bl/6J mice obtained from Charles River Laboratories were used. In the first experiment, only naïve animals were used. These animals were not food restricted or trained prior to recording. Only identified dopamine neurons located within VTA and SNc and identified non-dopamine neurons were included in the analysis. For the second experiment, animals received training in the task prior to recording and were kept under restricted access to food (as a motivator) with their weight maintained at 85 – 90 % of baseline. Both neurochemically identified (dopamine and non-dopamine) neurons located within VTA and SNc and putative dopamine neurons (defined by criteria detailed in section 2.5.5) were included in the analysis of the classical conditioning task. Identified and putative dopamine neurons were always analysed separately and are displayed in separate graphs. All recordings were performed in trained animals. Training criterion was reached with anticipatory licking and $\geq$ 90 of the 100 cued rewards given in a training session consumed. Note that tones and lights not associated with a reward are always referred to as "stimuli", whereas the reward-predicting tone is referred to as "cue". Detailed experimental methods are described in:

2.1 Animals

2.1.3 C57Bl/6J mice

2.4 Single-unit recordings and juxtacellular labelling

2.4.1 Single-unit recordings in rats and mice

2.4.2 Juxtacellular labelling and perfuse-fixation

2.4.3 Tissue processing to identify recorded and labelled neurons

2.5 Recordings in head-fixed awake mice

2.5.1 Headpost implantation

2.5.2 Treadmill, cue box and reward delivery system

2.5.3 Sensory stimuli experiments

2.5.4 Cued reward experiments

2.5.5 Analysis of head-fixed awake recordings

2.5.6 Statistical approach for head-fixed awake recordings

6.4 Results

6.4.1 Identified midbrain dopamine neurons exhibit diverse responses to sensory stimuli

To test whether and how the firing of midbrain dopamine neurons in naïve C57Bl/6J mice is modulated by neutral sensory stimuli, single-unit activity in head-fixed awake mice exposed to auditory and visual stimuli was recorded (Figure 6.2). Each animal was exposed to four different stimuli in a pseudorandom order: A low frequency tone (1 kHz), a high frequency tone (5 or 10 kHz), a blue LED light (wavelength 455 or 480 nm) and a green LED light (wavelength 520 nm). The median inter-stimulus interval was 2.5 s (minimum 2 s, maximum 45 s). Because the activity of midbrain dopamine neurons is modulated by spontaneous movements (Dodson, Dreyer, et al. 2016), individual stimuli were excluded from the analysis if movements of the animal overlapped with a stimulus trial (a trial being defined as 1 second either side of the stimulus). If movements occurred at any point within the trial, the trial was discarded. A minimum of 6 stimuli were delivered per cell (excluding movement-overlapping trials; median 17, maximum 30; pooled trials for all four stimuli). A total of 21 identified dopamine neurons were recorded in 9 animals (19 in SNc, 3 in VTA; see Figure 6.4E). One tyrosine hydroxylase-expressing neuron was located in SNr but considered as SNc dopamine neuron (Paxinos and Franklin 2013). One tyrosine hydroxylase-expressing neuron was located in the RRF and therefore was excluded from further analysis. Firing rates of recorded and identified dopamine neurons were converted to z-scores to compare rate modulation by sensory stimuli. Responses of identified midbrain dopamine neurons to sensory stimuli were highly variable showing firing increases (Figure 6.2A), firing decreases (Figure 6.2B), biphasic responses (Figure 6.2C) or no change in firing (Figure 6.2D). However, the average activity of identified midbrain dopamine neurons was not modulated by neutral sensory stimuli, irrespective of modality and property of the stimulus (blue LED: n = 20 neurons, median trial number per cell = 5; green LED: n = 21 neurons, median trial number = 6; high tone: n = 19 neurons, median trial number = 5; low tone: n = 19 neurons, median trial number = 3; Figure 6.3).

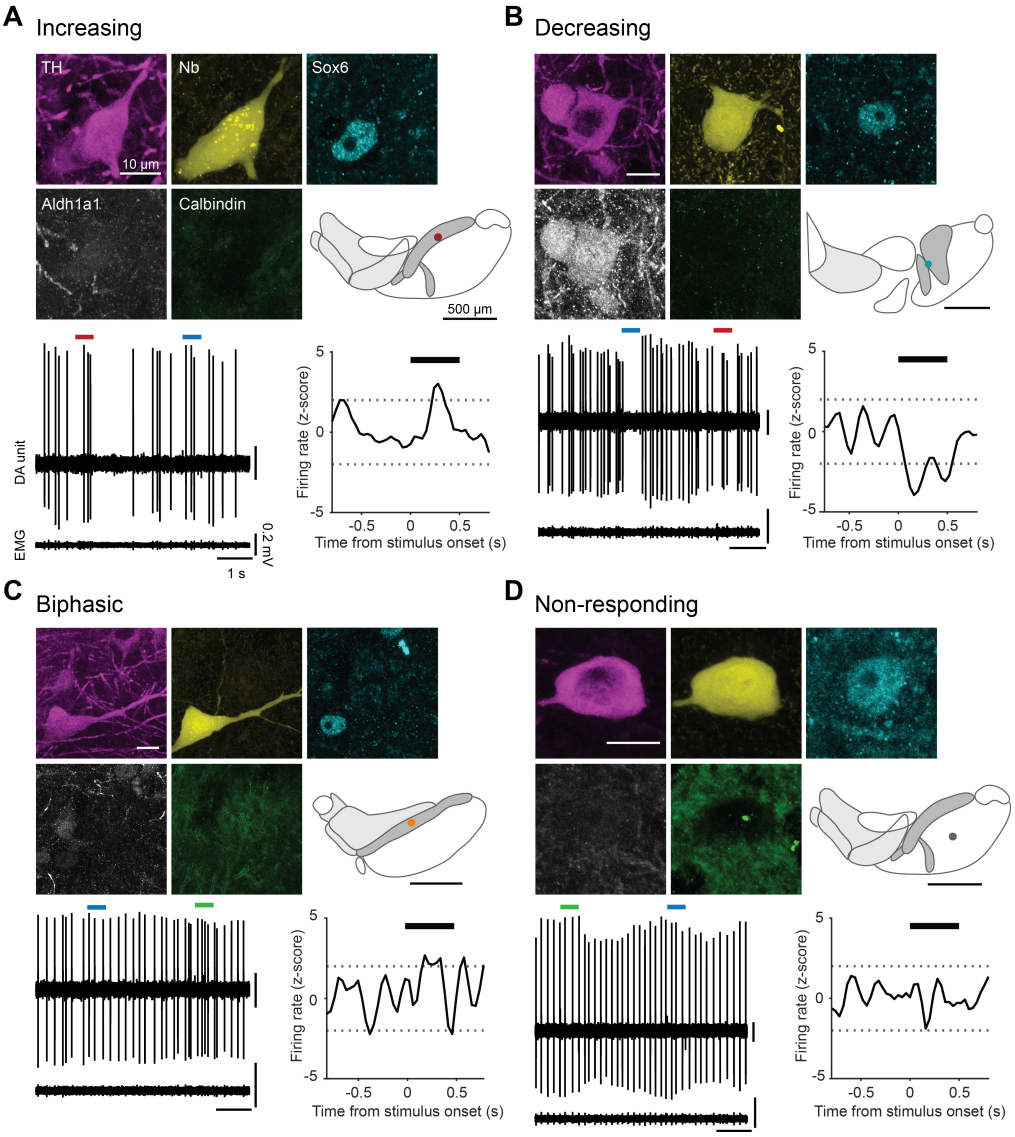

Figure 6.2: Diverse activity of identified midbrain dopamine neurons in the sensory stimuli experiment. After recording, individual neurons were juxtacellularly labelled with Neurobiotin (Nb) and confirmed to be dopaminergic by tyrosine hydroxylase (TH) immunoreactivity. Additionally, every neuron was tested for the expression of the molecular markers Sox6, Aldh1a1 and Calbindin (see Chapter 5). The SNc dopamine neuron in (B) was Sox6 $\oplus$ / Aldh1a1 $\oplus$ / Calbindin $\ominus$ and the neurons in (A,C-D) were Sox6 $\oplus$ / Aldh1a1 $\ominus$ / Calbindin $\ominus$. Identified midbrain dopamine neurons responded with (A) increased activity, (B) decreased activity, (C) biphasic activity or (D) no change in activity during sensory stimuli. (A-D) Coronal schematics show approximate locations of recorded and labelled dopamine neurons (light grey: VTA; dark grey: SNc). DA unit: Vertical lines represent individual action potentials, horizontal bars on top indicate sensory stimuli (blue: blue LED, green: green LED, red: high tone). Note that the "high frequency tone" sensory stimulus in (B) (red bar) was excluded from analysis because it overlapped with movement of the animal. PETH curves were constructed from pooled sensory stimuli. Black bars above PETH indicate stimulus duration; dashed horizontal lines are positioned at z-scores of ± 2. EMG, electromyogram.

Table 6.1: Response groups of identified midbrain dopamine neurons in sensory stimuli experiment. Baseline rate is shown as median.

Response group	n	Baseline rate spikes/s	Peak/trough z-score	Peak/trough time after stimulus onset
Increasing	4	3.7	2.8	280-320 ms
Decreasing	3	8.0	-2.8	160-200 ms
Biphasic	3	4.9	/	/
Non-responding	11	4.5	/	/

However, when analysed on a cell-by-cell basis, approximately half of the neurons (10 of 21) showed responses to neutral light and tone stimuli. Four of 21 of the midbrain dopamine neurons showed a significant increase during the presentation of sensory stimuli (z-score ≥ 2 during 500 ms stimulus presentation; Figure 6.4A) but not when randomly shuffling the sensory stimuli onset (Figure 6.4J). 3 of 21 neurons showed a significant decrease during stimulus presentation (z-score $\leq$ -2; Figure 6.4B) but not when randomly shuffling the sensory stimuli onset (Figure 6.4K). Three of 21 neurons showed significant biphasic responses during stimulus presentation (1 of 3 showed a decrease followed by an increase, 2 of 3 neurons showed an increase followed by a decrease; Figure 6.4C). 11 of 21 neurons showed no significant increase or decrease during stimulus presentation (-2 $<$ z-score $<$ 2; Figure 6.4D). Neurons with a significant increase to sensory stimuli peaked with a delay of 280 – 320 ms (mean peak z-score = 2.8), whereas neurons with a significant decrease to sensory stimuli reached their maximal decrease with a shorter delay of 160 – 200 ms after stimulus onset (mean trough z-score -2.8; see summary of properties in Table 6.1). All neurons showing significant decreases were located in SNc. 3 of 4 with a significant firing increase were located in SNc and 2 of 3 neurons with a biphasic response were located in SNc (Figure 6.4E). Baseline firing rate of neurons ascribed to the different response groups did not significantly differ (Figure 6.4I). However, it was notable that neurons with a significant decrease to sensory stimuli had very similar firing rates of $\sim$8 spikes/s and tended to be higher than the baseline rate of all but one of the other dopamine neurons (Figure 6.4I).

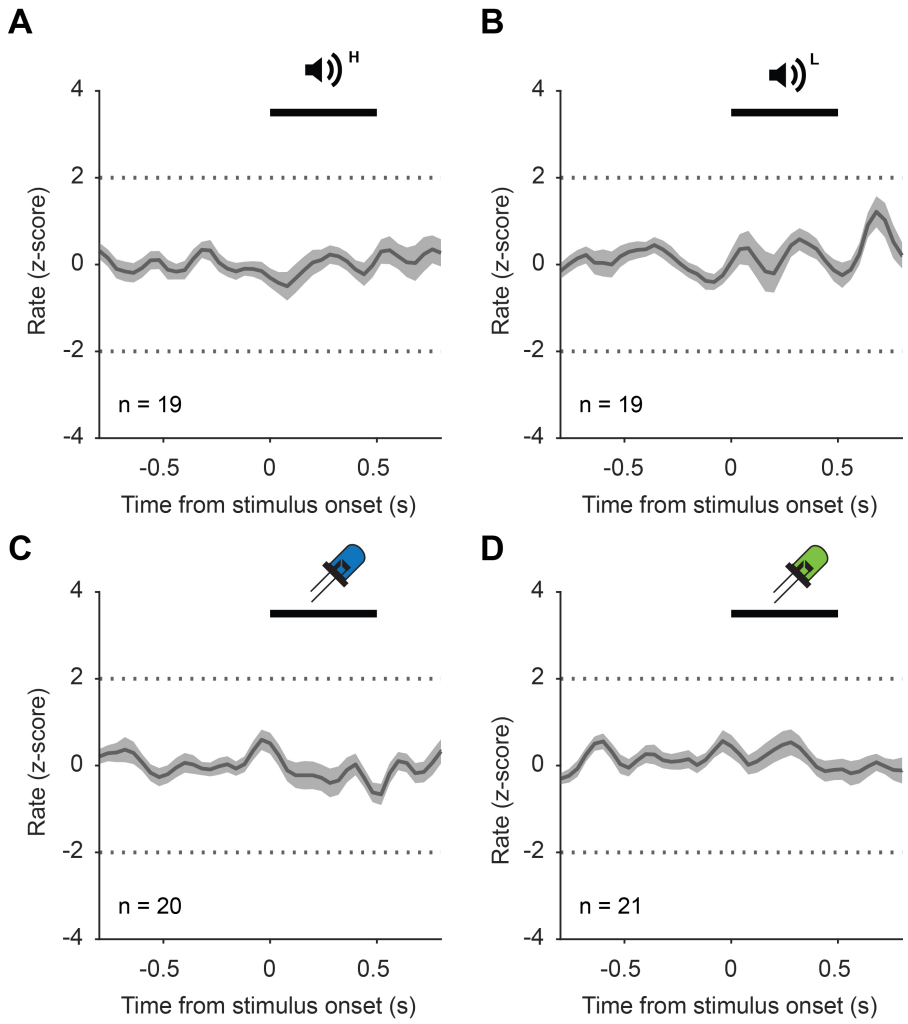

Figure 6.3: Average activity of identified midbrain dopamine neurons is not modulated by sensory stimuli of different sensory modality. Brief (500 ms) exposures to (A) high tones, (B) low tones, (C) blue light and (D) green light did not modulate spontaneous firing of midbrain dopamine neurons. n, neuron numbers per stimulus type; H, high tone; L, low tone. Data show mean ± SEM.

6.4.2 Responses of identified midbrain dopamine neurons depend on stimulus novelty

To test whether response magnitude of midbrain dopamine neurons following sensory stimuli was dependent on the "novelty" of the stimulus, the extent to which the animal had been exposed to neutral sensory stimuli was correlated with response magnitude. Stimulus-novelty was measured as the number of prior experienced sensory stimuli and response magnitude defined as the minimal and maximal rate (z-score) during stimulus presentation. Maximal rate during stimulus presentation

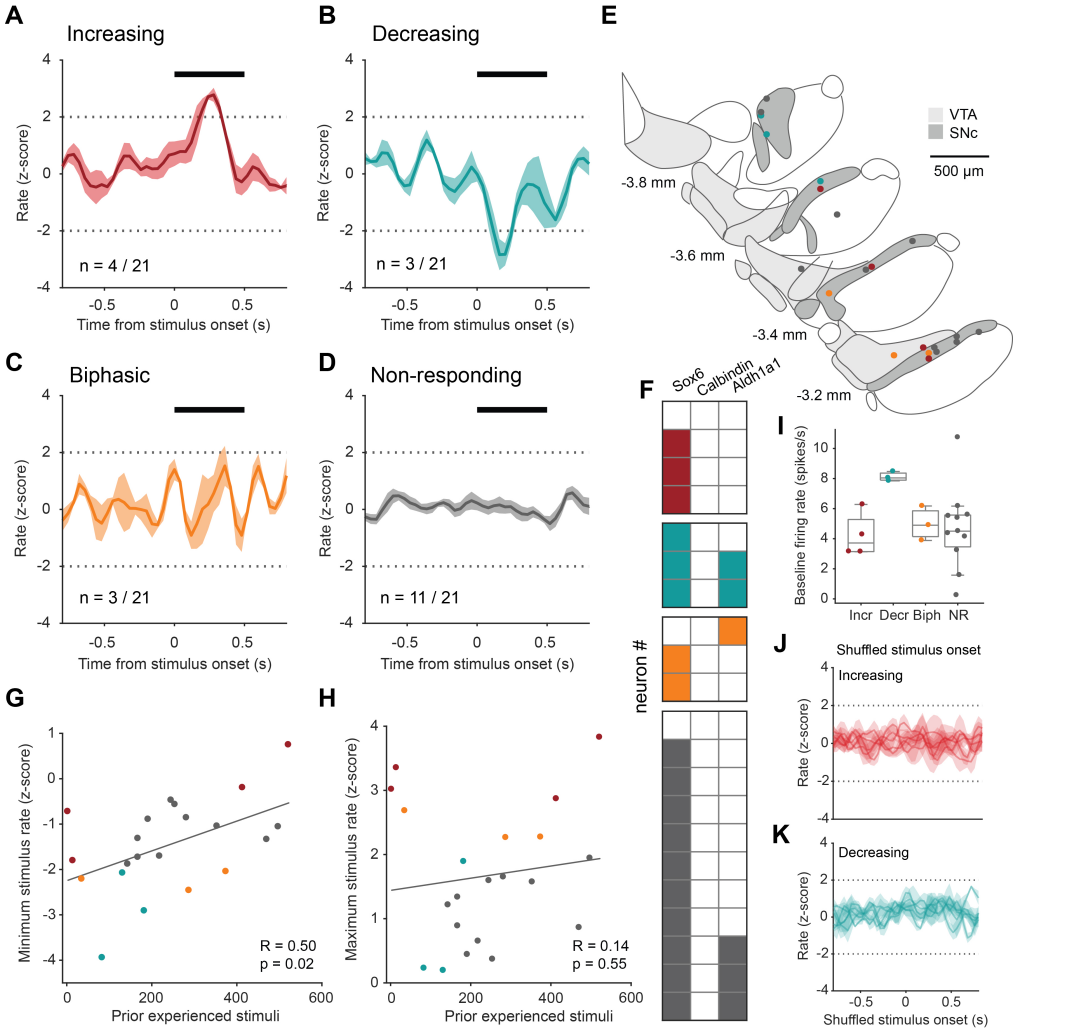

Figure 6.4: Individual analysis of identified midbrain dopamine neurons reveals diverse responses to sensory stimuli and novelty-dependency. Average activity pooled across sensory stimuli for (A) increasing (n = 4), (B) decreasing (n = 3), (C) biphasic (n = 3) and (D) non-responding (n = 11) dopamine neurons. (E) Locations of neurons in SNc and VTA (colour-coded as in (A-D); numbers indicate distance from Bregma). (F) Response groups did not correspond to molecular marker expression. Checkerboards are colour-coded as in (A-D); filled squares indicate marker expression of Sox6, Calbindin and Aldh1a1 (columns). Every neuron is represented in one row.(G-H) Response magnitude depended on stimulus novelty for (G) minimal firing rate (Pearson's correlation: R = 0.50, p = 0.02) but not (H) maximal firing rate during stimulus presentation (Pearson's correlation: R = 0.14, p = 0.55). (I) Firing rates of response groups (one-way ANOVA, p = 0.12). (J-K) Five randomly drawn examples of average activity for (J) increasing (n = 4) and (K) decreasing (n = 3) dopamine neurons with shuffled stimulus onset. X-axis labels in (K) also apply to (J). VTA, ventral tegmental area; SNc, substantia nigra pars compacta; Incr, increasing; Decr, decreasing; Biph, biphasic; NR, non-responding. Black bars in (A-D) depict stimulus duration. Data in (A-D) are shown as mean ± SEM; boxplots in (F) displays first quartile, median and third quartile.

did not correlate with stimulus novelty (Pearson's correlation, R = 0.14, p = 0.55; Figure 6.4H). However, minimal rate during stimulus presentation could be predicted from stimulus-novelty: Fewer exposures to the sensory stimuli correlated with a larger decrease in firing during sensory stimuli (Pearson's correlation, R = 0.50, p = 0.02; Figure 6.4G).

6.4.3 Response types of identified dopamine neurons are not segregated by marker expression

Midbrain dopamine neurons are molecularly heterogeneous (see Chapter 5). Distinct expression of molecular markers in subsets of dopamine neurons might be indicative of different functions or anatomical properties (e.g. projection target). To test whether different responses to neutral sensory stimuli corresponded to differential marker expression, identified midbrain dopamine neurons were immunolabelled for three subtype-selective markers (La Manno et al. 2016; Poulin, Zou, et al. 2014): The transcription factor Sox6, the calcium-binding protein Calbindin and the aldehyde dehydrogenase Aldh1a1. Calbindin and Sox6 were amongst the markers with the best projection-target discrimination of NAc- and DS-projecting midbrain dopamine neurons in Chapter 5. While SatB1 showed better projection-target discrimination than Sox6 (see Figure 5.4), Sox6 was selected as marker in this Chapter because single-cell gene-expression profiling studies indicated a stronger "all-or-nothing" expression pattern in midbrain dopamine neurons, potentially rendering it more suitable for a binary classification of expression as based on immunofluorescence (La Manno et al. 2016; Poulin, Zou, et al. 2014). None of the 21 identified midbrain dopamine neurons expressed Calbindin while 18 of 21 expressed Sox6 (Figure 6.4F). This might suggest that the identified midbrain dopamine neurons project to the dorsal striatum, while their expression of other markers did not correlate with distinct response types.

6.4.4 Diverse response types in identified non-dopamine neurons located in the midbrain

In many studies, putative midbrain dopamine neurons are classified based on approximate recording location, firing properties and width of extracellularly recorded action potentials (e.g. firing rate below 10 spikes/s and a spike width from threshold to trough of $\geq$ 1 ms) (Barter, Li, et al. 2015; Hyland et al. 2002; Janezic et al. 2013; Ungless et al. 2004; Wang and Tsien 2011). This does, however, not rule out that some neurons meeting some or all of these criteria are not dopaminergic nor that all dopamine neurons meet all these criteria. To gain further insight into this, the firing of non-dopamine neurons located in the midbrain (within or in close proximity to SNc or VTA), and which were recorded in the same animals as neurons presented in section 6.4.1, was analysed. The median inter-stimulus interval was 2.5 s (minimum 2 s, maximum 31 s) and stimulus trials overlapping with animal movements were excluded from the analysis. The minimum stimulus number per cell (excluding movement-overlapping trials) was 5 (median 18.5, maximum 30). A total of 27 non-dopamine cells were recorded in 8 animals (12 just dorsal to SNc/VTA, 6 in SNc, 4 in VTA, 3 in RRF, 1 in MT and 1 in SNr).

Table 6.2: Response groups of identified non-dopamine neurons in sensory stimuli experiment. Baseline rate shown as median.

Response group	n	Baseline rate spikes/s	Peak/trough z-score	Peak/trough time after stimulus onset
Increasing	8	12.0	5.1	80-120 ms
Decreasing/biphasic	5	3.2	-2.1	240-280 ms
Non-responding	14	6.8	/	/

When analysed individually, 8 of 27 neurons showed a significant increase in firing during sensory stimuli (2 SNc, 4 above SNc/VTA, 1 MT, 1 RRF; Figure 6.5C), 5 of 27 non-dopamine neurons showed a significant decrease in firing (2 VTA, 1 RRF, 2 above SNc/VTA; Figure 6.5D) and 14 of 27 non-dopamine neurons were not modulated by neutral sensory stimuli (Figure 6.5E; Table 6.2). Nine of 27

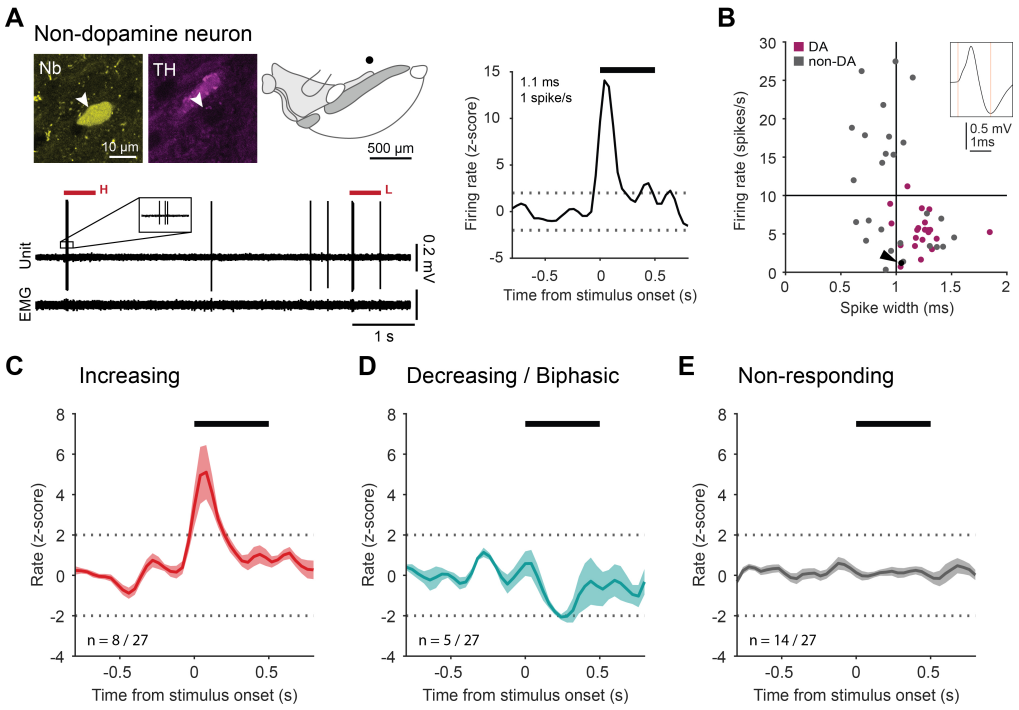

Figure 6.5: Identified non-dopamine neurons (in and around the SNc/VTA) show diverse responses to sensory stimuli. (A) Activity of one identified non-dopamine neuron with dopamine neuron-like firing characteristics (spike width = 1.1 ms; firing rate = 1 spike/s). PETHs were constructed using pooled sensory stimuli. The coronal midbrain schematic shows the location of the recorded neuron (black circle; dark grey area: SNc, light grey area: VTA). (B) Firing rate and spike width distribution of identified dopamine (magenta) and non-dopamine (grey/black) neurons. The neuron in (A) is depicted in black (arrowhead). Inset: spike width was measured from threshold to trough (orange vertical lines). (C-E) Average activity pooled across sensory stimuli for: (C) increasing (n = 8), (D) decreasing/biphasic (n = 5), and (E) non-responding (n = 14) non-dopamine neurons. Nb, neurobiotin; TH, tyrosine hydroxylase; DA, dopamine; EMG, electromyogram. Data in (C-E) show mean ± SEM.

non-dopamine neurons met the criteria commonly used to identify them as putative dopamine neurons (Figure 6.5B). 2 of 9 neurons meeting these selection criteria showed a significant increase during sensory stimuli (Figure 6.5A). Thus, some non-dopamine neurons which could be easily mistaken for dopamine neurons are responsive to neutral sensory stimuli. The same analysis showed that 2 of 21 identified dopamine neurons would not have met the criteria commonly used to identify them as putative dopamine neurons (one of which was non-responsive and the other one decreased firing to sensory stimuli) (Figure 6.5B). Taken together, these data highlight the need for better criteria to identify midbrain dopamine neurons.

6.4.5 Mice learn to associate cue with reward in a classical conditioning task

To investigate signalling of midbrain dopamine neurons in response to value-bearing cues and rewards, mice were trained in a classical conditioning task. For task training, mice were food restricted to 85 – 90 % of their baseline weight and received on average 6 days of training (in head-fixation) prior to recording. Task trials had a forward conditioning design and consisted of an auditory cue (4 kHz, ∼70 dB), followed by reward delivery after a delay of 1 second (8 – 9 µL strawberry milk; Figure 6.6A). Task trials during training were identical to task trials on recording days. To evaluate whether mice had learned to associate the auditory cue with the reward outcome, anticipatory licking during the cue was measured (in 17 of 28 mice used in recording experiments). Mean lick rate during the cue after an average of 6 training days was significantly higher than mean lick rate during the cue during the first two days of training (mean rate during 1 second cue; t-test, $p = 0.0002$; Figure 6.6B), indicating that animals had learned to associate the upcoming reward with the preceding cue. No significant difference was found in lick rate following reward delivery (mean rate for 1 second following reward delivery; t-test, $p = 0.13$) or during baseline 1 second before cue onset (t-test, $p = 0.18$).

6.4.6 Identified midbrain dopamine neurons show diverse responses in a classical conditioning task

Midbrain dopamine neuron activity was recorded in head-fixed mice trained to associate the conditioned cue with reward. The median inter-trial interval was 6.4 seconds (minimum 4.4 seconds, maximum 38.5 seconds). The minimum trial number per identified dopamine neuron was 5 (median 6, maximum 12). A total of 40 identified dopamine neurons were recorded in 21 animals (21 in SNc, 19 in VTA; see Figure 6.12A; 2 of 40 neurons were recorded with Ribena reward). 2 other cells were excluded from the analysis because they were located in the RRF. On average, rewards were consumed within 0.4 seconds following reward delivery on 94.44 ± 0.02 % of trials (mean ± SEM). Firing rates of recorded and identified dopamine

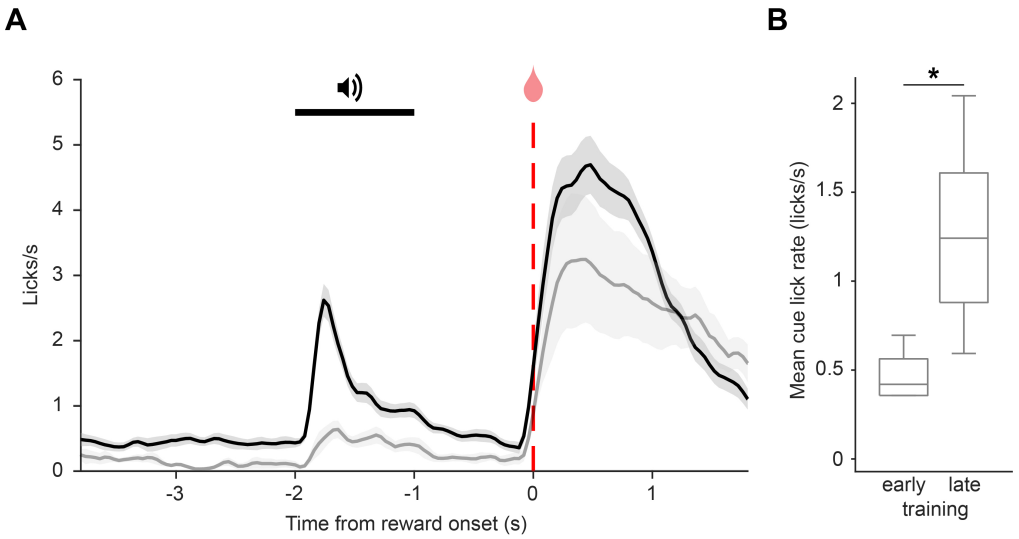

Figure 6.6: Animals trained in a classical conditioning task display anticipatory licking. (A) Lick frequency during early training (session on day 1 or 2; light grey line; data from 6 animals) and late training (last two sessions before recording; black line; data from 17 animals). The black horizontal bar indicates cue duration and the red dashed line marks reward delivery. (B) Anticipatory licking measured as mean lick frequency during the entire cue increased with training (t-test, $p = 0.0002$). Data in (A) show mean ± SEM, data in (B) depict first quartile, median and third quartile.

neurons were converted to z-scores to compare rate modulation during cue and reward. The average activity of all identified VTA dopamine neurons together showed a significant firing increase following reward delivery (peak z-score = 5.0, delay of peak: 160 – 200 ms; Figure 6.7A) as did all neurons located in SNc (peak z-score = 3.4, delay of peak: 160 – 200 ms; Figure 6.7B). No significant increase in firing to reward onset was present when data was shuffled by shifting the respective reward onset to a random position along the recording trace (Figure 6.7C). VTA and SNc dopamine neurons did not differ in maximum reward firing rate, baseline firing rate or baseline firing regularity (measured as mean CV2 during baseline; Table 6.3, Figure 6.7D-F). On average, neither VTA nor SNc dopamine neurons encoded the learned cue with changes in firing rate (Figure 6.7A-B).

When considered individually, not all identified midbrain dopamine neurons displayed firing increases following reward delivery (Figure 6.8). Furthermore, the firing of some identified dopamine neurons appeared to be well correlated to licking behaviour of the animal, irrespective of whether such behaviour co-

Table 6.3: Firing properties of identified midbrain dopamine neurons in cued reward task located in VTA and SNc. Baseline rate and baseline CV2 given as median.

Location	n	Baseline rate spikes/s	Baseline CV2	Peak reward response z-score	Peak delay
VTA	19	4.6	0.75	5.0	160-200 ms
SNc	21	6.2	0.62	3.4	160-200 ms

occurred with the reward delivery or not (Figure 6.8D). To test whether the firing of individual midbrain dopamine neurons correlated with cue, reward delivery, licking or combinations of the three, a generalised linear regression model was used on individual recording traces (see section 2.5.5). Cue, reward and licking were included as explanatory variables in the model to explain firing rate. Cue, reward and licking were defined as categorical variables with values of 1 (true) or 0 (false). Recording traces were subdivided into 100 ms bins. The number of spikes and the presence or absence of cue, reward and licking were determined for each bin of every recording.

Table 6.4: Response types of identified midbrain dopamine neurons in cued reward task. Each row marks a designated response group. The last three columns indicate how many neurons in each response group correlated positively (pos) or negatively (neg) with cue, reward and licking behaviour. Baseline rate (spikes/s) and baseline CV2 given as median.

Response type	n	Baseline rate	CV2	cue		reward		licking	
				pos	neg	pos	neg	pos	neg
Reward-only	9	5.7	0.79	0	0	**9**	0	0	0
Cue-negative	5	6.8	0.61	0	**5**	2	0	0	0
Licking-positive	7	4.6	0.51	0	1	2	2	**7**	0
Licking-negative	4	3.5	0.84	0	1	2	0	0	**4**
Cue-positive	2	6.8	0.69	**2**	0	1	0	0	0
Reward-negative	1	3.2	0.55	0	0	0	**1**	0	0
Non-responding	12	4.4	0.57	**0**	**0**	**0**	**0**	**0**	**0**

Regression coefficients and p-values were obtained for all explanatory variables for each neuron. An individual cell was considered responsive to any of the three variables if the corresponding p-value was equal to or lower than 0.05. Signs of

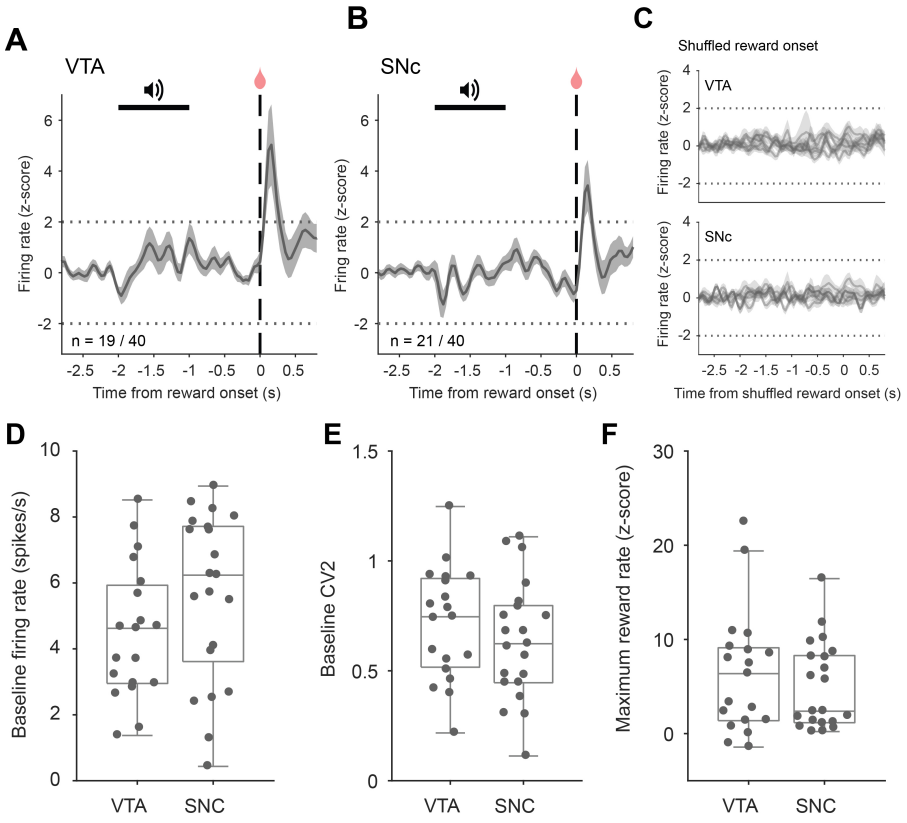

Figure 6.7: Identified VTA and SNc dopamine neurons signal reward after training in a classical conditioning task. (A-B) Average activity of identified dopamine neurons in (A) VTA (n = 19) and (B) SNc (n = 21) display significant firing increase following reward delivery (dashed vertical line). (C) Five randomly drawn examples of average activity for VTA (top) and SNc dopamine neurons (bottom) with shuffled reward onset. X-axis labels apply to both PETH plots. (D-F) SNc and VTA dopamine neurons are similar in (D) baseline firing rate (t-test, p = 0.14), (E) baseline firing regularity (measured as CV2) (t-test, p = 0.36) and (F) maximum firing rate during reward (Mann-Whitney rank sum, p = 0.59). Horizontal dashed lines in (A-B) indicate significance level (|z-score| $\geq$ 2). Data in (A-B) show mean $\pm$ SEM; boxplots in (D-F) display first quartile, median and third quartile.

coefficients were used to determine whether firing rate increased (positive sign) or decreased (negative sign) during cue, reward or licking. Data were then grouped and averaged based on response type (see Table 6.4 and Figure 6.9). Given that three explanatory variables were included in the model and that firing rate of an individual cell could be positively or negatively correlated with any one variable, the maximal theoretical number of response permutations is 27 (3^3). The overlap between response types is depicted in the Venn diagram in Figure 6.9E: Some neurons were only modulated by one of the three variables, whereas other neurons

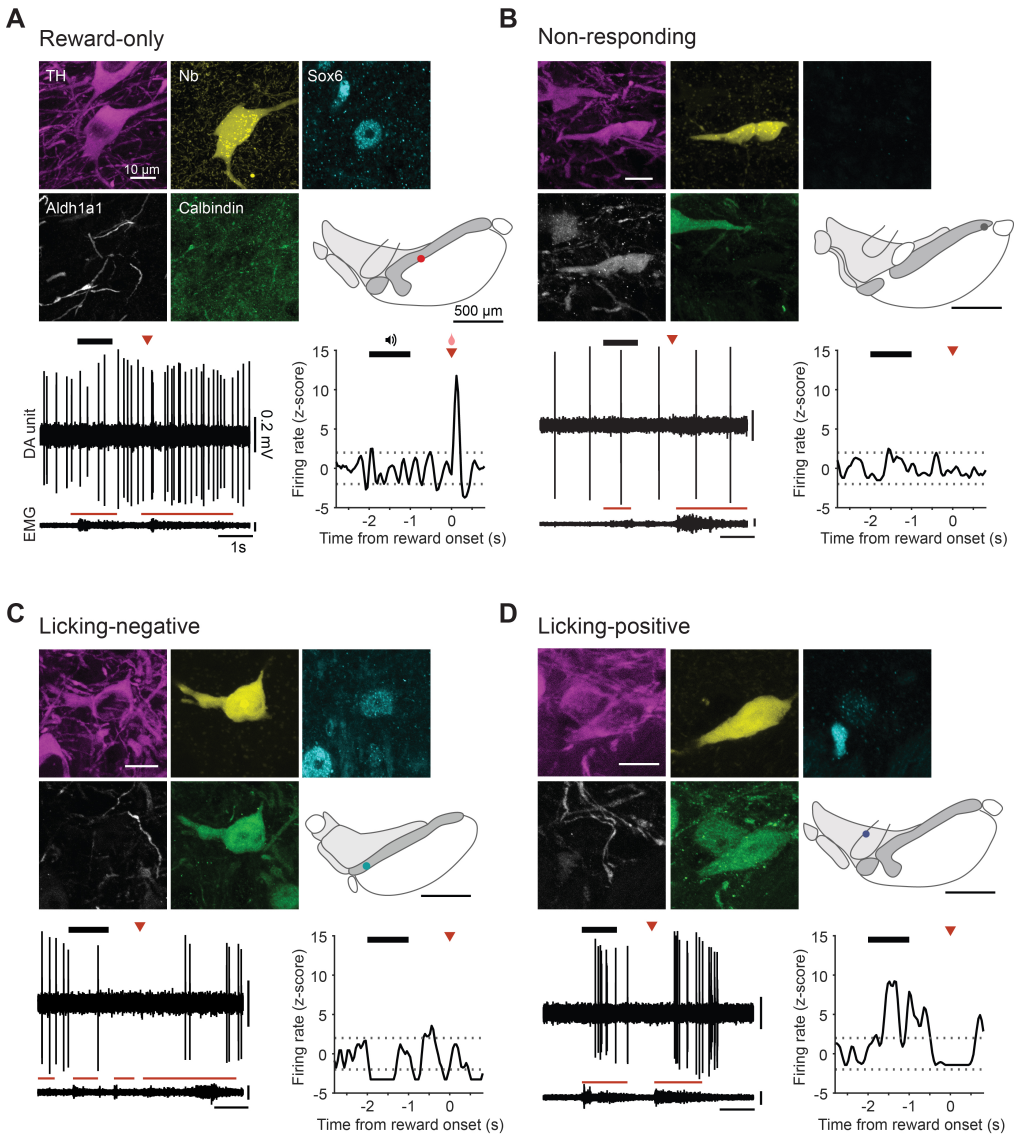

Figure 6.8: Diverse activity of identified midbrain dopamine neurons in the cued reward task. After recording, individual neurons were juxtacellularly labelled with Neurobiotin (Nb), confirmed to be dopaminergic by tyrosine hydroxylase (TH) immunoreactivity and tested for the expression of the molecular markers Sox6, Aldh1a1 and Calbindin (see Chapter 5). The SNc dopamine neuron in (A) was Sox6 ⊕ / Aldh1a1 ⊖ / Calbindin ⊖, the SNc dopamine neuron in (B) was Sox6 ⊖ / Aldh1a1 ⊕ / Calbindin ⊖, the SNc dopamine neuron in (C) was Sox6 ⊕ / Aldh1a1 ⊖ / Calbindin ⊕ and the VTA dopamine neuron in (D) was Sox6 ⊖ / Aldh1a1 ⊖ / Calbindin ⊕. Neurons were sub-divided into groups using a linear regression model. Example neurons categorised as (A) increasing firing to reward, (B) showing no response to either cue or reward, (C) decreasing firing during licking and (D) increasing firing during licking. (A-D) Coronal schematics show approximate locations of recorded and labelled dopamine neurons (light grey: VTA; dark grey: SNc). DA unit: Vertical lines are individual action potentials, horizontal black bars on top represent the cue, red arrowheads indicate reward delivery. Red bars on top of the EMG trace indicate licking behaviour. Dashed horizontal lines in PETH plots are positioned at z-scores ±2. EMG, electromyogram.

were modulated by combinations of them (note that the Venn diagram does not differentiate between positive or negative modulation). To simplify data display, neurons were allocated to the most prominent response groups (summarised in Table 6.4). To confirm response classifications obtained with the regression model, response characteristics of individual groups were compared. Differences in response class were reflected in reward-aligned average PETHs for individual response groups (Figure 6.9A-D,F) and absent for shuffled data, were respective reward onsets were randomly positioned within the recording trace (Figure 6.9M) . Reward-only dopamine neurons (Figure 6.9A) had a mean peak z-score of 10.9 (aligned to reward delivery) and their maximum reward rate (measured as maximal z-score in 400-ms window following reward onset) was significantly higher than the maximum reward rate of non-responding neurons (Kruskal-Wallis with Tukey-Kramer post-hoc, $p = 0.0019$; Figure 6.10A). The delay of the peak reward rate with respect to reward onset was identical to the delay seen when data were divided by midbrain region (160 – 200 ms; compare Figure 6.9A and Figure 6.7A-B). Cue-negative neurons were the only response group with significant decrease in firing during cue presentation (average minimum cue rate measured as z-score of -2.5; Figure 6.9B). If the mean firing rate of licking-positive dopamine neurons were plotted together with lick frequency, the traces overlapped at lick onset (Figure 6.9L); note, since lick frequency could not be measured during recording sessions due to electrical noise, mean lick frequency for this plot was taken from "late-training" training sessions as in Figure 6.6A. As anticipated, non-responding neurons did not show significant changes in firing to cue or reward (Figure 6.9F).

To compare licking-related changes in firing between response groups, plots were aligned to lick onset. Note that all lick phases were included in the average plots, irrespective of whether they co-occurred with a reward delivery or not. On average, one recording trace contained 14.5 "lick-phases" (median; minimum 7, maximum 32). When aligned to lick-onset, licking-positive neurons showed a prolonged increase in their average firing and licking-negative neurons a prolonged decrease (Figure 6.9J-K). The reward-only, non-responding and cue-negative response groups

did not show significant changes in firing if aligned to lick-onset (Figure 6.9G-I). The "bump" around licking onset in the average response of reward-only neurons (Figure 6.9G) is most likely explained by their reward response, since rewarded lick-phases were not excluded from the average PETH. To rule out the possibility that dopamine neurons classed as lick-responsive were recorded during unusually extensive lick-behaviour of the animal, the ratio between baseline recording length and licking recording length was calculated for individual cells in the reward-only and the licking-positive response groups. Baseline recording length was defined as the total length of recording periods during which the animal was not licking, exposed to the cue or receiving a reward. Licking recording length was defined as the total recording length during which the animal was licking but not exposed to a cue or receiving a reward. No difference in the ratio of total licking recording length to total baseline recording length could be seen between reward-only and licking-positive response groups (Figure 6.10C). To directly compare licking-related changes in firing rate between the licking-positive and reward-only response groups, the difference in firing rate between baseline and licking recording lengths (excluding cue and reward periods) was calculated for every cell in each of the two response groups. The licking-positive response group had a significantly higher firing rate difference between licking and baseline periods compared to the reward-only response group (Figure 6.10D), indicating their responsiveness to licking outside cued reward trials.

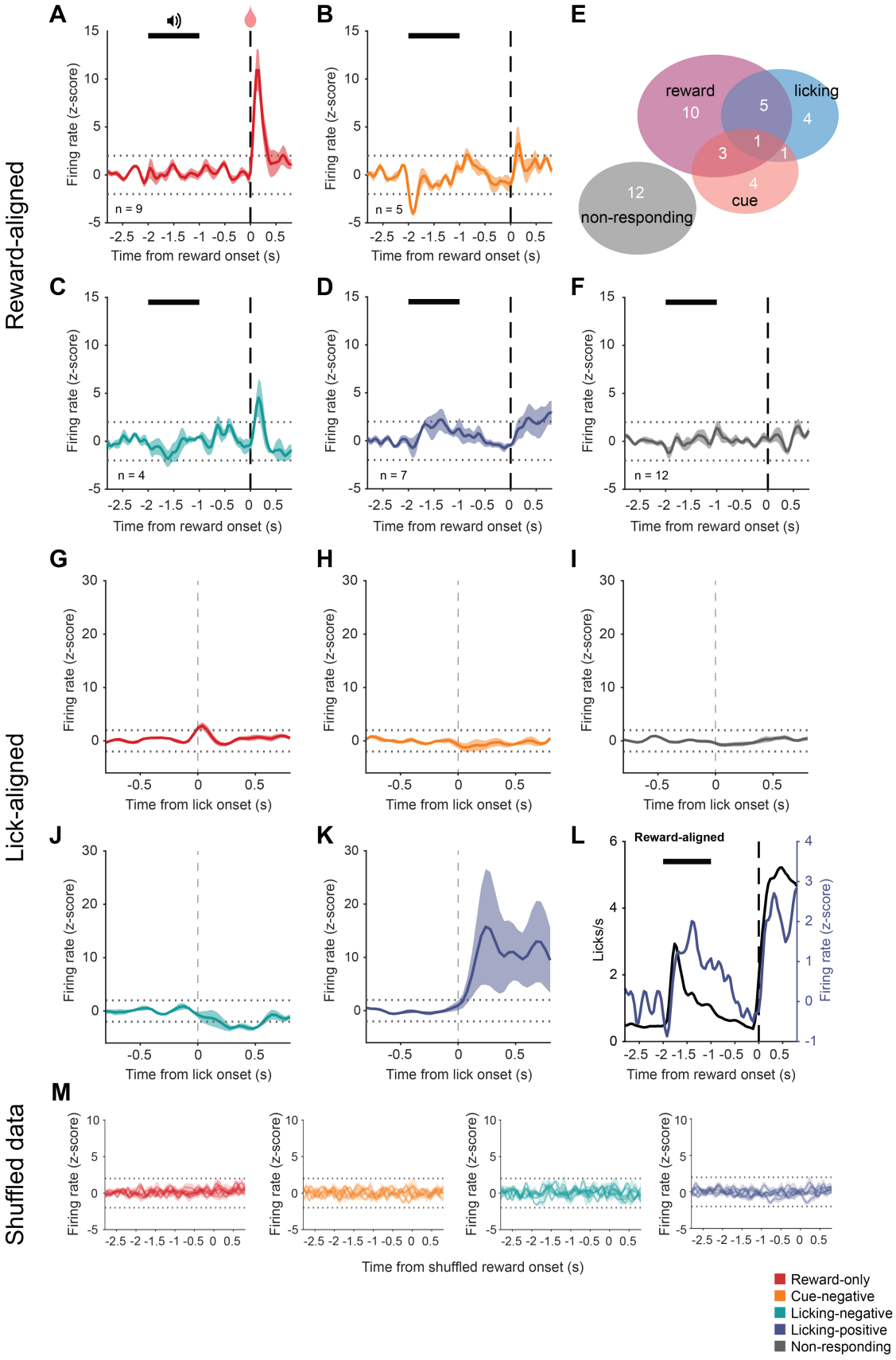
Reward-aligned
Lick-aligned
Shuffled data
A
B
C
D
E
F
G
H
I
J
K
L
M
Firing rate (z-score)
Time from reward onset (s)
Time from lick onset (s)
Time from shuffled reward onset (s)
n = 9
n = 5
n = 4
n = 7
n = 12
reward
licking
cue
non-responding
10
5
4
3
1
1
4
12
Reward-aligned
Licks/s
Firing rate (z-score)
Reward-only
Cue-negative
Licking-negative
Licking-positive
Non-responding

Figure 6.9: Linear regression-based response types of identified midbrain dopamine neurons in cued reward task. (A-D,F) Reward-aligned average activity of dopamine neurons responding with (A) rate increase to reward only (n = 9), (B) rate decrease during cue (n = 5), (C) rate decrease during licking behaviour (n = 4), (D) rate increase during licking behaviour (n = 7) or (F) not responding (n = 12). (E) Venn diagram showing numbers of neurons significantly correlated to reward, cue, licking or combinations thereof. Note: Venn diagram does not differentiate between positive or negative regression coefficients. (G-K) Licking-aligned average activity of the same response groups as in (A-D,F). (G-I) Reward-only, cue-negative and non-responding response groups are not modulated by licking behaviour. (J) Licking-negative neurons decrease activity after licking-onset, (K) licking-positive neurons increase activity after licking-onset. (L) Reward-aligned lick frequency measured during training (left axis, black; see Figure 6.6A) overlaid with the average activity of licking-positive neurons (right axis, blue) show similar time course. Horizontal black bars represent cue duration, vertical dashed lines indicate either reward delivery (A-D,F,L) or lick-onset (G-K). (M) Five examples of average activity for the response groups shown in (A-D) with shuffled reward onset. Data in (A-D,F-K, M) show mean ± SEM; data in (L) show means. Dashed horizontal lines are positioned at z-scores ±2.

Response groups in this Chapter were defined based on significant correlations with either licking, cue or reward presentation. To test whether this classification was linked to differences in basic firing properties of recorded and identified dopamine neurons, baseline firing rate and firing regularity (measured as CV2; see section 2.5.5) were calculated for each cell in each group. No significant differences in baseline firing rate or firing regularity of neurons were detected for any of the five response groups (Figure 6.10E-F).

All identified midbrain dopamine neurons were recorded over the course of one day because tissue had to be perfuse-fixated relatively shortly (∼10 hours) after labelling of recorded neurons to prevent the lysis of neurobiotin (used to label individual neurons). Some neurons were recorded early in the day and others in the afternoon or evening. Since circadian rhythms might influence dopamine levels (Friedman et al. 1979), it was tested whether the time of day impacted on the firing of dopamine neurons (Figure 6.10H). It was further tested whether recordings of response groups differed in the time since the last cued reward was obtained, since this potentially impacts on the animal's motivation for the reward (Figure 6.10G). Recordings of individual neurons also differed in the level of

task-experience of the mouse at time of recording (measured as number of total cue-reward trials the animal had received prior to a specific recording), e.g. an earlier recording corresponds with fewer prior received cued reward trials than a recording later in the day (Figure 6.10I). To rule out the possibility that any of these factors explained the observed response groups, time of day of the recording, time since last cued reward was obtained and the total number of prior received cue-reward trials (summed across training and recording days) were compared between response groups. Response groups did not systematically differ in time of day of the recording, time since the last cued reward was obtained, or number of prior cued reward trials (Figure 6.10G-I).

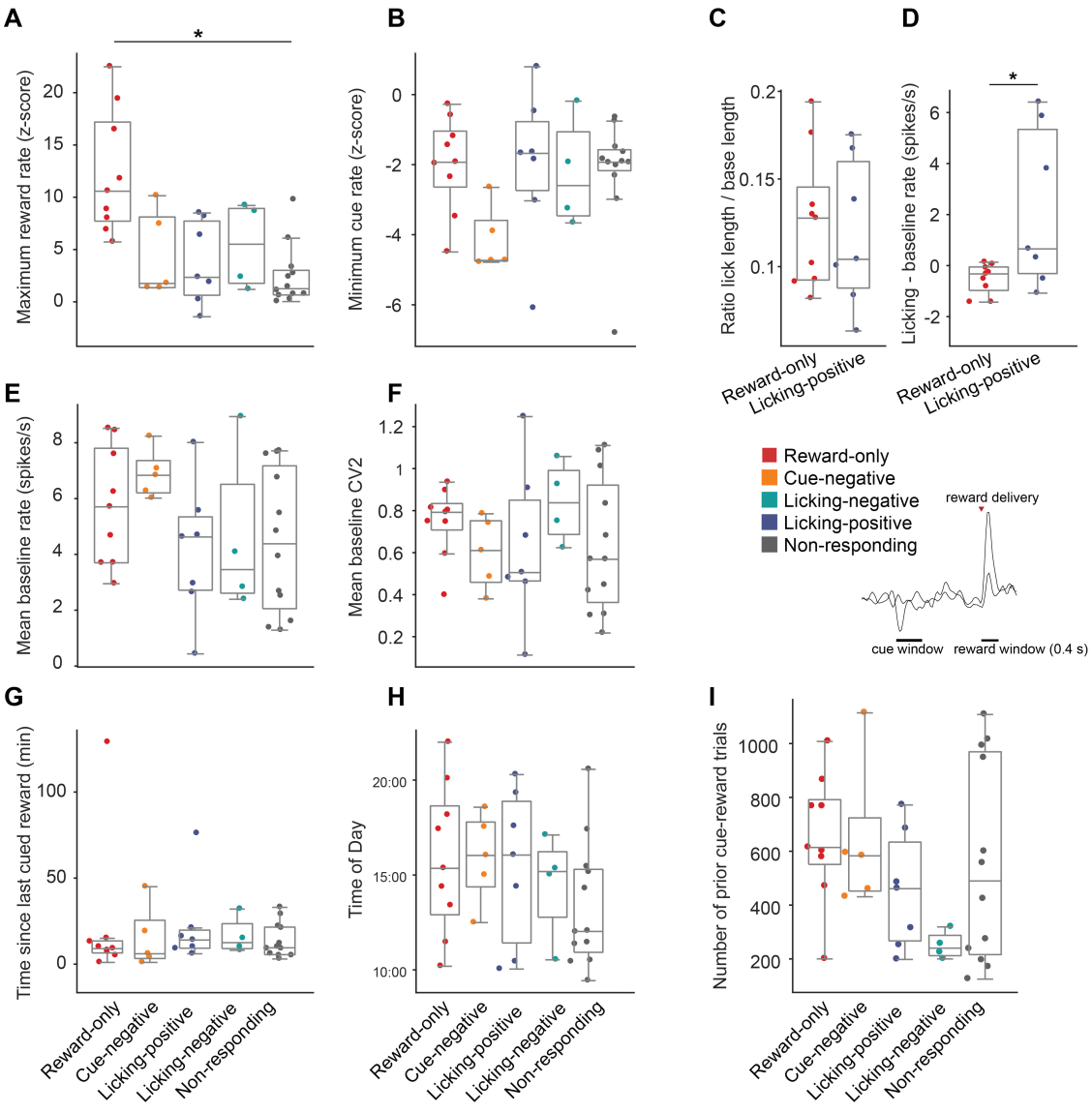
A
B
C
D
Maximum reward rate (z-score)
Minimum cue rate (z-score)
Ratio lick length / base length
Licking - baseline rate (spikes/s)
Reward-only
Licking-positive
E
F
Mean baseline rate (spikes/s)
Mean baseline CV2
Reward-only
Cue-negative
Licking-negative
Licking-positive
Non-responding
reward delivery
cue window
reward window (0.4 s)
G
H
I
Time since last cued reward (min)
Time of Day
Number of prior cue-reward trials
Reward-only
Cue-negative
Licking-positive
Licking-negative
Non-responding

Figure 6.10: Diversity in responses of identified midbrain dopamine neurons in cued reward task could not be explained by recording conditions. (A) Reward-only neurons had a significantly higher maximal reward rate than non-responding neurons (Kruskal-Wallis one-way ANOVA ($p = 0.005$) with Tukey Kramer post-hoc, $p = 0.0019$) and (B) there was no difference in minimum cue rate (Kruskal-Wallis one-way ANOVA, $p = 0.08$). (C) Licking-positive neurons did not differ in licking behaviour, measured as ratio between the length of lick-only phases and length of baseline periods) (t-test, $p = 0.75$) but (D) showed higher firing rate increases during non-rewarded lick-phases than reward-only neurons (calculated as difference between mean firing rate during lick-only phases and mean firing rate during baseline periods) (t-test, $p = 0.02$). Response groups did not differ in (E) mean baseline firing rate (one-way ANOVA, $p = 0.23$), (F) mean baseline firing regularity (measured as CV2; one-way ANOVA, $p = 0.55$), (G) time since the last cued reward was received prior to recording of individual neurons (Kruskal-Wallis one-way ANOVA, $p = 0.68$), (H) time of day (one-way ANOVA, $p = 0.46$) or (I) level of task experience (number of previously received cued reward trials, summed across training and recording days) (Kruskal-Wallis one-way ANOVA, $p = 0.17$). (A-D) Box plots illustrate effect of statistical separation of response groups shown in Figure 6.9 and should not be seen as separate informative analysis. Legend depicting colour-code for response groups. Black bars: Time windows used to determine minimal cue response in (B) (cue window) and maximal reward response in (A) (reward window). Red arrowhead marks reward delivery. Data are displayed with first quartile, median and third quartile.

Interestingly, the magnitude of the reward response (measured as maximum z-score during 400 ms window following reward delivery) scaled with experience (measured as prior received cued rewards; Figure 6.11). This relationship was seen when all identified dopamine neurons were included in the analysis (Pearson's correlation; $R = 0.31$, $p = 0.048$; Figure 6.11B; note that all identified dopamine neurons from seven classifications as listed in Table 6.4 were included in this analysis) as well as when only neurons with a positive reward response were included (Pearson's correlation; $R = 0.68$, $p = 0.004$; Figure 6.11C). There was no correlation between maximal rate during reward and time of day (Pearson's correlation; $R = 0.27$, $p = 0.30$) or time to last reward (Pearson's correlation; $R = 0.29$, $p = 0.28$). The correlation between maximum rate during the cue and trial number was not significant (Pearson's correlation; $R = 0.31$, $p = 0.053$; Figure 6.11A).

Taken together, identified dopamine neurons located in VTA and SNc responded to cue, reward and licking in a classical conditioning paradigm with diverse changes

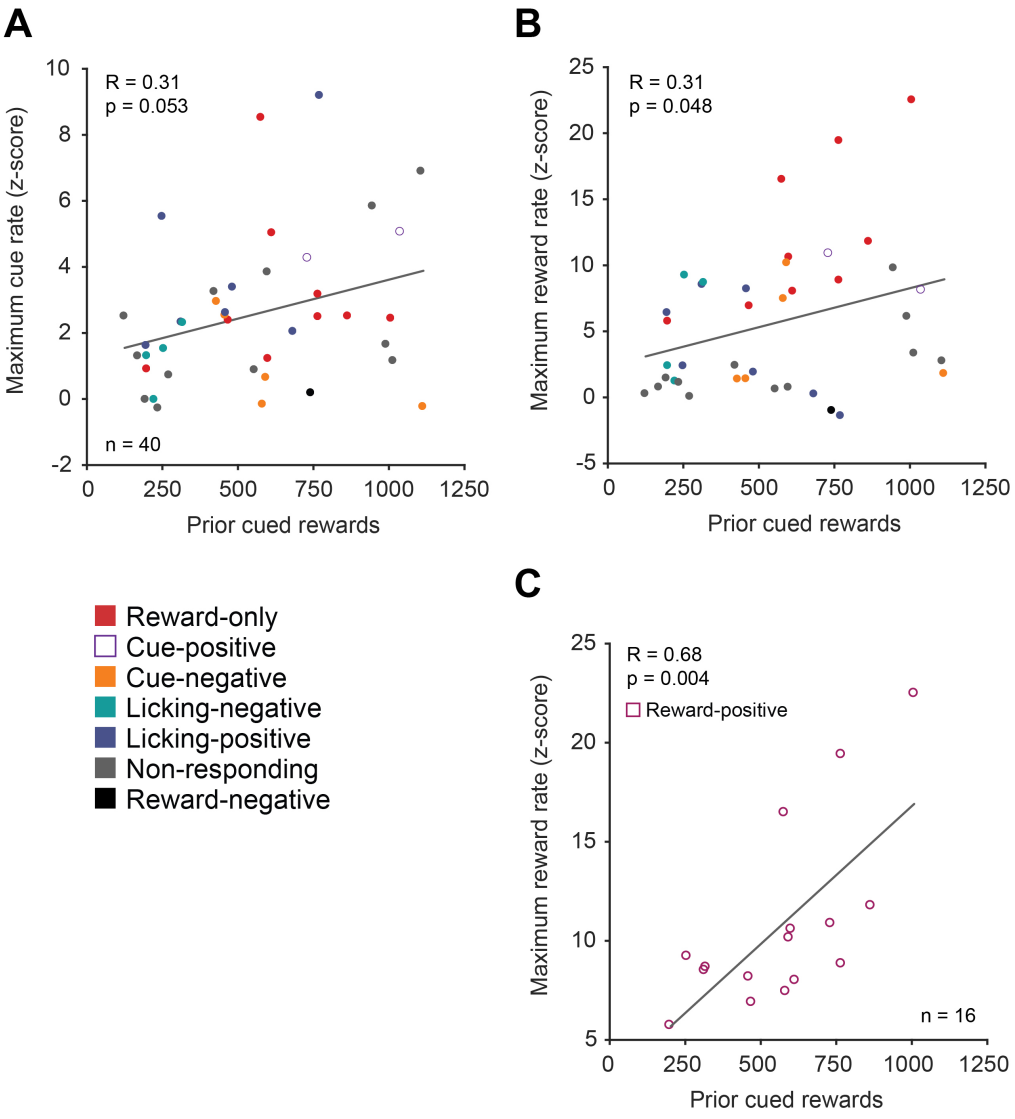

Figure 6.11: Magnitude of reward response scales with experience. (A) Maximum rate during cue (measured as peak z-score during cue presentation) did not correlate with experience (measured as prior received cued rewards) (n = 40; Pearson's correlation; R = 0.31, p = 0.053). (B-C) Magnitude of reward response was dependent on experience of cued reward trials both when (B) all neurons were included (n = 40; Pearson's correlation; R = 0.31, p = 0.048), as well as when (C) only selecting neurons with positive reward responses (see Table 6.4; n = 16 neurons; Pearson's correlation; R = 0.68, p = 0.004). Note that (A-B) includes all neurons from the seven classifications listed in Table 6.4.

in their firing. These different response types did not result from differences in recording condition such as time of day or time to last received cued reward. Additionally, reward response magnitude in reward-responding neurons scaled with prior experience.

6.4.7 Response types are not segregated by anatomical location

Midbrain dopamine neurons have diverse projection targets with medial SNc and VTA dopamine neurons mostly projecting to the nucleus accumbens and/or cortex, and with more laterally located SNc dopamine neurons projecting mostly to the dorsal striatum (see Chapter 5). This anatomical gradient has been suggested to map onto 'functional gradients' (encoding of behavioural events) observed in the midbrain (Bromberg-Martin et al. 2010). Single-unit recordings combined with juxtacellular labelling allow for retrieval of the exact anatomical location of an individual neuron. To test whether the response groups of identified midbrain dopamine neurons in this study (see section 6.4.6) were segregated by location, each neuron was assigned to either VTA or SNc and anatomical coordinates of each cell were measured as mediolateral (ML), anteroposterior (AP) and dorsoventral (DV) distance from Bregma (Paxinos and Franklin 2013). Response groups did not correspond to a preferred anatomical location when plotted onto schematics of coronal midbrain sections (Figure 6.12A): 4 of 9 reward-only, 3 of 5 cue-negative, 3 of 7 licking-positive, 3 of 4 licking-negative and 7 of 12 non-responding dopamine neurons were located in SNc. To investigate whether responses followed a gradient rather than a sharp separation between the midbrain nuclei VTA and SNc (as imposed by stereotaxic atlases), two-dimensional plots of rostrocaudal against mediolateral location were generated (Figure 6.12B-C). Neurons of distinct response types did not cluster or segregate along the mediolateral or rostrocaudal axis (Figure 6.12B).

16 of 40 identified dopamine neurons displayed phasic increases following reward delivery. To test whether neurons with positive reward responses were localized to

a discrete anatomical location in the midbrain (irrespective of modulation by the other explanatory variables), rostrocaudal location was plotted against mediolateral location for all cells with a positive reward response (16 of 40 identified dopamine neurons; Figure 6.12C). In accordance with the data classified into response groups, reward-responses were not predictable based on anatomical location (Figure 6.12C). Taken together, these data show that the responses of identified midbrain dopamine neurons were not correlated with anatomical location within the midbrain, and that neurons of each response type could be found both in VTA and SNc.

6.4.8 Response types are not segregated by molecular marker expression

Differences in the expression of molecular markers, e.g. transcription factors, calcium-binding proteins or specific enzymes, in midbrain dopamine neurons can inform on their projection target (see Chapter 5) as well as help identify subpopulations with differential vulnerability in diseases like Parkinson's. Differential expression of molecular markers in midbrain dopamine neurons was identified in early studies (Gerfen, Baimbridge, et al. 1985; Liang, Sinton, and German 1996; Schein et al. 1998) and analysed more recently on larger scales using microarray analysis and single-cell gene expression profiling (Chung, Seo, et al. 2005; Greene 2006; Greene, Dingledine, et al. 2005; Grimm et al. 2004; La Manno et al. 2016; Poulin, Zou, et al. 2014). To test whether the functional response types discussed in section 6.4.6 would map onto distinct expression of a selected subset of markers, individual identified dopamine neurons were tested (after recording and labelling) for the expression of the transcription factor Sox6, the calcium-binding protein Calbindin and the dehydrogenase enzyme Aldh1a1 (see Chapter 5). The three markers were selected based on the results for projection-target selectivity from Chapter 5. Sox6 was predominantly expressed in neurons projecting to the DS, Calbindin was predominantly expressed in midbrain dopamine neurons projecting to the NAc, and Aldh1a1 was expressed in midbrain dopamine neuron populations targeting NAc or DS (see Figure 5.2 and Figure 5.3). Furthermore, La Manno et al. (2016) showed

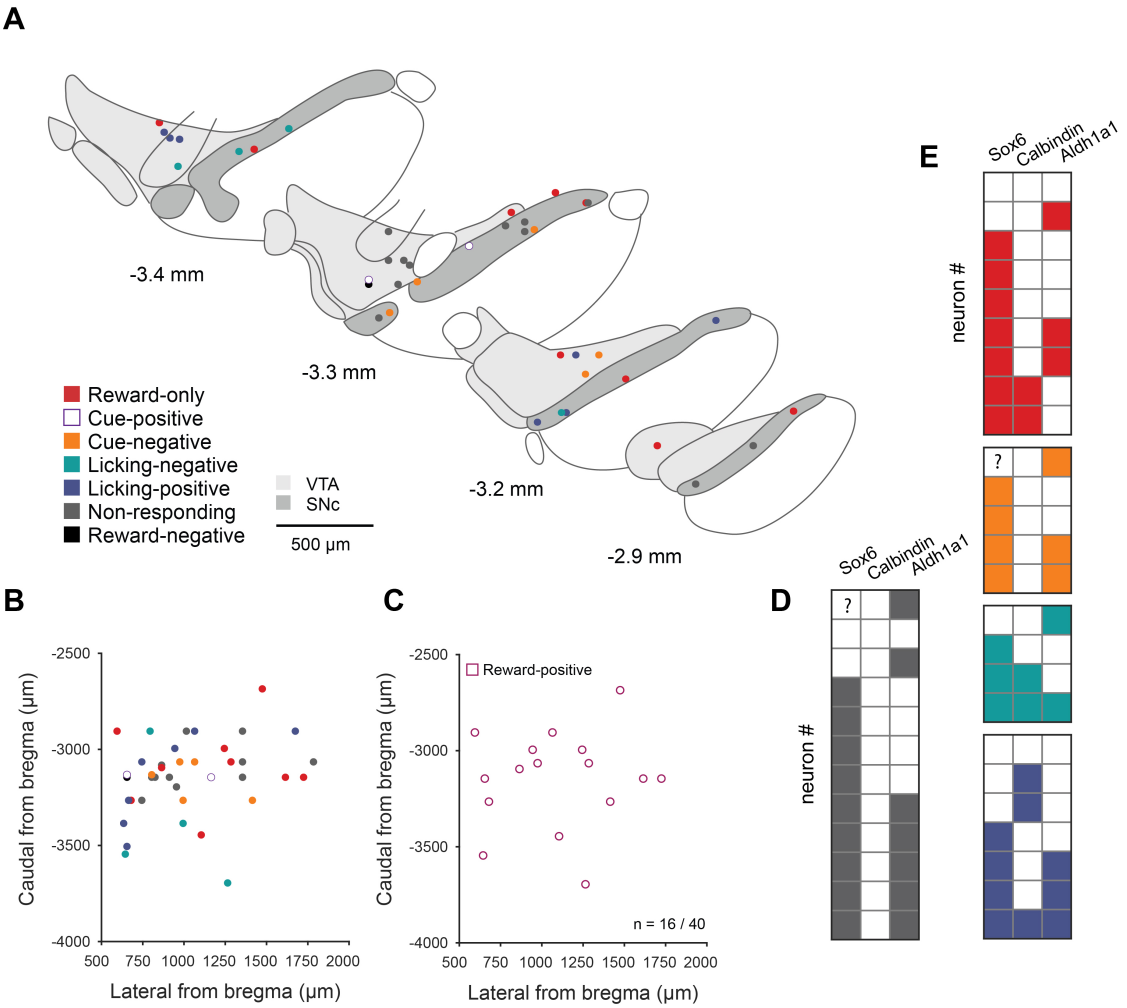

Figure 6.12: Response groups of identified midbrain dopamine neurons recorded in cued reward task are not segregated by anatomical location or marker expression. (A-C) Neurons with response types are not confined to specific locations within midbrain. (A) Approximate anatomical locations of identified midbrain dopamine neurons collapsed onto 4 rostrocaudal midbrain sections. Response groups are colour-coded (see legend); numbers indicate distance from Bregma (Paxinos and Franklin 2013). (B-C) Rostrocaudal location of individual neurons (circles) plotted against the mediolateral position colour-coded for (B) all response groups (n = 40 neurons) and (C) all neurons with positive reward response (magenta; n = 16). (D-E) Individual response groups do not map onto marker expression of the three molecular markers Sox6, Calbindin and Aldh1a1 (see Chapter 5). Checkerboards are colour-coded (see legend); filled squares indicate marker expression of Sox6, Calbindin and Aldh1a1 (columns). Each individual neuron is represented in one row. Question marks were placed where expression could not be determined due to missing nuclei in the section. Note that (A-B) includes all neurons from the seven classifications listed in Table 6.4.

that combinations of these three markers are differentially expressed in distinct (solely molecularly defined) populations of midbrain dopamine neurons.

When identified dopamine neurons were divided into functional response groups, each group contained diverse patterns of marker expression with three to five different patterns per group (out of the eight theoretically possible marker combinations; Figure 6.12D-E). Marker expression of individual neurons is displayed as checkerboard-plot, whereby each row represents an individual neuron and individual columns represent different molecular markers (Figure 6.12D-E). Note that tendencies of preferential marker expression are difficult to assess systematically with the relatively small sample size in each response group in this study.

To investigate the possibility that the response groups defined in section 6.4.6 could mask response differences in midbrain dopamine neurons with distinct marker expression, recordings from the classical conditioning task were regrouped based on the combinatorial expression of the three markers. Out of the eight theoretically possible marker combinations, seven were found in identified midbrain dopamine neurons (only 38 of 40 neurons were included in the analysis since Sox6 expression could not be examined for two neurons due to missing nuclei). 2 of 38 neurons were positive for Calbindin but not Aldh1a1 or Sox6 (Calbindin-only; Figure 6.13A), 3 of 38 neurons for Aldh1a1 but not Calbindin or Sox6 (Aldh1a1-only; Figure 6.13B) and 12 of 38 neurons for Sox6 but not Aldh1a1 or Calbindin (Sox6-only; Figure 6.13C). Four of 38 neurons co-expressed Calbindin and Sox6, but not Aldh1a1 (Calbindin-Sox6; Figure 6.13D), 11 of 38 neurons co-expressed Sox6 and Aldh1a1 but not Calbindin (Aldh1a1-Sox6; Figure 6.13F), and 3 of 38 neurons co-expressed all three markers (Aldh1a1-Calbindin-Sox6; Figure 6.13E). Three of 38 neurons were negative for Sox6, Calbindin and Aldh1a1 (Triple-negative; Figure 6.13G). Four of 7 marker combination-defined neuron groups showed significant short-latency increases within 0.4 seconds following reward delivery (Aldh1a1-only, Sox6-only, Calbindin-Sox6 and Triple-negative; assessed by a mean z-score above 2; Figure 6.13B-D,G), Aldh1a1-Sox6 neurons did not show such a short latency increase above a z-score of 2. Calbindin-only and Aldh1a1-Calbindin-Sox6 neurons showed

increased firing but with a longer latency following reward onset (> 500 ms; Figure 6.13A,E). Calbindin-only neurons were the only marker expression group restricted to one response type (Licking-positive; see section 6.4.6). However, since only two neurons were identified as Calbindin-only, these results are not conclusive. Taken together, marker expression for identified midbrain dopamine neurons was not confined to individual response groups with most marker combinations being present in each of the response groups.

6.4.9 Putative midbrain dopamine neurons show diverse responses in classical conditioning task

All analyses detailed above were performed on extracellular single-unit recordings of identified midbrain dopamine neurons. However, due to the challenging nature of the single-cell recording/labelling technique, not every single-unit recording could be completed with successful labelling of the neuron (e.g. extracellular spikes are 'lost' because the animal starts vigourously running at the end of the recording but before juxtacellular labelling can be employed to fill the neuron with neurobiotin). To investigate whether response groups observed in identified dopamine neurons were also present in the (larger) dataset of putatively-classified dopamine neurons, recording traces of unlabelled neurons were analysed. Unlabelled neurons were split into putative dopamine and non-dopamine neurons based on spike width and firing rate (Barter, Li, et al. 2015; Janezic et al. 2013; Pan et al. 2005; Wang and Tsien 2011). For a single-unit to be classified as a putative dopamine neuron, the width of its filtered spike (measured from threshold-to-trough) had to be bigger than 1 ms (see inset Figure 6.14A) and its firing rate lower than 10 spikes per second – more than 90 % of identified dopamine neurons met these two criteria (38 of 42 neurons; the 42 neurons include the two neurons located in RRF which were excluded from the other analyses); Figure 6.14A). 106 of 129 unlabelled neurons recorded in 24 animals were classified as putative dopamine neurons and included in the analysis (Figure 6.14A). Minimum trial number per recording was 4 (median 6, maximum 12) and median inter-trial interval was 6.3 seconds (minimum 3.4

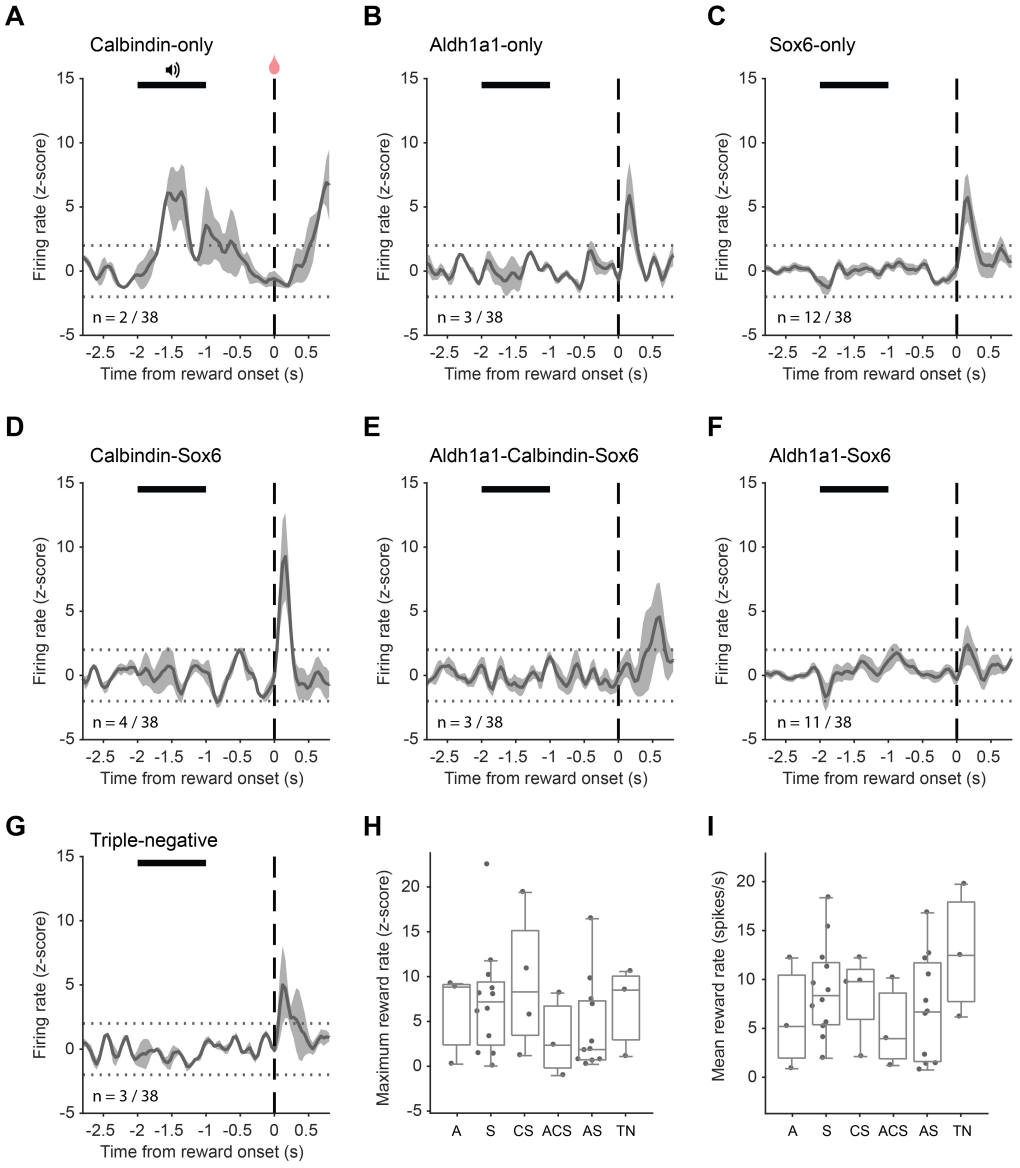

Figure 6.13: Average response of identified midbrain dopamine neurons in cued reward task split by marker expression. (A-G) Reward-aligned response PETHs for neurons expressing out of the three tested markers (A) only Calbindin (n = 2), (B) only Aldh1a1 (n = 3), (C) only Sox6 (n = 12), (D) Calbindin and Sox6 (n = 4), (E) Aldh1a1, Calbindin and Sox6 (n = 3), (F) Aldh1a1 and Sox6 (n = 11), or (G) not either (n = 3). (H-I) Reward response magnitude did not show significant differences between response groups for maximum reward rate (Kruskal-Wallis one-way ANOVA, p = 0.62) (H) or mean reward rate (one-way ANOVA, p = 0.47) (I); Calbindin-only neurons were not included in the analysis because there were only two. Two neurons for which Sox6 expression could not be determined were excluded from this analysis. A, Aldh1a1-positive; C, Calbindin-positive; S, Sox6-positive; TN, triple-negative. Data in (A-G) show mean ± SEM; boxplots in (H-I) display first quartile, median and third quartile. Horizontal black bars represent cue duration, vertical dashed lines indicate reward delivery, dashed horizontal lines are positioned at z-scores ±2.

s, maximum 25.0 s). The median firing rate for putative dopamine neurons was 4.9 spikes/s. The average response of putative dopamine neurons to cue/reward (Figure 6.14B) was similar to that of identified dopamine neurons in SNc and VTA (Figure 6.7A-B) and showed a significant phasic increase in firing following reward onset with a maximum reward z-score of 4.8 and a peak delay of 120 – 160 ms. To test whether putative dopamine neurons would divide into the response groups seen in identified dopamine neurons, the same generalised linear regression model was used on individual recording traces of putative dopamine neurons as for the identified midbrain dopamine neurons (see section 2.5.5 and 6.4.6). As before, recording traces were subdivided into 100 ms bins and cue, reward, and licking were included in the model as categorical variables to explain firing rate. As can be seen when plotted as Venn diagram, some neurons were only modulated by one of the three variables, whereas other neurons were modulated by combinations of them (note that the Venn diagram does not differentiate between positive or negative modulation; Figure 6.14C). Analysis of the Venn diagram shows that the proportions of reward, licking and cue responsive neurons were similar between identified and putative dopamine neurons: 27.4 % of neurons were reward-only responsive (25 % in identified dopamine neurons), 9.4 % were reward-licking responsive (12.5 % in identified dopamine neurons), 8.5 % were licking-only responsive (10 % in identified dopamine neurons), 9.4 % were cue-licking responsive (2.5 % in identified dopamine neurons), 3.8 % were cue-reward-licking responsive (2.5 % in identified dopamine neurons), 5.6 % were reward-cue responsive (2.5 % in identified dopamine neurons), 8.5 % were cue-only responsive (10 % in identified dopamine neurons) and 27.4 % were non-responding (30 % in identified dopamine neurons).

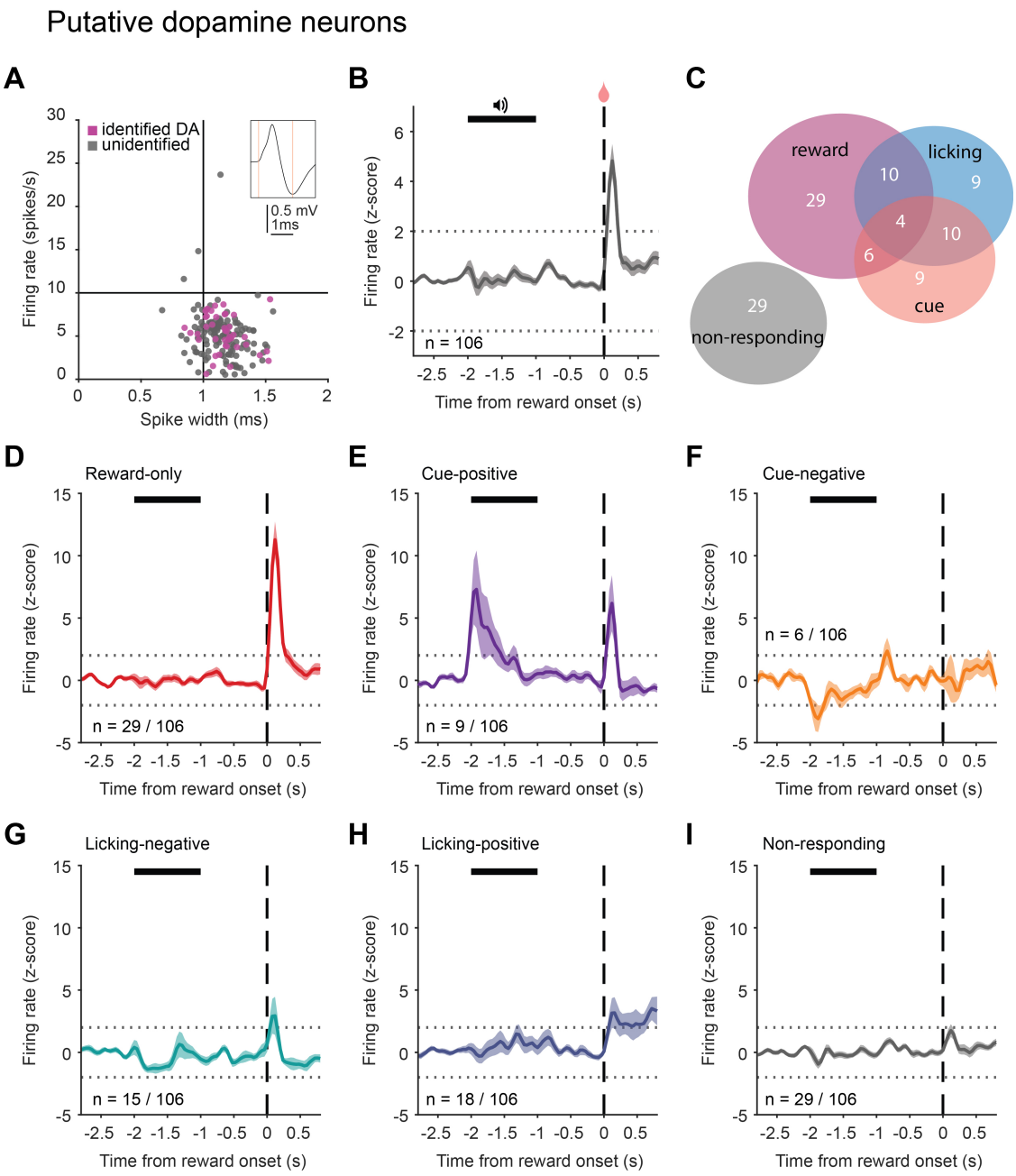

Figure 6.14: Linear regression reveals diverse response types of putative dopamine neurons in a cued reward task. (A) Putative dopamine neurons were classified based on their firing rate and spike width from threshold-to-trough (see inset). Unidentified neurons with a spike width $>$ 1 ms and a firing rate $<$ 10 spikes/s were considered putative dopamine neurons (n = 106; grey circles in bottom right quadrant of plot). Overlaid in magenta are the properties of identified dopamine neurons (see section 6.4.6). (B) Average activity of putative dopamine neurons shows phasic reward response. (C) Venn diagram showing numbers of neurons significantly correlated to reward, cue, licking or combinations thereof. Note: Venn diagram does not differentiate between positive or negative correlation coefficients. (D-I) Reward-aligned average activity of dopamine neurons responding with (D) rate increase to reward only (n = 29), (E) rate increase to cue (n = 9), (F) rate decrease to cue (n = 6), (G) rate decrease during licking behaviour (n = 15), (H) rate increase during licking behaviour (n = 18) or (I) not responding (n = 29). Horizontal black bars represent cue duration, vertical dashed lines indicate reward delivery. Data in (B,D-I) show mean ± SEM. DA, dopamine.

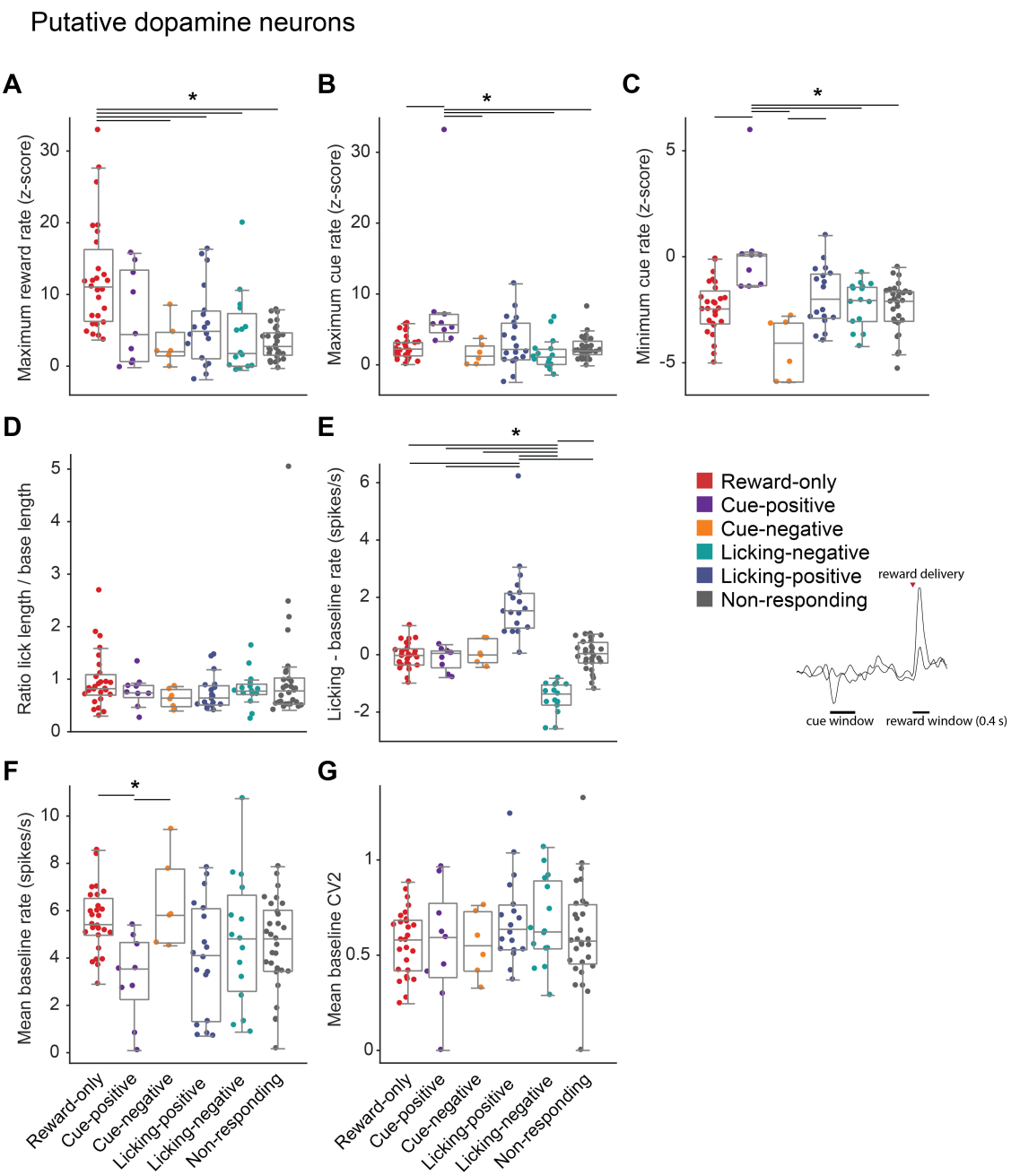
Putative dopamine neurons
A
B
C
D
E
F
G
Maximum reward rate (z-score)
Maximum cue rate (z-score)
Minimum cue rate (z-score)
Ratio lick length / base length
Licking - baseline rate (spikes/s)
Mean baseline rate (spikes/s)
Mean baseline CV2
Reward-only
Cue-positive
Cue-negative
Licking-positive
Licking-negative
Non-responding
reward delivery
cue window
reward window (0.4 s)

Figure 6.15: Comparison of response properties of putative midbrain dopamine neurons in cued reward task. (A) Reward-only neurons had a significantly higher maximal reward rate than most other response groups (Kruskal-Wallis one-way ANOVA with Tukey Kramer post-hoc, $p = 9*10^{-6}$ and (B) Cue-positive neurons had a significantly higher maximal cue response than most other response groups (Kruskal-Wallis one-way ANOVA with Tukey Kramer post-hoc, $p = 0.0001$). (C) Comparison of minimal cue response (Kruskal-Wallis one-way ANOVA with Tukey Kramer post-hoc, $p = 8*10^{-5}$. (D) Response groups did not differ in lick-phases (measured as ratio between the length of lick-only phases and length of baseline periods) (Kruskal-Wallis one-way ANOVA, $p = 0.43$). (E) Licking-positive neurons showed higher firing rate increases during non-rewarded lick-phases than most other response groups (calculated as difference between mean firing rate during lick-only phases and mean firing rate during baseline periods) and licking-negative neurons showed higher firing rate decreases during non-rewarded lick-phases than most other response groups (Kruskal-Wallis one-way ANOVA with Tukey Kramer post-hoc, $p = 8*10^{-13}$. (F) Some response groups differed in baseline firing rate (one-way ANOVA with Tukey Kramer post-hoc, $p = 0.009$). (G) Response groups were similar in baseline firing regularity (measured as CV2; one-way ANOVA, $p = 0.45$). (A-E) Box plots illustrate effect of statistical separation of response groups shown in Figure 6.14 and should not be seen as separate informative analysis. Legend depicting colour-code for response groups. Black bars below the graph represent the time windows used to determine minimal and maximal cue response in (B-C) (cue window) and maximal reward response in (A) (reward window). Red arrowhead marks reward delivery. Data display first quartile, median and third quartile.

After obtaining regression coefficients and p-values for each explanatory variable for every cell, data were grouped based on response type. Putative dopamine neurons were allocated to the same response groups as identified dopamine neurons (see Figure 6.14D-I; Table 6.5). Reward-aligned plots for putative dopamine neurons showed similar response patterns for individual response groups as identified dopamine neurons. Reward-only putative dopamine neurons had a mean peak z-score of 11.3 and a peak latency of 120 – 160 ms following reward onset. Maximum reward rate for reward-only dopamine neurons was significantly higher than the maximum reward rate of all other response groups apart from cue-positive neurons (Figure 6.15A). Cue-positive neurons increased their firing during the cue-presentation (average maximum cue rate measured as z-score was 7.3, peak delay of 80 – 120 ms; Figure 6.14E) and cue-negative neurons decreased their firing during cue presentation (average minimum cue rate measured as z-score of -3.1; Figure 6.14F). The latency of the maximal positive cue response in the cue-positive response group

of putative dopamine neurons is similar to previously reported delays (Eshel, Tian, et al. 2016; Matsumoto, Tian, et al. 2016). When comparing the maximum rate during cue (measured as maximum z-score within 600 ms window after cue onset), cue-positive neurons had a significantly higher response to the cue than almost all other response groups (Figure 6.15B). Like in the case of identified midbrain dopamine neurons, putative dopamine neurons assigned to different response groups did not differ in baseline firing regularity (Figure 6.15G). However, cue-positive neurons had a significantly lower baseline firing rate than reward-only neurons and cue-negative neurons (Figure 6.15F). To test whether lick behaviour of animals was similar across response groups, the ratio between baseline recording length (recording periods without licking, cue or reward) and licking recording length (recording periods with licking but no cue or reward) of individual cells was compared. Ratios did not differ between groups, indicating that lick behaviour was similar between response groups (Figure 6.15D). To compare firing rate changes between baseline and lick-phases, the difference between baseline firing and firing during licking (excluding cue and reward phases) was calculated. Licking-positive neurons were the only response group with exclusively positive rate changes (Figure 6.15E) and their rate change was significantly higher compared to most other response groups (Figure 6.15E). Licking-negative neurons had exclusively negative rate changes which were significantly smaller compared to all other response groups (Figure 6.15E). Taken together, response groups observed in identified midbrain dopamine neurons were also characteristic for the larger dataset of putative dopamine neurons and comparison of their response properties support the linear-regression based response classification.

6.4.10 Cue-response in identified non-dopamine neurons located in the midbrain

In the light of common concepts of reward prediction-signalling of dopamine neurons, a shift of the positive response from the outcome (reward) to the outcome-predicting cue would have been expected after mice had learned the classical conditioning task

Table 6.5: Response types of putative midbrain dopamine neurons in cued reward task. Each row marks a designated response group. The last three columns indicate how many neurons in each response group correlated positively (pos) or negatively (neg) with cue, reward and licking behaviour. Baseline rate (spikes/s) and baseline CV2 given as median.

Response type	n	Baseline rate	CV2	cue		reward		licking	
				pos	neg	pos	neg	pos	neg
Reward-only	27	5.4	0.58	0	0	**27**	0	0	0
Cue-negative	6	5.8	0.55	0	**6**	2	0	0	0
Licking-positive	18	4.1	0.64	2	6	5	3	**18**	0
Licking-negative	15	4.8	0.62	2	4	6	0	0	**15**
Cue-positive	9	3.5	0.59	**9**	0	4	0	0	0
Reward-negative	2	4.7	0.59	0	0	0	**2**	0	0
Non-responding	29	4.8	0.57	**0**	**0**	**0**	**0**	**0**	**0**

(Mirenowicz et al. 1994). However, despite a significant increase in anticipatory licking indicating that animals learned the cue-reward association (see Figure 6.6), only 2 of 40 (5%) identified midbrain dopamine neurons showed a significant positive cue response. In putative dopamine neurons, the proportion was slightly higher (∼12%) and the average plot of cue-positive neurons showed a significant cue response (Figure 6.14E). The significant increase in the firing of cue-positive putative dopamine neurons appeared with a delay of 80 – 120 ms following cue onset, identical to the delay of non-dopamine neurons with positive responses to sensory stimuli (see Figure 6.5C). To investigate the possibility that some of the cue-responsive single-units that were classified as putative dopamine neurons could in fact be cue-responsive non-dopamine neurons (see section 6.4.4), the small set of identified non-dopamine neurons with 'dopamine neuron-like' action potential waveforms and firing rates (i.e. firing rate < 10 spikes/s and spike width threshold-to-trough $>$ 1ms) were analysed (Figure 6.16). The average response of identified non-dopamine neurons did show a small but significant cue response (z-score 2.4; median baseline firing rate 2.4 spikes/s; median baseline CV2 = 0.68; n = 4; Figure 6.16A,C). These results indicate that the cue-positive group of putative dopamine

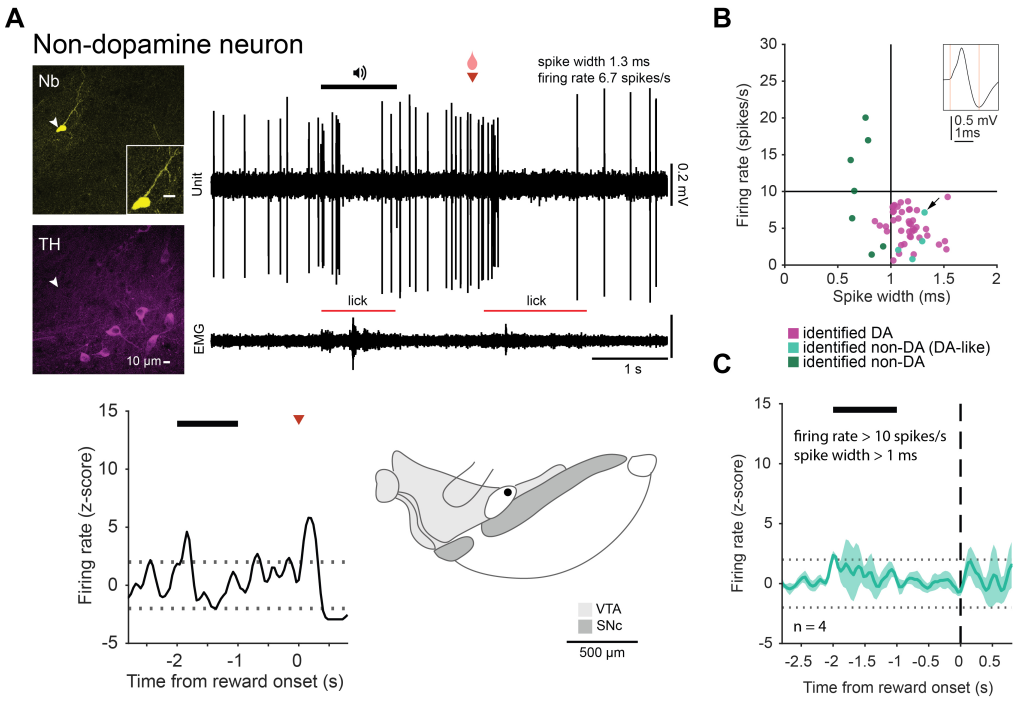

Figure 6.16: Cue response of identified non-dopamine neurons in a cued reward task. (A) A "dopamine neuron-like" non-dopamine neuron identified through juxtacellular labelling and absence of TH immunoreactivity. The neuron had a baseline firing rate of 6.7 spikes/s and a spike width of 1.3 ms. Horizontal black bar above the Unit trace represents cue duration, the red arrowhead marks reward delivery. Red bars above EMG indicate licking. The coronal schematic depicts the location of the recorded neuron (located in the medial terminal nucleus). (B) Firing rate and spike width of identified non-dopamine neurons (green/turquoise). The four neurons with spike width $>$ 1 ms and firing rate $<$ 10 spikes/s (turquoise) were included in the PETH in (C) The neuron displayed in (A) is marked with an arrow. Nb, neurobiotin; TH, tyrosine hydroxylase; DA, dopamine; EMG, electromyogram. Data in (C) show mean $\pm$ SEM.

neurons (Figure 6.14E) could be contaminated by the response of non-dopamine neurons. This reiterates the importance of identifying the type of cell recorded.

6.5 Discussion

The aim of this Chapter was to investigate responses of identified midbrain dopamine neurons to neutral sensory stimuli as well as to value-bearing cues and rewards. To avoid stimulus-generalisation between tasks, experiments addressing whether and how midbrain dopamine neurons signal sensory stimuli and whether and how they represent reward-predicting cues and predicted rewards were performed in separate cohorts of mice. Information representation in midbrain dopamine neurons has been studied since the late 1970s. Early studies have linked their firing changes to (presumably) neutral sensory stimuli. Recordings of putative dopamine neurons (classified by their response to apomorphine which activates D2-autoreceptors on dopamine neurons and results in decreased firing; Pan et al. 2005) in anaesthetised rats showed firing increases following light flashes or olfactory stimulation (Chiodo, Caggiula, et al. 1979; Chiodo, Antelman, et al. 1980), although the average response latencies of 400 ms (olfactory) and 1000 – 2000 ms (light flashes) were considerably longer than response latencies reported in studies performed on awake animals (see e.g. present study). Recordings of apomorphine-classified dopamine neurons in freely-moving cats showed mixed responses to auditory and visual stimuli: Studies using 113 dB click sounds or light flashes report phasic firing increases in all recorded neurons (Steinfels et al. 1983b) but more often a mix of phasic increase and decrease (with latencies ranging from 35 – 100 ms) observed in only a proportion of all recorded neurons (Horvitz et al. 1997; Steinfels et al. 1983a; Strecker et al. 1985). These previous findings in cats are in accordance with the results of the present study, where only half of the neurons showed responses to neutral light and tone stimuli (10 of 21), with some exhibiting firing increases (4 of 21), and others firing decreases (3 of 21), or biphasic responses (3 of 21) (see Figure 6.4) – although with an overall longer latency (280 – 320 ms for firing increases and 160 – 200 ms for firing decreases; Table 6.1). It is worth noting that clicks used in the cat studies had a sound-pressure level of 113 dB (which is equivalent to a live rock concert), while this study used milder tones at ∼70 dB (equivalent to conversation). Primate-studies have shown that differences in sound volume differentially affect

responses of midbrain dopamine neurons: While a proportion of putatively classified dopamine neurons in macaques responded with a phasic short-latency (80 ms) increase in firing to 90 dB sounds, they showed either no response or firing decrease with a longer latency (200 ms) to 70 dB sounds (Fiorillo et al. 2013). While stimuli used in the present study were selected to lie within the visible and audible range of mice (Ehret 1983; Henry et al. 1980; Huberman et al. 2011; Willott 1986) and to not elicit startle responses, in particular the 1 kHz auditory stimulus is located at the bottom edge of the audible range for most mice. This leaves the possibility that mice were not able to perceptually detect the cue. However, although not systematically assessed, mice often reacted with subtle muscle twitches to the first stimulus presented during recording of individual neurons (irrespective of stimulus type), indicating that mice were able to perceive the individual sensory stimuli.

One strength of the present study is that recorded neurons were unequivocally identified as dopamine neurons using juxtacellular labelling and post-hoc immunofluorescence. Interestingly, some neurons with a response to the auditory and visual stimuli were identified as non-dopamine neurons (Figure 6.5). Even though some of them would not have been classified as putative dopamine neuron based on waveform-classification and firing rate, others fell within commonly used cut-off criteria (Figure 6.5A-B). This highlights the importance of methods that allow identification of dopamine neurons to avoid misclassifications, especially in regions like the midbrain, where different cell types share some electrophysiological properties and are intermingled. The proposed function of responses to neutral sensory stimuli in dopamine neurons is the signalling of perceptually salient or novel events which could indicate value-bearing content in the present environment (Bromberg-Martin et al. 2010; Schultz 1998; Schultz 2007b). If responses to neutral stimuli are novelty signals, one would expect the response to disappear with increased exposure. To test this hypothesis, response magnitude of identified midbrain dopamine neurons to sensory stimuli was correlated with the level of prior exposure (Figure 6.4). While positive responses did not correlate with novelty of stimuli, the magnitude of negative responses was smaller for decreased novelty (see Figure 6.4G-H), indicating

that novelty might partially explain responses of midbrain dopamine neurons. A recent study using fibre photometry compared novelty and value coding in axonal fields of midbrain dopamine neurons (accessed and identified through Cre-dependent viral vectors) and concluded that novelty-related responses occurred in axons projecting to the tail of the striatum (TS), whereas value-related responses were found in axons projecting to the NAc (Menegas, Babayan, et al. 2017). In accordance with the present study, Menegas et al. (2017) observed that novelty-related responses decreased with increased familiarity (see e.g. Figure 2 of the study) (Menegas, Babayan, et al. 2017), but they only report response increases to novel stimuli (Menegas, Babayan, et al. 2017). However, the two studies are not directly comparable because tracking calcium signals in axon fields (which represents some form of population activity) is very different from measuring the firing of individual neurons. Additionally, while neutral stimuli (i.e. not predicting an outcome) seem to cause signal increases in TS-projecting dopamine neurons, they result in signal decreases in ventral striatum-projecting dopamine neurons (see "nothing odor" and "unpredicted tone" trials, Figure 6; Menegas, Babayan, et al. 2017), which could parallel the mix in responses found in the present study (see Figure 6.4). Responses shown in the present study are unlikely to be contaminated by movement-related responses (Dodson, Dreyer, et al. 2016) since trials containing movements were excluded from the analysis. However, it cannot be ruled out that responses to sensory stimuli involve some sort of motivational aspect rather than just perceptual salience. They could, for instance, be the result of aversive properties of the sensory stimuli, e.g. the volume of a sound (Bromberg-Martin et al. 2010; Matsumoto and Hikosaka 2009). In some studies, milder sensory stimuli were used to avoid stimuli being perceived as aversive (Fiorillo et al. 2013; Ison et al. 2007; Menegas, Babayan, et al. 2017). Some studies have attributed responses to neutral stimuli to stimulus generalisation, especially if neutral stimuli were of the same modality as value-bearing ones and presented in a reward context (Kobayashi et al. 2014; Romo et al. 1990; Schultz 2015; Schultz and Hollerman 1998). With such experimental designs incorporating neutral and valued stimuli, it is not clear

whether midbrain dopamine neurons respond to neutral, mild stimuli or whether it is purely a generalisation effect. The present study showed that some midbrain dopamine neurons respond with phasic firing changes to neutral sensory stimuli outside of a reward- or punishment-context. However, when all neurons were taken together, then no average change in their output was detected.

Reward prediction error learning was first proposed by Rescorla and Wagner (1972) and has since become a prominent concept to account for both instrumental as well as Pavlovian conditioning phenomena (Schultz, Apicella, et al. 1993; Schultz, Dayan, et al. 1997; Waelti et al. 2001). Phasic changes in the firing of midbrain dopamine neurons were found to be neural correlates for predictions from reward-based learning theory: In a Pavlovian forward conditioning paradigm, phasic firing changes are initially elicited following the unconditioned stimulus (e.g. a reward). This response shifts with trial repetition (i.e. learning) to the preceding conditioned stimulus (e.g. a tone) while being attenuated following the reward (see Figure 6.1). Should the expected reward differ from the actual reward, is this reflected in phasic firing changes of dopamine neurons at the time of the expected outcome, referred to as reward prediction error (RPE) signal (see Figure 6.1). It is often stated that most (if not all) midbrain dopamine neurons display RPE signalling (Frank and Surmeier 2009; Glimcher 2011; Schultz 2010; Schultz 2016). In the present study, reward and cue responses of identified midbrain dopamine neurons were assessed following classical conditioning. On average, both VTA and SNc dopamine neurons showed phasic firing increases following reward but no detectable response to the cue. However, analysed on a cell-by-cell basis, individual neurons fell into diverse response groups (see Figure 6.9) with some, but not all, neurons displaying phasic increases following reward delivery (16 of 40 identified neurons). It was shown that reward-related response magnitude is value-dependent (e.g. bigger rewards result in bigger response magnitude) (Cohen et al. 2012; Eshel, Tian, et al. 2016; Tobler, Fiorillo, et al. 2005). Hence, a possible explanation for reward responses seen in less than 50 % of identified midbrain dopamine neurons could be that mice did not ascribe much value to the rewarding solution; strawberry milk might not

have been their preferred reward. However, anticipatory licking behaviour indicated that mice were motivated to investigate the strawberry milk. Furthermore, in pilot experiments, others in the lab have detected the strongest preference for strawberry Yazoo when compared to sucrose solution or condensed milk. Previous studies rarely reported the response diversity of dopamine neurons and display population averages, which might mask underlying heterogeneity. However, some studies did report the proportions of reward-responsive dopamine neurons. Miller et al. (1981) found approximately 60 % of putative dopamine neurons to respond in a classical conditioning task, some increasing their firing and some decreasing their firing (Miller et al. 1981). Other studies mention 25 % (Schultz, Apicella, et al. 1993), 55 – 80 % (Schultz, Dayan, et al. 1997) or 53 % (Cohen et al. 2012) of reward and/or cue responsive putative dopamine neurons. Thus, reward responses are strong enough to be reflected in population averages but they are not characteristic for every dopamine neuron, highlighting the response diversity of individual midbrain dopamine neurons.

In addition to heterogeneity in encoding, another notable finding in this study was the lack of a clear or complete response shift of firing changes from the reward to the cue. While anticipatory licking indicated that animals had acquired the association between cue and reward (i.e. that learning had taken place), only 5 % (2 of 40) of identified dopamine neurons displayed positive cue responses after conditioning. Additionally, rather than being attenuated, the response to the (presumably) fully predicted reward persisted (Figure 6.7) and did not appear to decrease with increased experience (Figure 6.11). If the firing of midbrain dopamine neurons were the neural substrate of value prediction errors crucial to temporal difference (TD) learning and the Rescorla-Wagner model (Rescorla et al. 1972; Suri 2002; Sutton 1988), the dynamics in the firing of midbrain dopamine neurons should be time-locked to learning, including a response shift away from the reward to the reward-predicting cue. Notably, side comments in other reports mention similar discrepancies. Menegas et al. (2017) report response increases to the conditioned stimulus measured in dopamine axons only after “weeks of training” (with 300 trials

per day), Cohen et al. (2012) mention that "many neurons" but not all showed odour cue responses (after presumably 12 days of training with 400 – 1000 trials per day) and Matsumoto et al. (2016) report that only 50 % of light-identified midbrain dopamine neurons display conditioned-stimulus value coding (the amount of prior training is not clearly stated). Furthermore, these and other studies showed that phasic changes in firing of midbrain dopamine neurons to predicted rewards were retained to some extent. If extensive training is required for a complete response shift, the comparably low numbers of prior received cued-reward trials in the present study (accumulative 125 – 1114 trials) might explain the lack of dominant cue responses in identified midbrain dopamine neurons. Indeed, pioneering early studies on RPE signalling by dopamine neurons were largely conducted in heavily trained monkeys that had been exposed to 10,000 – 30,000 trials (Berridge and Robinson 1998). If the response shift from the reward to the reward-predicting cue happens well after learning, then it is unlikely to serve as a teaching signal in the associative cue-reward learning itself. However, since most studies using mice, including the present one, were performed using classical conditioning (Cohen et al. 2012; Eshel, Bukwich, et al. 2015; Eshel, Tian, et al. 2016; Matsumoto, Tian, et al. 2016), anticipatory licking is often the only behavioural readout to assess that learning has occurred (eye blink behaviour was measured in a previous study but did not change with learning; Matsumoto, Tian, et al. 2016). Notably, the pattern of anticipatory licking in the present study (see Figure 6.6) showed different temporal dynamics compared to other studies (e.g. Cohen et al. 2012), being briefer and less of a sustained build-up with respect to the time of reward delivery. A possible explanation for these differences could be that animals in the present study have not learned to fully predict the timing of the reward but instead assigned some value to the reward-predicting cue itself. Alternatively, different methods of lick detection could underlie the differences in anticipatory licking profiles: While the present study used a capacitive sensor for lick detection, which only registers licks with direct contact to the reward delivery spout, many other studies measure breaks of an infrared beam placed in front of the reward delivery tube, which might register

licks without direct contact to the delivery spout.

One possible experiment that could help to resolve the outlined issue with anticipatory licking being the only behavioural readout would be an instrumental learning task (e.g. lever pull- or lever press-contingent reward delivery), where learning can be inferred from task performance of the animal. Firing activity of midbrain dopamine neurons could then be measured throughout the course of learning to map it onto changes in performance. Since this is not feasible to do in the same animal with juxtacellular labelling (because the brain needs to be extracted relatively promptly after labelling), either different cohorts of mice could be used and trained to different performance levels, or other recording techniques (e.g. tetrodes) combined with opto-tagging identification (Cohen et al. 2012; Stauffer et al. 2016) could be used to track changes in firing of dopamine neurons over time to assess whether changes scale with task performance. Additionally, since many studies were performed in heavily trained monkeys but not rodents, experiments could be repeated in extensively trained mice to account for the possibility that the observed discrepancies are related to species differences. It is noteworthy that it has been suggested that cue-responses observed in classical conditioning could occur because the cue itself gains incentive value (i.e. becomes desirable) and that it is this characteristic rather than its predictive nature that relates to dopamine neuron activity (Berridge and Robinson 1998; Flagel et al. 2011).

One caveat of most electrophysiology studies looking at firing of midbrain dopamine neurons is their correlative nature: Co-occurrence of firing changes and behaviour is used as proxy to infer a more causal relationship. However, a previous study using behaviour and optogenetic stimulation, claims to have found a "causal link between prediction errors, dopamine neurons and learning" (Steinberg et al. 2013). Core to this study was a blocking experiment. Blocking is a phenomenon observed in associative cue conditioning and refers to the effect that the association between a cue and reward is blocked (i.e. prevented) if a separate cue present at the same time already reliably predicts the reward (Holland 1984; Waelti et al. 2001). Pairing

phasic unilateral optogenetic stimulation of dopamine neurons in channelrhodopsin-expressing TH-Cre rats with reward delivery in the blocking experiment (to mimic the otherwise absent teaching signal), Steinberg et al. (2013) show that the blocking effect is prevented and that association-learning for the second cue takes place. The authors concluded that by mimicking a teaching signal through optogentic stimulation of dopamine neurons, they were able to drive learning for the second cue which usually would have been prevented due to the blocking effect. However, this study did not rule out the possibility that the optogenetic stimulation of dopamine neurons in itself becomes a reward (separate from the paired sucrose-reward) and that their observations are better explained by parallel associative learning that takes place on top of the already learned association of a cue and sucrose. Further, the study does not measure dopamine neuron activity but uses behavioural readouts only, leaving it unclear how cue-related activity of midbrain dopamine neurons might vary during task performance (Steinberg et al. 2013).

Notably, the present study has revealed a gradual increase in the magnitude of reward response with increasing experience (see Figure 6.11C). It is assumed that response to the unconditioned reward stimulus should occur with maximal magnitude when it is least predicted. This reward prediction should be smaller for lower numbers of reward exposures and thus, maximal reward response would be expected with the very first trials. However, the present study reports the opposite. Once again, albeit not discussed extensively, other reports have shown similar results: Ljungberg et al. (1992) report that preceding their conditioning training phase, “most [dopamine] neurons lacked responses to light illumination and reward delivery” (see Table 4 and Figure 13; Ljungberg et al. 1992). The present study highlights that firing of midbrain dopamine neurons does not mirror learning model predictions as well as often assumed (Eshel, Tian, et al. 2016; Frank and Surmeier 2009; Schultz 2010; Schultz 2016).

In the dataset of putative dopamine neurons, 12 % of neurons (13 of 106) displayed a significant positive response to the predictive cue (see ‘cue pos’ column Table 6.5). This proportion might be slightly higher than the 5 % of identified midbrain

dopamine neurons positively modulated by the cue due to contamination by non-dopamine neurons with dopamine neuron-like firing and waveform-criteria that can show cue and reward responses (see Figure 6.5; Figure 6.16). Such contamination would render dopamine neuron classification based on hierarchical clustering of reward responses difficult (Cohen et al. 2012; Eshel, Tian, et al. 2016). This, again, highlights the importance to unequivocally identify midbrain dopamine neurons with techniques like juxtacellular labelling. While technical considerations have meant that few studies have used juxtacellular labelling in behaving animals, other identification methods (e.g. pharmacological or optogenetic) have been used to classify dopamine neurons. In early studies, drugs like apomorphine (which acts on D2-autoreceptors) were often used to identify dopamine neurons. More recently, 'opto-tagging' approaches replaced pharmacological identification methods: Channelrhodopsin is targeted to dopamine neurons by its expression under the control of the promoter for e.g. the dopamine transporter (DAT/Slc6a3), thought to be expressed in all midbrain dopamine neurons. Measurement of consistent short-latency spiking to light stimulation is then used to identify dopamine neurons (Cohen et al. 2012; Eshel, Tian, et al. 2016; Matsumoto, Tian, et al. 2016; Stauffer et al. 2016). One of the technical limitations of these two approaches is, however, that both D2-autoreceptors as well as DAT are not ubiquitously expressed in midbrain dopamine neurons: Some populations of midbrain dopamine neurons have low expression levels of DAT and D2-autoreceptors (Blanchard et al. 1994; González-Hernández, Barroso-Chinea, et al. 2004; Lammel et al. 2008; Li, Qi, et al. 2013; Poulin, Zou, et al. 2014; Sanghera, Manaye, et al. 1994). These populations might not be captured with pharmacological or opto-tagging identification methods, potentially excluding dopamine neurons with differential reward responses that were recorded in the present study. Furthermore, channelrhodopsin can be ectopically expressed by non-dopamine neurons (Stauffer et al. 2016). Some studies proposed hierarchical clustering of reward responses to classify recorded neurons as dopamine neurons (Eshel, Tian, et al. 2016). However, this might lead to artificial reduction of response diversity (e.g. although three neurons responded to opto-tagging in

Eshel et al. (2016), the same neurons showed no reward response and were therefore classified as non-dopamine neurons).

Interestingly, one of the response groups in the present study was characterised by a negative cue-response for both identified, as well as putative, dopamine neurons (see Figure 6.9). Negative responses to stimuli were also seen for a subpopulation of midbrain dopamine neurons in the sensory stimuli experiment (see Figure 6.4). These two subpopulations might represent identical or overlapping groups of dopamine neurons carrying value-independent cue responses, adding to the diversity of information represented in midbrain dopamine neurons. However, latencies of the two groups of dopamine neurons were not identical with a delay of 160 – 200 ms in sensory stimuli experiments and 80 – 120 ms in the cued-reward task, suggesting that different mechanisms (e.g. different efferent sources) might underlie them and that they each serve a separate role. It is further to be considered that animals used for the sensory stimuli experiment were not subjected to food restriction, while mice used for the cue-reward task had restricted access to food. While food restriction ensures motivation of the animal to reliably perform on the task, food restriction also alters neural activity of dopamine neurons (Branch, Goertz, et al. 2013) and dopamine release (Roseberry 2015) and might does underlie differences observed between sensory stimuli experiment and cue-reward task.

In addition to cue and reward responses, the present study also investigated the correlation of dopamine firing with the licking behaviour of the animal. The rationale for including this separate response dimension was the hypothesis that analysis restricted to cue and reward components might mask response modulation explained better by other factors such as licking. Masking is likely to happen when limiting analysis to reward-aligned peri-event time histograms. Hence, the present study used a general linear regression model applied to the whole recording trace of individual neurons (see section 2.5.5). Both in identified neurons as well as putative dopamine neurons, two subpopulations were identified which were either positively or negatively modulated by licking. Importantly, licking behaviour did not differ significantly between response groups and occurred within and outside reward trials

(Figure 6.10C-D and Figure 6.15D-E), suggesting that the response is not biased because of a particular behaviour. Other reports have shown that motor related aspects like spontaneous movements (Dodson, Dreyer, et al. 2016) or head-direction (Barter, Li, et al. 2015) are represented in the firing of midbrain dopamine neurons. It is difficult to disentangle whether the observed licking responses are "neutral" in nature and purely reflect motor aspects or whether they represent some sort of motivation (desire to consume reward), or a combination. Movements cost energy and it can thus be assumed that they only occur if there is a motivator for them; in the present study this could be the expectation of a reward still hanging on the spout or the possibility of a reward being delivered from the spout. However, licking-aligned plots showed prolonged modulation with ongoing licking (see Figure 6.9J-K), which would not be expected if expectation were the only modulator, and might support the idea of motor components of the behaviour being represented in addition to cues and rewards.

One issue arising is how dopamine neurons, whose activity correlates with so many different behavioural concepts, represent all these different aspects as a population. How can such diverse information be "decoded" in target regions like the dorsal striatum? This is particularly challenging since the complex axonal arbors of DS-projecting dopamine neurons cover large portions of the dorsal striatum (Matsuda et al. 2009). One possible mechanism could be that the precise spatiotemporal firing pattern of midbrain dopamine neurons – including phasic bursts and pauses – activate postsynaptic dopamine receptors in selective ways by differentially affecting receptor occupancy (Dreyer et al. 2010).

In the present study, three variables were included to explain firing changes of midbrain dopamine neurons: cue, reward and licking. The Venn diagrams in Figure 6.9E and Figure 6.14C show that the three variables are represented in a combinatorial fashion in 70 % of the neurons while not at all in the remaining 30 %. One proposed encoding scheme for neural populations which would match such a scattered combinatorial representation is sparse coding (Brunel et al. 2004; Földiák 2002; Olshausen et al. 1997), an intermediate between local coding (where

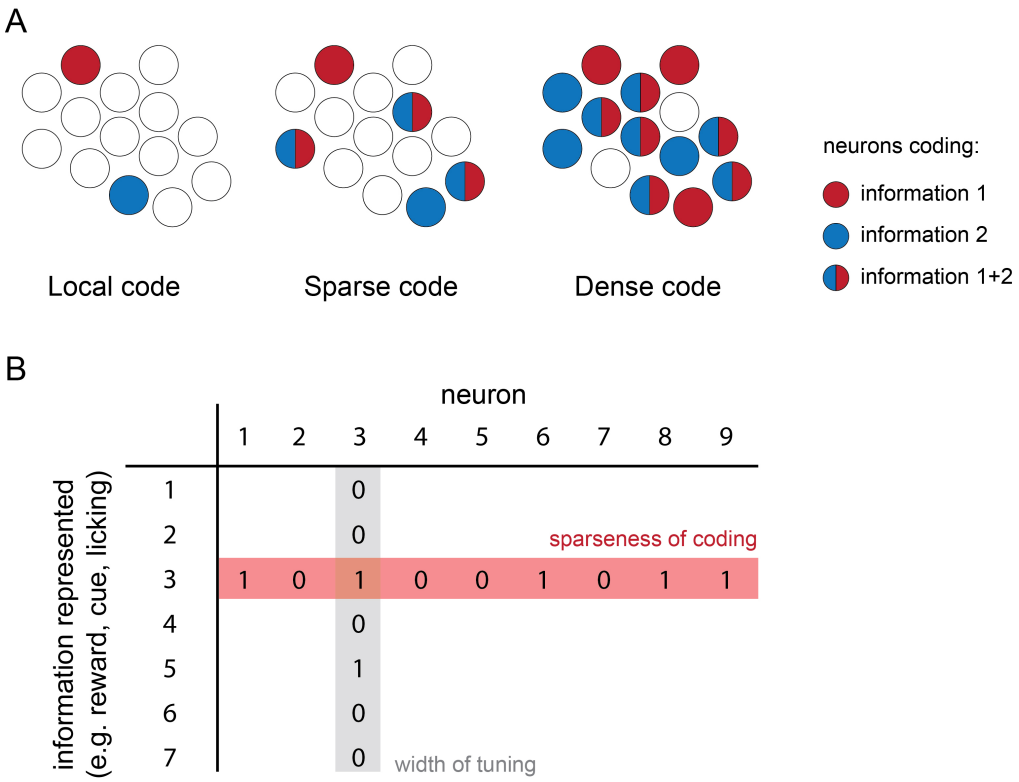

Figure 6.17: Sparse coding is an intermediate of local and dense coding. (A) Schematic of local coding (left), sparse coding (middle) and dense coding (right) neural population (one circle depicts one neuron). Circle colour represents information items represented by an individual neuron. Circles are left blank for neurons not representing the selected information items. (B) Comparison of sparseness of coding (how many neurons in the population represent an information item) and width of tuning (how many information items are represented by any one neuron). For instance, information item 3 is represented by neuron 1, 3, 6, 8 and 9 (red-coloured row; sparseness of coding across population); neuron 3 encodes information item 3 and 5 (grey-coloured column; width of tuning for neuron 3).

one neuron represents one item of information) and distributed dense coding (combinations of all neurons represent an item of information) (Figure 6.17). Due to its high representational capacity, sparse coding could accommodate the broadness of information representation seen in midbrain dopamine neurons. This is supported by the combinatorial diversity seen in this study which was not anatomically restricted (see Figure 6.12).

Given the range of projection targets of midbrain dopamine neurons, another important issue is whether defined response groups were linked to a preferential output target. To approximate this question, individual identified dopamine neurons

were tested for the expression of a subset of molecular markers shown to have relatively high projection target discrimination (see Chapter 5). While expressed marker combinations in the present study did not predict the response type, a substantially larger dataset might reveal underlying patterns. Furthermore, only three markers could be tested per neuron. It is possible that an alternative subset of markers might give more conclusive results. There was, however, a combination of marker expression only found in one response group: Two identified dopamine neurons with positive responses to licking were shown to express Calbindin but not Sox6 or Aldh1a1. These neurons had the highest positive regression coefficients for licking and showed no positive correlation with either reward or cue. Given the low percentage of Calbindin-positive neurons projecting to the dorsal striatum (1 %; see Figure 5.2), information represented in those neurons is unlikely to target this region and might instead send potentially motor-related signals to other brain regions.

Taken together, this Chapter provides new insights into the responses exhibited by identified and putative midbrain dopamine neurons to neutral sensory stimuli and in a classical conditioning task. Different response groups did not map onto defined anatomical locations. The finding that only 40 % (16 of 40 neurons) of identified dopamine neurons showed a positive reward response argues against the common notion that all dopamine neurons signal reward. Furthermore, the finding that there seems to be a combinatorial distribution of information across dopamine neurons (e.g. one neuron encodes reward and cue and another encodes only licking) suggests that dopamine neurons might employ sparse coding.

7 General Discussion

Contents

7.1 Summary

The objective of this thesis was to investigate the diversity of the functional properties of the midbrain dopamine system, how these properties are maintained in adulthood, and how they change when challenged with a genetic burden of relevance to Parkinson's. This objective was approached with a combination of *in vivo* single-cell recordings with juxtacellular labelling of individual neurons, both in anaesthetised and awake behaving rodents, immunolabelling, retrograde tracing and stereology. The importance of an intact midbrain dopamine system becomes apparent when its function is compromised in diseases like Parkinson's. With the discovery of genetic forms of Parkinson's, it became a possibility to model the impact of genetic variation on early disease stages with the help of transgenic animals. Investigating how such genetic burden manifests in altered functions of the midbrain dopamine system might serve fruitful in the development of novel treatments. In Chapter 3 of this thesis, a transgenic rat model was used to test how the R1441C point mutation in the *LRRK2* gene, shown to be linked to some forms of Parkinson's, affects the firing of SNc dopamine neurons and whether alterations are age-dependent. In contrast to the chronic and progressive genetic burden introduced in the *LRRK2* rat model, work on the midbrain dopamine system in Chapter 4 was designed to assess the impact of an acute genetic challenge introduced through conditional knock-out of the transcription factors Foxa1 and Foxa2. While Chapter 3 and Chapter 4 focused on a genetically-altered midbrain dopamine system, Chapter 5 and Chapter 6 focused on the functional diversity of the intact midbrain dopamine with a focus on molecular and structural properties of midbrain dopamine neurons (Chapter 5) and the electrophysiological properties of neurons as they pertain to the encoding of behaviourally relevant events (Chapter 6).

Chapter 3 and 4 – Chronic and acute genetic challenges of the midbrain dopamine system

The aim of Chapter 3 was to define *in vivo* firing properties of SNc dopamine neurons in a *LRRK2* rat model of Parkinson's following its behavioural characterisation. Since Parkinson's is described not only by motor symptoms, but also non-motor

symptoms like impaired olfaction (Ross et al. 2008), motor and olfactory performance were assessed in the R1441C rat model. It was shown that aged R1441C transgenic rats display impaired motor performance in a balance beam task compared to non-transgenic controls, whereas they did not show impaired olfactory performance in a hidden food or odour discrimination task. Motor impairments in aged R1441C rats were accompanied by reduced firing variability and burst firing of SNc dopamine neurons recorded *in vivo* under anaesthesia and identified through juxtacellular labelling. The changes in firing were age-dependent and absent in recordings of SNc dopamine neurons in young adult R1441C transgenic rats. The aim of Chapter 4 was to test how acute knock-out of the transcription factors Foxa1 and Foxa2 affect *in vivo* firing of SNc dopamine neurons in adulthood. Recordings of SNc dopamine neurons, identified through juxtacellular labelling, revealed that Foxa1 and Foxa2 were required for the maintenance of firing properties of SNc dopamine neurons and that the conditional knock-out of these transcription factors leads to reduced burst firing.

Reduced burst firing in SNc dopamine neurons was characteristic for aged R1441C *LRRK2* transgenic rats as well as conditional Foxa1/2 knock-out mice, indicating that both the mutated *LRRK2* as well as loss of Foxa1/2 might lead to similar network alterations. However, interestingly, the two animal models displayed very different behavioural phenotypes: While R1441C *LRRK2* rats showed motor and cognitive impairments (Sloan et al. 2016), Foxa1/2 knock-out mice had a severe feeding deficit and no gross motor impairment (Pristerà et al. 2015). A possible contributor to these two very different behavioural phenotypes is the chronic nature of the expression of mutated *LRRK2*, resulting in progressive effects from conception, compared to the acute knock-out of Foxa1 and Foxa2 induced in the adult mouse, leading to rapid alterations. While the intact and established midbrain dopamine system in Foxa1/2 mice is suddenly confronted with the loss of expression of Foxa1 and Foxa2, the chronic expression of mutated *LRRK2* in the rat model might allow for gradual network compensation, preventing severe feeding impairments as seen for the mouse model. It further suggests that altered firing pattern of SNc dopamine

neurons alone might contribute to, but does not account for, the entirety of the behavioural changes that might result from molecular disturbances of the intact system. Other alterations might contribute to the differential behavioural impact in both cases. For instance, transcript levels of tyrosine hydroxylase and levels of dopamine were shown to be reduced in Foxa1/2 knock-out mice (Pristerà et al. 2015), while tyrosine hydroxylase levels in the striatum of *LRRK2* transgenic rats were unaltered (Sloan et al. 2016).

Chapter 5 and 6 – Functional diversity of midbrain dopamine neurons

The overall aim of Chapter 5 was to characterise projection target-specific expression of molecular markers in midbrain dopamine neurons innervating the nucleus accumbens (NAc) or the dorsal striatum (DS). A set of seven markers was selected for investigation. Markers included Calbindin, Calretinin, Girk2, Aldh1a1, Otx2, SatB1 and Sox6. Retrograde tracing with Cholera toxin subunit b (CTB) was used to reveal NAc- or DS-projecting midbrain dopamine neurons, and combined with indirect immunofluorescence and stereology, marker expression was assessed in projecting dopamine neurons. It was shown that Calbindin, Calretinin and Otx2 were selectively expressed in midbrain dopamine neurons projecting to the NAc, whereas SatB1, Sox6 and Girk2 were selectively expressed in midbrain dopamine neurons projecting to the DS. Furthermore, individual markers differed in the magnitude of projection target specificity. While no markers exclusively defined projecting populations, Calbindin, Sox6 and SatB1 had the best projection target discrimination.

The overall aim of Chapter 6 was to assess functional diversity of midbrain dopamine neurons recorded in head-fixed awake mice during the presentation of sensory stimuli or the performance of a classical conditioning paradigm. In the first experiment, the firing of midbrain dopamine neurons in response to neutral auditory and visual stimuli was measured. Individual dopamine neurons were identified using the juxtacellular labelling method. In the second experiment, the firing of midbrain dopamine neurons was measured in a classical conditioning task and both identified and putative dopamine neurons were analysed. In both experiments, midbrain

dopamine neurons displayed response diversity, with firing rate increases or decreases occurring in time with defined task events. This functional diversity was not correlated with the anatomical location of the identified midbrain dopamine neurons, nor with the singular or combinatorial expression of the three markers Calbindin, Sox6 and Aldh1a1. The large proportion of non-responding neurons together with the combinatorial representation of different task-related events (e.g. licking or reward) in responding neurons, indicate that midbrain dopamine neurons might employ sparse coding to represent multiple contexts.

7.2 Technical and theoretical considerations

Neural recordings under anaesthesia. In Chapter 3 and Chapter 4 of this thesis, recordings of dopamine neurons were performed in anaesthetised rats and mice. The rats received combined urethane and ketamine-xylazine anaesthesia; mice were anaesthetised with urethane only. While recording in anaesthetised preparations has the advantage of providing a stable recording environment, anaesthetics not only affect respiratory and cardiovascular function (Field et al. 1993) but carry the potential to alter the activity of neurons (Nicoll et al. 1982). While the exact mode of action of urethane is not known, it was suggested that it affects the function of a range of ion channels including NMDA-receptors (Hara et al. 2002). NMDA-receptors are also the main site of action of ketamine (Kohrs et al. 1998; MacDonald et al. 1990; Yamamura et al. 1990), while xylazine is a selective Alpha 2 adrenoreceptor-agonist (Greene and Thurmon 1988; Kobinger et al. 1983). Both ketamine and urethane were shown to leave firing rates of putative dopamine neurons unaltered when compared to recordings from paralysed rats (Kelland et al. 1990). Additionally, recordings of identified SNc dopamine neurons have revealed that their firing rate in mice under urethane anaesthesia is similar to that in awake (head-fixed) mice (Dodson, Dreyer, et al. 2016; Janezic et al. 2013). However, urethane was found to suppress burst firing in putative dopamine neurons (Kelland et al. 1990). Burst frequencies obtained under urethane anaesthesia might thus not correspond to burst frequencies found in awake animals. However, urethane anaesthesia was

chosen over e.g. isoflurane anaesthesia because it results in relatively preserved cortical activity that resembles slow-wave sleep while higher doses of isoflurane can result in cortical burst-suppression, typically seen in hypoxia- or coma-induced cortical activity (Brenner 2005; Dahan et al. 2007). Additionally, isoflurane might reduce firing rates of dopamine neurons below frequencies seen in the awake state (Dodson, Dreyer, et al. 2016; Janezic et al. 2013; Subramaniam et al. 2014). Since cortical brain state activity impacts on firing properties of midbrain dopamine neurons (Brown et al. 2009; Walczak et al. 2017), it is crucial to monitor cortical activity in anaesthetised preparations (as was done in the present study).

Bias in selection of recorded neurons. Multiple sources of potential bias can be identified in the recording technique used in this study. Because neurons were recorded in an extracellular configuration, they had to be active (i.e. generate action potentials) to be sampled. As a consequence, recordings could be biased towards more active neurons, and in any case preclude the detection of quiescent dopamine neurons. Additionally, tracks of the glass pipette were always directional since it was lowered down from dorsal to ventral through the recording region. Recordings are therefore likely biased towards more dorsally located dopamine neurons since they would have been the first detected and then recorded and juxtacellularly labelled before retracting the recording pipette. Nevertheless, presumably due to a small radius of detectable firing, identified midbrain dopamine neurons were still distributed throughout the dorso-ventral extent of the midbrain dopamine nuclei. To avoid glass pipettes damaging the sagittal sinus, electrode penetrations were rarely attempted at very medial locations. Hence, the medial most dopamine neurons in the VTA were not recorded in this study. Furthermore, distinct subsets of midbrain dopamine neurons might be more challenging to label with the juxtacellular method, resulting in those neurons being less represented in the dataset of identified midbrain dopamine neurons. But the finding that proportions of response types in identified and putative dopamine neurons were similar suggests that this was unlikely the case.

Single-unit recordings and correlative nature of results. While the recording technique

used in this study typically results in only one neuron being recorded at any one time, it would be interesting to analyse populations of simultaneously recorded neurons, especially to reveal whether firing activity changes with learning or how sparsely information is represented by a larger neural population. However, the strength of single-unit with combined juxtacellular labelling is that it allows for identification of molecular characteristics as well as the anatomical location of the recorded neuron. A related question regarding single-unit and population recording of neural activity is its biological relevance. While biological relevance is often substituted with statistical significance, a statistically revealed effect (e.g. a significant change in neural activity) might not be biologically meaningful. It is thus important to consider whether and how spike trains measured within a particular circuit-component might impact on recipient regions, as well as how information might be read out downstream. This also needs taking into account that dopamine is a neuromodulator with some 'special features' such as non-synaptic volume transmission (Zoli et al. 1998) and cell-type selective modulatory effects in the striatum (Shen et al. 2008; Surmeier et al. 2007). Of particular interest is whether changes in firing activity are merely correlative with a certain context (e.g. licking or reward) or whether these changes are necessary to signal this context or aspects of it. Optogenetic stimulations are an approach that allows for targeted manipulation of circuit components to investigate whether mimicking activity patterns found to correlate with a behaviour is sufficient to elicit that same behaviour. Howe and Dombeck (2016) used calcium-imaging to reveal signals in dopamine axons in the striatum that correlated with locomotion. Subsequently, they used optogenetic stimulation of such dopamine axons to induce locomotion, concluding that their activity is sufficient to trigger it. However, it is difficult to replicate physiological firing patterns with optogenetics, i.e. temporally precise activity in only the subset of neurons active in a given context. The identification of molecular markers expressed in a subset of neurons linked to a defined behaviour might help develop more refined targets for optogenetics.

Recordings under head-fixation. To create relatively stable conditions for electrophysiological recordings, recordings in Chapter 6 of this thesis were performed in head-fixed awake mice. While this has experimental advantages, it does not provide a natural environment for the animal. Head-fixation prevents head-rotations, vestibular reflexes and restricts the environment that can be explored. However, these restrictions might also represent an advantage for the analysis of recording data since head-fixation limits parameter space. While head-rotation was implicated in the firing of midbrain dopamine neurons in other studies (Barter, Li, et al. 2015), it is unlikely to explain firing changes observed in this study because head-fixation prevented directional movement of the head. Hence, head-rotations did not have to be included as explanatory variables in the analysis. Nonetheless, head-fixation might present an aversive environment to the animal and put it into a mildly stressed state it wants to escape from. Indeed, in head-fixed rodents, physiological parameters linked to stress, such as respiratory and heart rate or blood levels of corticosterone, were shown to be increased initially but decreased with acclimation (King et al. 2005; Mizuma et al. 2010). Importantly, animals in this study did not seem to exhibit freezing responses, but continued whisking and performed the task in head-fixation, indicating that they were well habituated and not overtly stressed.
Species differences. While the mammalian nervous system is characterised by many similarities, species differences in neural representation might underlie certain aspects of behaviour. For instance, as noted in the general introduction, non-human primates and rodents differ substantially in the ratio of SNc to VTA dopamine neurons with a substantially higher proportion of SNc dopamine neurons in non-human primates (Bentivoglio et al. 2005; Brichta and Greengard 2014; German and Manaye 1993; Nair-Roberts et al. 2008; Nelson et al. 1996). While reward prediction error coding was first described in non-human primates, mouse studies are becoming increasingly popular due to the diverse genetic tools available for neural circuit manipulations. While this serves fruitful to dissect circuit mechanisms, it does not address the issue whether there are species differences in how information is represented in the midbrain dopamine system; prediction errors might be differently encoded in mice

compared to non-human primates. However, given the postulated importance of prediction error signalling for reinforcement learning and the importance of learning for the survival of an organism, it is likely that mechanisms would be preserved across species.

Tracer injections and counting strategy. While care was taken to restrict CTB-tracer injections to the region of interest, this does not control for the potential uptake by fibres of passage rather than axons innervating a region (whether or not they form synapses). While some studies suggest that only damaged fibres of passage take up the tracer (Luppi et al. 1990), others have indicated that the tracer is also taken up by intact fibres of passage (Chen and Aston-Jones 1995). If this were true for dopaminergic fibres of passage, midbrain dopamine neurons targeting e.g. cortical regions might contribute to the numbers obtained for NAc- or DS-projecting dopamine neurons in this study. However, considering the large axonal fields of midbrain dopamine neurons collateralizing/terminating in the striatum compared to individual fibres of passage, this contribution is likely to be minor (Aransay et al. 2015; Matsuda et al. 2009). It could further be compared to tracing results using novel retrogradely transported Adeno-associated virus (AAV) constructs, although they have not been assessed for fibre of passage uptake and revealed surprisingly low numbers of projecting neurons in the SNc for DS-targeted injections (Tervo et al. 2016). Marker expression in tracer studies as well as of recorded midbrain dopamine neurons in Chapter 6 was evaluated with indirect immunofluorescence and a binary system only distinguishing between detected expression or non-detected expression. However, while such a binary system represents a useful classification tool, it does not take into account differential expression intensities. For instance, the calcium-binding proteins Calbindin and Calretinin were both shown to differ in the intensity of immunoreactivity in different midbrain dopamine neurons (Liang, Sinton, and German 1996). Such differential expression levels of calcium-binding protein were dynamic and behavioural context-dependent in the hippocampus (Donato et al. 2013). This highlights two aspects that need to be considered regarding the present study: First, expression levels of at least some molecular

markers might follow a continuous not a binary scale and second, this continuum might not be static but could be context-dependent. Furthermore, subgroups of dopamine neurons with weaker or stronger expression levels of the same marker might themselves form a 'subtype' of neurons not accounted for in the present study. Differences in expression levels of markers could further be related to the state the animal was in before brain tissue was extracted; the counts in this study then representing a snapshot of that particular state. Another technical consideration already mentioned in the discussion section of Chapter 5 is the interpretation of projection target-specific marker expression: While the employed tracer strategy revealed proportions of marker expression in projecting neurons, it did not inform about the proportion of non-projecting neurons expressing the same marker. This is because it is nearly impossible to have complete coverage of the target region (e.g. NAc); marker expressing neurons might thus be projecting neurons not captured with the respective tracer injection or marker expressing neurons that actually do not target the respective region.

7.3 Future directions

7.3.1 Subterritory-specific innervation of the nucleus accumbens

While injections in Chapter 5 were targeted at the nucleus accumbens (NAc) as a whole, it was shown that some markers might be expressed in midbrain dopamine neurons that selectively innervate identified subterritories of the NAc, such as the medial shell (for example Aldh1a1 in the present study). To investigate subterritory-specific innervation more systematically, tracer injections could be adjusted to target only the NAc medial shell region (selectivity could perhaps be further enhanced by employing Cre-dependent tracing). Molecular marker expression could then be assessed in midbrain dopamine neurons selectively innervating those subterritories. Additionally, further molecular markers shown to be expressed in subtypes of midbrain dopamine neurons could be included in the analyses to expand the dataset of seven selected markers used in this study (La Manno et al. 2016; Poulin, Zou,

et al. 2014). Additionally, including further projection targets like the prefrontal cortex or the lateral septum could shed light on specific marker expression in those projection-defined subtypes of midbrain dopamine neurons.

7.3.2 Recordings of midbrain dopamine neurons after extensive learning

While the current study indicated that the reward response in identified midbrain dopamine neurons is still detectable after training (unlike predicted from reinforcement learning theories and unlike reported in some monkey studies), recordings of midbrain dopamine neurons that have undergone more extensive training could be performed to reveal whether such responses are experience-dependent and vanish after extensive repetition of the task. Additionally, an instrumental learning task could be used instead of Pavlovian conditioning to get a better readout for behavioural performance to measure progression of learning. Additionally, retrograde tracer injections into target regions of midbrain dopamine neurons prior to extracellular single-unit recordings could be used to identify projection targets of juxtacellularly-labelled midbrain dopamine neurons and thus, to identify recipient regions for the diverse responses identified in this study. However, tracer-load might potentially affect firing properties of midbrain dopamine neurons. For instance, it was shown that expression of enhanced green fluorescent protein (eGFP) could alone alter burst firing in midbrain dopamine neurons (Schiemann, Schlaudraff, et al. 2012). Since trial-and-error based reinforcement learning was shown to be impaired in Parkinson's patients (Cools et al. 2007; Dagher et al. 2009; Frank, Seeberger, et al. 2004; Schonberg et al. 2010), a further proposed experiment is to repeat recordings in a suitable mouse model of Parkinson's to test whether reward-related signals are altered. Recently, it was found that initiation of spontaneous movements are represented in midbrain dopamine neuron firing and that such signals are lost in SNc dopamine neurons of an α-synuclein Parkinson's model (Dodson, Dreyer, et al. 2016). The same model could be used to investigate whether reward-related signals are also altered in identified midbrain dopamine neurons.

7.3.3 Simultaneous recordings of populations of dopamine neurons

Recordings in this study indicate that midbrain dopamine neurons might represent different behavioural variables with a sparse coding scheme. However, this reference was drawn from a combination of single-unit recordings carried out at different times. To further investigate whether such a sparse code is represented in a simultaneously recorded population of neurons, tetrode recordings combined with opto-identification of midbrain dopamine neurons could be used. This would ensure that recordings of multiple neurons are made while the animal is in an identical state (e.g. regarding level of learning or motivation). Additionally, tetrode recordings might be used in freely moving animals performing similar tasks as in head-fixation to investigate whether exploratory freedom might alter response types or proportions of responding neurons.

References

Abdi, A., Mallet, N., Mohamed, F. Y., Sharott, A., Dodson, P. D., Nakamura, K. C., Suri, S., Avery, S. V., Larvin, J. T., Garas, F. N., Garas, S. N., Vinciati, F., Morin, S., Bezard, E., Baufreton, J., and Magill, P. J. (2015). "Prototypic and arkypallidal neurons in the dopamine-intact external globus pallidus." In: *Journal of Neuroscience* 35 (17): pp. 6667–6688.

Acampora, D., Avantaggiato, V., Tuorto, F., and Simeone, A. (1997). "Genetic control of brain morphogenesis through Otx gene dosage requirement." In: *Development* 124 (18): pp. 3639–3650.

Adinolfi, A. M. (1969). "Degenerative changes in the entopeduncular nucleus following lesions of the caudate nucleus: An electron microscopic study". In: *Experimental Neurology* 25 (2): pp. 246–254.

Aebischer, P. and Schultz, W. (1984). "The activity of pars compacta neurons of the monkey substantia nigra is depressed by apomorphine". In: *Neuroscience Letters* 50 (1-3): pp. 25–29.

Airaksinen, M. S., Thoenen, H., and Meyer, M. (1997). "Vulnerability of midbrain dopaminergic neurons in calbindin-D28k-deficient mice: lack of evidence for a neuroprotective role of endogenous calbindin in MPTP-treated and weaver mice." In: *European Journal of Neuroscience* 9 (1): pp. 120–127.

Aizman, O., Brismar, H., Uhlén, P., Zettergren, E., Levey, A. I., Forssberg, H., Greengard, P., and Aperia, A. (2000). "Anatomical and physiological evidence for D1 and D2 dopamine receptor colocalization in neostriatal neurons". In: *Nature Neuroscience* 3 (3): pp. 226–230.

Alberico, S. L., Cassell, M. D., and Narayanan, N. S. (2015). "The vulnerable ventral tegmental area in Parkinson's disease". In: *Basal Ganglia* 5 (2-3): pp. 51–55.

Albin, R. L., Young, A. B., and Penney, J. B. (1989). "The functional anatomy of basal ganglia disorders". In: *Trends in Neurosciences* 12 (10): pp. 366–375.

Alexander, G. E. and Crutcher, M. D. (1990). "Functional architecture of basal ganglia circuits: neural substrates of parallel processing". In: *Trends in Neurosciences* 13 (7): pp. 266–271.

Alexander, G. E., DeLong, M. R., and Strick, P. L. (1986). "Parallel organization of functionally segregated circuits linking basal ganglia and cortex." In: *Annual Review of Neuroscience* 9 (1): pp. 357–381.

Ammari, R., Lopez, C., Fiorentino, H., Gonon, F. G., and Hammond, C. (2009). "A mouse juvenile or adult slice with preserved functional nigro-striatal dopaminergic neurons". In: *Neuroscience* 159 (1): pp. 3–6.

Anderson, D. W., Schray, R. C., Duester, G., and Schneider, J. S. (2011). "Functional significance of aldehyde dehydrogenase ALDH1A1 to the nigrostriatal dopamine system." In: *Brain Research* 1408: pp. 81–87.

Anderson, M. and Turner, R. (1991). "A quantitative analysis of pallidal discharge during targeted reaching movement in the monkey". In: *Experimental Brain Research* 86 (3): pp. 623–632.

Andersson, E., Tryggvason, U., Deng, Q., Friling, S., Alekseenko, Z., Robert, B., Perlmann, T., and Ericson, J. (2006). "Identification of Intrinsic Determinants of Midbrain Dopamine Neurons". In: *Cell* 124 (2): pp. 393–405.

Ang, S.-L. (2009). "Foxa1 and Foxa2 Transcription Factors Regulate Differentiation of Midbrain Dopaminergic Neurons". In: *Development and Engineering of Dopamine Neurons*. Ed. by Pasterkamp, R. J., Smidt, M. P., and Burbach, J. P. H. New York, NY: Springer New York, pp. 58–65.

Aransay, A., Rodríguez-López, C., García-Amado, M., Clascá, F., and Prensa, L. (2015). "Long-range projection neurons of the mouse ventral tegmental area: a single-cell axon tracing analysis". In: *Frontiers in Neuroanatomy* 9: p. 59.

Baldo, B. A., Sadeghian, K., Basso, A. M., and Kelley, A. E. (2002). "Effects of selective dopamine D1 or D2 receptor blockade within nucleus accumbens subregions on ingestive behavior and associated motor activity". In: *Behavioural Brain Research* 137 (1): pp. 165–177.

Balopole, D. C., Hansult, C. D., and Dorph, D. (1979). "Effect of cocaine on food intake in rats". In: *Psychopharmacology* 64 (1): pp. 121–122.

Barker, D. J., Root, D. H., Zhang, S., and Morales, M. (2016). "Multiplexed neurochemical signaling by neurons of the ventral tegmental area". In: *Journal of Chemical Neuroanatomy* 73: pp. 33–42.

Barter, J. W., Castro, S., Sukharnikova, T., Rossi, M. A., and Yin, H. H. (2014). "The role of the substantia nigra in posture control". In: *European Journal of Neuroscience* 39 (9): pp. 1465–1473.

Barter, J. W., Li, S., Lu, D., Bartholomew, R. A., Rossi, M. A., Shoemaker, C. T., Salas-Meza, D., Gaidis, E., and Yin, H. H. (2015). "Beyond reward prediction errors: the role of dopamine in movement kinematics". In: *Frontiers in Integrative Neuroscience* 9: p. 39.

Beccano-Kelly, D. A., Volta, M., Munsie, L. N., Paschall, S. A., Tatarnikov, I., Co, K., Chou, P., Cao, L.-P., Bergeron, S., Mitchell, E., Han, H., Melrose, H. L., Tapia, L., Raymond, L. A., Farrer, M. J., and Milnerwood, A. J. (2015). "LRRK2 overexpression alters glutamatergic presynaptic plasticity, striatal dopamine tone, postsynaptic signal transduction, motor activity and memory." In: *Human Molecular Genetics* 24 (5): pp. 1336–1349.

Beckstead, M. J., Grandy, D. K., Wickman, K., and Williams, J. T. (2004). "Vesicular Dopamine Release Elicits an Inhibitory Postsynaptic Current in Midbrain Dopamine Neurons." In: *Neuron* 42 (6): pp. 939–946.

Beckstead, R. M. (1983). "A pallidostriatal projection in the cat and monkey." In: *Brain Research Bulletin* 11 (6): pp. 629–632.

Beckstead, R. M., Domesick, V. B., and Nauta, W. J. (1979). "Efferent connections of the substantia nigra and ventral tegmental area in the rat". In: *Brain Research* 175 (2): pp. 191–217.

Beier, K. T., Steinberg, E. E., DeLoach, K. E., Xie, S., Miyamichi, K., Schwarz, L., Gao, X. J., Kremer, E. J., Malenka, R. C., and Luo, L. (2015). "Circuit Architecture of VTA Dopamine Neurons Revealed by Systematic Input-Output Mapping". In: *Cell* 162 (3): pp. 622–634.

Beninato, M. and Spencer, R. F. (1987). "A cholinergic projection to the rat substantia nigra from the pedunculopontine tegmental nucleus". In: *Brain Research* 412 (1): pp. 169–174.

— (1988). "The cholinergic innervation of the rat substantia nigra: a light and electron microscopic immunohistochemical study". In: *Experimental Brain Research* 72 (1): pp. 178–184.

Bentivoglio, M. and Morelli, M. (2005). "Chapter I: The organization and circuits of mesencephalic dopaminergic neurons and the distribution of dopamine receptors in the brain". In: *Handbook of Chemical Neuroanatomy*. Ed. by Dunnett, S., Bentivoglio, M., Björklund, A., and Hökfelt, T. Elsevier, pp. 100–107.

Bernard, V., Normand, E., and Bloch, B. (1992). "Phenotypical characterization of the rat striatal neurons expressing muscarinic receptor genes". In: *Journal of Neuroscience* 12 (9): pp. 3591–3600.

Berridge, K. C. (2007). "The debate over dopamine's role in reward: the case for incentive salience". In: *Psychopharmacology* 191 (3): pp. 391–431.

Berridge, K. C. and Robinson, T. E. (1998). "What is the role of dopamine in reward: hedonic impact, reward learning, or incentive salience?" In: *Brain Research Reviews* 28 (3): pp. 309–369.

Berridge, K. C., Venier, I. L., and Robinson, T. E. (1989). "Taste reactivity analysis of 6-hydroxydopamine-induced aphagia: Implications for arousal and anhedonia hypotheses of dopamine function." In: *Behavioral Neuroscience* 103 (1): pp. 36–45.

Besnard, V., Wert, S. E., Hull, W. M., and Whitsett, J. A. (2004). "Immunohistochemical localization of Foxa1 and Foxa2 in mouse embryos and adult tissues." In: *Gene Expression Patterns* 5 (2): pp. 193–208.

Bevan, M. D., Booth, P. A. C., Eaton, S. A., and Bolam, J. P. (1998). "Selective innervation of neostriatal interneurons by a subclass of neuron in the globus pallidus of the rat". In: *Journal of Neuroscience* 18 (22): pp. 9438–9452.

Bichler, Z., Lim, H. C., Zeng, L., and Tan, E. K. (2013). "Non-Motor and Motor Features in LRRK2 Transgenic Mice". In: *PLoS ONE* 8 (7): e70249.

Bingmer, M., Schiemann, J., Roeper, J., and Schneider, G. (2011). "Measuring burstiness and regularity in oscillatory spike trains". In: *Journal of Neuroscience Methods* 201 (2): pp. 426–437.

Birkmayer, W. and Hornykiewicz, O. (1961). "The L-3,4-dioxyphenylalanine (DOPA)-effect in Parkinson-akinesia". In: *Wiener Klinische Wochenschrift* 73: pp. 787–788.

Bishop, M. W., Chakraborty, S., Matthews, G. A. C., Dougalis, A., Wood, N. W., Festenstein, R., and Ungless, M. A. (2010). "Hyperexcitable Substantia Nigra Dopamine Neurons in PINK1- and HtrA2/Omi-Deficient Mice." In: *Journal of Neurophysiology* 104 (6): pp. 3009–3020.

Biskup, S., Moore, D. J., Celsi, F., Higashi, S., West, A. B., Andrabi, S. A., Kurkinen, K., Yu, S.-W., Savitt, J. M., Waldvogel, H. J., Faull, R. L. M., Emson, P. C., Torp, R., Ottersen, O. P., Dawson, T. M., and Dawson, V. L. (2006). "Localization of LRRK2 to membranous and vesicular structures in mammalian brain". In: *Annals of Neurology* 60 (5): pp. 557–569.

Björklund, A. and Dunnett, S. B. (2007). "Dopamine neuron systems in the brain: an update." In: *Trends in Neurosciences* 30 (5): pp. 194–202.

Björklund, A. and Lindvall, O. (1975). "Dopamine in dendrites of substantia nigra neurons: suggestions for a role in dendritic terminals". In: *Brain Research* 83 (3): pp. 531–537.

Blaess, S. and Ang, S.-L. (2015). "Genetic control of midbrain dopaminergic neuron development." In: *Wiley Interdisciplinary Reviews. Developmental Biology* 4 (2): pp. 113–134.

Blanchard, V., Raisman-Vozari, R., Vyas, S., Michel, P. P., Javoy-Agid, F., Uhl, G., and Agid, Y. A. (1994). "Differential expression of tyrosine hydroxylase and membrane

dopamine transporter genes in subpopulations of dopaminergic neurons of the rat mesencephalon". In: *Molecular Brain Research* 22 (1-4): pp. 29–38.

Blythe, S. N., Atherton, J. F., and Bevan, M. D. (2007). "Synaptic Activation of Dendritic AMPA and NMDA Receptors Generates Transient High-Frequency Firing in Substantia Nigra Dopamine Neurons In Vitro." In: *Journal of Neurophysiology* 97 (4): pp. 2837–2850.

Bodea, G. O. and Blaess, S. (2015). "Establishing diversity in the dopaminergic system." In: *FEBS Letters* 589 (24 Pt A): pp. 3773–3785.

Bolam, J. P., Clarke, D. J., Smith, A. D., and Somogyi, P. (1983). "A type of aspiny neuron in the rat neostriatum accumulates [3H]γ-aminobutyric acid: Combination of golgi-staining, autoradiography, and electron microscopy". In: *The Journal of Comparative Neurology* 213 (2): pp. 121–134.

Bolam, J. P., Hanley, J. J., Booth, P. A. C., and Bevan, M. D. (2000). "Synaptic organisation of the basal ganglia". In: *Journal of Anatomy* 196 (4): pp. 527–542.

Bolam, J. P. and Moss, J. (2010). "The relationship between dopaminergic axons and glutamatergic synapses in the striatum: structural considerations". In: *Dopamine Handbook*. Ed. by Iversen, L. L., Iversen, S. D., Dunnett, S. B., and Björklund, A. 4th ed. New York: Oxford University Press, pp. 49–59.

Bolam, J. P. and Pissadaki, E. K. (2012). "Living on the edge with too many mouths to feed: why dopamine neurons die." In: *Movement Disorders* 27 (12): pp. 1478–1483.

Bolam, J. P. and Smith, Y. (1990). "The GABA and substance P input to dopaminergic neurones in the substantia nigra of the rat". In: *Brain Research* 529 (1-2): pp. 57–78.

— (1992). "The striatum and the globus pallidus send convergent synaptic inputs onto single cells in the entopeduncular nucleus of the rat: A double anterograde labelling study combined with postembedding immunocytochemistry for GABA". In: *The Journal of Comparative Neurology* 321 (3): pp. 456–476.

Bonilla, S., Hall, A. C., Pinto, L., Attardo, A., Götz, M., Huttner, W. B., and Arenas, E. (2008). "Identification of midbrain floor plate radial glia-like cells as dopaminergic progenitors". In: *Glia* 56 (8): pp. 809–820.

Borgkvist, A., Puelles, E., Carta, M., Acampora, D., Ang, S.-L., Wurst, W., Goiny, M., Fisone, G., Simeone, A., and Usiello, A. (2006). "Altered dopaminergic innervation and amphetamine response in adult Otx2 conditional mutant mice". In: *Molecular and Cellular Neuroscience* 31 (2): pp. 293–302.

Bostantjopoulou, S., Katsarou, Z., Papadimitriou, A., Veletza, V., Hatzigeorgiou, G., and Lees, A. (2001). "Clinical features of parkinsonian patients with the α-synuclein (G209A) mutation". In: *Movement Disorders* 16 (6): pp. 1007–1013.

Branch, S. Y., Goertz, R. B., Sharpe, A. L., Pierce, J., Roy, S., Ko, D., Paladini, C. A., and Beckstead, M. J. (2013). "Food Restriction Increases Glutamate Receptor-Mediated Burst Firing of Dopamine Neurons". In: *Journal of Neuroscience* 33 (34): pp. 13861–13872.

Branch, S. Y., Sharma, R., and Beckstead, M. J. (2014). "Aging Decreases L-Type Calcium Channel Currents and Pacemaker Firing Fidelity in Substantia Nigra Dopamine Neurons". In: *Journal of Neuroscience* 34 (28): pp. 9310–9318.

Brenner, R. P. (2005). "The interpretation of the EEG in stupor and coma." In: *The neurologist* 11 (5): pp. 271–284.

Brichta, L. and Greengard, P. (2014). "Molecular determinants of selective dopaminergic vulnerability in Parkinson's disease: an update". In: *Frontiers in Neuroanatomy* 8: p. 152.

Brichta, L., Shin, W., Jackson-Lewis, V., Blesa, J., Yap, E.-L., Walker, Z., Zhang, J., Roussarie, J.-P., Alvarez, M. J., Califano, A., Przedborski, S., and Greengard, P. (2015). "Identification of neurodegenerative factors using translatome-regulatory network analysis." In: *Nature Neuroscience* 18 (9): pp. 1325–1333.

Brog, J. S., Salyapongse, A., Deutch, A. Y., and Zahm, D. S. (1993). "The patterns of afferent innervation of the core and shell in the accumbens part of the rat ventral striatum: Immunohistochemical detection of retrogradely transported fluoro-gold". In: *The Journal of Comparative Neurology* 338 (2): pp. 255–278.

Bromberg-Martin, E. S., Matsumoto, M., and Hikosaka, O. (2010). "Dopamine in motivational control: rewarding, aversive, and alerting." In: *Neuron* 68 (5): pp. 815–834.

Brotchie, P., Iansek, R., and Horne, M. K. (1991). "Motor function of the monkey globus pallidus. 2. Cognitive aspects of movement and phasic neuronal activity." In: *Brain* 114 (Pt 4): pp. 1685–1702.

Brown, M. T. C., Henny, P., Bolam, J. P., and Magill, P. J. (2009). "Activity of neurochemically heterogeneous dopaminergic neurons in the substantia nigra during spontaneous and driven changes in brain state." In: *Journal of Neuroscience* 29 (9): pp. 2915–2925.

Brunel, N., Hakim, V., Isope, P., Nadal, J.-P., and Barbour, B. (2004). "Optimal Information Storage and the Distribution of Synaptic Weights: Perceptron versus Purkinje Cell". In: *Neuron* 43 (5): pp. 745–757.

Burbach, J. P. H., Smidt, M. P., Asbreuk, C. H. J., Cox, J. J., Chen, H., and Johnson, R. L. (2000). "A second independent pathway for development of mesencephalic dopaminergic neurons requires Lmx1b". In: *Nature Neuroscience* 3 (4): pp. 337–341.

Campbell, G. A., Eckardt, M. J., and Weight, F. F. (1985). "Dopaminergic mechanisms in subthalamic nucleus of rat: analysis using horseradish peroxidase and microiontophoresis". In: *Brain Research* 333 (2): pp. 261–270.

Canteras, N. S., Shammah-Lagnado, S. J., Silva, B. A., and Ricardo, J. A. (1990). "Afferent connections of the subthalamic nucleus: a combined retrograde and anterograde horseradish peroxidase study in the rat". In: *Brain Research* 513 (1): pp. 43–59.

Cardozo Pinto, D. F. and Lammel, S. (2017). "Viral vector strategies for investigating midbrain dopamine circuits underlying motivated behaviors". In: *Pharmacology, Biochemistry, and Behavior* pii: S0091 (16): pp. 30318–30325.

Carlsson, A. (1959). "The occurrence, distribution and physiological role of catecholamines in the nervous system." In: *Pharmacological reviews* 11 (2, Part 2): pp. 490–493.

Carlsson, A., Falck, B., and Hillarp, N. A. (1962). "Cellular localization of brain monoamines". In: *Acta Physiologica Scandinavica Supplement* 56: pp. 1–28.

Carr, D. B. and Sesack, S. R. (2000a). "GABA-containing neurons in the rat ventral tegmental area project to the prefrontal cortex". In: *Synapse* 38 (2): pp. 114–123.

— (2000b). "Projections from the rat prefrontal cortex to the ventral tegmental area: target specificity in the synaptic associations with mesoaccumbens and mesocortical neurons." In: *Journal of Neuroscience* 20 (10): pp. 3864–3873.

Carter, C. J. (1982). "Topographical distribution of possible glutamatergic pathways from the frontal cortex to the striatum and substantia nigra in rats". In: *Neuropharmacology* 21 (5): pp. 379–383.

Carter, D. A. and Fibiger, H. C. (1978). "The projections of the entopeduncular nucleus and globus pallidus in rat as demonstrated by autoradiography and horseradish peroxidase histochemistry". In: *The Journal of Comparative Neurology* 177 (1): pp. 113–123.

Celada, P., Paladini, C. A., and Tepper, J. M. (1999). "Gabaergic control of rat substantia nigra dopaminergic neurons: role of globus pallidus and substantia nigra pars reticulata". In: *Neuroscience* 89 (3): pp. 813–825.

Celio, M. (1990). "Calbindin D-28k and parvalbumin in the rat nervous system". In: *Neuroscience* 35 (2): pp. 375–475.

Cenci, M. A., Whishaw, I. Q., and Schallert, T. (2002). "Opinion: Animal models of neurological deficits: how relevant is the rat?" In: *Nature Reviews Neuroscience* 3 (7): pp. 574–579.

Chan, C. S., Guzman, J. N., Ilijic, E., Mercer, J. N., Rick, C., Tkatch, T., Meredith, G. E., and Surmeier, D. J. (2007). "'Rejuvenation' protects neurons in mouse models of Parkinson's disease." In: *Nature* 447 (7148): pp. 1081–1086.

Chang, H., Wilson, C. J., and Kitai, S. T. (1981). "Single neostriatal efferent axons in the globus pallidus: a light and electron microscopic study". In: *Science* 213 (4510): pp. 915–918.

Charara, A., Smith, Y., and Parent, A. (1996). "Glutamatergic inputs from the pedunculopontine nucleus to midbrain dopaminergic neurons in primates: Phaseolus vulgaris-leucoagglutinin anterograde labeling combined with postembedding glutamate and GABA immunohistochemistry." In: *Journal of Comparative Neurology* 364 (2): pp. 254–266.

Chartier-Harlin, M.-C., Kachergus, J., Roumier, C., Mouroux, V., Douay, X., Lincoln, S., Levecque, C., Larvor, L., Andrieux, J., Hulihan, M., Waucquier, N., Defebvre, L., Amouyel, P., Farrer, M. J., and Destée, A. (2004). "α-synuclein locus duplication as a cause of familial Parkinson's disease". In: *Lancet* 364 (9440): pp. 1167–1169.

Chen, C.-Y., Weng, Y.-H., Chien, K.-Y., Lin, K.-J., Yeh, T.-H., Cheng, Y.-P., Lu, C.-S., and Wang, H.-L. (2012). "(G2019S) LRRK2 activates MKK4-JNK pathway and causes degeneration of SN dopaminergic neurons in a transgenic mouse model of PD". In: *Cell Death and Differentiation* 19 (10): pp. 1623–1633.

Chen, S. and Aston-Jones, G. (1995). "Evidence that cholera toxin B subunit (CTb) can be avidly taken up and transported by fibers of passage". In: *Brain Research* 674 (1): pp. 107–111.

Chen, T.-Y., Duh, S.-L., Huang, C.-C., Lin, T.-B., and Kuo, D.-Y. (2001). "Evidence for the involvement of dopamine D1 and D2 receptors in mediating the decrease of food intake during repeated treatment with amphetamine". In: *Journal of Biomedical Science* 8 (6): pp. 462–466.

Cheramy, A., Leviel, V., and Glowinski, J. (1981). "Dendritic release of dopamine in the substantia nigra". In: *Nature* 289 (5798): pp. 537–543.

Chergui, K., Suaud-Chagny, M., and Gonon, F. G. (1994). "Nonlinear relationship between impulse flow, dopamine release and dopamine elimination in the rat brain in vivo." In: *Neuroscience* 62 (3): pp. 641–645.

Chergui, K., Akaoka, H., Charléty, P. J., Saunier, C. F., Buda, M., and Chouvet, G. (1994). "Subthalamic nucleus modulates burst firing of nigral dopamine neurones via NMDA receptors". In: *NeuroReport* 5 (10): pp. 1185–1188.

Chesselet, M.-F. (1996). "Basal ganglia and movement disorders: an update". In: *Trends in Neurosciences* 19 (10): pp. 417–422.

Chesselet, M.-F., Fleming, S., Mortazavi, F., and Meurers, B. (2008). "Strengths and limitations of genetic mouse models of Parkinson's disease." In: *Parkinsonism & Related Disorders* 14 (Supplement 2): S84–87.

Chesselet, M.-F., Richter, F., Zhu, C., Magen, I., Watson, M. B., and Subramaniam, S. R. (2012). "A Progressive Mouse Model of Parkinson's Disease: The Thy1-aSyn ("Line 61") Mice". In: *Neurotherapeutics* 9 (2): pp. 297–314.

Chevalier, G., Vacher, S., Deniau, J. M., and Desban, M. (1985). "Disinhibition as a basic process in the expression of striatal functions. I. The striato-nigral influence on tecto-spinal/tecto-diencephalic neurons". In: *Brain Research* 334 (2): pp. 215–226.

Chiba, T., Kayahara, T., and Nakano, K. (2001). "Efferent projections of infralimbic and prelimbic areas of the medial prefrontal cortex in the Japanese monkey, Macaca fuscata". In: *Brain Research* 888 (1): pp. 83–101.

Chiodo, L. A., Antelman, S. M., Caggiula, A. R., and Lineberry, C. G. (1980). "Sensory stimuli alter discharge rate of dopamine (DA) neurons: evidence for two functional types of DA cells in the substantia nigra". In: *Brain Research* 189 (2): pp. 544–549.

Chiodo, L. A., Caggiula, A. R., Antelman, S. M., and Lineberry, C. G. (1979). "Reciprocal influences of activating and immobilizing stimuli on the activity of nigrostriatal dopamine neurons". In: *Brain Research* 176 (2): pp. 385–390.

Chung, C. Y., Licznerski, P., Alavian, K. N., Simeone, A., Lin, Z., Martin, E., Vance, J., and Isacson, O. (2010). "The transcription factor orthodenticle homeobox 2 influences axonal projections and vulnerability of midbrain dopaminergic neurons." In: *Brain* 133 (Pt 7): pp. 2022–2031.

Chung, C. Y., Seo, H., Sonntag, K. C., Brooks, A., Lin, L., and Isacson, O. (2005). "Cell type-specific gene expression of midbrain dopaminergic neurons reveals molecules involved in their vulnerability and protection." In: *Human Molecular Genetics* 14 (13): pp. 1709–1725.

Cirillo, L. A., Lin, F. R., Cuesta, I., Friedman, D., Jarnik, M., and Zaret, K. S. (2002). "Opening of compacted chromatin by early developmental transcription factors HNF3 (FoxA) and GATA-4." In: *Molecular Cell* 9 (2): pp. 279–289.

Clarke, P. B. S., Hommer, D., Pert, A., and Skirboll, L. (1987). "Innervation of substantia nigra neurons by cholinergic afferents from pedunculopontine nucleus in the rat: neuroanatomical and electrophysiological evidence". In: *Neuroscience* 23 (3): pp. 1011–1019.

Cleland, T. A., Morse, A., Yue, E. L., and Linster, C. (2002). "Behavioral models of odor similarity." In: *Behavioral Neuroscience* 116 (2): pp. 222–231.

Cohen, J. Y., Haesler, S., Vong, L., Lowell, B. B., and Uchida, N. (2012). "Neuron-type-specific signals for reward and punishment in the ventral tegmental area." In: *Nature* 482 (7383): pp. 85–88.

Comoli, E., Coizet, V., Boyes, J., Bolam, J. P., Canteras, N. S., Quirk, R. H., Overton, P. G., and Redgrave, P. (2003). "A direct projection from superior colliculus to substantia nigra for detecting salient visual events". In: *Nature Neuroscience* 6 (9): pp. 974–980.

Cools, R., Lewis, S. J. G., Clark, L., Barker, R. A., and Robbins, T. W. (2007). "L-DOPA Disrupts Activity in the Nucleus Accumbens during Reversal Learning in Parkinson's Disease". In: *Neuropsychopharmacology* 32 (1): pp. 180–189.

Coon, D. J. (1982). "Eponymy, obscurity, Twitmyer, and Pavlov." In: *Journal of the History of the Behavioral Sciences* 18 (3): pp. 255–262.

Cote, P.-Y., Sadikot, A. F., and Parent, A. (1991). "Complementary Distribution of Calbindin D-28k and Parvalbumin in the Basal Forebrain and Midbrain of the Squirrel Monkey". In: *European Journal of Neuroscience* 3 (12): pp. 1316–1329.

Cotzias, G. C., Van Woert, M. H., and Schiffer, L. M. (1967). "Aromatic Amino Acids and Modification of Parkinsonism". In: *New England Journal of Medicine* 276 (7): pp. 374–379.

Cragg, S. J. (2003). "Variable dopamine release probability and short-term plasticity between functional domains of the primate striatum." In: *Journal of Neuroscience* 23 (10): pp. 4378–4385.

Cragg, S. J., Rice, M. E., and Greenfield, S. A. (1997). "Heterogeneity of electrically evoked dopamine release and reuptake in substantia nigra, ventral tegmental area, and striatum." In: *Journal of Neurophysiology* 77 (2): pp. 863–873.

Criscuolo, C., De Rosa, A., Guacci, A., Simons, E. J., Breedveld, G. J., Peluso, S., Volpe, G., Filla, A., Oostra, B. A., Bonifati, V., and De Michele, G. (2011). "The LRRK2 R1441C mutation is more frequent than G2019S in Parkinson's disease patients from Southern Italy". In: *Movement Disorders* 26 (9): pp. 1732–1736.

Dagher, A. and Robbins, T. W. (2009). "Personality, Addiction, Dopamine: Insights from Parkinson's Disease". In: *Neuron* 61 (4): pp. 502–510.

Dahan, L., Astier, B., Vautrelle, N., Urbain, N., Kocsis, B., and Chouvet, G. (2007). "Prominent burst firing of dopaminergic neurons in the ventral tegmental area during paradoxical sleep." In: *Neuropsychopharmacology* 32 (6): pp. 1232–1241.

Dahlström, A. and Fuxe, K. (1964). "Evidence for the existence of monoamine-containing neurons in the central nervous system. I. Demonstration of monoamines in the cell bodies of brain stem neurons." In: *Acta Physiologica Scandinavica Supplement* 62 (232): pp. 1–55.

Dawson, T. M., Ko, H. S., Dawson, V. L., Lichtner, P., Farrer, M. J., Lincoln, S., Kachergus, J., Hulihan, M., Uitti, R., and Calne, D. (2010). "Genetic animal models of Parkinson's disease." In: *Neuron* 66 (5): pp. 646–661.

Day, J. J., Jones, J. L., Wightman, R. M., and Carelli, R. M. (2010). "Phasic Nucleus Accumbens Dopamine Release Encodes Effort- and Delay-Related Costs". In: *Biological Psychiatry* 68 (3): pp. 306–309.

Deacon, R. M. J. (2013). "Measuring motor coordination in mice." In: *Journal of Visualized Experiments* (75): e2609.

DeLong, M. R. (1971). "Activity of pallidal neurons during movement." In: *Journal of Neurophysiology* 34 (3): pp. 414–427.

— (1973). "Putamen: activity of single units during slow and rapid arm movements." In: *Science* 179 (4079): pp. 1240–1242.

— (1990). "Primate models of movement disorders of basal ganglia origin". In: *Trends in Neurosciences* 13 (7): pp. 281–285.

DeLong, M. R., Crutcher, M. D., and Georgopoulos, A. P. (1983). "Relations between movement and single cell discharge in the substantia nigra of the behaving monkey." In: *Journal of Neuroscience* 3 (8): pp. 1599–1606.

Deniau, J. M., Feger, J., and Le Guyader, C. (1976). "Striatal evoked inhibition of identified nigro-thalamic neurons". In: *Brain Research* 104 (1): pp. 152–156.

Deniau, J. M., Kitai, S. T., Donoghue, J., and Grofova, I. (1982). "Neuronal interactions in the substantia nigra pars reticulata through axon collaterals of the projection neurons". In: *Experimental Brain Research* 47 (1): pp. 105–113.

Deniau, J. M., Mailly, P., Maurice, N., and Charpier, S. (2007). "The pars reticulata of the substantia nigra: a window to basal ganglia output". In: *Progress in Brain Research* 160: pp. 151–172.

Deumens, R., Blokland, A., and Prickaerts, J. (2002). "Modeling Parkinson's disease in rats: an evaluation of 6-OHDA lesions of the nigrostriatal pathway." In: *Experimental Neurology* 175 (2): pp. 303–317.

Di Chiara, G. and Imperato, A. (1988). "Drugs abused by humans preferentially increase synaptic dopamine concentrations in the mesolimbic system of freely moving rats." In: *Proceedings of the National Academy of Sciences* 85 (14): pp. 5274–5278.

Di Chiara, G., Porceddu, M., Morelli, M., Mulas, M., and Gessa, G. (1979). "Evidence for a gabaergic projection from the substantia nigra to the ventromedial thalamus and to the superior colliculus of the rat". In: *Brain Research* 176 (2): pp. 273–284.

Di Fonzo, A., Rohé, C. F., Ferreira, J. J., Chien, H. F., Vacca, L., Stocchi, F., Guedes, L., Fabrizio, E., Manfredi, M., Vanacore, N., Goldwurm, S., Breedveld, G., Sampaio, C., Meco, G., Barbosa, E., Oostra, B. A., and Bonifati, V. (2005). "A frequent LRRK2 gene mutation associated with autosomal dominant Parkinson's disease." In: *Lancet* 365 (9457): pp. 412–415.

Di Giovannantonio, L. G., Di Salvio, M., Acampora, D., Prakash, N., Wurst, W., and Simeone, A. (2013). "Otx2 selectively controls the neurogenesis of specific neuronal subtypes of the ventral tegmental area and compensates En1-dependent neuronal loss and MPTP vulnerability". In: *Developmental Biology* 373 (1): pp. 176–183.

Di Porzio, U., Zuddas, A., Cosenza-Murphy, D. B., and Barker, J. L. (1990). "Early appearance of tyrosine hydroxylase immunoreactive cells in the mesencephalon of mouse embryos". In: *International Journal of Developmental Neuroscience* 8 (5): pp. 523–532.

Di Salvio, M., Di Giovannantonio, L. G., Omodei, D., Acampora, D., and Simeone, A. (2010). "Otx2 expression is restricted to dopaminergic neurons of the ventral tegmental area in the adult brain." In: *The International Journal of Developmental Biology* 54 (5): pp. 939–945.

Di Salvio, M., Di Giovannantonio, L. G., Acampora, D., Prosperi, R., Omodei, D., Prakash, N., Wurst, W., and Simeone, A. (2010). "Otx2 controls neuron subtype identity in ventral tegmental area and antagonizes vulnerability to MPTP." In: *Nature Neuroscience* 13 (12): pp. 1481–1488.

Dobi, A., Margolis, E. B., Wang, H.-L., Harvey, B. K., and Morales, M. (2010). "Glutamatergic and Nonglutamatergic Neurons of the Ventral Tegmental Area Establish Local Synaptic Contacts with Dopaminergic and Nondopaminergic Neurons". In: *Journal of Neuroscience* 30 (1): pp. 218–229.

Dodson, P. D., Dreyer, J. K., Jennings, K. A., Syed, E. C. J., Wade-Martins, R., Cragg, S. J., Bolam, J. P., and Magill, P. J. (2016). "Representation of spontaneous movement by dopaminergic neurons is cell-type selective and disrupted in parkinsonism". In: *Proceedings of the National Academy of Sciences* 113 (15): E2180–E2188.

Dodson, P. D., Larvin, J. T., Duffell, J. M., Garas, F. N., Doig, N. M., Kessaris, N., Duguid, I. C., Bogacz, R., Butt, S. J., and Magill, P. J. (2015). "Distinct Developmental Origins Manifest in the Specialized Encoding of Movement by Adult Neurons of the External Globus Pallidus". In: *Neuron* 86 (2): pp. 501–513.

Doig, N. M., Moss, J., and Bolam, J. P. (2010). "Cortical and Thalamic Innervation of Direct and Indirect Pathway Medium-Sized Spiny Neurons in Mouse Striatum". In: *Journal of Neuroscience* 30 (44): pp. 14610–14618.

Domanskyi, A., Alter, H., Vogt, M. A., Gass, P., and Vinnikov, I. A. (2014). "Transcription factors Foxa1 and Foxa2 are required for adult dopamine neurons maintenance". In: *Frontiers in Cellular Neuroscience* 8: p. 275.

Donato, F., Rompani, S. B., and Caroni, P. (2013). "Parvalbumin-expressing basket-cell network plasticity induced by experience regulates adult learning". In: *Nature* 504 (7479): pp. 272–276.

Dopeso-Reyes, I. G., Rico, A. J., Roda, E., Sierra, S., Pignataro, D., Lanz, M., Sucunza, D., Chang-Azancot, L., and Lanciego, J. L. (2014). "Calbindin content and differential vulnerability of midbrain efferent dopaminergic neurons in macaques." In: *Frontiers in Neuroanatomy* 8: p. 146.

Doty, R. L., Deems, D. A., and Stellar, S. (1988). "Olfactory dysfunction in parkinsonism: a general deficit unrelated to neurologic signs, disease stage, or disease duration." In: *Neurology* 38 (8): pp. 1237–1244.

Doty, R. L., Shaman, P., and Dann, M. (1984). "Development of the university of pennsylvania smell identification test: A standardized microencapsulated test of olfactory function". In: *Physiology & Behavior* 32 (3): pp. 489–502.

Dranka, B. P., Gifford, A., Ghosh, A., Zielonka, J., Joseph, J., Kanthasamy, A. G., and Kalyanaraman, B. (2013). "Diapocynin prevents early Parkinson's disease symptoms in the leucine-rich repeat kinase 2 (LRRK2R1441G) transgenic mouse". In: *Neuroscience Letters* 549: pp. 57–62.

Dranka, B. P., Gifford, A., McAllister, D., Zielonka, J., Joseph, J., O'Hara, C. L., Stucky, C. L., Kanthasamy, A. G., and Kalyanaraman, B. (2014). "A novel mitochondrially-targeted apocynin derivative prevents hyposmia and loss of motor function in the leucine-rich repeat kinase 2 (LRRK2(R1441G)) transgenic mouse model of Parkinson's disease." In: *Neuroscience Letters* 583: pp. 159–164.

Dreyer, J. K. and Herrik, K. (2010). "Influence of phasic and tonic dopamine release on receptor activation". In: *Journal of Neuroscience* 30 (42): pp. 14273–14283.

Ehret, G. (1983). "Psychoacoustics". In: *The Auditory Psychobiology of the Mouse*. Ed. by Willott, J. F. Springfield: C.C. Thomas. Chap. 2, pp. 13–56.

Ehringer, H. and Hornykiewicz, O. (1960). "Verteilung Von Noradrenalin Und Dopamin (3-Hydroxytyramin) Im Gehirn Des Menschen Und Ihr Verhalten Bei Erkrankungen Des Extrapyramidalen Systems". In: *Klinische Wochenschrift* 38 (24): pp. 1236–1239.

Ekstrand, M. I., Nectow, A. R., Knight, Z. A., Latcha, K. N., Pomeranz, L. E., and Friedman, J. M. (2014). "Molecular Profiling of Neurons Based on Connectivity". In: *Cell* 157 (5): pp. 1230–1242.

Eshel, N., Bukwich, M., Rao, V., Hemmelder, V., Tian, J., and Uchida, N. (2015). "Arithmetic and local circuitry underlying dopamine prediction errors." In: *Nature* 525 (7568): pp. 243–246.

Eshel, N., Tian, J., Bukwich, M., and Uchida, N. (2016). "Dopamine neurons share common response function for reward prediction error". In: *Nature Neuroscience* 19 (3): pp. 479–486.

Eulitz, D., Prüss, H., Derst, C., and Veh, R. W. (2007). "Heterogeneous Distribution of Kir3 Potassium Channel Proteins Within Dopaminergic Neurons in the Mesencephalon of the Rat Brain". In: *Cellular and Molecular Neurobiology* 27 (3): pp. 285–302.

Fadel, J. and Deutch, A. Y. (2002). "Anatomical substrates of orexin–dopamine interactions: lateral hypothalamic projections to the ventral tegmental area". In: *Neuroscience* 111 (2): pp. 379–387.

Fallon, J. H. (1981). "Collateralization of monoamine neurons: mesotelencephalic dopamine projections to caudate, septum, and frontal cortex." In: *Journal of Neuroscience* 1 (12): pp. 1361–1368.

Fallon, J. H., Koziell, D. A., and Moore, R. Y. (1978). "Catecholamine innervation of the basal forebrain II. Amygdala, suprarhinal cortex and entorhinal cortex". In: *The Journal of Comparative Neurology* 180 (3): pp. 509–531.

Fallon, J. H. and Loughlin, S. E. (1995). "Substantia Nigra". In: *The Rat Nervous System*. Ed. by Paxinos, G. 2nd ed. San Diego ; London: Academic Press. Chap. 12, pp. 215–237.

Fallon, J. H. and Moore, R. Y. (1978a). "Catecholamine innervation of the basal forebrain III. Olfactory bulb, anterior olfactory nuclei, olfactory tubercle and piriform cortex". In: *The Journal of Comparative Neurology* 180 (3): pp. 533–544.

— (1978b). "Catecholamine innervation of the basal forebrain. IV. Topography of the dopamine projection to the basal forebrain and neostriatum." In: *The Journal of Comparative Neurology* 180 (3): pp. 545–80.

Fallon, J. H., Riley, J. N., and Moore, R. Y. (1978). "Substantia nigra dopamine neurons: separate populations project to neostriatum and allocortex". In: *Neuroscience Letters* 7 (2): pp. 157–162.

Fan, D., Rossi, M. A., and Yin, H. H. (2012). "Mechanisms of Action Selection and Timing in Substantia Nigra Neurons". In: *Journal of Neuroscience* 32 (16): pp. 5534–5548.

Farrell, K. F., Krishnamachari, S., Villanueva, E., Lou, H., Alerte, T. N. M., Peet, E., Drolet, R. E., and Perez, R. G. (2014). "Non-motor parkinsonian pathology in aging A53T α-Synuclein mice is associated with progressive synucleinopathy and altered enzymatic function". In: *Journal of Neurochemistry* 128 (4): pp. 536–546.

Fearnley, J. M. and Lees, A. J. (1991). "Ageing and Parkinson's Disease: Substantia Nigra Regional Selectivity". In: *Brain* 114 (5): pp. 2283–2301.

Feil, R., Wagner, J., Metzger, D., and Chambon, P. (1997). "Regulation of Cre Recombinase Activity by Mutated Estrogen Receptor Ligand-Binding Domains". In: *Biochemical and Biophysical Research Communications* 237 (3): pp. 752–757.

Ferreira, J. G. P., Del-Fava, F., Hasue, R. H., and Shammah-Lagnado, S. J. (2008). "Organization of ventral tegmental area projections to the ventral tegmental area-nigral complex in the rat." In: *Neuroscience* 153 (1): pp. 196–213.

Ferreira, J. J., Guedes, L. C., Rosa, M. M., Coelho, M., Doeselaar, M. van, Schweiger, D., Di Fonzo, A., Oostra, B. A., Sampaio, C., and Bonifati, V. (2007). "High prevalence of LRRK2 mutations in familial and sporadic Parkinson's disease in Portugal". In: *Movement Disorders* 22 (8): pp. 1194–1201.

Ferri, A. L. M., Lin, W., Mavromatakis, Y. E., Wang, J. C., Sasaki, H., Whitsett, J. A., and Ang, S.-L. (2007). "Foxa1 and Foxa2 regulate multiple phases of midbrain dopaminergic neuron development in a dosage-dependent manner." In: *Development* 134 (15): pp. 2761–2769.

Field, K. J., White, W. J., and Lang, C. M. (1993). "Anaesthetic effects of chloral hydrate, pentobarbitone and urethane in adult male rats". In: *Laboratory Animals* 27 (3): pp. 258–269.

Fiorillo, C. D., Song, M. R., and Yun, S. R. (2013). "Multiphasic temporal dynamics in responses of midbrain dopamine neurons to appetitive and aversive stimuli." In: *Journal of Neuroscience* 33 (11): pp. 4710–4725.

Flagel, S. B., Clark, J. J., Robinson, T. E., Mayo, L., Czuj, A., Willuhn, I., Akers, C. A., Clinton, S. M., Phillips, P. E. M., and Akil, H. (2011). "A selective role for dopamine in stimulus–reward learning". In: *Nature* 469 (7328): pp. 53–57.

Fleming, S. M., Salcedo, J., Fernagut, P.-O., Rockenstein, E., Masliah, E., Levine, M. S., and Chesselet, M.-F. (2004). "Early and progressive sensorimotor anomalies in mice overexpressing wild-type human alpha-synuclein." In: *Journal of Neuroscience* 24 (42): pp. 9434–9440.

Fleming, S. M., Tetreault, N. A., Mulligan, C. K., Hutson, C. B., Masliah, E., and Chesselet, M.-F. (2008). "Olfactory deficits in mice overexpressing human wildtype α-synuclein". In: *European Journal of Neuroscience* 28 (2): pp. 247–256.

Floresco, S. B., West, A. R., Ash, B., Moore, H., and Grace, A. A. (2003). "Afferent modulation of dopamine neuron firing differentially regulates tonic and phasic dopamine transmission". In: *Nature Neuroscience* 6 (9): pp. 968–973.

Földiák, P. (2002). *Sparse Coding in the Primate Cortex*. Ed. by Arbib, M. A. 2nd ed. Cambridge, MA: The MIT Press.

Foltynie, T., Brayne, C. E. G., Robbins, T. W., and Barker, R. A. (2003). "The cognitive ability of an incident cohort of Parkinson's patients in the UK. The CamPaIGN study". In: *Brain* 127 (3): pp. 550–560.

Ford, C. P., Gantz, S. C., Phillips, P. E. M., and Williams, J. T. (2010). "Control of extracellular dopamine at dendrite and axon terminals." In: *Journal of Neuroscience* 30 (20): pp. 6975–6983.

Francois, C., Savy, C., Jan, C., Tande, D., Hirsch, E. C., and Yelnik, J. (2000). "Dopaminergic innervation of the subthalamic nucleus in the normal state, in MPTP-treated monkeys, and in Parkinson's disease patients". In: *The Journal of Comparative Neurology* 425 (1): pp. 121–129.

Frank, M. J., Seeberger, L. C., and O'reilly, R. C. (2004). "By carrot or by stick: cognitive reinforcement learning in parkinsonism." In: *Science* 306 (5703): pp. 1940–1943.

Frank, M. J. and Surmeier, D. J. (2009). "Do substantia nigra dopaminergic neurons differentiate between reward and punishment?" In: *Journal of Molecular Cell Biology* 1 (1): pp. 15–16.

Freeze, B. S., Kravitz, A. V., Hammack, N., Berke, J. D., and Kreitzer, A. C. (2013). "Control of Basal Ganglia Output by Direct and Indirect Pathway Projection Neurons". In: *Journal of Neuroscience* 33 (47): pp. 18531–18539.

Friedman, A. H. and Piepho, R. W. (1979). "Effect of photoperiod reversal on twenty-four hour patterns for dopamine levels in the corpus striatum and upper and lower brainstem of the rat." In: *International Journal of Chronobiology* 6 (1): pp. 57–65.

Fu, Y., Yuan, Y., Halliday, G., Rusznák, Z., Watson, C., and Paxinos, G. (2012). "A cytoarchitectonic and chemoarchitectonic analysis of the dopamine cell groups in the substantia nigra, ventral tegmental area, and retrorubral field in the mouse." In: *Brain Structure & Function* 217 (2): pp. 591–612.

Furuta, T., Koyano, K., Tomioka, R., Yanagawa, Y., and Kaneko, T. (2004). "GABAergic basal forebrain neurons that express receptor for neurokinin B and send axons to the cerebral cortex". In: *The Journal of Comparative Neurology* 473 (1): pp. 43–58.

Futami, T., Takakusaki, K., and Kitai, S. T. (1995). "Glutamatergic and cholinergic inputs from the pedunculopontine tegmental nucleus to dopamine neurons in the substantia nigra pars compacta". In: *Neuroscience Research* 21 (4): pp. 331–342.

Fuxe, K., Hökfelt, T., Johansson, O., Jonsson, G., Lidbrink, P., and Ljundahl, Å. (1974). "The origin of the dopamine nerve terminals in limbic and frontal cortex. Evidence for meso-cortico dopamine neurons". In: *Brain Research* 82 (2): pp. 349–355.

Galter, D., Buervenich, S., Carmine, A., Anvret, M., and Olson, L. (2003). "ALDH1 mRNA: presence in human dopamine neurons and decreases in substantia nigra in Parkinson's disease and in the ventral tegmental area in schizophrenia". In: *Neurobiology of Disease* 14 (3): pp. 637–647.

Gan, J. O., Walton, M. E., and Phillips, P. E. M. (2010). "Dissociable cost and benefit encoding of future rewards by mesolimbic dopamine." In: *Nature Neuroscience* 13 (1): pp. 25–27.

García-Cabezas, M. Á., Martínez-Sánchez, P., Sánchez-González, M. A., Garzón, M., Cavada, C., Garcia-Cabezas, M. A., Martinez-Sanchez, P., Sanchez-Gonzalez, M. A., and Garzon, M. (2009). "Dopamine innervation in the thalamus: monkey versus rat." In: *Cerebral Cortex* 19 (2): pp. 424–434.

García-Cabezas, M. Á., Rico, B., Sánchez-González, M. Á., and Cavada, C. (2007). "Distribution of the dopamine innervation in the macaque and human thalamus". In: *NeuroImage* 34 (3): pp. 965–984.

Gauthier, J., Parent, M., Levesque, M., and Parent, A. (1999). "The axonal arborization of single nigrostriatal neurons in rats". In: *Brain Research* 834 (1): pp. 228–232.

Geffen, L., Jessell, T., Cuello, A., and Iversen, L. (1976). "Release of dopamine from dendrites in rat substantia nigra". In: *Nature* 260 (5548): pp. 619–621.

Georgopoulos, A. P., DeLong, M. R., and Crutcher, M. D. (1983). "Relations between parameters of step-tracking movements and single cell discharge in the globus pallidus and subthalamic nucleus of the behaving monkey." In: *Journal of Neuroscience* 3 (8): pp. 1586–1598.

Gerfen, C. R. (1984). "The neostriatal mosaic: compartmentalization of corticostriatal input and striatonigral output systems." In: *Nature* 311 (5985): pp. 461–464.

— (1992). "The neostriatal mosaic: multiple levels of compartmental organization". In: *Trends in Neurosciences* 15 (4): pp. 133–139.

— (2004). "Basal Ganglia". In: *The Rat Nervous System*. Ed. by Paxinos, G. 3rd ed. Amsterdam ; London: Elsevier/Academic Press, pp. 455–508.

Gerfen, C. R., Baimbridge, K. G., and Miller, J. J. (1985). "The neostriatal mosaic: compartmental distribution of calcium-binding protein and parvalbumin in the basal ganglia of the rat and monkey." In: *Proceedings of the National Academy of Sciences* 82 (24): pp. 8780–8784.

Gerfen, C. R., Engber, T. M., Mahan, L. C., Susel, Z., Chase, T. N., Monsma, F. J., and Sibley, D. R. (1990). "D1 and D2 dopamine receptor regulated gene expression of striatonigral and striatopallidal neurons". In: *Science* 250 (1986): pp. 1429–1432.

Gerfen, C. R., Herkenham, M., and Thibault, J. (1987). "The neostriatal mosaic: II. Patch- and matrix-directed mesostriatal dopaminergic and non-dopaminergic systems". In: *Journal of Neuroscience* 7 (12): pp. 3915–3934.

Gerfen, C. R., Paletzki, R., and Heintz, N. (2013). "GENSAT BAC Cre-Recombinase Driver Lines to Study the Functional Organization of Cerebral Cortical and Basal Ganglia Circuits". In: *Neuron* 80 (6): pp. 1368–1383.

Gerfen, C. R. and Young, W. S. I. (1988). "Distribution of striatonigral and striatopallidal peptidergic neurons in both patch and matrix compartments: an in situ hybridization histochemistry and fluorescent retrograde tracing study". In: *Brain Research* 460 (1): pp. 161–167.

German, D. C. and Manaye, K. F. (1993). "Midbrain dopaminergic neurons (nuclei A8, A9, and A10): Three-dimensional reconstruction in the rat". In: *The Journal of Comparative Neurology* 331 (3): pp. 297–309.

German, D. C., Manaye, K. F., Sonsalla, P. K., and Brooks, B. A. (1992). "Midbrain Dopaminergic Cell Loss in Parkinson's Disease and MPTP-Induced Parkinsonism: Sparing of Calbindin-D 28k Containing Cells". In: *Annals of the New York Academy of Sciences* 648: pp. 42–62.

Gershman, S. J. and Niv, Y. (2015). "Novelty and Inductive Generalization in Human Reinforcement Learning". In: *Topics in Cognitive Science* 7 (3): pp. 391–415.

Gervais, J. and Rouillard, C. (2000). "Dorsal raphe stimulation differentially modulates dopaminergic neurons in the ventral tegmental area and substantia nigra". In: *Synapse* 35 (4): pp. 281–291.

Gilks, W. P., Abou-Sleiman, P. M., Gandhi, S., Jain, S., Singleton, A., Lees, A. J., Shaw, K., Bhatia, K. P., Bonifati, V., Quinn, N. P., Lynch, J., Healy, D. G., Holton, J. L., Revesz, T., and Wood, N. W. (2005). "A common LRRK2 mutation in idiopathic Parkinson's disease." In: *Lancet* 365 (9457): pp. 415–416.

Giovanni, A., Sieber, B. A., Heikkila, R. E., and Sonsalla, P. K. (1994). "Studies on species sensitivity to the dopaminergic neurotoxin 1-methyl-4-phenyl-1,2,3,6-tetrahydropyridine. Part 1: Systemic administration." In: *The Journal of Pharmacology and Experimental Therapeutics* 270 (3): pp. 1000–1007.

Glasl, L., Kloos, K., Giesert, F., Roethig, A., Di Benedetto, B., Kühn, R., Zhang, J., Hafen, U., Zerle, J., Hofmann, A., Hrabé De Angelis, M., Winklhofer, K. F., Hölter, S. M., Vogt Weisenhorn, D. M., and Wurst, W. (2012). "Pink1-deficiency in mice impairs gait, olfaction and serotonergic innervation of the olfactory bulb". In: *Experimental Neurology* 235 (1): pp. 214–227.

Glimcher, P. W. (2011). "Understanding dopamine and reinforcement learning: the dopamine reward prediction error hypothesis." In: *Proceedings of the National Academy of Sciences* 108 (Supplement 3): pp. 15647–15654.

Gonon, F. G. (1988). "Nonlinear relationship between impulse flow and dopamine released by rat midbrain dopaminergic neurons as studied by in vivo electrochemistry." In: *Neuroscience* 24 (1): pp. 19–28.

— (1997). "Prolonged and Extrasynaptic Excitatory Action of Dopamine Mediated by D1 Receptors in the Rat Striatum In Vivo". In: *Journal of Neuroscience* 17 (15): pp. 5972–5978.

González-Hernández, T., Barroso-Chinea, P., de la Cruz Muros, I., del Mar Pérez-Delgado, M., and Rodríguez, M. (2004). "Expression of dopamine and vesicular monoamine transporters and differential vulnerability of mesostriatal dopaminergic neurons". In: *Journal of Comparative Neurology* 479 (2): pp. 198–215.

González-Hernández, T., Cruz-Muros, I., Afonso-Oramas, D., Salas-Hernandez, J., and Castro-Hernandez, J. (2010). "Vulnerability of mesostriatal dopaminergic neurons in Parkinson's disease." In: *Frontiers in Neuroanatomy* 4: p. 140.

González-Hernández, T. and Rodríguez, M. (2000). "Compartmental organization and chemical profile of dopaminergic and GABAergic neurons in the substantia nigra of the rat." In: *Journal of Comparative Neurology* 421 (1): pp. 107–135.

Gould, E., Woolf, N., and Butcher, L. (1989). "Cholinergic projections to the substantia nigra from the pedunculopontine and laterodorsal tegmental nuclei". In: *Neuroscience* 28 (3): pp. 611–623.

Gourévitch, B. and Eggermont, J. J. (2007). "A nonparametric approach for detection of bursts in spike trains." In: *Journal of Neuroscience Methods* 160 (2): pp. 349–358.

Grace, A. A. and Bunney, B. S. (1980). "Nigral dopamine neurons: intracellular recording and identification with L-dopa injection and histofluorescence". In: *Science* 210 (4470): pp. 654–656.

— (1984a). "The control of firing pattern in nigral dopamine neurons: burst firing." In: *Journal of Neuroscience* 4 (11): pp. 2877–2890.

— (1984b). "The control of firing pattern in nigral dopamine neurons: single spike firing". In: *Journal of Neuroscience* 4 (11): pp. 2866–2876.

Grace, A. A. and Onn, S. P. (1989). "Morphology and electrophysiological properties of immunocytochemically identified rat dopamine neurons recorded in vitro." In: *Journal of Neuroscience* 9 (10): pp. 3463–3481.

Graveland, G. and Difiglia, M. (1985). "The frequency and distribution of medium-sized neurons with indented nuclei in the primate and rodent neostriatum". In: *Brain Research* 327 (1): pp. 307–311.

Graybiel, A. M. and Ragsdale, C. W. (1978). "Histochemically distinct compartments in the striatum of human, monkeys, and cat demonstrated by acetylthiocholinesterase staining." In: *Proceedings of the National Academy of Sciences* 75 (11): pp. 5723–5726.

Greene, J. G. (2006). "Gene expression profiles of brain dopamine neurons and relevance to neuropsychiatric disease." In: *The Journal of Physiology* 575 (Pt 2): pp. 411–416.

Greene, J. G., Dingledine, R., and Greenamyre, J. T. (2005). "Gene expression profiling of rat midbrain dopamine neurons: implications for selective vulnerability in parkinsonism." In: *Neurobiology of Disease* 18 (1): pp. 19–31.

Greene, S. A. and Thurmon, J. C. (1988). "Xylazine – a review of its pharmacology and use in veterinary medicine". In: *Journal of Veterinary Pharmacology and Therapeutics* 11 (4): pp. 295–313.

Grimm, J., Mueller, A., Hefti, F., and Rosenthal, A. (2004). "Molecular basis for catecholaminergic neuron diversity." In: *Proceedings of the National Academy of Sciences* 101 (38): pp. 13891–13896.

Grofová, I. (1975). "The identification of striatal and pallidal neurons projecting to substantia nigra. An experimental study by means of retrograde axonal transport of horseradish peroxidase". In: *Brain Research* 91 (2): pp. 286–291.

Grofová, I. and Rinvik, E. (1970). "An experimental electron microscopic study on the striatonigral projection in the cat". In: *Experimental Brain Research* 11 (3): pp. 249–262.

Groves, P. M., Wilson, C. J., Young, S. J., and Rebec, G. V. (1975). "Self-inhibition by dopaminergic neurons." In: *Science* 190 (4214): pp. 522–528.

Gründemann, J., Schlaudraff, F., Haeckel, O., and Liss, B. (2008). "Elevated α-synuclein mRNA levels in individual UV-laser-microdissected dopaminergic substantia nigra neurons in idiopathic Parkinson's disease". In: *Nucleic Acids Research* 36 (7): e38.

Gulley, J. M., Kuwajima, M., Mayhill, E., and Rebec, G. V. (1999). "Behavior-related changes in the activity of substantia nigra pars reticulata neurons in freely moving rats". In: *Brain Research* 845 (1): pp. 68–76.

Guo, C., Qiu, H.-Y., Huang, Y., Chen, H., Yang, R.-Q., Chen, S.-D., Johnson, R. L., Chen, Z.-F., and Ding, Y.-Q. (2007). "Lmx1b is essential for Fgf8 and Wnt1

expression in the isthmic organizer during tectum and cerebellum development in mice". In: *Development* 134 (2): pp. 317–325.

Gusmão, I. D., Monteiro, B. M. M., Cornélio, G. O. S., Fonseca, C. S., Moraes, M. F. D., and Pereira, G. S. (2012). "Odor-enriched environment rescues long-term social memory, but does not improve olfaction in social isolated adult mice." In: *Behavioural Brain Research* 228 (2): pp. 440–446.

Guttmacher, A. E., Collins, F. S., Nussbaum, R. L., and Ellis, C. E. (2003). "Alzheimer's Disease and Parkinson's Disease". In: *New England Journal of Medicine* 348 (14): pp. 1356–1364.

Haber, S. (2014). "The place of dopamine in the cortico-basal ganglia circuit". In: *Neuroscience* 282: pp. 248–257.

Hajós, M. and Greenfield, S. A. (1994). "Synaptic connections between pars compacta and pars reticulata neurones: electrophysiological evidence for functional modules within the substantia nigra". In: *Brain Research* 660 (2): pp. 216–224.

Halliday, G. M. and Törk, I. (1986). "Comparative anatomy of the ventromedial mesencephalic tegmentum in the rat, cat, monkey and human". In: *Journal of Comparative Neurology* 252 (4): pp. 423–445.

Hamid, A. A., Pettibone, J. R., Mabrouk, O. S., Hetrick, V. L., Schmidt, R., Vander Weele, C. M., Kennedy, R. T., Aragona, B. J., and Berke, J. D. (2015). "Mesolimbic dopamine signals the value of work". In: *Nature Neuroscience* 19 (1): pp. 117–126.

Hammond, C., Deniau, J. M., Rizk, A., and Feger, J. (1978). "Electrophysiological demonstration of an excitatory subthalamonigral pathway in the rat". In: *Brain Research* 151 (2): pp. 235–244.

Hansen, C., Björklund, T., Petit, G. H., Lundblad, M., Murmu, R. P., Brundin, P., and Li, J.-Y. (2013). "A novel α-synuclein-GFP mouse model displays progressive motor impairment, olfactory dysfunction and accumulation of α-synuclein-GFP". In: *Neurobiology of Disease* 56: pp. 145–155.

Hara, K. and Harris, R. A. (2002). "The Anesthetic Mechanism of Urethane: The Effects on Neurotransmitter-Gated Ion Channels". In: *Anesthesia & Analgesia* 94 (2): pp. 313–318.

Hardman, C. D., Henderson, J. M., Finkelstein, D. I., Horne, M. K., Paxinos, G., and Halliday, G. M. (2002). "Comparison of the basal ganglia in rats, marmosets, macaques, baboons, and humans: Volume and neuronal number for the output, internal relay, and striatal modulating nuclei". In: *The Journal of Comparative Neurology* 445 (3): pp. 238–255.

Hassani, O.-K., François, C., Yelnik, J., and Féger, J. (1997). "Evidence for a dopaminergic innervation of the subthalamic nucleus in the rat". In: *Brain Research* 749 (1): pp. 88–94.

Hassler, R. (1938). "Zur Pathologie der Paralysis agitans und des postenzephalitischen Parkinsonismus". In: *Journal für Psychologie und Neurologie* 48 (48): pp. 387–476.

Häusser, M., Stuart, G., Racca, C., and Sakmann, B. (1995). "Axonal initiation and active dendritic propagation of action potentials in substantia nigra neurons". In: *Neuron* 15 (3): pp. 637–647.

Hawkes, C. H. (2008). "The prodromal phase of sporadic Parkinson's disease: Does it exist and if so how long is it?" In: *Movement Disorders* 23 (13): pp. 1799–1807.

Hawkes, C. H., Del Tredici, K., and Braak, H. (2010). "A timeline for Parkinson's disease". In: *Parkinsonism & Related Disorders* 16 (2): pp. 79–84.

Healy, D. G., Falchi, M., O'Sullivan, S. S., Bonifati, V., Durr, A., Bressman, S., Brice, A., Aasly, J., Zabetian, C. P., Goldwurm, S., Ferreira, J. J., Tolosa, E., Kay, D. M., Klein, C., Williams, D. R., Marras, C., Lang, A. E., Wszolek, Z. K., Berciano, J., Schapira, A. H., Lynch, T., Bhatia, K. P., Gasser, T., Lees, A. J., and Wood, N. W. (2008). "Phenotype, genotype, and worldwide genetic penetrance of LRRK2-associated Parkinson's disease: a case-control study". In: *The Lancet Neurology* 7 (7): pp. 583–590.

Hedreen, J. C. (1999). "Tyrosine hydroxylase-immunoreactive elements in the human globus pallidus and subthalamic nucleus". In: *Journal of Comparative Neurology* 409 (3): pp. 400–410.

Heffner, T. G., Zigmond, M. J., and Stricker, E. M. (1977). "Effects of dopaminergic agonists and antagonists of feeding in intact and 6-hydroxydopamine-treated rats." In: *Journal of Pharmacology and Experimental Therapeutics* 201 (2): pp. 386–399.

Heimer, L. and Wilson, R. D. (1975). "The subcortical projections of the allocortex: similarities in the neural associations of the hippocampus, the piriform cortex, and the neocortex." In: *Golgi Centennial Symposium: Perspectives in Neurobiology.* Ed. by Santini, M. New York: Raven Press, pp. 177–193.

Heimer, L., Zahm, D. S., Churchill, L., Kalivas, P., and Wohltmann, C. (1991). "Specificity in the projection patterns of accumbal core and shell in the rat". In: *Neuroscience* 41 (1): pp. 89–125.

Henry, K. R. and Chole, R. A. (1980). "Genotypic differences in behavioral, physiological and anatomical expressions of age-related hearing loss in the laboratory mouse." In: *Audiology* 19 (5): pp. 369–383.

Herkenham, M. (1979). "The afferent and efferent connections of the ventromedial thalamic nucleus in the rat". In: *The Journal of Comparative Neurology* 183 (3): pp. 487–517.

Herkenham, M., Edley, S. M., and Stuart, J. (1984). "Cell clusters in the nucleus accumbens of the rat, and the mosaic relationship of opiate receptors, acetylcholinesterase and subcortical afferent terminations". In: *Neuroscience* 11 (3): pp. 561–593.

Hernandez, P. J., Andrzejewski, M. E., Sadeghian, K., Panksepp, J. B., and Kelley, A. E. (2005). "AMPA/kainate, NMDA, and dopamine D1 receptor function in the nucleus accumbens core: a context-limited role in the encoding and consolidation of instrumental memory." In: *Learning & Memory* 12 (3): pp. 285–295.

Hikosaka, O. and Wurtz, R. H. (1983a). "Visual and oculomotor functions of monkey substantia nigra pars reticulata. I. Relation of visual and auditory responses to saccades." In: *Journal of Neurophysiology* 49 (5): pp. 1230–1253.

— (1983b). "Visual and oculomotor functions of monkey substantia nigra pars reticulata. II. Visual responses related to fixation of gaze." In: *Journal of Neurophysiology* 49 (5): pp. 1254–1267.

— (1983c). "Visual and oculomotor functions of monkey substantia nigra pars reticulata. III. Memory-contingent visual and saccade responses." In: *Journal of Neurophysiology* 49 (5): pp. 1268–1284.

Hille, B. (1992). "G protein-coupled mechanisms and nervous signaling". In: *Neuron* 9 (2): pp. 187–195.

Hinkle, K. M., Yue, M., Behrouz, B., Dächsel, J. C., Lincoln, S. J., Bowles, E. E., Beevers, J. E., Dugger, B., Winner, B., Prots, I., Kent, C. B., Nishioka, K., Lin, W.-L., Dickson, D. W., Janus, C. J., Farrer, M. J., and Melrose, H. L. (2012).

"LRRK2 knockout mice have an intact dopaminergic system but display alterations in exploratory and motor co-ordination behaviors". In: *Molecular Neurodegeneration* 7 (25).

Hirsch, E. C., Graybiel, A. M., and Agid, Y. A. (1988). "Melanized dopaminergic neurons are differentially susceptible to degeneration in Parkinson's disease". In: *Nature* 334 (6180): pp. 345–348.

— (1989). "Selective vulnerability of pigmented dopaminergic neurons in Parkinson's disease". In: *Acta Neurologica Scandinavica* 80 (s126): pp. 19–22.

Hoek, G. A. van der and Cooper, S. J. (1994). "The selective dopamine uptake inhibitor GBR 12909: Its effects on the microstructure of feeding in rats". In: *Pharmacology Biochemistry and Behavior* 48 (1): pp. 135–140.

Holland, P. C. (1984). "Unblocking in Pavlovian appetitive conditioning." In: *Journal of Experimental Psychology: Animal Behavior Processes* 10 (4): pp. 476–497.

Holt, G. R., Softky, W. R., Koch, C., and Douglas, R. J. (1996). "Comparison of discharge variability in vitro and in vivo in cat visual cortex neurons". In: *Journal of Neurophysiology* 75 (5): pp. 1806–1814.

Hoover, B. R. and Marshall, J. F. (2002). "Further characterization of preproenkephalin mRNA-containing cells in the rodent globus pallidus". In: *Neuroscience* 111 (1): pp. 111–125.

Hoover, B. R. and Marshall, J. F. (1999). "Population characteristics of preproenkephalin mRNA-containing neurons in the globus pallidus of the rat". In: *Neuroscience Letters* 265 (3): pp. 199–202.

Horvitz, J. C., Stewart, T., and Jacobs, B. L. (1997). "Burst activity of ventral tegmental dopamine neurons is elicited by sensory stimuli in the awake cat". In: *Brain Research* 759 (2): pp. 251–258.

Hosp, J. A., Nolan, H. E., and Luft, A. R. (2015). "Topography and collateralization of dopaminergic projections to primary motor cortex in rats." In: *Experimental Brain Research* 233 (5): pp. 1365–1375.

Howe, M. W. and Dombeck, D. A. (2016). "Rapid signalling in distinct dopaminergic axons during locomotion and reward". In: *Nature* 535: pp. 505–510.

Huang, Y., Zhang, L., Song, N.-N., Hu, Z.-L., Chen, J.-Y., and Ding, Y.-Q. (2011). "Distribution of Satb1 in the central nervous system of adult mice." In: *Neuroscience Research* 71 (1): pp. 12–21.

Huberman, A. D. and Niell, C. M. (2011). "What can mice tell us about how vision works?" In: *Trends in Neurosciences* 34 (9): pp. 464–473.

Hughes, A. J., Daniel, S. E., Kilford, L., and Lees, A. J. (1992). "Accuracy of clinical diagnosis of idiopathic Parkinson's disease: a clinico-pathological study of 100 cases." In: *Journal of Neurology, Neurosurgery, and Psychiatry* 55 (3): pp. 181–184.

Hyland, B. I., Reynolds, J. N. J., Hay, J., Perk, C. G., and Miller, R. (2002). "Firing modes of midbrain dopamine cells in the freely moving rat". In: *Neuroscience* 114 (2): pp. 475–492.

Hynes, M. A., Porter, J. A., Chiang, C., Chang, D., Tessier-Lavigne, M., Beachy, P. A., and Rosenthal, A. (1995). "Induction of midbrain dopaminergic neurons by Sonic hedgehog". In: *Neuron* 15 (1): pp. 35–44.

Hynes, M. A., Poulsen, K., Tessier-Lavigne, M., and Rosenthal, A. (1995). "Control of neuronal diversity by the floor plate: Contact-mediated induction of midbrain dopaminergic neurons". In: *Cell* 80 (1): pp. 95–101.

Hynes, M. A. and Rosenthal, A. (1999). "Specification of dopaminergic and serotonergic neurons in the vertebrate CNS". In: *Current Opinion in Neurobiology* 9 (1): pp. 26–36.

Iacopino, A. M., Christakos, S., German, D. C., Sonsalla, P. K., and Altar, C. A. (1992). "Calbindin-D28K-containing neurons in animal models of neurodegeneration: possible protection from excitotoxicity". In: *Molecular Brain Research* 13 (3): pp. 251–261.

Iacopino, A. M., Rhoten, W. B., and Christakos, S. (1990). "Calcium binding protein (calbindin-D28k) gene expression in the developing and aging mouse cerebellum". In: *Molecular Brain Research* 8 (4): pp. 283–290.

Ichimiya, Y., Emson, P. C., Mountjoy, C. Q., Lawson, D. E. M., and Heizmann, C. W. (1988). "Loss of calbindin-28K immunoreactive neurones from the cortex in Alzheimer-type dementia". In: *Brain Research* 475 (1): pp. 156–159.

Ikai, Y., Takada, M., and Mizuno, N. (1994). "Single neurons in the ventral tegmental area that project to both the cerebral and cerebellar cortical areas by way of axon collaterals". In: *Neuroscience* 61 (4): pp. 925–934.

Ikemoto, S. (2007). "Dopamine reward circuitry: Two projection systems from the ventral midbrain to the nucleus accumbens–olfactory tubercle complex". In: *Brain Research Reviews* 56 (1): pp. 27–78.

Ingham, C. A., Bolam, J. P., and Smith, A. D. (1988). "GABA-immunoreactive synaptic boutons in the rat basal forebrain: Comparison of neurons that project to the neocortex with pallidosubthalamic neurons". In: *The Journal of Comparative Neurology* 273 (2): pp. 263–282.

Isaacs, K. and Jacobowitz, D. (1994). "Mapping of the colocalization of calretinin and tyrosine hydroxylase in the rat substantia nigra and ventral tegmental area". In: *Experimental Brain Research* 99 (1): pp. 34–42.

Ison, J. R., Allen, P. D., and O'Neill, W. E. (2007). "Age-related hearing loss in C57BL/6J mice has both frequency-specific and non-frequency-specific components that produce a hyperacusis-like exaggeration of the acoustic startle reflex." In: *Journal of the Association for Research in Otolaryngology* 8 (4): pp. 539–550.

Jacobs, F. M. J., Smits, S. M., Noorlander, C. W., Oerthel, L. von, Linden, A. J. A. van der, Burbach, J. P. H., and Smidt, M. P. (2007). "Retinoic acid counteracts developmental defects in the substantia nigra caused by Pitx3 deficiency." In: *Development* 134 (14): pp. 2673–2684.

Jan, C., Francois, C., Tande, D., Yelnik, J., Tremblay, L., Agid, Y. A., and Hirsch, E. (2000). "Dopaminergic innervation of the pallidum in the normal state, in MPTP-treated monkeys and in parkinsonian patients". In: *European Journal of Neuroscience* 12 (12): pp. 4525–4535.

Jande, S. S., Maler, L., and Lawson, D. E. M. (1981). "Immunohistochemical mapping of vitamin D-dependent calcium-binding protein in brain". In: *Nature* 294 (5843): pp. 765–767.

Janezic, S., Threlfell, S., Dodson, P. D., Dowie, M. J., Taylor, T. N., Potgieter, D., Parkkinen, L., Senior, S. L., Anwar, S., Ryan, B., Deltheil, T., Kosillo, P., Cioroch, M., Wagner, K., Ansorge, O., Bannerman, D. M., Bolam, J. P., Magill, P. J., Cragg, S. J., and Wade-Martins, R. (2013). "Deficits in dopaminergic transmission precede neuron loss and dysfunction in a new Parkinson model". In: *Proceedings of the National Academy of Sciences* 110 (42): E4016–E4025.

Javitch, J. A., D'Amato, R. J., Strittmatter, S. M., and Snyder, S. H. (1985). "Parkinsonism-inducing neurotoxin, N-methyl-4-phenyl-1,2,3,6 -tetrahydropyridine:

uptake of the metabolite N-methyl-4-phenylpyridine by dopamine neurons explains selective toxicity." In: *Proceedings of the National Academy of Sciences* 82 (7): pp. 2173–2177.

Javitch, J. A. and Snyder, S. H. (1984). "Uptake of MPP(+) by dopamine neurons explains selectivity of parkinsonism-inducing neurotoxin, MPTP". In: *European Journal of Pharmacology* 106 (2): pp. 455–456.

Jeon, B. S., Jackson-Lewis, V., and Burke, R. E. (1995). "6-Hydroxydopamine Lesion of the Rat Substantia Nigra: Time Course and Morphology of Cell Death". In: *Neurodegeneration* 4 (2): pp. 131–137.

Ji, H. and Shepard, P. D. (2006). "SK Ca2+-activated K+ channel ligands alter the firing pattern of dopamine-containing neurons in vivo." In: *Neuroscience* 140 (2): pp. 623–633.

Jimenez-Castellanos, J. and Graybiel, A. M. (1987). "Subdivisions of the dopamine-containing A8-A9-A10 complex identified by their differential mesostriatal innervation of striosomes and extrastriosomal matrix". In: *Neuroscience* 23 (1): pp. 223–242.

Jin, X. and Costa, R. M. (2010). "Start/stop signals emerge in nigrostriatal circuits during sequence learning". In: *Nature* 466 (7305): pp. 457–462.

Joel, D. and Weiner, I. (2000). "The connections of the dopaminergic system with the striatum in rats and primates: an analysis with respect to the functional and compartmental organization of the striatum". In: *Neuroscience* 96 (3): pp. 451–474.

Johnson, S. W. and North, R. A. (1992). "Two types of neurone in the rat ventral tegmental area and their synaptic inputs." In: *The Journal of Physiology* 450 (1): pp. 455–468.

Johnson, S. W., Seutin, V., and North, R. A. (1992). "Burst firing in dopamine neurons induced by N-methyl-D-aspartate: role of electrogenic sodium pump." In: *Science* 258 (5082): pp. 665–667.

Juraska, J. M., Wilson, C. J., and Groves, P. M. (1977). "The substantia nigra of the rat: a Golgi study." In: *Journal of Comparative Neurology* 172 (4): pp. 585–600.

Kadkhodaei, B., Alvarsson, A., Schintu, N., Ramsköld, D., Volakakis, N., Joodmardi, E., Yoshitake, T., Kehr, J., Decressac, M., Björklund, A., Sandberg, R., Svenningsson, P., and Perlmann, T. (2013). "Transcription factor Nurr1 maintains fiber integrity and nuclear-encoded mitochondrial gene expression in dopamine neurons." In: *Proceedings of the National Academy of Sciences* 110 (6): pp. 2360–2365.

Kakade, S. and Dayan, P. (2002). "Dopamine: generalization and bonuses". In: *Neural Networks* 15 (4): pp. 549–559.

Kalivas, P., Churchill, L., and Klitenick, M. (1993). "GABA and enkephalin projection from the nucleus accumbens and ventral pallidum to the ventral tegmental area". In: *Neuroscience* 57 (4): pp. 1047–1060.

Kanazawa, I., Emson, P. C., and Cuello, A. C. (1977). "Evidence for the existence of substance P-containing fibres in striato-nigral and pallido-nigral pathways in rat brain". In: *Brain Research* 119 (2): pp. 447–453.

Kawaguchi, Y., Wilson, C. J., and Emson, P. C. (1990). "Projection subtypes of rat neostriatal matrix cells revealed by intracellular injection of biocytin". In: *Journal of Neuroscience* 10 (10): pp. 3421–3438.

Kawano, M., Kawasaki, A., Sakata-Haga, H., Fukui, Y., Kawano, H., Nogami, H., and Hisano, S. (2006). "Particular subpopulations of midbrain and hypothalamic

dopamine neurons express vesicular glutamate transporter 2 in the rat brain". In: *The Journal of Comparative Neurology* 498 (5): pp. 581–592.

Kelland, M. D., Chiodo, L. A., and Freeman, A. S. (1990). "Anesthetic influences on the basal acticity and pharmacological responsiveness of nigrostriatal dopamine neurons". In: *Synapse* 6 (2): pp. 207–209.

Kemp, J. M. and Powell, T. P. S. (1971). "The Structure of the Caudate Nucleus of the Cat: Light and Electron Microscopy". In: *Philosophical Transactions of the Royal Society of London B: Biological Sciences* 262 (845): pp. 383–401.

Khaliq, Z. M. and Bean, B. P. (2008). "Dynamic, Nonlinear Feedback Regulation of Slow Pacemaking by A-Type Potassium Current in Ventral Tegmental Area Neurons". In: *Journal of Neuroscience* 28 (43): pp. 10905–10917.

— (2010). "Pacemaking in Dopaminergic Ventral Tegmental Area Neurons: Depolarizing Drive from Background and Voltage-Dependent Sodium Conductances". In: *Journal of Neuroscience* 30 (21): pp. 7401–7413.

Khan, N. L., Jain, S., Lynch, J. M., Pavese, N., Abou-Sleiman, P., Holton, J. L., Healy, D. G., Gilks, W. P., Sweeney, M. G., Ganguly, M., Gibbons, V., Gandhi, S., Vaughan, J., Eunson, L. H., Katzenschlager, R., Gayton, J., Lennox, G., Revesz, T., Nicholl, D., Bhatia, K. P., Quinn, N., Brooks, D., Lees, A. J., Davis, M. B., Piccini, P., Singleton, A. B., and Wood, N. W. (2005). "Mutations in the gene LRRK2 encoding dardarin (PARK8) cause familial Parkinson's disease: clinical, pathological, olfactory and functional imaging and genetic data". In: *Brain* 128 (12): pp. 2786–2796.

Khan, S., Stott, S., Chabrat, A., Truckenbrodt, A. M., Spencer-Dene, B., Nave, K.-A., Guillemot, F., Levesque, M., and Ang, S.-L. (2017). "Survival of a novel subset of midbrain dopaminergic neurons projecting to the lateral septum is dependent on NeuroD proteins". In: *Journal of Neuroscience* 37 (9): pp. 2305–2316.

Kim, H. F., Ghazizadeh, A., and Hikosaka, O. (2015). "Dopamine Neurons Encoding Long-Term Memory of Object Value for Habitual Behavior". In: *Cell* 163 (5): pp. 1165–1175.

Kim, J.-I., Ganesan, S., Luo, S. X., Wu, Y.-W., Park, E., Huang, E. J., Chen, L. L., and Ding, J. B. (2015). "Aldehyde dehydrogenase 1a1 mediates a GABA synthesis pathway in midbrain dopaminergic neurons." In: *Science* 350 (6256): pp. 102–106.

Kincaid, A. E., Penney, J. B., Young, A. B., and Newman, S. W. (1991). "Evidence for a projection from the globus pallidus to the entopeduncular nucleus in the rat". In: *Neuroscience Letters* 128 (1): pp. 121–125.

King, J. A., Garelick, T. S., Brevard, M. E., Chen, W., Messenger, T. L., Duong, T. Q., and Ferris, C. F. (2005). "Procedure for minimizing stress for fMRI studies in conscious rats". In: *Journal of Neuroscience Methods* 148 (2): pp. 154–160.

Kita, H. (2007). "Globus pallidus external segment". In: *GABA and the Basal Ganglia: From Molecules to Systems*. Ed. by Tepper, J. M., Abercrombie, E. D., and Bolam, J. P. Vol. 160. Amsterdam; Oxford: Elsevier, pp. 111–133.

Kita, H. and Kita, T. (2001). "Number, origins, and chemical types of rat pallidostriatal projection neurons". In: *The Journal of Comparative Neurology* 437 (4): pp. 438–448.

Kita, H. and Kitai, S. T. (1987). "Efferent projections of the subthalamic nucleus in the rat: Light and electron microscopic analysis with the PHA-L method". In: *The Journal of Comparative Neurology* 260 (3): pp. 435–452.

— (1988). "Glutamate decarboxylase immunoreactive neurons in rat neostriatum: their morphological types and populations". In: *Brain Research* 447 (2): pp. 346–352.

Kita, H. and Kitai, S. T. (1994). "The morphology of globus pallidus projection neurons in the rat: an intracellular staining study". In: *Brain Research* 636 (2): pp. 308–319.

Kita, T., Kita, H., and Kitai, S. T. (1986). "Electrical membrane properties of rat substantia nigra compacta neurons in an in vitro slice preparation". In: *Brain Research* 372 (1): pp. 21–30.

Kittappa, R., Chang, W. W., Awatramani, R. B., and McKay, R. D. G. (2007). "The foxa2 gene controls the birth and spontaneous degeneration of dopamine neurons in old age." In: *PLoS biology* 5 (12): e325.

Kiyama, H., Seto-Ohshima, A., and Emson, P. (1990). "Calbindin D28K as a marker for the degeneration of the striatonigral pathway in Huntington's disease". In: *Brain Research* 525 (2): pp. 209–214.

Ko, D., Wilson, C. J., Lobb, C. J., and Paladini, C. A. (2012). "Detection of bursts and pauses in spike trains." In: *Journal of Neuroscience Methods* 211 (1): pp. 145–158.

Kobayashi, S. and Schultz, W. (2014). "Reward contexts extend dopamine signals to unrewarded stimuli." In: *Current Biology* 24 (1): pp. 56–62.

Kobinger, W. and Pichler, L. (1983). "$\alpha 1\alpha 2$ selectivity ratio in a series of agonists and their relation to pre/postsynaptic activity ratios". In: *European Journal of Pharmacology* 91 (1): pp. 129–133.

Kofuji, P., Davidson, N., and Lester, H. A. (1995). "Evidence that neuronal G-protein-gated inwardly rectifying K+ channels are activated by G beta gamma subunits and function as heteromultimers." In: *Proceedings of the National Academy of Sciences* 92 (14): pp. 6542–6546.

Kohrs, R. and Durieux, M. E. (1998). "Ketamine: Teaching an old drug new tricks". In: *Anesthesia & Analgesia* 87 (5): pp. 1186–1193.

Koob, G. F. and Bloom, F. E. (1988). "Cellular and molecular mechanisms of drug dependence." In: *Science* 242 (4879): pp. 715–723.

Kosobud, A., Harris, G., and Chapin, J. (1994). "Behavioral associations of neuronal activity in the ventral tegmental area of the rat". In: *Journal of Neuroscience* 14 (11): pp. 7117–7129.

Kraeuchi, K., Rudolph, K., Wirz-Justice, A., and Feer, H. (1985). "Similarities in feeding behavior of chronic methamphetamine treated and withdrawn rats to VMH lesioned rats". In: *Pharmacology Biochemistry and Behavior* 23 (6): pp. 917–920.

Krüger, R., Kuhn, W., Müller, T., Woitalla, D., Graeber, M., Kösel, S., Przuntek, H., Epplen, J. T., Schols, L., and Riess, O. (1998). "AlaSOPro mutation in the gene encoding α-synuclein in Parkinson's disease". In: *Nature Genetics* 18 (2): pp. 106–108.

Kuo, D.-Y. (2002). "Co-administration of dopamine D1 and D2 agonists additively decreases daily food intake, body weight and hypothalamic neuropeptide Y level in rats". In: *Journal of Biomedical Science* 9 (2): pp. 126–132.

Kupchik, Y. M., Brown, R. M., Heinsbroek, J. A., Lobo, M. K., Schwartz, D. J., and Kalivas, P. W. (2015). "Coding the direct/indirect pathways by D1 and D2 receptors is not valid for accumbens projections." In: *Nature Neuroscience* 18 (9): pp. 1230–1232.

La Manno, G., Gyllborg, D., Codeluppi, S., Nishimura, K., Salto, C., Zeisel, A., Borm, L. E., Stott, S. R. W., Toledo, E. M., Villaescusa, J. C., Lönnerberg, P., Ryge, J., Barker, R. A., Arenas, E., and Linnarsson, S. (2016). "Molecular Diversity of Midbrain Development in Mouse, Human, and Stem Cells." In: *Cell* 167 (2): 566–580.e19.

Lammel, S., Hetzel, A., Häckel, O., Jones, I., Liss, B., and Roeper, J. (2008). "Unique properties of mesoprefrontal neurons within a dual mesocorticolimbic dopamine system." In: *Neuron* 57 (5): pp. 760–773.

Lanciego, J. L., Gonzalo, N., Castle, M., Sanchez-Escobar, C., Aymerich, M. S., and Obeso, J. A. (2004). "Thalamic innervation of striatal and subthalamic neurons projecting to the rat entopeduncular nucleus". In: *European Journal of Neuroscience* 19 (5): pp. 1267–1277.

Langer, L. F. and Graybiel, A. M. (1989). "Distinct nigrostriatal projection systems innervate striosomes and matrix in the primate striatum". In: *Brain Research* 498 (2): pp. 344–350.

Langston, J. W., Ballard, P., Tetrud, J. W., and Irwin, I. (1983). "Chronic Parkinsonism in humans due to a product of meperidine-analog synthesis." In: *Science* 219 (4587): pp. 979–980.

Langston, J. W., Forno, L. S., Tetrud, J., Reeves, A. G., Kaplan, J. A., and Karluk, D. (1999). "Evidence of active nerve cell degeneration in the substantia nigra of humans years after 1-methyl-4-phenyl-1,2,3,6-tetrahydropyridine exposure". In: *Annals of Neurology* 46 (4): pp. 598–605.

Lantz, K. A., Vatamaniuk, M. Z., Brestelli, J. E., Friedman, J. R., Matschinsky, F. M., and Kaestner, K. H. (2004). "Foxa2 regulates multiple pathways of insulin secretion." In: *The Journal of Clinical Investigation* 114 (4): pp. 512–520.

Lau, L. M. de and Breteler, M. M. (2006). "Epidemiology of Parkinson's disease". In: *The Lancet Neurology* 5 (6): pp. 525–535.

Lavoie, B. and Parent, A. (1991). "Dopaminergic neurons expressing calbindin in normal and parkinsonian monkeys." In: *NeuroReport* 2 (10): pp. 601–604.

Lavoie, B., Smith, Y., and Parent, A. (1989). "Dopaminergic innervation of the basal ganglia in the squirrel monkey as revealed by tyrosine hydroxylase immunohistochemistry". In: *The Journal of Comparative Neurology* 289 (1): pp. 36–52.

Le Moine, C., Normand, E., and Bloch, B. (1991). "Phenotypical characterization of the rat striatal neurons expressing the D1 dopamine receptor gene." In: *Proceedings of the National Academy of Sciences* 88 (10): pp. 4205–4209.

Le Moine, C., Normand, E., Guitteny, A. F., Fouque, B., Teoule, R., and Bloch, B. (1990). "Dopamine receptor gene expression by enkephalin neurons in rat forebrain." In: *Proceedings of the National Academy of Sciences* 87: pp. 230–234.

Lee, J.-W., Tapias, V., Di Maio, R., Greenamyre, J. T., and Cannon, J. R. (2014). "Behavioral, neurochemical, and pathologic alterations in bacterial artificial chromosome transgenic G2019S leucine-rich repeated kinase 2 rats." In: *Neurobiology of Aging* 36 (1): pp. 505–518.

Legéndy, C. R. and Salcman, M. (1985). "Bursts and recurrences of bursts in the spike trains of spontaneously active striate cortex neurons." In: *Journal of Neurophysiology* 53 (4): pp. 926–939.

Lerner, T. N., Shilyansky, C., Davidson, T. J., Evans, K. E., Beier, K. T., Zalocusky, K. A., Crow, A. K., Malenka, R. C., Luo, L., Tomer, R., and Deisseroth, K. (2015). "Intact-Brain Analyses Reveal Distinct Information Carried by SNc Dopamine Subcircuits". In: *Cell* 162 (3): pp. 635–647.

Lesage, S., Dürr, A., Tazir, M., Lohmann, E., Leutenegger, A.-L., Janin, S., Pollak, P., and Brice, A. (2006). "LRRK2 G2019S as a Cause of Parkinson's Disease in North African Arabs". In: *New England Journal of Medicine* 354 (4): pp. 422–423.

Lévesque, M. and Parent, A. (2005). "The striatofugal fiber system in primates: a reevaluation of its organization based on single-axon tracing studies." In: *Proceedings of the National Academy of Sciences* 102 (33): pp. 11888–11893.

Li, X., Patel, J. C., Wang, J., Avshalumov, M. V., Nicholson, C., Buxbaum, J. D., Elder, G. A., Rice, M. E., and Yue, Z. (2010). "Enhanced Striatal Dopamine Transmission and Motor Performance with LRRK2 Overexpression in Mice Is Eliminated by Familial Parkinson's Disease Mutation G2019S". In: *Journal of Neuroscience* 30 (5): pp. 1788–1797.

Li, X., Qi, J., Yamaguchi, T., Wang, H.-L., and Morales, M. (2013). "Heterogeneous composition of dopamine neurons of the rat A10 region: molecular evidence for diverse signaling properties." In: *Brain Structure & Function* 218 (5): pp. 1159–1176.

Li, Y., Liu, W., Oo, T. F., Wang, L., Tang, Y., Jackson-Lewis, V., Zhou, C., Geghman, K., Bogdanov, M., Przedborski, S., Beal, M. F., Burke, R. E., and Li, C. (2009). "Mutant LRRK2(R1441G) BAC transgenic mice recapitulate cardinal features of Parkinson's disease." In: *Nature Neuroscience* 12 (7): pp. 826–828.

Liang, C.-L., Sinton, C. M., Sonsalla, P. K., and German, D. C. (1996). "Midbrain Dopaminergic Neurons in the Mouse that Contain Calbindin-D28k Exhibit Reduced Vulnerability to MPTP-induced Neurodegeneration". In: *Neurodegeneration* 5 (4): pp. 313–318.

Liang, C.-L., Sinton, C. M., and German, D. C. (1996). "Midbrain dopaminergic neurons in the mouse: co-localization with Calbindin-D28k and calretinin". In: *Neuroscience* 75 (2): pp. 523–533.

Ligmond, M. J. and Stricker, E. M. (1972). "Deficits in Feeding Behavior after Intraventricular Injection of 6-Hydroxydopamine in Rats". In: *Science* 177 (4055): pp. 1211–1214.

Lin, X., Parisiadou, L., Gu, X.-L., Wang, L., Shim, H., Sun, L., Xie, C., Long, C.-X., Yang, W.-J., Ding, J., Chen, Z. Z., Gallant, P. E., Tao-Cheng, J.-H., Rudow, G., Troncoso, J. C., Liu, Z., Li, Z., and Cai, H. (2009). "Leucine-rich repeat kinase 2 regulates the progression of neuropathology induced by Parkinson's-disease-related mutant alpha-synuclein." In: *Neuron* 64 (6): pp. 807–827.

Lindvall, O. and Björklund, A. (1979). "Dopaminergic innervation of the globus pallidus by collaterals from the nigrostriatal pathway". In: *Brain Research* 172 (1): pp. 169–173.

Lindvall, O., Björklund, A., Moore, R. Y., and Stenevi, U. (1974). "Mesencephalic dopamine neurons projecting to neocortex". In: *Brain Research* 81 (2): pp. 325–331.

Liss, B., Haeckel, O., Wildmann, J., Miki, T., Seino, S., and Roeper, J. (2005). "K-ATP channels promote the differential degeneration of dopaminergic midbrain neurons". In: *Nature Neuroscience* 8 (12): pp. 1742–1751.

Liss, B. and Roeper, J. (2010). "Ion channels and regulation of dopamine neuron activtiy". In: *Dopamine Handbook*. Ed. by Iversen, L. L., Iversen, S. D., Dunnett, S. B., and Björklund, A. 4th ed. New York: Oxford University Press, pp. 118–138.

Liu, G., Yu, J., Ding, J., Xie, C., Sun, L., Rudenko, I., Zheng, W., Sastry, N., Luo, J., Rudow, G., Troncoso, J. C., and Cai, H. (2014). "Aldehyde dehydrogenase 1 defines and protects a nigrostriatal dopaminergic neuron subpopulation." In: *The Journal of Clinical Investigation* 124 (7): pp. 3032–3046.

Liu, H.-F., Lu, S., Ho, P. W.-L., Tse, H.-M., Pang, S. Y.-Y., Kung, M. H.-W., Ho, J. W.-M., Ramsden, D. B., Zhou, Z.-J., and Ho, S.-L. (2014). "LRRK2 R1441G

mice are more liable to dopamine depletion and locomotor inactivity". In: *Annals of Clinical and Translational Neurology* 1 (3): pp. 199–208.

Ljungberg, T., Apicella, P., and Schultz, W. (1992). "Responses of monkey dopamine neurons during learning of behavioral reactions". In: *Journal of Neurophysiology* 67 (1): pp. 145–163.

Lobb, C. (2014). "Abnormal bursting as a pathophysiological mechanism in Parkinson's disease." In: *Basal Ganglia* 3 (4): pp. 187–195.

Lobo, M. K., Cui, Y., Ostlund, S. B., Balleine, B. W., and William Yang, X. (2007). "Genetic control of instrumental conditioning by striatopallidal neuron–specific S1P receptor Gpr6". In: *Nature Neuroscience* 10 (11): pp. 1395–1397.

Lodge, D. J. and Grace, A. A. (2006a). "The laterodorsal tegmentum is essential for burst firing of ventral tegmental area dopamine neurons." In: *Proceedings of the National Academy of Sciences* 103 (13): pp. 5167–5172.

Lodge, D. J. and Grace, A. A. (2006b). "The Hippocampus Modulates Dopamine Neuron Responsivity by Regulating the Intensity of Phasic Neuron Activation". In: *Neuropsychopharmacology* 31 (7): pp. 1356–1361.

Lokwan, S. J. A., Overton, P. G., Berry, M. S., and Clark, D. (1999). "Stimulation of the pedunculopontine tegmental nucleus in the rat produces burst firing in A9 dopaminergic neurons". In: *Neuroscience* 92 (1): pp. 245–254.

Longo, F., Russo, I., Shimshek, D. R., Greggio, E., and Morari, M. (2014). "Genetic and pharmacological evidence that G2019S LRRK2 confers a hyperkinetic phenotype, resistant to motor decline associated with aging." In: *Neurobiology of Disease* 71: pp. 62–73.

Loughlin, S. E. and Fallon, J. H. (1983). "Dopaminergic and non-dopaminergic projections to amygdala from substantia nigra and ventral tegmental area". In: *Brain Research* 262 (2): pp. 334–338.

— (1984). "Substantia nigra and ventral tegmental area projections to cortex: Topography and collateralization". In: *Neuroscience* 11 (2): pp. 425–435.

Luo, L., Callaway, E. M., and Svoboda, K. (2008). "Genetic Dissection of Neural Circuits". In: *Neuron* 57 (5): pp. 634–660.

Luppi, P.-H., Fort, P., and Jouvet, M. (1990). "Iontophoretic application of unconjugated cholera toxin B subunit (CTb) combined with immunohistochemistry of neurochemical substances: a method for transmitter identification of retrogradely labeled neurons". In: *Brain Research* 534 (1-2): pp. 209–224.

Luthman, J., Fredriksson, A., Sundström, E., Jonsson, G., and Archer, T. (1989). "Selective lesion of central dopamine or noradrenaline neuron systems in the neonatal rat: motor behavior and monoamine alterations at adult stage." In: *Behavioural Brain Research* 33 (3): pp. 267–277.

Macchi, G., Bentivoglio, M., Molinari, M., and Minciacchi, D. (1984). "The thalamo-caudate versus thalamo-cortical projections as studied in the cat with fluorescent retrograde double labeling". In: *Experimental Brain Research* 54 (2): pp. 225–239.

Macchi, G. and Bentivoglio, M. (1986). "The Thalamic Intralaminar Nuclei and the Cerebral Cortex". In: *Cerebral Cortex*. Ed. by Jones, E. G. and Peters, A. New York; London: Springer US, pp. 355–401.

MacDonald, J. F. and Nowak, L. M. (1990). "Mechanisms of blockade of excitatory amino acid receptor channels". In: *Trends in Pharmacological Sciences* 11 (4): pp. 167–172.

Madisen, L., Garner, A. R., Shimaoka, D., Chuong, A. S., Klapoetke, N. C., Li, L., Bourg, A. van der, Niino, Y., Egolf, L., Monetti, C., Gu, H., Mills, M., Cheng, A., Tasic, B., Nguyen, T. N., Sunkin, S. M., Benucci, A., Nagy, A., Miyawaki, A., Helmchen, F., Empson, R. M., Knöpfel, T., Boyden, E. S., Reid, R. C., Carandini, M., and Zeng, H. (2015). "Transgenic Mice for Intersectional Targeting of Neural Sensors and Effectors with High Specificity and Performance". In: *Neuron* 85 (5): pp. 942–958.

Maekawa, T., Mori, S., Sasaki, Y., Miyajima, T., Azuma, S., Ohta, E., and Obata, F. (2012). "The I2020T Leucine-rich repeat kinase 2 transgenic mouse exhibits impaired locomotive ability accompanied by dopaminergic neuron abnormalities." In: *Molecular Neurodegeneration* 7 (15).

Magerkurth, C., Schnitzer, R., and Braune, S. (2005). "Symptoms of autonomic failure in Parkinson's disease: prevalence and impact on daily life". In: *Clinical Autonomic Research* 15 (2): pp. 76–82.

Magill, P. J., Bolam, J. P., and Bevan, M. D. (2000). "Relationship of Activity in the Subthalamic Nucleus–Globus Pallidus Network to Cortical Electroencephalogram". In: *Journal of Neuroscience* 20 (2): pp. 820–833.

— (2001). "Dopamine regulates the impact of the cerebral cortex on the subthalamic nucleus–globus pallidus network". In: *Neuroscience* 106 (2): pp. 313–330.

Mailly, P., Charpier, S., Menetrey, A., and Deniau, J. M. (2003). "Three-dimensional organization of the recurrent axon collateral network of the substantia nigra pars reticulata neurons in the rat". In: *Journal of Neuroscience* 23 (12): pp. 5347–5257.

Mallet, N., Micklem, B. R., Henny, P., Brown, M. T. C., Williams, C., Bolam, J. P., Nakamura, K. C., and Magill, P. J. (2012). "Dichotomous Organization of the External Globus Pallidus". In: *Neuron* 74 (6): pp. 1075–1086.

Mallet, N., Pogosyan, A., Márton, L. F., Bolam, J. P., Brown, P., and Magill, P. J. (2008). "Parkinsonian Beta Oscillations in the External Globus Pallidus and Their Relationship with Subthalamic Nucleus Activity". In: *Journal of Neuroscience* 28 (52): pp. 14245–14258.

Mandairon, N., Sultan, S., Rey, N., Kermen, F., Moreno, M., Busto, G., Farget, V., Messaoudi, B., Thevenet, M., and Didier, A. (2009). "A computer-assisted odorized hole-board for testing olfactory perception in mice." In: *Journal of Neuroscience Methods* 180 (2): pp. 296–303.

Mandel, S. A., Fishman, T., and Youdim, M. B. (2007). "Gene and protein signatures in sporadic Parkinson's disease and a novel genetic model of PD". In: *Parkinsonism & Related Disorders* 13 (Suppl 3): S242–S247.

Marchitti, S. A., Deitrich, R. A., and Vasiliou, V. (2007). "Neurotoxicity and Metabolism of the Catecholamine-Derived 3,4-Dihydroxyphenylacetaldehyde and 3,4-Dihydroxyphenylglycolaldehyde: The Role of Aldehyde Dehydrogenase". In: *Pharmacological Reviews* 59 (2): pp. 125–150.

Markopoulou, K., Larsen, K. W., Wszolek, E. K., Denson, M. A., Lang, A. E., Pfeiffer, R. F., and Wszolek, Z. K. (1997). "Olfactory dysfunction in familial parkinsonism." In: *Neurology* 49 (5): pp. 1262–1267.

Marras, C., Schuele, B., Munhoz, R., Rogaeva, E., Langston, J., Kasten, M., Meaney, C., Klein, C., Wadia, P., Lim, S.-Y., Chuang, R.-I., Zadikof, C., Steeves, T., Prakash, K., Bie, R. de, Adeli, G., Thomsen, T., Johansen, K., Teive, H., Asante, A., Reginold, W., and Lang, A. (2011). "Phenotype in parkinsonian and nonparkinsonian LRRK2 G2019S mutation carriers". In: *Neurology* 77 (4): pp. 325–333.

Matsuda, W., Furuta, T., Nakamura, K. C., Hioki, H., Fujiyama, F., Arai, R., and Kaneko, T. (2009). "Single nigrostriatal dopaminergic neurons form widely spread and highly dense axonal arborizations in the neostriatum." In: *Journal of Neuroscience* 29 (2): pp. 444–453.

Matsumoto, H., Tian, J., Uchida, N., and Watabe-Uchida, M. (2016). "Midbrain dopamine neurons signal aversion in a reward-context-dependent manner." In: *eLife* 5: e17328.

Matsumoto, M. and Hikosaka, O. (2009). "Two types of dopamine neuron distinctly convey positive and negative motivational signals." In: *Nature* 459 (7248): pp. 837–841.

Matsumoto, M. and Takada, M. (2013). "Distinct representations of cognitive and motivational signals in midbrain dopamine neurons." In: *Neuron* 79 (5): pp. 1011–1024.

Mattiace, L., Baring, M., Manaye, K., Mihailoff, G., and German, D. C. (1989). "Mesostriatal projections in BALB/c and CBA mice: A quantitative retrograde neuroanatomical tracing study". In: *Brain Research Bulletin* 23 (1-2): pp. 61–68.

Mavromatakis, Y. E., Lin, W., Metzakopian, E., Ferri, A. L. M., Yan, C. H., Sasaki, H., Whisett, J., and Ang, S.-L. (2011). "Foxa1 and Foxa2 positively and negatively regulate Shh signalling to specify ventral midbrain progenitor identity." In: *Mechanisms of Development* 128 (1-2): pp. 90–103.

Maxwell, S. L., Ho, H.-Y., Kuehner, E., Zhao, S., and Li, M. (2005). "Pitx3 regulates tyrosine hydroxylase expression in the substantia nigra and identifies a subgroup of mesencephalic dopaminergic progenitor neurons during mouse development". In: *Developmental Biology* 282 (2): pp. 467–479.

McCaffery, P. and Dräger, U. C. (1994). "High levels of a retinoic acid-generating dehydrogenase in the meso-telencephalic dopamine system." In: *Proceedings of the National Academy of Sciences* 91 (16): pp. 7772–7776.

McFarland, N. R. and Haber, S. N. (2000). "Convergent inputs from thalamic motor nuclei and frontal cortical areas to the dorsal striatum in the primate." In: *Journal of Neuroscience* 20 (10): pp. 3798–3813.

McGeer, P. L., McGeer, E. G., and Suzuki, J. S. (1977). "Aging and extrapyramidal function." In: *Archives of Neurology* 34 (1): pp. 33–35.

McRitchie, D., Cartwright, H., and Halliday, G. (1997). "Specific A10 Dopaminergic Nuclei in the Midbrain Degenerate in Parkinson's Disease". In: *Experimental Neurology* 144 (1): pp. 202–213.

Meibach, R. C. and Katzman, R. (1979). "Catecholaminergic innervation of the subthalamic nucleus: evidence for a rostral continuation of the A9 (substantia nigra) dopaminergic cell group". In: *Brain Research* 173 (2): pp. 364–368.

Melrose, H. L., Dächsel, J. C., Behrouz, B., Lincoln, S. J., Yue, M., Hinkle, K. M., Kent, C. B., Korvatska, E., Taylor, J. P., Witten, L., Liang, Y.-Q., Beevers, J. E., Boules, M., Dugger, B. N., Serna, V. A., Gaukhman, A., Yu, X., Castanedes-Casey, M., Braithwaite, A. T., Ogholikhan, S., Yu, N., Bass, D., Tyndall, G., Schellenberg, G. D., Dickson, D. W., Janus, C., and Farrer, M. J. (2010). "Impaired dopaminergic neurotransmission and microtubule-associated protein tau alterations in human LRRK2 transgenic mice." In: *Neurobiology of Disease* 40 (3): pp. 503–517.

Mena-Segovia, J., Winn, P., and Bolam, J. P. (2008). "Cholinergic modulation of midbrain dopaminergic systems". In: *Brain Research Reviews* 58 (2): pp. 265–271.

Mendez, I., Sanchez-Pernaute, R., Cooper, O., Viñuela, A., Ferrari, D., Björklund, L., Dagher, A., and Isacson, O. (2005). "Cell type analysis of functional fetal dopamine cell suspension transplants in the striatum and substantia nigra of patients with Parkinson's disease". In: *Brain* 128 (7): pp. 1498–1510.

Menegas, W., Babayan, B. M., Uchida, N., and Watabe-Uchida, M. (2017). "Opposite initialization to novel cues in dopamine signaling in ventral and posterior striatum in mice". In: *eLife* 6: e21886.

Menegas, W., Bergan, J. F., Ogawa, S. K., Isogai, Y., Umadevi Venkataraju, K., Osten, P., Uchida, N., and Watabe-Uchida, M. (2015). "Dopamine neurons projecting to the posterior striatum form an anatomically distinct subclass." In: *eLife* 4: e10032.

Metzakopian, E., Lin, W., Salmon-Divon, M., Dvinge, H., Andersson, E., Ericson, J., Perlmann, T., Whitsett, J. A., Bertone, P., and Ang, S.-L. (2012). "Genome-wide characterization of Foxa2 targets reveals upregulation of floor plate genes and repression of ventrolateral genes in midbrain dopaminergic progenitors." In: *Development* 139 (14): pp. 2625–2634.

Miller, J. D., Sanghera, M. K., and German, D. C. (1981). "Mesencephalic dopaminergic unit activity in the behaviorally conditioned rat". In: *Life Sciences* 29 (12): pp. 1255–1263.

Mingazzini, G. (1888). *Sulla Fine Struttura Della Substantia Nfigra Sömmeringii*. Vol. 5. Rome, pp. 36–40.

Mink, J. W. and Thach, W. T. (1991). "Basal ganglia motor control. I. Nonexclusive relation of pallidal discharge to five movement modes." In: *Journal of Neurophysiology* 65 (2): pp. 273–300.

Mirenowicz, J. and Schultz, W. (1994). "Importance of unpredictability for reward responses in primate dopamine neurons". In: *Journal of Neurophysiology* 72 (2): pp. 1024–1027.

Mirenowicz, J. and Schultz, W. (1996). "Preferential activation of midbrain dopamine neurons by appetitive rather than aversive stimuli." In: *Nature* 379 (6564): pp. 449–451.

Mizuma, H., Shukuri, M., Hayashi, T., Watanabe, Y., and Onoe, H. (2010). "Establishment of in vivo brain imaging method in conscious mice." In: *Journal of Nuclear Medicine* 51 (7): pp. 1068–1075.

Mizuno, Y., Sone, N., and Saitoh, T. (1987). "Effects of 1-methyl-4-phenyl-1,2,3,6-tetrahydropyridine and 1-methyl-4-phenylpyridinium ion on activities of the enzymes in the electron transport system in mouse brain." In: *Journal of Neurochemistry* 48 (6): pp. 1787–1793.

Monakow, K. H., Akert, K., and Kunzle, H. (1978). "Projections of the precentral motor cortex and other cortical areas of the frontal lobe to the subthalamic nucleus in the monkey". In: *Experimental Brain Research* 33 (3): pp. 395–403.

Moore, R. Y. (1978). "Catecholamine innervation of the basal forebrain. I. The septal area". In: *The Journal of Comparative Neurology* 177 (4): pp. 665–683.

Moore, R. Y. and Bloom, F. E. (1979). "Central Catecholamine Neuron Systems: Anatomy and Physiology of the Norepinephrine and Epinephrine Systems". In: *Annual Review of Neuroscience* 2 (1): pp. 113–168.

Morales, M. and Margolis, E. B. (2017). "Ventral tegmental area: cellular heterogeneity, connectivity and behaviour". In: *Nature Reviews Neuroscience* 18 (2): pp. 73–85.

Moriizumi, T., Nakamura, Y., Okoyama, S., and Kitao, Y. (1987). "Synaptic organization of the cat entopeduncular nucleus with special reference to the relationship between

the afferents to entopedunculothalamic projection neurons: An electron microscope study by a combined degeneration and horseradish peroxidase tracin". In: *Neuroscience* 20 (3): pp. 797–816.

Morikawa, H. and Paladini, C. A. (2011). "Dynamic regulation of midbrain dopamine neuron activity: intrinsic, synaptic, and plasticity mechanisms." In: *Neuroscience* 198: pp. 95–111.

Morley, J. E. and Flood, J. F. (1987). "An investigation of tolerance to the actions of leptogenic and anorexigenic drugs in mice". In: *Life Sciences* 41 (18): pp. 2157–2165.

Morris, G., Nevet, A., Arkadir, D., Vaadia, E., and Bergman, H. (2006). "Midbrain dopamine neurons encode decisions for future action". In: *Nature Neuroscience* 9 (8): pp. 1057–1063.

Mroz, E. A., Brownstein, M. J., and Leeman, S. E. (1977). "Evidence for substance P in the striato-nigral tract". In: *Brain Research* 125 (2): pp. 305–311.

Nair-Roberts, R., Chatelain-Badie, S., Benson, E., White-Cooper, H., Bolam, J. P., and Ungless, M. (2008). "Stereological estimates of dopaminergic, GABAergic and glutamatergic neurons in the ventral tegmental area, substantia nigra and retrorubral field in the rat". In: *Neuroscience* 152 (4): pp. 1024–1031.

Nalls, M. A., Pankratz, N., Lill, C. M., Do, C. B., Hernandez, D. G., Saad, M., DeStefano, A. L., Kara, E., Bras, J., Sharma, M., Schulte, C., Keller, M. F., Arepalli, S., Letson, C., Edsall, C., Stefansson, H., Liu, X., Pliner, H., Lee, J. H., Cheng, R., Ikram, M. A., Ioannidis, J. P. A., Hadjigeorgiou, G. M., Bis, J. C., Martinez, M., Perlmutter, J. S., Goate, A., Marder, K., Fiske, B., Sutherland, M., Xiromerisiou, G., Myers, R. H., Clark, L. N., Stefansson, K., Hardy, J. A., Heutink, P., Chen, H., Wood, N. W., Houlden, H., Payami, H., Brice, A., Scott, W. K., Gasser, T., Bertram, L., Eriksson, N., Foroud, T., Singleton, A. B., Heutink, P., Chen, H., Wood, N. W., Houlden, H., Payami, H., Brice, A., Scott, W. K., Gasser, T., Bertram, L., Eriksson, N., Foroud, T., and Singleton, A. B. (2014). "Large-scale meta-analysis of genome-wide association data identifies six new risk loci for Parkinson's disease". In: *Nature Genetics* 46 (9): pp. 989–993.

Nambu, A., Takada, M., Inase, M., and Tokuno, H. (1996). "Dual somatotopical representations in the primate subthalamic nucleus: evidence for ordered but reversed body-map transformations from the primary motor cortex and the supplementary motor area". In: *Journal of Neuroscience* 16 (8): pp. 2671–2683.

Nambu, A., Tokuno, H., Hamada, I., Kita, H., Imanishi, M., Akazawa, T., Ikeuchi, Y., and Hasegawa, N. (2000). "Excitatory cortical inputs to pallidal neurons via the subthalamic nucleus in the monkey." In: *Journal of Neurophysiology* 84 (1): pp. 289–300.

Nambu, A., Tokuno, H., and Takada, M. (2002). "Functional significance of the cortico–subthalamo–pallidal 'hyperdirect' pathway". In: *Neuroscience Research* 43 (2): pp. 111–117.

Al-Naser, H. A. and Cooper, S. J. (1994). "A-68930, a novel potent dopamine D1 receptor agonist: a microstructural analysis of its effects on feeding and other behaviour in the rat". In: *Behavioural Pharmacology* 5 (2): pp. 210–218.

Nedergaard, S., Bolam, J. P., and Greenfield, S. A. (1988). "Facilitation of a dendritic calcium conductance by 5-hydroxytryptamine in the substantia nigra". In: *Nature* 333 (6169): pp. 174–177.

Nelson, E. L., Liang, C.-L., Sinton, C. M., and German, D. C. (1996). "Midbrain dopaminergic neurons in the mouse: computer-assisted mapping." In: *Journal of Comparative Neurology* 369 (3): pp. 361–371.

Nemoto, C., Hida, T., and Arai, R. (1999). "Calretinin and calbindin-D28k in dopaminergic neurons of the rat midbrain: a triple-labeling immunohistochemical study". In: *Brain Research* 846 (1): pp. 129–136.

Nicoll, R. A. and Madison, D. V. (1982). "General anesthetics hyperpolarize neurons in the vertebrate central nervous system." In: *Science* 217 (4564): pp. 1055–1057.

Nieoullon, A., Cheramy, A., and Glowinski, J. (1977). "Nigral and striatal dopamine release under sensory stimuli". In: *Nature* 269 (5626): pp. 340–342.

Nissbrandt, H., Elverfors, A., and Engberg, G. (1994). "Pharmacologically induced cessation of burst activity in nigral dopamine neurons: Significance for the terminal dopamine efflux". In: *Synapse* 17 (4): pp. 217–224.

Nitsch, C. and Riesenberg, R. (1988). "Immunocytochemical demonstration of GABAergic synaptic connections in rat substantia nigra after different lesions of the striatonigral projection". In: *Brain Research* 461 (1): pp. 127–142.

Oades, R. and Halliday, G. (1987). "Ventral tegmental (A10) system: neurobiology. 1. Anatomy and connectivity". In: *Brain Research Reviews* 12 (2): pp. 117–165.

Oertel, W. and Mugnaini, E. (1984). "Immunocytochemical studies of GABAergic neurons in rat basal ganglia and their relations to other neuronal systems". In: *Neuroscience Letters* 47 (3): pp. 233–238.

Ogawa, S. K., Cohen, J. Y., Hwang, D., Uchida, N., and Watabe-Uchida, M. (2014). "Organization of Monosynaptic Inputs to the Serotonin and Dopamine Neuromodulatory Systems". In: *Cell Reports* 8 (4): pp. 1105–1118.

Olshausen, B. A. and Fieldt, D. J. (1997). "Sparse Coding with an Overcomplete Basis Set: A Strategy Employed by V1?" In: *Vision Research* 37 (23): pp. 3311–3325.

Olson, L., Seiger, Å., and Fuxe, K. (1972). "Heterogeneity of striatal and limbic dopamine innervation: Highly fluorescent islands in developing and adult rats". In: *Brain Research* 44 (1): pp. 283–288.

Olson, V. G. and Nestler, E. J. (2007). "Topographical organization of GABAergic neurons within the ventral tegmental area of the rat". In: *Synapse* 61 (2): pp. 87–95.

Omelchenko, N. and Sesack, S. R. (2005). "Laterodorsal tegmental projections to identified cell populations in the rat ventral tegmental area". In: *The Journal of Comparative Neurology* 483 (2): pp. 217–235.

— (2006). "Cholinergic axons in the rat ventral tegmental area synapse preferentially onto mesoaccumbens dopamine neurons". In: *The Journal of Comparative Neurology* 494 (6): pp. 863–875.

Omodei, D., Acampora, D., Mancuso, P., Prakash, N., Di Giovannantonio, L. G., Wurst, W., and Simeone, A. (2008). "Anterior-posterior graded response to Otx2 controls proliferation and differentiation of dopaminergic progenitors in the ventral mesencephalon." In: *Development* 135 (20): pp. 3459–3470.

Ono, Y., Nakatani, T., Sakamoto, Y., Mizuhara, E., Minaki, Y., Kumai, M., Hamaguchi, A., Nishimura, M., Inoue, Y., Hayashi, H., Takahashi, J., and Imai, T. (2007). "Differences in neurogenic potential in floor plate cells along an anteroposterior location: midbrain dopaminergic neurons originate from mesencephalic floor plate cells." In: *Development* 134 (17): pp. 3213–3225.

Oorschot, D. E. (1996). "Total number of neurons in the neostriatal, pallidal, subthalamic, and substantia nigral nuclei of the rat basal ganglia: A stereological

study using the cavalieri and optical disector methods". In: *The Journal of Comparative Neurology* 366 (4): pp. 580–599.

Orr-Urtreger, A., Shifrin, C., Rozovski, U., Rosner, S., Bercovich, D., Gurevich, T., Yagev-More, H., Bar-Shira, A., and Giladi, N. (2007). "The LRRK2 G2019S mutation in Ashkenazi Jews with Parkinson disease: is there a gender effect?" In: *Neurology* 69 (16): pp. 1595–1602.

Overton, P. G. and Clark, D. (1997). "Burst firing in midbrain dopaminergic neurons." In: *Brain Research Reviews* 25 (3): pp. 312–334.

Overton, P. G. and Clark, D. (1992). "Iontophoretically administered drugs acting at the N-methyl-D-aspartate receptor modulate burst firing in A9 dopamine neurons in the rat". In: *Synapse* 10 (2): pp. 131–140.

Ozelius, L. J., Senthil, G., Saunders-Pullman, R., Ohmann, E., Deligtisch, A., Tagliati, M., Hunt, A. L., Klein, C., Henick, B., Hailpern, S. M., Lipton, R. B., Soto-Valencia, J., Risch, N., and Bressman, S. B. (2006). "LRRK2 G2019S as a Cause of Parkinson's Disease in Ashkenazi Jews". In: *New England Journal of Medicine* 354 (4): pp. 424–425.

Paisan-Ruiz, C., Jain, S., Evans, E., Gilks, W. P., Simón, J., Brug, M. van der, Munain, A. L. de, Aparicio, S., Gil, A. M., Khan, N., Johnson, J., Martinez, J. R., Nicholl, D., Carrera, I. M., Peňa, A. S., Silva, R. de, Lees, A., Marti-Massó, J. F., Pérez-Tur, J., Wood, N. W., and Singleton, A. B. (2004). "Cloning of the Gene Containing Mutations that Cause PARK8-Linked Parkinson's Disease". In: *Neuron* 44 (4): pp. 595–600.

Paladini, C. A., Celada, P., and Tepper, J. M. (1999). "Striatal, pallidal, and pars reticulata evoked inhibition of nigrostriatal dopaminergic neurons is mediated by GABAA receptors in vivo". In: *Neuroscience* 89 (3): pp. 799–812.

Pan, W.-X., Schmidt, R., Wickens, J. R., and Hyland, B. I. (2005). "Dopamine Cells Respond to Predicted Events during Classical Conditioning: Evidence for Eligibility Traces in the Reward-Learning Network". In: *Journal of Neuroscience* 25 (26): pp. 6235–6242.

Panman, L., Andersson, E., Alekseenko, Z., Hedlund, E., Kee, N., Mong, J., Uhde, C. W., Deng, Q., Sandberg, R., Stanton, L. W., Ericson, J., and Perlmann, T. (2011). "Transcription Factor-Induced Lineage Selection of Stem-Cell-Derived Neural Progenitor Cells". In: *Cell Stem Cell* 8 (6): pp. 663–675.

Panman, L., Papathanou, M., Laguna, A., Oosterveen, T., Volakakis, N., Acampora, D., Kurtsdotter, I., Yoshitake, T., Kehr, J., Joodmardi, E., Muhr, J., Simeone, A., Ericson, J., and Perlmann, T. (2014). "Sox6 and Otx2 control the specification of substantia nigra and ventral tegmental area dopamine neurons." In: *Cell Reports* 8 (4): pp. 1018–1025.

Parent, A. and Hazrati, L.-N. (1995). "Functional anatomy of the basal ganglia. I. The cortico-basal ganglia-thalamo-cortical loop". In: *Brain Research Reviews* 20 (1): pp. 91–127.

Parker, P. R., Lalive, A. L., and Kreitzer, A. C. (2016). "Pathway-Specific Remodeling of Thalamostriatal Synapses in Parkinsonian Mice". In: *Neuron* 89 (4): pp. 734–740.

Patil, N., Cox, D. R., Bhat, D., Faham, M., Myers, R. M., and Peterson, A. S. (1995). "A potassium channel mutation in weaver mice implicates membrane excitability in granule cell differentiation". In: *Nature Genetics* 11 (2): pp. 126–129.

Pavlov, I. P. and Petrovitch, I. (1928). "Experimental psychology and psycho-pathology in animals." In: *Lectures on Conditioned Reflexes: Twenty-five Years of Objective*

Study of the Higher Nervous Activity (Behaviour) of Animals. New York: Liverwright Publishing Corporation, pp. 47–60.

Paxinos, G. and Franklin, K. B. J. (2013). *Paxinos and Franklin's the Mouse Brain in Stereotaxic Coordinates*. 4th ed. London: Academic Press.

Paxinos, G. and Watson, C. (2007). *The Rat Brain in Stereotaxic Coordinates*. 6th ed. London: Academic Press.

Penny, G., Afsharpour, S., and Kitai, S. T. (1986). "The glutamate decarboxylase-, leucine enkephalin-, methionine enkephalin-and substance P-immunoreactive neurons in the neostriatum of the rat and cat: Evidence for partial population overlap". In: *Neuroscience* 17 (4): pp. 1011–1045.

Perese, D., Ulman, J., Viola, J., Ewing, S., and Bankiewicz, K. (1989). "A 6-hydroxydopamine-induced selective parkinsonian rat model". In: *Brain Research* 494 (2): pp. 285–293.

Phillipson, O. T. (1979). "Afferent projections to the ventral tegmental area of Tsai and interfascicular nucleus: A horseradish peroxidase study in the rat". In: *The Journal of Comparative Neurology* 187 (1): pp. 117–143.

Pinault, D. (1996). "A novel single-cell staining procedure performed in vivo under electrophysiological control: morpho-functional features of juxtacellularly labeled thalamic cells and other central neurons with biocytin or Neurobiotin." In: *Journal of Neuroscience Methods* 65 (2): pp. 113–136.

Pissadaki, E. K. and Bolam, J. P. (2013). "The energy cost of action potential propagation in dopamine neurons: clues to susceptibility in Parkinson's disease". In: *Frontiers in Computational Neuroscience* 7: p. 13.

Plowey, E. D., Cherra, S. J., Liu, Y.-J., and Chu, C. T. (2008). "Role of autophagy in G2019S-LRRK2-associated neurite shortening in differentiated SH-SY5Y cells". In: *Journal of Neurochemistry* 105 (3): pp. 1048–1056.

Polymeropoulos, M. H., Lavedan, C., Leroy, E., Ide, S. E., Dehejia, A., Dutra, A., Pike, B., Root, H., Rubenstein, J., Boyer, R., Stenroos, E. S., Chandrasekharappa, S., Athanassiadou, A., Papapetropoulos, T., Johnson, W. G., Lazzarini, A. M., Duvoisin, R. C., Di Iorio, G., Golbe, L. I., and Nussbaum, R. L. (1997). "Mutation in the α-Synuclein Gene Identified in Families with Parkinson's Disease". In: *Science* 276 (5321): pp. 2045–2047.

Poulin, J.-F., Tasic, B., Hjerling-Leffler, J., Trimarchi, J. M., and Awatramani, R. (2016). "Disentangling neural cell diversity using single-cell transcriptomics". In: *Nature Neuroscience* 19 (9): pp. 1131–1141.

Poulin, J.-F., Zou, J., Drouin-Ouellet, J., Kim, K.-Y. A., Cicchetti, F., and Awatramani, R. B. (2014). "Defining Midbrain Dopaminergic Neuron Diversity by Single-Cell Gene Expression Profiling". In: *Cell Reports* 9 (3): pp. 930–943.

Powell, T. P. S. and Cowan, W. M. (1956). "A study of thalamo-striate relations in the monkey". In: *Brain* 79 (2): pp. 364–366.

Prakash, N., Brodski, C., Naserke, T., Puelles, E., Gogoi, R., Hall, A., Panhuysen, M., Echevarria, D., Sussel, L., Weisenhorn, D. M. V., Martinez, S., Arenas, E., Simeone, A., and Wurst, W. (2006). "A Wnt1-regulated genetic network controls the identity and fate of midbrain-dopaminergic progenitors in vivo." In: *Development* 133 (1): pp. 89–98.

Prensa, L. and Parent, A. (2001). "The Nigrostriatal Pathway in the Rat: A Single-Axon Study of the Relationship between Dorsal and Ventral Tier Nigral Neurons and the

Striosome/Matrix Striatal Compartments". In: *Journal of Neuroscience* 21 (18): pp. 7247–7260.

Prensa, L., Richard, S., and Parent, A. (2003). "Chemical anatomy of the human ventral striatum and adjacent basal forebrain structures". In: *The Journal of Comparative Neurology* 460 (3): pp. 345–367.

Preston, R., Bishop, G., and Kitai, S. T. (1980). "Medium spiny neuron projection from the rat striatum: An intracellular horseradish peroxidase study". In: *Brain Research* 183 (2): pp. 253–263.

Pristerà, A., Lin, W., Kaufmann, A.-K., Brimblecombe, K. R., Threlfell, S., Dodson, P. D., Magill, P. J., Fernandes, C., Cragg, S. J., and Ang, S.-L. (2015). "Transcription factors FOXA1 and FOXA2 maintain dopaminergic neuronal properties and control feeding behavior in adult mice." In: *Proceedings of the National Academy of Sciences* 112 (35): E4929–E4938.

Przedborski, S., Jackson-Lewis, V., Naini, A. B., Jakowec, M., Petzinger, G., Miller, R., and Akram, M. (2001). "The parkinsonian toxin 1-methyl-4-phenyl-1,2,3,6-tetrahydropyridine (MPTP): a technical review of its utility and safety". In: *Journal of Neurochemistry* 76 (5): pp. 1265–1274.

Puelles, E., Annino, A., Tuorto, F., Usiello, A., Acampora, D., Czerny, T., Brodski, C., Ang, S.-L., Wurst, W., and Simeone, A. (2004). "Otx2 regulates the extent, identity and fate of neuronal progenitor domains in the ventral midbrain." In: *Development* 131 (9): pp. 2037–2048.

Puopolo, M., Raviola, E., and Bean, B. P. (2007). "Roles of subthreshold calcium current and sodium current in spontaneous firing of mouse midbrain dopamine neurons." In: *Journal of Neuroscience* 27 (3): pp. 645–656.

Ramón y Cajal, S. (1909). *Histologie du Système Nerveux de l'Homme et des Vertébrés*. Ed. by Maloine, A. Paris.

Ramonet, D., Daher, J. P. L., Lin, B. M., Stafa, K., Kim, J., Banerjee, R., Westerlund, M., Pletnikova, O., Glauser, L., Yang, L., Liu, Y., Swing, D. A., Beal, M. F., Troncoso, J. C., McCaffery, J. M., Jenkins, N. A., Copeland, N. G., Galter, D., Thomas, B., Lee, M. K., Dawson, T. M., Dawson, V. L., and Moore, D. J. (2011). "Dopaminergic neuronal loss, reduced neurite complexity and autophagic abnormalities in transgenic mice expressing G2019S mutant LRRK2." In: *PloS One* 6 (4): e18568.

Redgrave, P., Gurney, K., and Reynolds, J. (2008). "What is reinforced by phasic dopamine signals?" In: *Brain Research reviews* 58 (2): pp. 322–339.

Reisner, P. D., Christakos, S., and Vanaman, T. C. (1992). "In vitro enzyme activation with calbindin-D28k , the vitamin D-dependent 28 kDa calcium binding protein". In: *FEBS Letters* 297 (1-2): pp. 127–131.

Rescorla, R. A. and Wagner, A. R. (1972). "A theory of Pavlovian conditioning: variations in the effectiveness of reinforcement and nonreinforcement." In: *Classical Conditioning II: Current Research and Theory*. Ed. by Black, A. H. and Prokasy, W. F. New York: Appleton-Century-Crofts, pp. 64–99.

Reyes, S., Fu, Y., Double, K., Thompson, L., Kirik, D., Paxinos, G., and Halliday, G. M. (2012). "GIRK2 expression in dopamine neurons of the substantia nigra and ventral tegmental area." In: *Journal of Comparative Neurology* 520 (12): pp. 2591–2607.

Rhinn, M. and Brand, M. (2001). "The midbrain–hindbrain boundary organizer". In: *Current Opinion in Neurobiology* 11 (1): pp. 34–42.

Roeper, J. (2013). "Dissecting the diversity of midbrain dopamine neurons." In: *Trends in Neurosciences* 36 (6): pp. 336–342.

Roffler-Tarlov, S. and Graybiel, A. M. (1984). "Weaver mutation has differential effects on the dopamine-containing innervation of the limbic and nonlimbic striatum". In: *Nature* 307 (5946): pp. 62–66.

Rogers, J. H. (1987). "Calretinin: a gene for a novel calcium-binding protein expressed principally in neurons." In: *The Journal of Cell Biology* 105 (3): pp. 1343–1353.

Rogers, J. H. (1992). "Immunohistochemical markers in rat brain: colocalization of calretinin and calbindin-D28k with tyrosine hydroxylase". In: *Brain Research* 587 (2): pp. 203–210.

Romo, R. and Schultz, W. (1990). "Dopamine neurons of the monkey midbrain: contingencies of responses to active touch during self-initiated arm movements". In: *Journal of Neurophysiology* 63 (3): pp. 592–606.

Roseberry, A. G. (2015). "Acute fasting increases somatodendritic dopamine release in the ventral tegmental area". In: *Journal of Neurophysiology* 114 (2): pp. 1072–1082.

Ross, G. W., Petrovitch, H., Abbott, R. D., Tanner, C. M., Popper, J., Masaki, K., Launer, L., and White, L. R. (2008). "Association of olfactory dysfunction with risk for future Parkinson's disease". In: *Annals of Neurology* 63 (2): pp. 167–173.

Roussa, E. and Krieglstein, K. (2004). "Induction and specification of midbrain dopaminergic cells: focus on SHH, FGF8, and TGF-β". In: *Cell and Tissue Research* 318 (1): pp. 23–33.

Sachdev, R. N., Gilman, S., and Aldridge, J. W. (1989). "Effects of excitotoxic striatal lesions on single unit activity in globus pallidus and entopeduncular nucleus of the cat". In: *Brain Research* 501 (2): pp. 295–306.

Sadacca, B. F., Jones, J. L., and Schoenbaum, G. (2016). "Midbrain dopamine neurons compute inferred and cached value prediction errors in a common framework." In: *eLife* 5: e13665.

Sadek, A. R., Magill, P. J., and Bolam, J. P. (2007). "A Single-Cell Analysis of Intrinsic Connectivity in the Rat Globus Pallidus". In: *Journal of Neuroscience* 27 (24): pp. 6352–6362.

Salamone, J. D., Correa, M., Farrar, A., and Mingote, S. M. (2007). "Effort-related functions of nucleus accumbens dopamine and associated forebrain circuits". In: *Psychopharmacology* 191 (3): pp. 461–482.

Salamone, J. D., Correa, M., Nunes, E. J., Randall, P. A., and Pardo, M. (2012). "The Behavioral Pharmacology of Effort-related Choice Behavior: Dopamine, Adenosine and Beyond". In: *Journal of the Experimental Analysis of Behavior* 97 (1): pp. 125–146.

Samii, A., Nutt, J. G., and Ransom, B. R. (2004). "Parkinson's disease". In: *Lancet* 363 (9423): pp. 1783–1793.

Sánchez-González, M. A., García-Cabezas, M. Á., Rico, B., and Cavada, C. (2005). "The primate thalamus is a key target for brain dopamine." In: *Journal of Neuroscience* 25 (26): pp. 6076–6083.

Sanderson, P., Mavoungou, R., and Albe-Fessard, D. (1986). "Changes in substantia nigra pars reticulata activity following lesions of the substantia nigra pars compacta". In: *Neuroscience Letters* 67 (1): pp. 25–30.

Sanghera, M. K., Manaye, K. F., Liang, C.-L., Lacopino, A. M., Bannon, M. J., and German, D. C. (1994). "Low dopamine transporter mRNA levels in midbrain regions containing calbindin". In: *NeuroReport* 5 (13): pp. 1641–1644.

Sanghera, M., Trulson, M., and German, D. C. (1984). "Electrophysiological properties of mouse dopamine neurons: In vivo and in vitro studies". In: *Neuroscience* 12 (3): pp. 793–801.

Satake, W., Nakabayashi, Y., Mizuta, I., Hirota, Y., Ito, C., Kubo, M., Kawaguchi, T., Tsunoda, T., Watanabe, M., Takeda, A., Tomiyama, H., Nakashima, K., Hasegawa, K., Obata, F., Yoshikawa, T., Kawakami, H., Sakoda, S., Yamamoto, M., Hattori, N., Murata, M., Nakamura, Y., and Toda, T. (2009). "Genome-wide association study identifies common variants at four loci as genetic risk factors for Parkinson's disease." In: *Nature Genetics* 41 (12): pp. 1303–1307.

Saunders-Pullman, R., Lipton, R. B., Senthil, G., Katz, M., Costan-Toth, C., Derby, C., Bressman, S., Verghese, J., and Ozelius, L. J. (2006). "Increased frequency of the LRRK2 G2019S mutation in an elderly Ashkenazi Jewish population is not associated with dementia." In: *Neuroscience Letters* 402 (1-2): pp. 92–96.

Schein, J. C., Hunter, D. D., and Roffler-Tarlov, S. (1998). "Girk2 Expression in the Ventral Midbrain, Cerebellum, and Olfactory Bulb and Its Relationship to the Murine Mutation Weaver". In: *Developmental Biology* 204 (2): pp. 432–450.

Schiemann, J., Puggioni, P., Dacre, J., Pelko, M., Domanski, A., Rossum, M. C. van, and Duguid, I. (2015). "Cellular Mechanisms Underlying Behavioral State-Dependent Bidirectional Modulation of Motor Cortex Output". In: *Cell Reports* 11 (8): pp. 1319–1330.

Schiemann, J., Schlaudraff, F., Klose, V., Bingmer, M., Seino, S., Magill, P. J., Zaghloul, K. A., Schneider, G., Liss, B., and Roeper, J. (2012). "K-ATP channels in dopamine substantia nigra neurons control bursting and novelty-induced exploration." In: *Nature Neuroscience* 15 (9): pp. 1272–1280.

Schiffmann, S. N., Jacobs, O., and Vanderhaeghen, J.-J. (1991). "Striatal Restricted Adenosine A2 Receptor (RDC8) Is Expressed by Enkephalin but Not by Substance P Neurons: An In Situ Hybridization Histochemistry Study". In: *Journal of Neurochemistry* 57 (3): pp. 1062–1067.

Schmidt, H. (2012). "Three functional facets of calbindin D-28k." In: *Frontiers in Molecular Neuroscience* 5: p. 25.

Schober, A. (2004). "Classic toxin-induced animal models of Parkinson's disease: 6-OHDA and MPTP." In: *Cell and Tissue Research* 318 (1): pp. 215–224.

Schoenbaum, G., Esber, G. R., and Iordanova, M. D. (2013). "Dopamine signals mimic reward prediction errors". In: *Nature Neuroscience* 16 (7): pp. 777–779.

Schonberg, T., O'Doherty, J. P., Joel, D., Inzelberg, R., Segev, Y., and Daw, N. D. (2010). "Selective impairment of prediction error signaling in human dorsolateral but not ventral striatum in Parkinson's disease patients: evidence from a model-based fMRI study". In: *NeuroImage* 49 (1): pp. 772–781.

Schultz, W. (1986). "Responses of midbrain dopamine neurons to behavioral trigger stimuli in the monkey." In: *Journal of Neurophysiology* 56 (5): pp. 1439–1461.

— (1998). "Predictive Reward Signal of Dopamine Neurons". In: *Journal of Neurophysiology* 80 (1): pp. 1–27.

— (2007a). "Behavioral dopamine signals." In: *Trends in Neurosciences* 30 (5): pp. 203–210.

— (2007b). "Multiple dopamine functions at different time courses." In: *Annual Review of Neuroscience* 30: pp. 259–288.

— (2010). "Dopamine signals for reward value and risk: basic and recent data." In: *Behavioral and Brain Functions* 6 (1): p. 24.

Schultz, W. (2015). “Neuronal Reward and Decision Signals: From Theories to Data”. In: *Physiological Reviews* 95 (3): pp. 853–951.

— (2016). “Dopamine reward prediction-error signalling: a two-component response.” In: *Nature Reviews Neuroscience* 17 (3): pp. 183–195.

Schultz, W., Apicella, P., and Ljungberg, T. (1993). “Responses of Monkey Dopamine Neurons to Reward and Conditioned Stimuli during Successive Steps of Learning a Delayed Response Task”. In: *Journal of Neuroscience* 13 (3): pp. 900–913.

Schultz, W., Dayan, P., and Montague, P. R. (1997). “A Neural Substrate of Prediction and Reward”. In: *Science* 275 (5306): pp. 1593–1599.

Schultz, W. and Hollerman, J. R. (1998). “Dopamine neurons report an error in the temporal prediction of reward during learning”. In: *Nature Neuroscience* 1 (4): pp. 304–309.

Schultz, W. and Romo, R. (1988). “Neuronal activity in the monkey striatum during the initiation of movements”. In: *Experimental Brain Research* 71 (2): pp. 431–436.

— (1990). “Dopamine neurons of the monkey midbrain: contingencies of responses to stimuli eliciting immediate behavioral reactions”. In: *Journal of Neurophysiology* 63 (3): pp. 607–624.

Schultz, W., Ruffieux, A., and Aebischer, P. (1983). “The activity of pars compacta neurons of the monkey substantia nigra in relation to motor activation”. In: *Experimental Brain Research* 51 (3): pp. 377–387.

Scott, O., Pugh, J., Kiddoo, D., Sonnenberg, L. K., Bamforth, S., and Goez, H. R. (2014). “Global Developmental Delay, Progressive Relapsing-Remitting Parkinsonism, and Spinal Syrinx in a Child With SOX6 Mutation”. In: *Journal of Child Neurology* 29 (11): NP164–NP167.

Seeman, P., Guan, H. C., and Van Tol, H. H. (1993). “Dopamine D4 receptors elevated in schizophrenia.” In: *Nature* 365 (6445): pp. 441–445.

Seifert, U., Härtig, W., Grosche, J., Brückner, G., Riedel, A., and Brauer, K. (1998). “Axonal expression sites of tyrosine hydroxylase, calretinin- and calbindin-immunoreactivity in striato-pallidal and septal nuclei of the rat brain: a double-immunolabelling study”. In: *Brain Research* 795 (1-2): pp. 227–246.

Seite, R., Vuillet-Luciani, J., Vio, M., and Cataldo, C. (1977). “Sur la présence d’inclusions nucléaires dans certains neurones du noyau caudé du rat: répartition, fréquence et organisation ultrastructurale.” In: *Biologie Cellulaire* 30: pp. 73–76.

Sesack, S. R. and Pickel, V. M. (1992). “Prefrontal cortical efferents in the rat synapse on unlabeled neuronal targets of catecholamine terminals in the nucleus accumbens septi and on dopamine neurons in the ventral tegmental area”. In: *The Journal of Comparative Neurology* 320 (2): pp. 145–160.

Shen, W., Flajolet, M., Greengard, P., and Surmeier, D. J. (2008). “Dichotomous dopaminergic control of striatal synaptic plasticity.” In: *Science* 321 (5890): pp. 848–851.

Shimizu, N., Kitada, T., Asakawa, S., Hattori, N., Matsumine, H., Yamamura, Y., Minoshima, S., Yokochi, M., and Mizuno, Y. (1998). “Mutations in the parkin gene cause autosomal recessive juvenile parkinsonism”. In: *Nature* 392 (6676): pp. 605–608.

Shimo, Y. and Wichmann, T. (2009). “Neuronal activity in the subthalamic nucleus modulates the release of dopamine in the monkey striatum”. In: *European Journal of Neuroscience* 29 (1): pp. 104–113.

Shin, N., Jeong, H., Kwon, J., Heo, H. Y., Kwon, J. J., Yun, H. J., Kim, C.-H., Han, B. S., Tong, Y., Shen, J., Hatano, T., Hattori, N., Kim, K.-S., Chang, S., and

Seol, W. (2008). "LRRK2 regulates synaptic vesicle endocytosis". In: *Experimental Cell Research* 314 (10): pp. 2055–2065.

Sidransky, E., Lopez, G., Qin, Z., Muthane, U., Shankar, S., and Raju, T. (2012). "The link between the GBA gene and parkinsonism." In: *The Lancet Neurology* 11 (11): pp. 986–998.

Siegert, S., Cabuy, E., Scherf, B. G., Kohler, H., Panda, S., Le, Y.-Z., Fehling, H. J., Gaidatzis, D., Stadler, M. B., and Roska, B. (2012). "Transcriptional code and disease map for adult retinal cell types". In: *Nature Neuroscience* 15 (3): pp. 487–495.

Silva, N. L., Pechura, C. M., and Barker, J. L. (1990). "Postnatal rat nigrostriatal dopaminergic neurons exhibit five types of potassium conductances." In: *Journal of Neurophysiology* 64 (1): pp. 262–272.

Silveira-Moriyama, L., Guedes, L. C., Kingsbury, A., Ayling, H., Shaw, K., Barbosa, E. R., Bonifati, V., Quinn, N. P., Abou-Sleiman, P., Wood, N. W., Petrie, A., Sampaio, C., Ferreira, J. J., Holton, J., Revesz, T., and Lees, A. J. (2008). "Hyposmia in G2019S LRRK2-related parkinsonism". In: *Neurology* 71 (13): pp. 1021–1026.

Silveira-Moriyama, L., Munhoz, R. P., de J. Carvalho, M., Raskin, S., Rogaeva, E., de C. Aguiar, P., Bressan, R. A., Felicio, A. C., Barsottini, O. G., Andrade, L. A. F., Chien, H. F., Bonifati, V., Barbosa, E. R., Teive, H. A., and Lees, A. J. (2010). "Olfactory heterogeneity in LRRK2 related Parkinsonism". In: *Movement Disorders* 25 (16): pp. 2879–2883.

Simon, H. H., Saueressig, H., Wurst, W., Goulding, M. D., and O'Leary, D. D. (2001). "Fate of midbrain dopaminergic neurons controlled by the engrailed genes." In: *Journal of Neuroscience* 21 (9): pp. 3126–3134.

Simon, H. H., Bhatt, L., Gherbassi, D., Sgadó, P., and Alberí, L. (2003). "Midbrain dopaminergic neurons: determination of their developmental fate by transcription factors." In: *Annals of the New York Academy of Sciences* 991: pp. 36–47.

Simón-Sánchez, J., Schulte, C., Bras, J. M., Sharma, M., Gibbs, J. R., Berg, D., Paisan-Ruiz, C., Lichtner, P., Scholz, S. W., Hernandez, D. G., Krüger, R., Federoff, M., Klein, C., Goate, A., Perlmutter, J., Bonin, M., Nalls, M. A., Illig, T., Gieger, C., Houlden, H., Steffens, M., Okun, M. S., Racette, B. A., Cookson, M. R., Foote, K. D., Fernandez, H. H., Traynor, B. J., Schreiber, S., Arepalli, S., Zonozi, R., Gwinn, K., Brug, M. van der, Lopez, G., Chanock, S. J., Schatzkin, A., Park, Y., Hollenbeck, A., Gao, J., Huang, X., Wood, N. W., Lorenz, D., Deuschl, G., Chen, H., Riess, O., Hardy, J. A., Singleton, A. B., and Gasser, T. (2009). "Genome-wide association study reveals genetic risk underlying Parkinson's disease." In: *Nature Genetics* 41 (12): pp. 1308–1312.

Singleton, A. B., Farrer, M. J., Johnson, J., Singleton, A., Hague, S., Kachergus, J., Hulihan, M., Peuralinna, T., Dutra, A., Nussbaum, R., Lincoln, S., Crawley, A., Hanson, M., Maraganore, D., Adler, C., Cookson, M. R., Muenter, M., Baptista, M., Miller, D., Blancato, J., Hardy, J., and Gwinn-Hardy, K. (2003). "α-Synuclein Locus Triplication Causes Parkinson's Disease". In: *Science* 302 (5646): p. 841.

Sloan, M., Alegre-Abarrategui, J., Potgieter, D., Kaufmann, A.-K., Exley, R., Deltheil, T., Threlfell, S., Connor-Robson, N., Brimblecombe, K., Wallings, R., Cioroch, M., Bannerman, D. M., Bolam, J. P., Magill, P. J., Cragg, S. J., Dodson, P. D., and Wade-Martins, R. (2016). "LRRK2 BAC transgenic rats develop progressive, L-DOPA-responsive motor impairment, and deficits in dopamine circuit function." In: *Human Molecular Genetics* 25 (5): pp. 951–963.

Smeyne, R. J. and Jackson-Lewis, V. (2005). "The MPTP model of Parkinson's disease". In: *Molecular Brain Research* 134 (1): pp. 57–66.

Smidt, M. P. and Burbach, J. P. H. (2007). "How to make a mesodiencephalic dopaminergic neuron". In: *Nature Reviews Neuroscience* 8 (1): pp. 21–32.

Smidt, M. P., Schaick, H. S. van, Lanctôt, C., Tremblay, J. J., Cox, J. J., Kleij, A. A. van der, Wolterink, G., Drouin, J., and Burbach, J. P. (1997). "A homeodomain gene Ptx3 has highly restricted brain expression in mesencephalic dopaminergic neurons." In: *Proceedings of the National Academy of Sciences* 94 (24): pp. 13305–13310.

Smith, A. D. and Bolam, J. P. (1990a). "The neural network of the basal ganglia as revealed by the study of synaptic connections of identified neurones". In: *Trends in Neurosciences* 13 (7): pp. 259–265.

Smith, J. B., Klug, J. R., Ross, D. L., Howard, C. D., Hollon, N. G., Ko, V. I., Hoffman, H., Callaway, E. M., Gerfen, C. R., and Jin, X. (2016). "Genetic-Based Dissection Unveils the Inputs and Outputs of Striatal Patch and Matrix Compartments". In: *Neuron* 91 (5): pp. 1069–1084.

Smith, R. J., Lobo, M. K., Spencer, S., and Kalivas, P. W. (2013). "Cocaine-induced adaptations in D1 and D2 accumbens projection neurons (a dichotomy not necessarily synonymous with direct and indirect pathways)". In: *Current Opinion in Neurobiology* 23 (4): pp. 546–552.

Smith, Y., Bevan, M. D., Shink, E., and Bolam, J. P. (1998). "Microcircuitry of the direct and indirect pathway of the basal ganglia". In: *Neuroscience* 86 (2): pp. 353–387.

Smith, Y. and Bolam, J. P. (1989). "Neurons of the substantia nigra reticulata receive a dense GABA-containing input from the globus pallidus in the rat". In: *Brain Research* 493 (1): pp. 160–167.

— (1990b). "The output neurones and the dopaminergic neurones of the substantia nigra receive a GABA-Containing input from the globus pallidus in the rat". In: *The Journal of Comparative Neurology* 296 (1): pp. 47–64.

Smith, Y. and Parent, A. (1988). "Neurons of the subthalamic nucleus in primates display glutamate but not GABA immunoreactivity". In: *Brain Research* 453 (1): pp. 353–356.

Smith, Y., Parent, A., Seguela, P., and Descarries, L. (1987). "Distribution of GABA-immunoreactive neurons in the basal ganglia of the squirrel monkey (Saimiri sciureus)". In: *The Journal of Comparative Neurology* 259 (1): pp. 50–64.

Smits, S. M., Burbach, J. P. H., and Smidt, M. P. (2006). "Developmental origin and fate of meso-diencephalic dopamine neurons". In: *Progress in Neurobiology* 78 (1): pp. 1–16.

Smits, S. M., Oerthel, L. von, Hoekstra, E. J., Burbach, J. P. H., and Smidt, M. P. (2013). "Molecular marker differences relate to developmental position and subsets of mesodiencephalic dopaminergic neurons." In: *PloS One* 8 (10): e76037.

Solomon, P. R., Vander Schaaf, E. R., Thompson, R. F., and Weisz, D. J. (1986). "Hippocampus and trace conditioning of the rabbit's classically conditioned nictitating membrane response." In: *Behavioral Neuroscience* 100 (5): pp. 729–744.

Somogyi, P., Bolam, J. P., and Smith, A. D. (1981). "Monosynaptic cortical input and local axon collaterals of identified striatonigral neurons. A light and electron microscopic study using the golgi-peroxidase transport-degeneration procedure". In: *The Journal of Comparative Neurology* 195 (4): pp. 567–584.

Somogyi, P. and Smith, A. D. (1979). "Projection of neostriatal spiny neurons to the substantia nigra. Application of a combined golgi-staining and horse-radish peroxidase transport procedure at both light and electron microscopic levels". In: *Brain Research* 178 (1): pp. 3–15.

Sotak, B. N., Hnasko, T. S., Robinson, S., Kremer, E. J., and Palmiter, R. D. (2005). "Dysregulation of dopamine signaling in the dorsal striatum inhibits feeding". In: *Brain Research* 1061 (2): pp. 88–96.

Spillantini, M. G., Schmidt, M. L., Lee, V. M., Trojanowski, J. Q., Jakes, R., and Goedert, M. (1997). "Alpha-synuclein in Lewy bodies." In: *Nature* 388 (6645): pp. 839–840.

Stafa, K., Tsika, E., Moser, R., Musso, A., Glauser, L., Jones, A., Biskup, S., Xiong, Y., Bandopadhyay, R., Dawson, V. L., Dawson, T. M., and Moore, D. J. (2013). "Functional Interaction of Parkinson's Disease-Associated LRRK2 with Members of the Dynamin GTPase Superfamily." In: *Human Molecular Genetics* 23 (8): pp. 2055–2077.

Staines, W., Atmadja, S., and Fibiger, H. (1981). "Demonstration of a pallidostriatal pathway by retrograde transport of HRP-labeled lectin". In: *Brain Research* 206 (2): pp. 446–450.

Stauffer, W. R., Lak, A., Yang, A., Borel, M., Paulsen, O., Boyden, E. S., and Schultz, W. (2016). "Dopamine Neuron-Specific Optogenetic Stimulation in Rhesus Macaques". In: *Cell* 166 (6): 1564–1571.e6.

Steinberg, E. E., Keiflin, R., Boivin, J. R., Witten, I. B., Deisseroth, K., and Janak, P. H. (2013). "A causal link between prediction errors, dopamine neurons and learning." In: *Nature Neuroscience* 16 (7): pp. 966–973.

Steinfels, G. F., Heym, J., Strecker, R. E., and Jacobs, B. L. (1983a). "Behavioral correlates of dopaminergic unit activity in freely moving cats." In: *Brain Research* 258 (2): pp. 217–228.

— (1983b). "Response of dopaminergic neurons in cat to auditory stimuli presented across the sleep-waking cycle." In: *Brain Research* 277 (1): pp. 150–154.

Stephenson-Jones, M., Yu, K., Ahrens, S., Tucciarone, J. M., Huijstee, A. N. van, Mejia, L. A., Penzo, M. A., Tai, L.-H., Wilbrecht, L., and Li, B. (2016). "A basal ganglia circuit for evaluating action outcomes". In: *Nature* 539 (7628): pp. 289–293.

Stern, E. A., Kincaid, A. E., and Wilson, C. J. (1997). "Spontaneous subthreshold membrane potential fluctuations and action potential variability of rat corticostriatal and striatal neurons in vivo." In: *Journal of Neurophysiology* 77 (4): pp. 1697–1715.

Stolt, C. C., Schlierf, A., Lommes, P., Hillgärtner, S., Werner, T., Kosian, T., Sock, E., Kessaris, N., Richardson, W. D., Lefebvre, V., and Wegner, M. (2006). "SoxD Proteins Influence Multiple Stages of Oligodendrocyte Development and Modulate SoxE Protein Function". In: *Developmental Cell* 11 (5): pp. 697–709.

Stoof, J. C. and Kebabian, J. W. (1981). "Opposing roles for D-1 and D-2 dopamine receptors in efflux of cyclic AMP from rat neostriatum". In: *Nature* 294 (5839): pp. 366–368.

Stott, S. R. W., Metzakopian, E., Lin, W., Kaestner, K. H., Hen, R., and Ang, S.-L. (2013). "Foxa1 and foxa2 are required for the maintenance of dopaminergic properties in ventral midbrain neurons at late embryonic stages." In: *Journal of Neuroscience* 33 (18): pp. 8022–8034.

Strecker, R. E. and Jacobs, B. L. (1985). "Substantia nigra dopaminergic unit activity in behaving cats: Effect of arousal on spontaneous discharge and sensory evoked activity". In: *Brain Research* 361 (1-2): pp. 339–350.

Su, A. I., Wiltshire, T., Batalov, S., Lapp, H., Ching, K. A., Block, D., Zhang, J., Soden, R., Hayakawa, M., Kreiman, G., Cooke, M. P., Walker, J. R., and Hogenesch, J. B. (2004). "A gene atlas of the mouse and human protein-encoding transcriptomes." In: *Proceedings of the National Academy of Sciences* 101 (16): pp. 6062–6067.

Suaud-Chagny, M., Brun, P., Buda, M., and Gonon, F. G. (1992). "Fast in vivo monitoring of electrically evoked dopamine release by differential pulse amperometry with untreated carbon fibre electrodes". In: *Journal of Neuroscience Methods* 45 (3): pp. 183–190.

Suaud-Chagny, M., Chergui, K., Chouvet, G., and Gonon, F. G. (1992). "Relationship between dopamine release in the rat nucleus accumbens and the discharge activity of dopaminergic neurons during local in vivo application of amino acids in the ventral tegmental area". In: *Neuroscience* 49 (1): pp. 63–72.

Subramaniam, M., Althof, D., Gispert, S., Schwenk, J., Auburger, G., Kulik, A., Fakler, B., and Roeper, J. (2014). "Mutant α-Synuclein Enhances Firing Frequencies in Dopamine Substantia Nigra Neurons by Oxidative Impairment of A-Type Potassium Channels". In: *Journal of Neuroscience* 34 (41): pp. 13586–13599.

Sugimoto, T., Hattori, T., Mizuno, N., Itoh, K., and Sato, M. (1983). "Direct projections from the centre median-parafascicular complex to the subthalamic nucleus in the cat and rat". In: *The Journal of Comparative Neurology* 214 (2): pp. 209–216.

Sulzer, D. and Surmeier, D. J. (2013). "Neuronal vulnerability, pathogenesis, and Parkinson's disease". In: *Movement Disorders* 28 (6): pp. 715–724.

Sund, N. J., Vatamaniuk, M. Z., Casey, M., Ang, S. L., Magnuson, M. A., Stoffers, D. A., Matschinsky, F. M., and Kaestner, K. H. (2001). "Tissue-specific deletion of Foxa2 in pancreatic beta cells results in hyperinsulinemic hypoglycemia." In: *Genes & Development* 15 (13): pp. 1706–1715.

Suri, R. E. (2002). "TD models of reward predictive responses in dopamine neurons". In: *Neural Networks* 15 (4-6): pp. 523–533.

Surmeier, D. J., Ding, J., Day, M., Wang, Z., and Shen, W. (2007). "D1 and D2 dopamine-receptor modulation of striatal glutamatergic signaling in striatal medium spiny neurons". In: *Trends in Neurosciences* 30 (5): pp. 228–235.

Sutton, R. S. (1988). "Learning to predict by the methods of temporal differences". In: *Machine Learning* 3 (1): pp. 9–44.

Sutton, R. S. and Barto, A. (1990). "Time-derivative models of Pavlovian reinforcement." In: *Learning and Computational Neuroscience: Foundations of Adaptive Networks.* Ed. by Gabriel, M. and Moore, J. Cambridge, MA: MIT Press, pp. 497–537.

Swanson, C. J., Heath, S., Stratford, T. R., and Kelley, A. E. (1997). "Differential Behavioral Responses to Dopaminergic Stimulation of Nucleus Accumbens Subregions in the Rat". In: *Pharmacology Biochemistry and Behavior* 58 (4): pp. 933–945.

Swanson, L. W. (1982). "The projections of the ventral tegmental area and adjacent regions: a combined fluorescent retrograde tracer and immunofluorescence study in the rat." In: *Brain Research Bulletin* 9 (1-6): pp. 321–353.

Szczypka, M. S., Rainey, M. A., Kim, D. S., Alaynick, W. A., Marck, B. T., Matsumoto, A. M., and Palmiter, R. D. (1999). "Feeding behavior in

dopamine-deficient mice." In: *Proceedings of the National Academy of Sciences* 96 (21): pp. 12138–12143.

Takada, M., Tokuno, H., Hamada, I., Inase, M., Ito, Y., Imanishi, M., Hasegawa, N., Akazawa, T., Hatanaka, N., and Nambu, A. (2001). "Organization of inputs from cingulate motor areas to basal ganglia in macaque monkey". In: *European Journal of Neuroscience* 14 (10): pp. 1633–1650.

Takikawa, Y., Kawagoe, R., and Hikosaka, O. (2004). "A possible role of midbrain dopamine neurons in short- and long-term adaptation of saccades to position-reward mapping." In: *Journal of Neurophysiology* 92 (4): pp. 2520–2529.

Taymans, J.-M., Van den Haute, C., and Baekelandt, V. (2006). "Distribution of PINK1 and LRRK2 in rat and mouse brain". In: *Journal of Neurochemistry* 98 (3): pp. 951–961.

Tepper, J. M., Martin, L. P., and Anderson, D. R. (1995). "GABAA receptor-mediated inhibition of rat substantia nigra dopaminergic neurons by pars reticulata projection neurons." In: *Journal of Neuroscience* 15 (4): pp. 3092–3103.

Tepper, J. M., Tecuapetla, F., Koós, T., and Ibáñez-Sandoval, O. (2010). "Heterogeneity and Diversity of Striatal GABAergic Interneurons". In: *Frontiers in Neuroanatomy* 4: p. 150.

Tervo, D. G. R., Hwang, B.-Y., Viswanathan, S., Gaj, T., Lavzin, M., Ritola, K. D., Lindo, S., Michael, S., Kuleshova, E., Ojala, D., Huang, C.-C., Gerfen, C. R., Schiller, J., Dudman, J. T., Hantman, A. W., Looger, L. L., Schaffer, D. V., and Karpova, A. Y. (2016). "A Designer AAV Variant Permits Efficient Retrograde Access to Projection Neurons". In: *Neuron* 92 (2): pp. 372–382.

Thierry, A. M., Blanc, G., Sobel, A., Stinus, L., and Glowinski, J. (1973). "Dopaminergic terminals in the rat cortex." In: *Science* 182 (4111): pp. 499–501.

Thorndike, E. L. (1911). *Animal Intelligence: Experimental Studies*. New York: The Macmillan Company.

Tian, J., Huang, R., Cohen, J. Y., Osakada, F., Kobak, D., Machens, C. K., Callaway, E. M., Uchida, N., and Watabe-Uchida, M. (2016). "Distributed and Mixed Information in Monosynaptic Inputs to Dopamine Neurons". In: *Neuron* 91 (6): pp. 1374–1389.

Tobler, P. N., Fiorillo, C. D., and Schultz, W. (2005). "Adaptive Coding of Reward Value by Dopamine Neurons". In: *Science* 307 (5715): pp. 1642–1645.

Tobler, P. N., Dickinson, A., and Schultz, W. (2003). "Coding of predicted reward omission by dopamine neurons in a conditioned inhibition paradigm." In: *Journal of Neuroscience* 23 (32): pp. 10402–10410.

Tokuno, H., Moriizumi, T., Kudo, M., and Nakamura, Y. (1988). "A morphological evidence for monosynaptic projections from the nucleus tegmenti pedunculopontinus pars compacta (TPC) to nigrostriatal projection neurons". In: *Neuroscience Letters* 85 (1): pp. 1–4.

Tong, Y., Pisani, A., Martella, G., Karouani, M., Yamaguchi, H., Pothos, E. N., and Shen, J. (2009). "R1441C mutation in LRRK2 impairs dopaminergic neurotransmission in mice." In: *Proceedings of the National Academy of Sciences* 106 (34): pp. 14622–14627.

Tritsch, N. X., Ding, J. B., and Sabatini, B. L. (2012). "Dopaminergic neurons inhibit striatal output through non-canonical release of GABA". In: *Nature* 490 (7419): pp. 262–266.

Tritsch, N. X., Granger, A. J., and Sabatini, B. L. (2016). "Mechanisms and functions of GABA co-release". In: *Nature Reviews Neuroscience* 17 (3): pp. 139–145.

Tritsch, N. X., Oh, W.-J., Gu, C., and Sabatini, B. L. (2014). "Midbrain dopamine neurons sustain inhibitory transmission using plasma membrane uptake of GABA, not synthesis." In: *eLife* 3: e01936.

Tsai, C. (1925). "The optic tracts and centers of the opossum. Didelphis virginiana". In: *The Journal of Comparative Neurology* 39 (2): pp. 173–216.

Tsika, E., Kannan, M., Foo, C. S.-Y., Dikeman, D., Glauser, L., Gellhaar, S., Galter, D., Knott, G. W., Dawson, T. M., Dawson, V. L., and Moore, D. J. (2014). "Conditional expression of Parkinson's disease-related R1441C LRRK2 in midbrain dopaminergic neurons of mice causes nuclear abnormalities without neurodegeneration." In: *Neurobiology of Disease* 71: pp. 345–358.

Ungerstedt, U. (1971a). "Adipsia and Aphagia after 6-Hydroxydopamine Induced Degeneration of the Nigro-striatal Dopamine System". In: *Acta Physiologica Scandinavica* 82 (S367): pp. 95–122.

Ungerstedt, U. (1971b). "Stereotaxic mapping of the monoamine pathways in the rat brain." In: *Acta Physiologica Scandinavica. Supplement* 367: pp. 1–48.

Ungerstedt, U. (1968). "6-hydroxy-dopamine induced degeneration of central monoamine neurons". In: *European Journal of Pharmacology* 5 (1): pp. 107–110.

Ungless, M. A. (2004). "Dopamine: the salient issue." In: *Trends in Neurosciences* 27 (12): pp. 702–706.

Ungless, M. A., Magill, P. J., and Bolam, J. P. (2004). "Uniform inhibition of dopamine neurons in the ventral tegmental area by aversive stimuli." In: *Science* 303 (5666): pp. 2040–2042.

Usunoff, K. G., Romansky, K. V., Malinov, G. B., Ivanov, D. P., Blagov, Z. A., and Galabov, G. P. (1982). "Electron microscopic evidence for the existence of a corticonigral tract in the cat." In: *Journal für Hirnforschung* 23 (1): pp. 23–29.

Valente, E. M., Abou-Sleiman, P. M., Caputo, V., Muqit, M. M. K., Harvey, K., Gispert, S., Ali, Z., Del Turco, D., Bentivoglio, A. R., Healy, D. G., Albanese, A., Nussbaum, R., González-Maldonado, R., Deller, T., Salvi, S., Cortelli, P., Gilks, W. P., Latchman, D. S., Harvey, R. J., Dallapiccola, B., Auburger, G., and Wood, N. W. (2004). "Hereditary Early-Onset Parkinson's Disease Caused by Mutations in PINK1". In: *Science* 304 (5674): pp. 1158–1160.

Valente, E. M., Bentivoglio, A. R., Dixon, P. H., Ferraris, A., Ialongo, T., Frontali, M., Albanese, A., and Wood, N. W. (2001). "Localization of a Novel Locus for Autosomal Recessive Early-Onset Parkinsonism, PARK6, on Human Chromosome 1p35-p36". In: *The American Journal of Human Genetics* 68 (4): pp. 895–900.

Valente, E. M., Brancati, F., Ferraris, A., Graham, E. A., Davis, M. B., Breteler, M. M., Gasser, T., Bonifati, V., Bentivoglio, A. R., De Michele, G., Dürr, A., Cortelli, P., Wassilowsky, D., Harhangi, B. S., Rawal, N., Caputo, V., Filla, A., Meco, G., Oostra, B. A., Brice, A., Albanese, A., Dallapiccola, B., and Wood, N. W. (2002). "Park6-linked parkinsonism occurs in several European families". In: *Annals of Neurology* 51 (1): pp. 14–18.

Van Bockstaele, E. and Pickel, V. (1995). "GABA-containing neurons in the ventral tegmental area project to the nucleus accumbens in rat brain". In: *Brain Research* 682 (1-2): pp. 215–221.

Van Bockstaele, E. J., Cestari, D. M., and Pickel, V. M. (1994). "Synaptic structure and connectivity of serotonin terminals in the ventral tegmental area: potential sites for

modulation of mesolimbic dopamine neurons". In: *Brain Research* 647 (2): pp. 307–322.

Van Der Kooy, D., Hattori, T., Shannak, K., and Hornykiewicz, O. (1981). "The pallido-subthalamic projection in rat: Anatomical and biochemical studies". In: *Brain Research* 204 (2): pp. 253–268.

Venton, B. J., Zhang, H., Garris, P. A., Phillips, P. E. M., Sulzer, D., and Wightman, R. M. (2003). "Real-time decoding of dopamine concentration changes in the caudate-putamen during tonic and phasic firing". In: *Journal of Neurochemistry* 87 (5): pp. 1284–1295.

Vertes, R. P. (1991). "A PHA-L analysis of ascending projections of the dorsal raphe nucleus in the rat". In: *The Journal of Comparative Neurology* 313 (4): pp. 643–668.

Veyrac, A., Nguyen, V., Marien, M., Didier, A., and Jourdan, F. (2007). "Noradrenergic control of odor recognition in a nonassociative olfactory learning task in the mouse." In: *Learning & Memory* 14 (12): pp. 847–854.

Veyrac, A., Sacquet, J., Nguyen, V., Marien, M., Jourdan, F., and Didier, A. (2009). "Novelty determines the effects of olfactory enrichment on memory and neurogenesis through noradrenergic mechanisms." In: *Neuropsychopharmacology* 34 (3): pp. 786–795.

Vincent, S., Hökfelt, T., Christensson, I., and Terenius, L. (1982). "Immunohistochemical evidence for a dynorphin immunoreactive striato-nigral pathway". In: *European Journal of Pharmacology* 85 (2): pp. 251–252.

Vogt Weisenhorn, D. M., Giesert, F., and Wurst, W. (2016). "Diversity matters - heterogeneity of dopaminergic neurons in the ventral mesencephalon and its relation to Parkinson's Disease." In: *Journal of Neurochemistry* 139 (S1): pp. 8–26.

Voorn, P., Gerfen, C. R., and Groenewegen, H. J. (1989). "Compartmental organization of the ventral striatum of the rat: immunohistochemical distribution of enkephalin, substance P, dopamine, and calcium-binding protein." In: *Journal of Comparative Neurology* 289 (2): pp. 189–201.

Voorn, P., Vanderschuren, L. J., Groenewegen, H. J., Robbins, T. W., and Pennartz, C. M. (2004). "Putting a spin on the dorsal–ventral divide of the striatum". In: *Trends in Neurosciences* 27 (8): pp. 468–474.

Waelti, P., Dickinson, A., and Schultz, W. (2001). "Dopamine responses comply with basic assumptions of formal learning theory". In: *Nature* 412 (6842): pp. 43–48.

Walczak, M. and Błasiak, T. (2017). "Midbrain dopaminergic neuron activity across alternating brain states of urethane anaesthetized rat". In: *European Journal of Neuroscience* 45 (8): pp. 1068–1077.

Walker, M. D., Volta, M., Cataldi, S., Dinelle, K., Beccano-Kelly, D., Munsie, L., Kornelsen, R., Mah, C., Chou, P., Co, K., Khinda, J., Mroczek, M., Bergeron, S., Yu, K., Cao, L. P., Funk, N., Ott, T., Galter, D., Riess, O., Biskup, S., Milnerwood, A. J., Stoessl, A. J., Farrer, M. J., and Sossi, V. (2014). "Behavioral Deficits and Striatal DA Signaling in LRRK2 p.G2019S Transgenic Rats: A Multimodal Investigation Including PET Neuroimaging". In: *Journal of Parkinson's Disease* 4 (3): pp. 483–498.

Wang, D. V. and Tsien, J. Z. (2011). "Convergent processing of both positive and negative motivational signals by the VTA dopamine neuronal populations." In: *PloS One* 6 (2): e17047.

Wang, X., Yan, M. H., Fujioka, H., Liu, J., Wilson-Delfosse, A., Chen, S. G., Perry, G., Casadesus, G., and Zhu, X. (2012). "LRRK2 regulates mitochondrial dynamics and

function through direct interaction with DLP1". In: *Human Molecular Genetics* 21 (9): pp. 1931–1944.

Ward, C. D., Hess, W. A., and Calne, D. B. (1983). "Olfactory impairment in Parkinson's disease." In: *Neurology* 33 (7): pp. 943–946.

Waroux, O., Massotte, L., Alleva, L., Graulich, A., Thomas, E., Liégeois, J.-F., Scuvée-Moreau, J., and Seutin, V. (2005). "SK channels control the firing pattern of midbrain dopaminergic neurons in vivo." In: *European Journal of Neuroscience* 22 (12): pp. 3111–3121.

Wassef, M., Berod, A., and Sotelo, C. (1981). "Dopaminergic dendrites in the pars reticulata of the rat substantia nigra and their striatal input. combined immunocytochemical localization of tyrosine hydroxylase and anterograde degeneration". In: *Neuroscience* 6 (11): pp. 2125–2139.

Watabe-Uchida, M., Zhu, L., Ogawa, S. K., Vamanrao, A., and Uchida, N. (2012). "Whole-Brain Mapping of Direct Inputs to Midbrain Dopamine Neurons". In: *Neuron* 74 (5): pp. 858–873.

Weber, P., Metzger, D., and Chambon, P. (2001). "Temporally controlled targeted somatic mutagenesis in the mouse brain". In: *European Journal of Neuroscience* 14 (11): pp. 1777–1783.

Wellman, P., Ho, D., Cepeda-Benito, A., Bellinger, L., and Nation, J. (2002). "Cocaine-induced hypophagia and hyperlocomotion in rats are attenuated by prazosin". In: *European Journal of Pharmacology* 455 (2): pp. 117–126.

West, M. J. (1993). "New stereological methods for counting neurons". In: *Neurobiology of Aging* 14 (4): pp. 275–285.

Wey, M. C.-Y., Fernandez, E., Martinez, P. A., Sullivan, P., Goldstein, D. S., and Strong, R. (2012). "Neurodegeneration and motor dysfunction in mice lacking cytosolic and mitochondrial aldehyde dehydrogenases: implications for Parkinson's disease." In: *PloS One* 7 (2): e31522.

Wichmann, T. and Kliem, M. A. (2004). "Neuronal activity in the primate substantia nigra pars reticulata during the performance of simple and memory-guided elbow movements." In: *Journal of Neurophysiology* 91 (2): pp. 815–827.

Wickersham, I. R., Lyon, D. C., Barnard, R. J., Mori, T., Finke, S., Conzelmann, K.-K., Young, J. A., and Callaway, E. M. (2007). "Monosynaptic Restriction of Transsynaptic Tracing from Single, Genetically Targeted Neurons". In: *Neuron* 53 (5): pp. 639–647.

Wickman, K. D., Iñiguez-Lluhi, J. A., Davenport, P. A., Taussig, R., Krapivinsky, G. B., Linder, M. E., Gilman, A. G., and Clapham, D. E. (1994). "Recombinant G-protein $\beta\gamma$-subunits activate the muscarinic-gated atrial potassium channel". In: *Nature* 368 (6468): pp. 255–257.

Willott, J. F. (1986). "Effects of aging, hearing loss, and anatomical location on thresholds of inferior colliculus neurons in C57BL/6 and CBA mice". In: *Journal of Neurophysiology* 56 (2): pp. 391–408.

Wilson, C. J. and Groves, P. M. (1981). "Spontaneous firing patterns of identified spiny neurons in the rat neostriatum." In: *Brain Research* 220 (1): pp. 67–80.

Wilson, C. J., Young, S. J., and Groves, P. M. (1977). "Statistical properties of neuronal spike trains in the substantia nigra: Cell types and their interactions". In: *Brain Research* 136 (2): pp. 243–260.

Wolfart, J., Neuhoff, H., Franz, O., and Roeper, J. (2001). "Differential Expression of the Small-Conductance, Calcium-Activated Potassium Channel SK3 Is Critical for

Pacemaker Control in Dopaminergic Midbrain Neurons". In: *Journal of Neuroscience* 21 (10): pp. 3443–3456.

Wolfart, J. and Roeper, J. (2002). "Selective Coupling of T-Type Calcium Channels to SK Potassium Channels Prevents Intrinsic Bursting in Dopaminergic Midbrain Neurons". In: *Journal of Neuroscience* 22 (9): pp. 3404–3413.

Wood-Kaczmar, A., Gandhi, S., and Wood, N. W. (2006). "Understanding the molecular causes of Parkinson's disease". In: *Trends in Molecular Medicine* 12 (11): pp. 521–528.

Wurst, W. and Prakash, N. (2010). "Genetic control of meso-diencephalic dopaminergic neuron development in rodents". In: *Dopamine Handbook*. Ed. by Iversen, L. L., Iversen, S. D., Dunnett, S. B., and Björklund, A. 4th ed. New York: Oxford University Press, pp. 141–159.

Yamada, T., McGeer, P. L., Baimbridge, K. G., and McGeer, E. G. (1990). "Relative sparing in Parkinson's disease of substantia nigra dopamine neurons containing calbindin-D28K." In: *Brain Research* 526 (2): pp. 303–307.

Yamaguchi, T., Sheen, W., and Morales, M. (2007). "Glutamatergic neurons are present in the rat ventral tegmental area". In: *European Journal of Neuroscience* 25 (1): pp. 106–118.

Yamamura, T., Harada, K., Okamura, A., and Kemmotsu, O. (1990). "Is the site of action of ketamine anesthesia the N-methyl-D-aspartate receptor?" In: *Anesthesiology* 72 (4): pp. 704–710.

Yetnikoff, L., Lavezzi, H. N., Reichard, R. A., and Zahm, D. S. (2014). "An update on the connections of the ventral mesencephalic dopaminergic complex." In: *Neuroscience* 282: pp. 23–48.

Yung, K., Bolam, J. P., Smith, A. D., Hersch, S., Ciliax, B., and Levey, A. (1995). "Immunocytochemical localization of D1 and D2 dopamine receptors in the basal ganglia of the rat: Light and electron microscopy". In: *Neuroscience* 65 (3): pp. 709–730.

Záborszky, L., Alheid, G., Beinfeld, M., Eiden, L., Heimer, L., and Palkovits, M. (1985). "Cholecystokinin innervation of the ventral striatum: A morphological and radioimmunological study". In: *Neuroscience* 14 (2): pp. 427–453.

Záborszky, L. and Vadasz, C. (2001). "The Midbrain Dopaminergic System: Anatomy and Genetic Variation in Dopamine Neuron Number of Inbred Mouse Strains". In: *Behavior Genetics* 31 (1): pp. 47–59.

Zahm, D. S. and Heimer, L. (1990). "Two transpallidal pathways originating in the rat nucleus accumbens". In: *The Journal of Comparative Neurology* 302 (3): pp. 437–446.

— (1993). "Specificity in the efferent projections of the nucleus accumbens in the rat: Comparison of the rostral pole projection patterns with those of the core and shell". In: *The Journal of Comparative Neurology* 327 (2): pp. 220–232.

Zahm, D. S., Williams, E., and Wohltmann, C. (1996). "Ventral striatopallidothalamic projection: IV. Relative involvements of neurochemically distinct subterritories in the ventral pallidum and adjacent parts of the rostroventral forebrain". In: *The Journal of Comparative Neurology* 364 (2): pp. 340–362.

Zariwala, H. A., Kepecs, A., Uchida, N., Hirokawa, J., and Mainen, Z. F. (2013). "The Limits of Deliberation in a Perceptual Decision Task". In: *Neuron* 78 (2): pp. 339–351.

Zarranz, J. J., Alegre, J., Gómez-Esteban, J. C., Lezcano, E., Ros, R., Ampuero, I., Vidal, L., Hoenicka, J., Rodriguez, O., Atarés, B., Llorens, V., Tortosa, E. G., Ser, T. del, Muñoz, D. G., and Yebenes, J. G. de (2004). "The new mutation, E46K,

of α-synuclein causes parkinson and Lewy body dementia". In: *Annals of Neurology* 55 (2): pp. 164–173.

Zervas, M., Millet, S., Ahn, S., and Joyner, A. L. (2004). "Cell Behaviors and Genetic Lineages of the Mesencephalon and Rhombomere 1". In: *Neuron* 43 (3): pp. 345–357.

Zetterström, R. H., Williams, R., Perlmann, T., and Olson, L. (1996). "Cellular expression of the immediate early transcription factors Nurr1 and NGFI-B suggests a gene regulatory role in several brain regions including the nigrostriatal dopamine system". In: *Molecular Brain Research* 41 (1): pp. 111–120.

Zhou, H., Huang, C., Tong, J., Hong, W. C., Liu, Y.-J., and Xia, X.-G. (2011). "Temporal Expression of Mutant LRRK2 in Adult Rats Impairs Dopamine Reuptake". In: *International Journal of Biological Sciences* 7 (6): pp. 753–761.

Zhou, Q.-Y. and Palmiter, R. D. (1995). "Dopamine-deficient mice are severely hypoactive, adipsic, and aphagic". In: *Cell* 83 (7): pp. 1197–1209.

Zimprich, A., Biskup, S., Leitner, P., Lichtner, P., Farrer, M. J., Lincoln, S., Kachergus, J., Hulihan, M., Uitti, R. J., Calne, D. B., Stoessl, A. J., Pfeiffer, R. F., Patenge, N., Carbajal, I. C., Vieregge, P., Asmus, F., Müller-Myhsok, B., Dickson, D. W., Meitinger, T., Strom, T. M., Wszolek, Z. K., and Gasser, T. (2004). "Mutations in LRRK2 cause autosomal-dominant parkinsonism with pleomorphic pathology." In: *Neuron* 44 (4): pp. 601–607.

Zoli, M., Torri, C., Ferrari, R., Jansson, A., Zini, I., Fuxe, K., and Agnati, L. F. (1998). "The emergence of the volume transmission concept". In: *Brain Research Reviews* 26 (2-3): pp. 136–147.

Zweifel, L. S., Parker, J. G., Lobb, C. J., Rainwater, A., Wall, V. Z., Fadok, J. P., Darvas, M., Kim, M. J., Mizumori, S. J. Y., Paladini, C. A., Phillips, P. E. M., and Palmiter, R. D. (2009). "Disruption of NMDAR-dependent burst firing by dopamine neurons provides selective assessment of phasic dopamine-dependent behavior." In: *Proceedings of the National Academy of Sciences* 106 (18): pp. 7281–7288.